Analysis of cell-cell communication during reproductive processes by EA1-like peptides in maize

DISSERTATION

ZUR ERLANGUNG DES DOKTORGRADES DER NATURWISSENSCHAFTEN

(DR. RER. NAT.) DER FAKULTÄT FÜR BIOLOGIE UND VORKLINISCHE MEDIZIN

UNIVERSITÄT REGENSBURG

Vorgelegt von

Susanne Uebler

aus Vilshofen an der Donau

im September 2015

Das Promotionsgesuch wurde eingereicht am 24.09.2015

Die Arbeit wurde angeleitet von Dr. Mihaela-Luiza Márton

Unterschrift: _____

Susanne Uebler

Meinen Eltern.

Meiner Liebe.

„Coming back to where you started is not the same as never leaving."

Terry Pratchett

This thesis is partially composed of the manuscripts listed below:

CHAPTER 2

Uebler, S., Márton, M. L. and Dresselhaus, T. (under review in *Plant Reproduction*). Classification of EA1-box proteins and new insights into their role during reproduction in grasses.

S. Uebler conducted bioinformatical analysis and performed all experimental procedures except RT-PCR of rice genes and generation of constructs for transient transformation of *ZmEA1*, *AtEAG1*, *OsEAL1* and *OsEAL3*. The manuscript was written by S. Uebler and edited by T. Dresselhaus. The paragraphs about generation and analysis of transgenic maize lines and promoter analysis are excluded from the publication.

CHAPTER 3

Márton, M. L., Fastner, A., Uebler, S. and Dresselhaus, T. (2012). Overcoming hybridization barriers by the secretion of the maize pollen tube attractant ZmEA1 from *Arabidopsis* ovules. *Current Biology* 22, 1194–1198.

S. Uebler performed the immunoblot experiments (Figure 3.4 E) and wrote the corresponding paragraph in the section of experimental design (3. 2. 6).

CHAPTER 4

Uebler, S., Dresselhaus, T. and Márton, M. L. (2013). Species-specific interaction of EA1 with the maize pollen tube apex. *Plant Signaling & Behavior* 8, e25682.

S. Uebler performed all experiments and wrote the manuscript except the introduction paragraph. The manuscript was edited by T. Dresselhaus and M. L. Márton.

CHAPTER 5

Uebler, S. and Dresselhaus, T. (2014). Identifying plant cell-surface receptors: combining "classical" techniques with novel methods. *Biochemical Society Transactions* 42, 395–400.

The manuscript was written by S. Uebler and edited by T. Dresselhaus.

CONTENTS

SUMMARY **1**

CHAPTER 1 - GENERAL INTRODUCTION TO SEXUAL REPRODUCTION IN ANGIOSPERMS **3**

1. 1 Development of gametophytes in flowering plants **3**

1. 1. 1 Development of the female gametophyte 3

1. 1. 2 Development of the male gametophyte 5

1. 2 Progamic phase **6**

1. 2. 1 Growth of the pollen tube through sporophytic tissue 6

1. 2. 2 Control of pollen tube growth by male-female communication 7

1. 3 Embryogenesis in model flowering plants **9**

1. 3. 1 Developmental steps of embryo formation 9

1. 3. 2 Peptide signaling during embryogenesis 11

1. 4 Aims of this work **12**

CHAPTER 2 - CLASSIFICATION OF EA1-BOX PROTEINS AND NEW INSIGHTS INTO THEIR ROLE DURING REPRODUCTION IN GRASSES **13**

2. 1 Introduction **13**

2. 2 Experimental procedures **15**

2. 2. 1 Bioinformatic analysis 15

2. 2. 2 Generation of constructs for transformation of BMS cells 15

2. 2. 3 Transient transformation of maize BMS suspension cells 16

2. 2. 4 Extraction of total RNA and generation of cDNA 16

2. 2. 5 Semi-quantitative reverse transcriptase-PCR (RT-PCR) and quantitative real–time PCR (qRT-PCR) 17

2. 2. 6 Immunoblot analysis and generation of anti-ZmEAL2 antiserum 17

2. 2. 7 Immunohistochemical detection of ZmEAL2 18

2. 2. 8 Generation of stable transgenic maize lines 18

2. 2. 8. 1 Constructs for Agrobacterium-mediated transformation of maize 18

2. 2. 8. 2 Agrobacterium-mediated transformation of maize 19

2. 3 Results and discussion 21

2. 3. 1 EA1-box containing proteins can be separated into three classes 21

2. 3. 2 EA1-box proteins show a highly variable expression pattern..... 26

2. 3. 3 EALs and EACs enter the secretory pathway, while EAGs localize to the cytoplasm and nucleus 28

2. 3. 4 ZmEAL2 potentially plays a role during late embryogenesis..... 32

2. 4 Conclusions 39

CHAPTER 3 - OVERCOMING HYBRIDIZATION BARRIERS BY THE SECRETION OF THE MAIZE POLLEN TUBE ATTRACTANT ZMEA1 FROM *ARABIDOPSIS* OVULES 41

3. 1 Introduction 41

3. 2 Experimental procedures 41

3. 2. 1 Plant material and growth 41

3. 2. 2 Generation of constructs and transgenic plants..... 42

3. 2. 3 Chemical labeling of synthetic ZmEA1 peptide 43

3. 2. 4 *In vitro* pollen tube guidance and competition assays and ZmEA1 bioassay..... 43

3. 2. 5 Microscopy 44

3. 2. 6 Immunoblot analysis 45

3. 3 Results and discussion 46

3. 3. 1 Mature ZmEA1 attracts and arrests maize pollen tubes *in vitro* and binds to the subapical region of their tips 46

3. 3. 2 ZmEA1-GFP fusion proteins are predominantly localized to the filiform apparatus, the secretory zone of synergid cells in *Arabidopsis* ovules..... 50

3. 3. 3 Maize PTs are attracted *in vitro* by *Arabidopsis* ovules expressing ZmEA1-GFP fusion protein in synergid cells..... 53

3. 4 Conclusions 57

CHAPTER 4 - SPECIES-SPECIFIC INTERACTION OF EA1 WITH THE MAIZE POLLEN TUBE APEX 58

4. 1 Introduction 58

4. 2 Experimental procedures 59

4. 2. 1 Chemical labeling of synthetic peptides 59
4. 2. 2 Pollen tube binding assay 59
4. 3 Results and discussion 60
4. 4 Conclusions 64

CHAPTER 5 - IDENTIFYING PLANT CELL-SURFACE RECEPTORS: COMBINING "CLASSICAL" TECHNIQUES WITH NOVEL METHODS. 66
5. 1 Introduction 66
5. 2 Genetic and bioinformatic approaches are limited to identify peptide ligand interaction partners 67
5. 3 Cross-linking: Panacea for receptor-fishing? 68
5. 4 Innovative novel method: Ligand-based receptor-capture technology 71
5. 5 Alternative "classical" method: mRNA-display libraries 73
5. 6 Concluding remarks 73

CHAPTER 6 - IDENTIFICATION OF CANDIDATE INTERACTION PARTNERS OF THE POLLEN TUBE ATTRACTOR ZMEA1 75
6. 1 Introduction 75
6. 2 Experimental procedures 78
6. 2. 1 Cultivation of organisms 78
6. 2. 1. 1 Plant material and growth conditions 78
6. 2. 1. 2 Bacterial strains and culture conditions 78
6. 2. 2 Transformation of bacteria 79
6. 2. 3 Molecular cloning and PCR 79
6. 2. 3. 1 PCR and quantitative real-time PCR (qRT-PCR) 79
6. 2. 3. 2 Determination of UTR sequences 80
6. 2. 3. 3 Constructs for heterologous expression in E. coli 80
6. 2. 3. 4 Constructs for transient expression in N. benthamiana 81
6. 2. 3. 5 Constructs for in vitro transcription/translation (IVT/T) 81
6. 2. 4 Heterologous expression in *E. coli* and protein purification 82
6. 2. 4. 1 Purification of His-tagged protein 82

6. 2. 4. 2 On-column refolding of His-tagged protein *83*

6. 2. 4. 3 Native protein purification of GST-tagged protein *83*

6. 2. 5 Heterologous expression in *N. benthamiana* leaves and protein purification 83

6. 2. 5. 1 Transient transgene expression in tobacco *83*

6. 2. 5. 2 Extraction of recombinant protein produced in tobacco *84*

6. 2. 5. 3 Purification of sEA1-GFP produced in tobacco *84*

6. 2. 5. 4 Pull-down of recombinant Myc-WSL3 with sEA1-biotin *85*

6. 2. 5. 5 Pull-down of candidate proteins fused to GFP with sEA1-biotin *86*

6. 2. 6 Protein analysis 86

6. 2. 6. 1 Generation of polyclonal peptide antibodies against EA1, WSL1a/b and WSL3 ..... *86*

6. 2. 6. 2 SDS-PAGE, gel staining and immunoblot analysis *86*

6. 2. 7 *In vitro* transcription/translation (IVT/T) of proteins 87

6. 2. 8 Protein extraction from maize pollen tubes 88

6. 2. 9 Pull-down with sEA1-biotin and germinated maize pollen 88

6. 2. 9. 1 With crosslinking, analysis by immunoblot *88*

6. 2. 9. 2 No crosslinking, analysis by mass spectrometry *89*

6. 2. 10 Bioinformatic analysis 89

6. 3 Results 90

6. 3. 1 Heterologous expression of predicted mature *ZmEA1* (*sEA1*) 90

6. 3. 1. 1 Expression of sEA1 in Escherichia coli *90*

6. 3. 1. 2 Expression of sEA1 in Nicotiana benthamiana leaves *97*

6. 3. 2 Potential interaction partners of sEA1 100

6. 3. 2. 1 Visualization of sEA1 binding to other proteins *100*

6. 3. 2. 2 Identification of potential interaction partners of sEA1 ..... *104*

6. 3. 2. 3 Sequence analysis of the potential interaction partners *107*

6. 3. 3 WSL1a/b and WSL3 exhibit structural similarities to DEFLs 110

6. 3. 4 Interaction studies with sEA1 and WSLs 111

6. 3. 4. 1 Expression of WSLs and ZmEA1/sEA1 in IVT/T systems *111*

6. 3. 4. 2 Expression in Nicotiana benthamiana leaves *114*

6. 3. 5 Characterization of WSL peptides 116

6. 3. 5. 1 Expression profile of WSL peptides 116

6. 3. 5. 2 WSL1 is highly abundant in maize pollen 119

6. 3. 5. 3 WSL peptides enter the secretory pathway 121

6. 3. 5. 4 WSL peptides are exclusively found in maize and Sorghum bicolor 124

6. 4 Conclusions 125

6. 4. 1 Candidates for interaction with predicted mature ZmEA1 are secreted CRPs related to defensins 125

6. 4. 2 Future tasks to verify WSL peptides as interaction partners of ZmEA1 126

6. 4. 3 Model for interaction of WSL peptides with ZmEA1 129

CHAPTER 7 - COMPREHENSIVE DISCUSSION AND OUTLOOK 132

7. 1 EA1-box as potential protein-protein interaction motive 132

7. 2 Structure and posttranslational modifications of EALs: Open questions that need to be answered 134

7. 3 WSL-EA1 interaction – a novel reproductive isolation mechanism? 138

REFERENCES 140

SUPPLEMENTARY MATERIAL 165

Genomic locations of EA1-box proteins 165

Primer sequences 166

Vector maps 169

ABBREVIATIONS 174

FIGURES AND TABLES 176

ACKNOWLEDGEMENTS 179

SUMMARY

Signaling processes mediated by secreted peptides are of eminently importance in cell-cell-communication of plants. This work focuses on extracellular signaling peptides containing the EA1-box and their involvement in control of reproductive processes in maize (*Zea mays* L.). In maize, the EA1-box protein ZmEA1 was already demonstrated to act as a secreted signaling peptide in micropylar pollen tube guidance, whereas the closely related peptide ZmEAL1 is necessary for cell fate determination of the female gametophyte. To extent our knowledge about EA1-box proteins, several plant genomes of monocotyledonous and dicotyledonous plants were searched for this motif and EA1-box proteins could be identified in all of the analyzed plant species. Based on similarities of structural features and subcellular localization, a new classification and phylogenetic analysis is presented, dividing these proteins into three classes, the EAL, EAG and EAC proteins. The EA1-like (EAL) proteins, including ZmEA1 and ZmEAL1, consist of less than 200 amino acids and are predicted to be secreted using either an N-terminal or internal signal sequence. Besides the EA1-box, they contain the so-called P-box and a C-terminal alanine-rich region as conserved motifs. All analyzed EAL proteins were demonstrated to enter the secretory pathway in transiently transformed plant suspension cells. In contrast, the EA1-box containing glycine-rich (EAG) proteins show cytoplasmic localization and are expected to act as intracellular components. The third class, the EA1-box containing (EAC) proteins, includes EA1-box proteins that could not be classified as EALs or EAGs and contains proteins with up to several transmembrane domains. The expression pattern of rice EALs was analyzed and comparison with maize EALs indicated that these proteins might act as orthologs. Furthermore, the final member of the small maize EAL family, *ZmEAL2*, was analyzed in detail and was demonstrated to exhibit a broader expression pattern compared to *ZmEA1* and *ZmEAL1*, and showed a remarkable strong expression pattern in the embryo during later stages of development. Using immunohistochemical analysis, ZmEAL2 was localized in the scutellar parenchym and surrounding the vascular system of the embryo. Taken together, these results suggest a role of ZmEAL2 during embryogenesis.

To gain deeper insights into the role of ZmEA1 during micropylar pollen tube attraction, it was expressed as GFP-fusion protein in the synergids of *Arabidopsis thaliana*. Interestingly, dissected transgenic *Arabidopsis* ovules placed on solid media were demonstrated to attract *in vitro* germinated maize pollen tubes, whereas no impact on tube growth direction could be

detected for wild-type ovules. As this indicates the direct binding of secreted ZmEA1 protein to the pollen tube, germinated maize pollen was further incubated with predicted mature ZmEA1 (sEA1), labeled with a fluorophore to visualize the interaction. The peptide bound to the surface of the pollen tube apex and was internalized quickly, probably for degradation. To identify the interaction partner(s) located on the pollen tube surface binding to sEA1, a large number of pull-down experiments were performed. Immunoblot analysis of the isolated fractions indicated binding to one or more interaction partners, which should be identified by Orbitrap mass spectrometry. Three different protein sequences were identified as candidates for interaction with sEA1 and named as WHY SO LATE (WSL) proteins. Contrary to the expected membranous proteins, WSL proteins represent putative secreted cysteine-rich peptides. They were shown to enter the secretory pathway in transiently transformed tobacco leaves. WSL1 is encoded by two genes which were named as *WSL1a* and *WSL1b*. WSL1a/b and WSL3 protein sequences are highly similar, therefore they were classified to form a small protein family sharing structural similarities to defensin-like proteins (DEFLs). All WSL peptides are strongly and specifically expressed in pollen and are exclusively found in maize and the closely related grass *Sorghum bicolor*. First attempts were performed to confirm the interaction of WSL peptides with sEA1. Taken together, potential factors acting in the pathway of ZmEA1-signaling could be identified and were made available for further research. In case, the direct binding between ZmEA1 and WSL peptides as well as the involvement of this complex in micropylar pollen tube guidance can be demonstrated in future, this would be the first report of a heterodimeric signaling ligand generated both by male and female gametophytes, which would provide a highly specific interaction representing a prerequisite for a molecular mechanism contributing to reproductive isolation barriers in plants.

CHAPTER 1 - GENERAL INTRODUCTION TO SEXUAL REPRODUCTION IN ANGIOSPERMS

Flowering plants (angiosperms) exhibit a life cycle with alteration of generations in which the diploid sporophyte represents the dominant generation and strongly reduced haploid male and female gametophytes are formed by meiosis within flowers of the sporophyte (for review see Reiser and Fischer, 1993). For sexual reproduction, the gametophytes produce male and female gametes, which fuse to form a diploid zygote giving rise to the next diploid sporophytic generation containing both parental and maternal genetic information. A characteristic trait of flowering plants is double fertilization, in which the two male gametes, the sperm cells, fuse with two gametic cells of the female gametophyte, the egg cell and the central cell, respectively. Whereas fertilization of the egg cell gives rise to the embryo, fertilization of the central cell results in formation of the endosperm tissue, nourishing the embryo (Boavida *et al.*, 2005). Both developments of the gametophytes as well as fertilization procedures follow a defined and precisely controlled pattern to ensure successful reproduction.

1. 1 Development of gametophytes in flowering plants

1. 1. 1 Development of the female gametophyte

The female gametophyte (FG), also called megagametophyte or embryo sac, develops in the ovules. Many different types of FG development exist in angiosperms, with the *Polygonum*-type pattern representing the most abundant one. Maize and *Arabidopsis* gametophytes studied in this thesis exhibit this pattern, therefore FG development of both plants will be described here (for reviews see Evans and Grossniklaus, 2009; Drews and Koltunow, 2011). FG development can be distinguished into two phases called megasporogenesis and megagametogenesis. Stages of the megagametogenesis are outlined in Figure 1.1. During megasporogenesis in both species, one archesporial cell derived from a hypodermal cell differentiates into the megaspore mother cell, which enlarges before undergoing meiosis to give rise to four haploid megaspores. Three of these cells degenerate, whereas the last one forms the functional megaspore, representing the first stage of megagametogenesis (stage FG1). Subsequently, the functional megaspore enlarges by increasing vacuole volume. An eight-nucleated coenocyte is produced by three rounds of mitosis without cell division, during stages FG2 until FG5. Cel-

lularization takes place during stage FG5 and the seven-celled megagametophyte is formed. It consists of three antipodal cells at the chalazal pole of the FG, two synergid cells and one egg cell at the micropylar pole, and one central cell. Egg cell, antipodal and synergid cells are haploid, whereas the central cell contains two polar nuclei migrating towards each other to the micropylar pole of the central cell, defining stage FG6. During fertilization, both egg cell and central cell fuse with a sperm cell, giving rise to the diploid embryo (egg cell) and the triploid endosperm (central cell). In maize, the antipodal cells continue to divide during maturation of the embryo sac, to form a cluster of antipodal cells (Diboll and Larson, 1966). Contrary to this pattern, the three antipodal cells of *Arabidopsis* do not proliferate further (Christensen *et al.*, 1998). In both plant species, the synergid cells are specialized at the micropylar pole by thickening and invagination of the cell walls, forming the secretory highly active filiform apparatus. Mutants with defects in filiform apparatus formation exhibit a lack of pollen tube attraction during fertilization, suggesting that it represents a cell structure necessary for secretion of pollen tube attractant (Kasahara *et al.*, 2005).

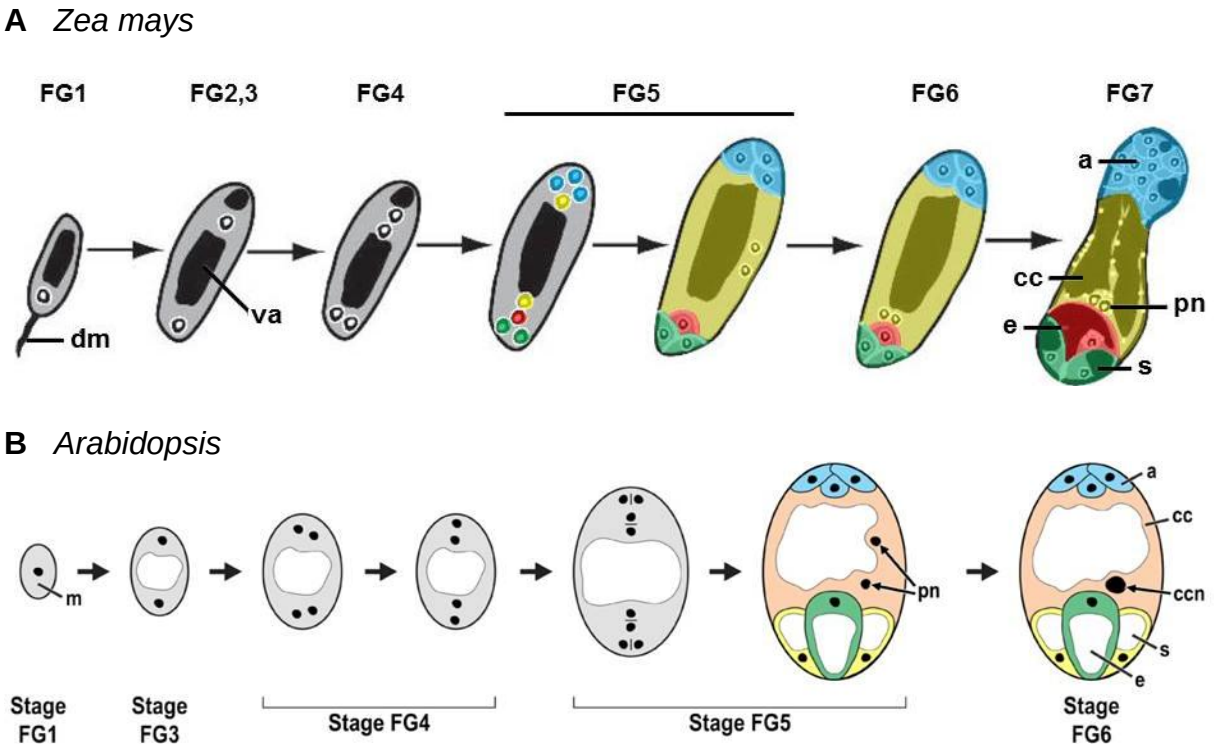

Figure 1.1 Megagametogenesis of *Zea mays* and *Arabidopsis*. Stages of megagametophyte development in (**A**) *maize* (image adapted from Evans and Grossniklaus, 2009) and (**B**) *Arabidopsis* (image taken from Drews and Koltunow, 2011) as detailed in the text, according to Christensen *et al.*, 1998. Abbreviations: a = antipodal cells, cc = central cell, ccn = central cell nucleus, dm = degenerated megaspores, e = egg cell, m = megaspore, pn = polar nuclei, s = synergid cell, va = vacuole.

1. 1. 2 Development of the male gametophyte

Successful seed formation requires a functional male gametophyte interacting with sporophytic tissue and the female gametophyte during the fertilization process. During male gametophyte development, the pollen is formed by coordinated interaction with surrounding tissue, giving rise to haploid cells after meiosis. Maize is a valuable model for studying male gametogenesis and will represent the object of interest in the following paragraph. For review of pollen development in *Arabidopsis* see McCormick, 2004. In maize, each male flower within the tassels contains three stamen with four anther locules, in which the pollen develops (Vollbrecht and Schmidt, 2009). These developmental processes can be distinguished into three phases, first premeiotic development, followed by microsporogenesis and microgametogenesis and finally postpollination events as the last phase (for review see Bedinger and Fowler, 2009). During premeiotic development, archesporial cells surrounded by a layer of primary parietal cells are formed, both originating from divided hypodermal cells (Figure 1.2 A). The archesporial cells further differentiate during microsporogenesis into pollen mother cells, also called microsporocytes. The primary parietal cell layer differentiates and gives rise to inner anther wall layers and the tapetum (Figure 1.2 B). Subsequently, the pollen mother cell undergoes meiosis to produce a tetrade of four haploid microspores, whereas the tapetal cells secretes substances for formation of the pollen coat as well as enzymes, like callase, to release the microspores from the tetrade (Figure 1.2 C) (Quilichini *et al.*, 2015).

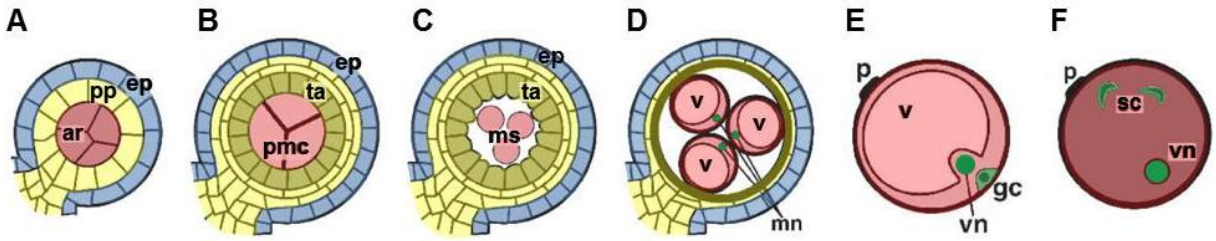

Figure 1.2 Development of the male gametophyte in maize. (**A**) Archesporial cells, embedded in a primary parietal cell layer, differentiate into (**B**) pollen mother cells, surrounded from the tapetum cells, which are derived from the primary parietal layer. (**C, D**) Pollen mother cells undergo meiosis to form enlarging microspores. (**E**) Microspores undergo mitosis to produce a vegetative and a generative nucleus and cellularization gives rise to the generative cell. (**F**) Two sperm cells located in the cytoplasm of the vegetative cell are formed by mitosis of the generative cell. Abbreviations: ar = archesporial cells, ep = epidermis, gc = generative cell, mn = microspore nucleus, ms = microspores, pmc = pollen mother cells, pp = primary parietal layer, sc = sperm cells, ta = tapetum, v = vacuole, vn = vegetative nucleus. Image adapted from Bedinger and Fowler, 2009.

The enlarging microspores generate a vacuole and the surrounding sporophytic cell layers collapse. Tapetum cells undergo programmed cell-death (Solís *et al.,* 2014) (Figure 1.2 D). Asymmetric mitosis of the microspores marks the beginning of microgameteogenesis and produces a large transcriptionally active vegetative nucleus and a generative smaller nucleus with more compact chromatin. Cellularization around the generative nucleus leads to formation of the generative cell adjacent to the pollen wall, which later migrates into the cytoplasm of the larger vegetative cell (Figure 1.2 E). A second mitosis event of the generative cell produces two sperm cells (Figure 1.2 F). The final steps of pollen maturation include starch accumulation, pollen wall maturation and dehydration, preparing the pollen to be released out of the anthers after anthesis.

1. 2 Progamic phase

1. 2. 1 Growth of the pollen tube through sporophytic tissue

After the pollen is released from the anthers, it attaches to the silks of the female flower, representing the maize stigma. The vegetative cell germinates as pollen tube to transport the embedded sperm cells towards the FG. The journey of the maize pollen tube can be divided into different phases based on Lausser *et al.,* 2010. During phase I, the pollen grains get attached on hairs covering the silk, hydrate and germinate (Figure 1.3 A). Growth of pollen tubes into the sporophytic silk tissue marks the beginning of phase II, in which the pollen tubes enter one of the two transmitting tracts inside of the silk to begin phase III of tube growth. Penetration of the multicellular silk hairs by pollen tubes during phase II is thought to be necessary for directed growth of the pollen tube towards the basis of the silk during phase III (Booy *et al.,* 1992; Lausser *et al.,* 2010). Growth of pollen tubes through the transmitting tract causes degeneration of the silk abscission zone to prevent supernumerous pollen tubes reaching the female gametophyte (Heslop-Harrison *et al.,* 1985). During phase IV, pollen tubes exit the transmitting tract and enter the ovular cavity to grow towards the embryo sac (Figure 1.3 B). Finally, in phase V, the pollen tubes are directed to the micropylar region of the FG, which is covered with several cell layers of nucellus cells. This is contrary to the FG of *Arabidopsis*, which is covered by integuments, leaving a pore for penetration of the micropylar region with the pollen tube. In grasses, pollen tubes have to penetrate these cell layers to release the sperm cells for double fertilization, a unique feature of flowering plants. One sperm cell fuses with

the haploid egg cell to develop the embryo, whereas the second sperm cell fuses with the diploid central cell to arise the triploid endosperm.

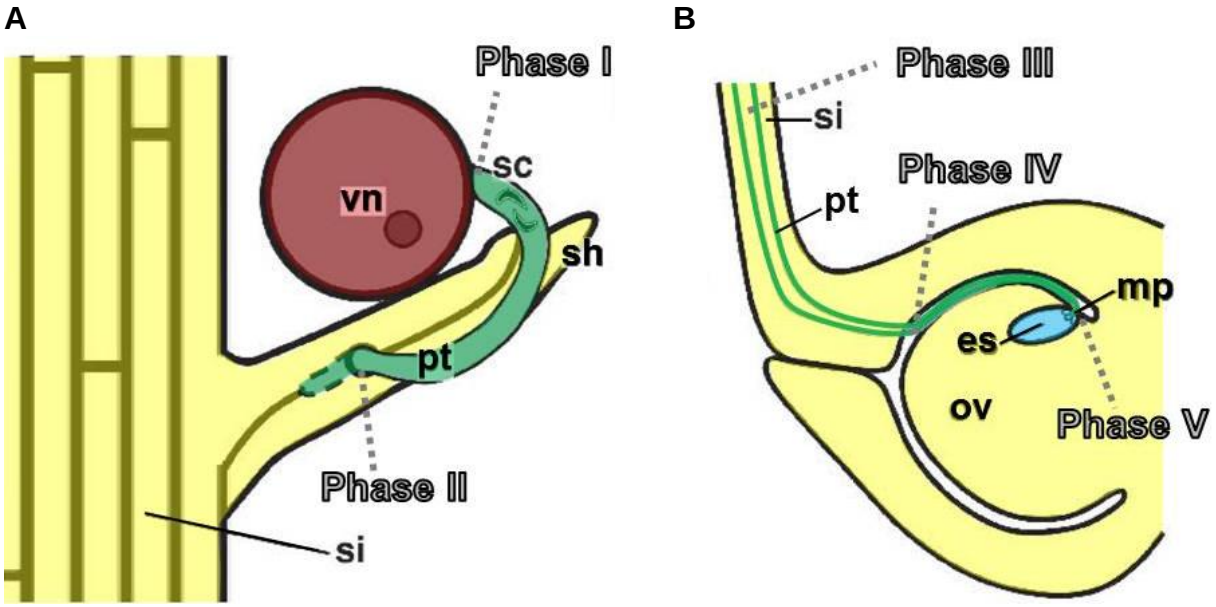

Figure 1.3 Growth of pollen tube for fertilization of the female gametophyte in maize. In maize, the journey of the pollen tube towards the female gametophyte can be distinguished into different phases (Lausser *et al.*, 2010). (**A**) A pollen grain attaches to the silk hairs and germinates (phase I). In phase II, the pollen tube penetrates the sporophytic tissue to enter the transmitting tract inside of the silk. (**B**) Pollen tubes pass through the transmitting tracts (phase III) and exit into the ovarial cavity in phase IV, to grow towards the female gametophyte. In phase V, one pollen tube enters the embryo sac to release the sperm cells for fertilization. Images adapted from Bedinger and Fowler, 2009.

1. 2. 2 Control of pollen tube growth by male-female communication

The growth of the pollen tube through the style towards the female gametophyte has to be controlled precisely, requiring communication between the pollen tube and the surrounding tissues. Several substances contributing to these communication processes were identified during the last years in different plant species (for review see Dresselhaus and Franklin-Tong, 2013; Higashiyama and Takeuchi, 2015). These factors are influencing pollen germination and growth rate as well as guidance of the growth direction mediated by sporophytic tissue or the female gametophyte, partially with overlapping functions. Germination of the pollen in *Arabidopsis* is stimulated for example by sulfinylated azadecalin, a substance isolated from pistil extract (Qin *et al.*, 2011) as well as epibrassinolide, which also accelerates tube growth

(Vogler *et al.,* 2014). With γ-aminobutyric acid (GABA), another substance was identified to promote pollen tube germination and growth. Additionally, GABA is involved in ovular guidance during the last steps of pollen tube growth (Palanivelu *et al.,* 2003; Ling *et al.,* 2013). Growth of the pollen tube through the transmitting tract seems to be guided by an interplay of various factors with the tube cell, although also mechanical guidance of the tube growth was observed (Jauh *et al.,* 1997; Higashiyama and Hamamura, 2008). An arabinogalactan protein named Transmitting-Tissue-Specific (TTS) from tobacco styles was reported to act as directional cue (Cheung *et al.,* 1995; Wu *et al.,* 2000), just as several cysteine-rich peptides (CRPs) secreted by the sporophytic transmitting tract tissue like chemocyanin (Kim *et al.,* 2003), plantacyanin (Dong *et al.,* 2005) or the adhesine SCA, which was demonstrated to be involved in formation of the adhesive matrix necessary for pollen tube guidance through the transmitting tract (Mollet *et al.,* 2000). As mentioned before, not only sporophytic tissue but also the female gametophyte contributes to the correct growth direction of the pollen tube, as functional female gametophytes are a prerequisite for the last steps of the pollen tube journey (Ray *et al.,* 1997; Higashiyama *et al.,* 2001). With ZmEA1, the first described secreted peptide with pollen tube attraction capability was isolated from maize (Márton *et al.,* 2005). *ZmEA1* encodes a small 94 amino-acid propeptide which is secreted after passing the secretory pathway from the egg apparatus (egg cell and synergids) towards the nucellus cells at the micropylar cone covering the female gametophyte. Down-regulation of *ZmEA1* using the RNAi technique resulted in a loss of short-range guidance of the pollen tube, which failed to grow through the micropylar region (Márton *et al.,* 2005). Later, pollen tube attracting peptides secreted from the synergids were also discovered in the dicotyledonous plants *Torenia fournieri* (TfLURE1-2; Okuda *et al.,* 2009), *Torenia concolor* (TcCRP1; Kanaoka *et al.,* 2011), *Arabidopsis thaliana* (AtLURE1.1 - 1.6; Takeuchi and Higashiyama, 2012) and *Arabidopsis lyrata* (AlLURE1.1 - 1.10; Takeuchi and Higashiyama, 2012). In contrast to ZmEA1, all of these attractants are defensin-like CRPs.

Communication between the pollen tube and the pistil is also required during the last steps of tube growth, the penetration of the female gametophyte to release the sperm cells. The pollen tube is perceived by the FG, its growth has to be arrested and tube burst has to be initiated. These procedures require intensive cross-talk of both pollen tube and FG cells. As examples for female factors localized on the synergid surface, the small putative glucosylphsophatidylinositol-anchored protein LORELEI (LRE) (Capron *et al.,* 2008) and the receptor-like kinase (RLK) FERONIA (FER), containing a putative extracellular carbohydrate-binding malectin-

like domain (Lindner *et al.,* 2012), are necessary for pollen tube growth arrest (Escobar-Restrepo *et al.,* 2007). Mutants lacking these proteins display overgrowing pollen tubes that fail to burst. Regarding the male side, the FER-related pollen tube derived RLKs ANXUR1 (ANX1) and (ANX2) seem to be involved in maintaining pollen tube integrity until it reaches the FG (Boisson-Dernier *et al.,* 2009). To release the sperm cells for fertilization, the defensin-like cysteine-rich peptide ZmES4 from maize was identified to induce pollen tube burst. It is accumulating in the synergids and gets discharged upon pollen tube arrival (Amien *et al.,* 2010).

To summarize, there are many key players involved in pollen-pistil communication to guide the pollen tube towards the FG. Many of them, like above described pollen tube attractants and ZmES4 (Amien *et al.,* 2010), are thought to act in a species-preferential manner and provide reproductive barriers between different plant species. In this paragraph, only a selection of them was described. Further factors mediating successful sperm cell delivery to the FG will be discussed in CHAPTER 6.

1. 3 Embryogenesis in model flowering plants

1. 3. 1 Developmental steps of embryo formation

Following fertilization, the basic plant body is formed during embryogenesis by establishing polarity, differentiation of primary tissue and accumulation of storage nutrients. As embryo development marks the first steps after changing from gametophytic to sporophytic phase of the plant life cycle, these processes are extensively studied. In general, the detailed pattern of embryo body formation is species-specific. The following paragraph will focus on morphologically described stages of embryogenesis of maize and will point out differences to the dicotyledonous model plant *Arabidopsis* (Figure 1.4) (for review see Vernoud *et al.,* 2005 and Lau *et al.,* 2012).

The zygote of maize divides asymmetrically into a small apical and a large basal cell giving rise to the proembryo. The proembryo consist of small cytoplasm-rich cells of the embryo proper and larger vacuolized cells forming the suspensor (Randolph, 1936). During the transition stage, the protoderm is formed as external cell layer surrounding the embryo proper. The embryo proper cells representing the future scutellum enlarge during the following coleoptilar stage, whereas a group of cells facing towards the ear stays densely packed. At this position, formation of the shoot apical meristem (SAM) is initiated close to a protuberance marking the

future coleoptile. Additionally, the root apical meristem (RAM) is formed at a more basal position. Depending on genotype and environmental conditions, the coleoptilar stage lasts until 10 to 15 days after pollination. In contrast to *Arabidopsis*, in which the SAM does not generate leaf primordia before germination, the SAM of the maize embryo initiates the formation of 5-6 leaves, with the number of leaf primordia naming the developmental stage of the embryo (stage 1-6) (Nardmann and Werr, 2009). To protect the leaf primordia, they are covered by the coleoptile. During these stages, the vascular system is established in the embryo. With proceeding maturation, the embryo grows further, the suspensor degenerates and storage nutrients like lipids are accumulated (Giuliani *et al.*, 2002).

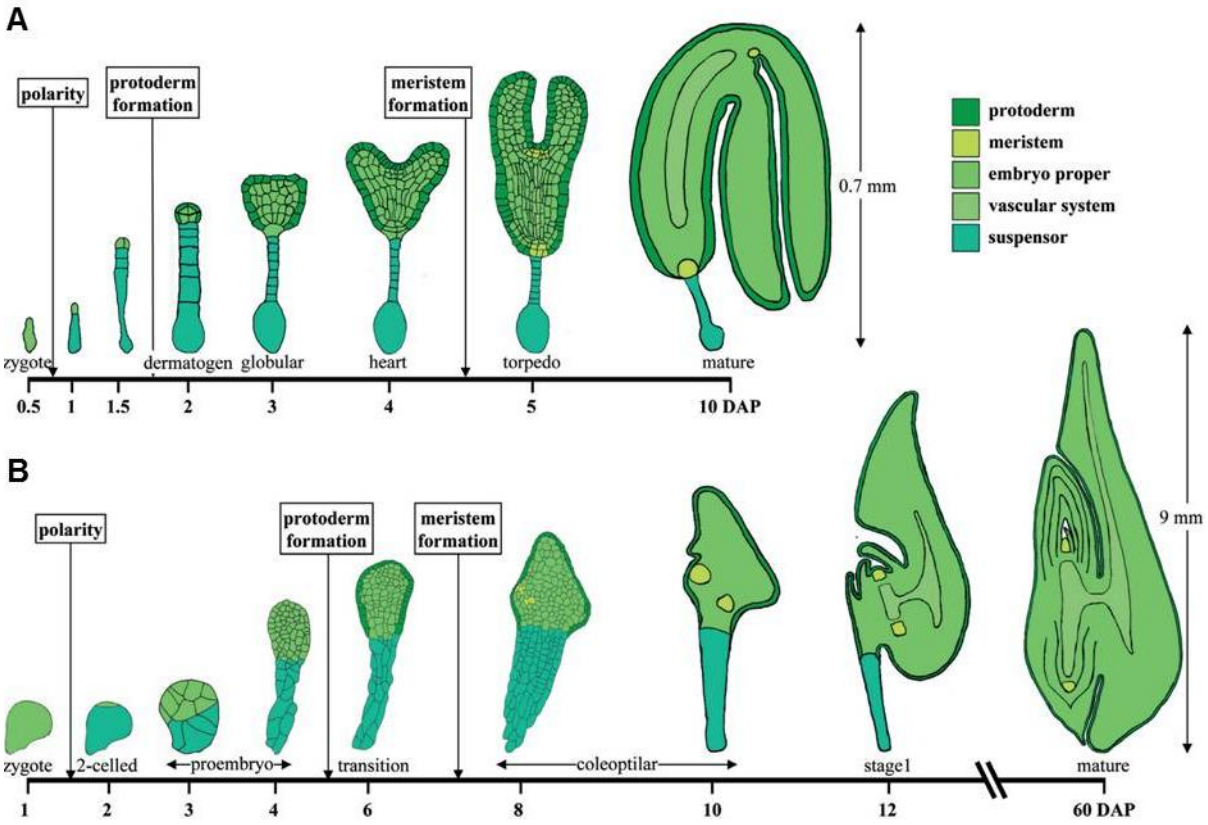

Figure 1.4 Morphological stages of embryogenesis of *Arabidopsis* and *Zea mays*. The different embryo stages are indicated. (**A**) In *Arabidopsis*, asymmetric cell divisions of the zygote give rise to the embryo proper and suspensor, followed by protoderm formation in the dermatogen stage. After the globular stage, meristems are formed during the heart stage and a vascular system starts to develop during the torpedo stage. (**B**) Like in *Arabidopsis*, the maize zygote divides asymmetrically to form embryo proper and suspensor, respectively. The transition stage is characterized by formation of the protoderm. At the coleoptilar stage, meristems start to develop and formation of the coleoptile is initiated. Up to six leaf primordia are initiated during the following stages 1-6 and a vascular system develops. The timeline marks approximate days after pollination (DAP). Images taken from Vernoud *et al.*, 2005.

During early stages of embryogenesis, maize and *Arbidopsis* share some general features like the establishment of apical-basal axis polarity to form a proembryo consisting of embryo proper and suspensor formed after asymmetric zygote division, protoderm formation, organization of the root and shoot meristem as well as accumulation of reserve substances (Vernoud *et al.,* 2005). Nevertheless, there are some differences in embryo development of both plant species besides the aforementioned earlier activity of the maize SAM, embryo size and cell number. Cell divisions in *Arabidopsis* are stronger synchronized leading to a more geometric and stereotypic histological appearance than the maize embryo, as depicted in Figure 1.4. Additionally, SAM and RAM are arranged along the apical-basal axis by contrast to the oblique arrangement in maize.

1. 3. 2 Peptide signaling during embryogenesis

Several communication events have to take place to orchestrate embryogenesis. Besides plant hormones (Chen *et al.,* 2014), secreted peptides were demonstrated to act as signaling components during embryo and endosperm development (for review see Ingram and Gutierrez-Marcos, 2015). In *Arabidopsis*, the cysteine-rich peptides of the EMBRYO SURROUNDING FACTOR 1 (ESF1) family are expressed in the central cell and endosperm cells of the embryo surrounding region and are involved in formation of the zygotic basal cell lineage (Costa *et al.,* 2014). Furthermore, they act in non-cell autonomous signaling by promoting suspensor elongation in the signaling pathway of the receptor-like cytoplasmic kinase SHORT SUSPENSOR (SSP) and YODA (YDA) mitogen-activated protein kinase (Bayer *et al.,* 2009). Another class of peptides controlling the embryo suspensor is the embryo-expressed KISS OF DEATH (KOD) peptide, which positively regulates controlled cell-death (Blanvillain *et al.,* 2011). In maize, MATERNAL EXPRESSED GENE 1 (MEG1) peptides are involved in development of transfer cells of the basal endosperm transfer layer, mediating nutrient translocation in seeds (Costa *et al.,* 2012). Another signaling peptide involved in seed development is CLE8 from the CLE (CLAVATA3/ENDOSPERM SURROUNDING REGION) protein family, which can be found in young embryos and endosperm. Together with the transcription factor WUSCHEL-like homeobox 8 (WOX8), it acts by regulating the basal embryo cell division patterning, endosperm proliferation and endosperm differentiation (Fiume and Fletcher, 2012).

Like in many plant signaling pathways, receptors for most of the signaling peptides are not yet identified. Nevertheless, some putative receptors potentially representing interaction partners of secreted peptides were already demonstrated to be involved in signaling processes

during seed development, like the leucine-rich repeat (LRR) receptor protein kinase HAIKU2 (IKU2). Mutations of *IKU2* result in reduced growth of the early endosperm (Luo *et al.*, 2005). The LRR receptor protein kinases GASSHO1 (GSO1) and GASSHO2 (GSO2), located within the developing embryo, ensure formation of a functional embryonic cuticle in *Arabidopsis* (Tsuwamoto *et al.*, 2008).

1. 4 Aims of this work

The aim of the following work was to examine peptide signaling during sexual reproduction of *Zea mays* by studying the EAL-like (EAL) gene family in more detail. The small peptide ZmEA1, secreted from the maize egg apparatus for short range growth guidance of the pollen towards the female gametophyte, was previously reported to be member of a small peptide family exclusively found in grasses (Dresselhaus *et al.*, 2011). A detailed phylogenetic classification of peptides related to ZmEA1 as well as investigations on yet uncharacterized family members should be performed and a manuscript was recently submitted for publication (Uebler *et al.*, under review). These data are now shown in CHAPTER 2. Another task was to study the ability of ZmEA1 to overcome species-specific hybridization barriers by transgenic expression in *Arabidopsis thaliana*. These data are published in Márton *et al.*, 2012, and my results of experiments contributing to this work are given in CHAPTER 3. Based on this work, the capability of ZmEA1 to directly bind the attracted pollen tubes should be tested and could be visualized in a species-specific manner as described in CHAPTER 4 and published in Uebler *et al.*, 2013. Binding of ZmEA1 as ligand on the pollen tube surface requires interaction with surface located pollen tube protein(s) for initiating change in growth direction. As identification of membranous ligand binding partners is a highly challenging field of research, an overview and discussion of current methods to isolate surface receptor proteins is given in CHAPTER 5 (Uebler and Dresselhaus, 2014). Various methods to identify ZmEA1 receptors and interaction partners by biochemical approaches should be tested and applied. This work is described in CHAPTER 6 and includes the expression and purification of recombinant ZmEA1 protein in a variety of systems as well as isolation of potential ZmEA1 binding candidates. Some candidates are further characterized regarding their classification, expression pattern, subcellular localization and protein level. Finally, a comprehensive conclusion is given in CHAPTER 7, which also provides an outlook for future research.

CHAPTER 2 - CLASSIFICATION OF EA1-BOX PROTEINS AND NEW INSIGHTS INTO THEIR ROLE DURING REPRODUCTION IN GRASSES

This CHAPTER is based on the manuscript Uebler *et al.*, under review in *Plant Reproduction*, excluding the paragraphs about generation and analysis of transgenic maize lines and promoter analysis. S. Uebler conducted bioinformatical analysis and performed all experimental procedures except RT-PCR of rice genes and generation of constructs for transient transformation of *ZmEA1*, *AtEAG1*, *OsEAL1* and *OsEAL3*. The manuscript was written by S. Uebler and edited by T. Dresselhaus.

2. 1 Introduction

Peptide signaling plays an elementary role during various vegetative and reproductive processes in plants, including development of vegetative organs, fertilization and embryogenesis (Murphy *et al.*, 2012; Costa *et al.*, 2014; Qu *et al.*, 2015; Ingram and Gutierrez-Marcos, 2015). During reproduction, the secretion and perception of peptides enables plants, for example, to distinguish self from non-self pollen, to support pollen tube growth and to mediate successful fertilization. The identification and characterization of signaling components is therefore of great importance to unveil the underlying communication mechanisms. Several thousand of potentially secreted peptides are predicted to exist in *Arabidopsis* (Lease and Walker, 2006), and many of them are indicated to play essential roles in reproductive processes (Huang *et al.*, 2015). However, until now only a few of them could be successfully associated with signaling processes. Many signaling peptides can be grouped into protein families with shared conserved features. Based on single or several well-characterized founding peptides, sequence homology searches offer a possibility to identify more members of these families (Olsen *et al.*, 2002; Lease and Walker, 2010). Classifications of yet unknown peptides into protein families might give further hints about their role in cellular processes.

One of the largest protein families of secreted peptides is formed by CLE (CLAVATA3/ENDOSPERM SURROUNDING REGION) proteins (Miyawaki *et al.*, 2013). Members of this protein family are supposed to function as processed 12- or 13- amino acid peptides derived of larger precursor proteins containing the conserved CLE-motive (Ito *et al.*, 2006; Kondo *et al.*, 2006; Ohyama *et al.*, 2009). They are differentially expressed during plant development and are involved in regulation of the meristem activity in shoots (Fletcher *et al.*,

1999) and roots (Stahl *et al.,* 2009) as well as in development of vascular tissues (Hirakawa *et al.,* 2008). Originally, this protein family was assumed to consist of 65 members in both monocotyledonous and dicotyledonous plants (Cock and McCormick, 2001; Oelkers *et al.,* 2008). Based on similarity to the CLE domain, 114 new members were identified in a variety of plants and could be classified into 13 groups, thus nearly tripling the number of previously known CLE proteins (Oelkers *et al.,* 2008). A similar case can be depicted regarding the CEP (C-TERMINALLY ENCODED PEPTIDE) proteins, which are supposed to act as negative regulators that mediate environmental influences on root and shoot development in seed plants (Delay *et al.,* 2013) and which were originally identified by an *in silico* approach (Ohyama *et al.,* 2008). Additional bioinformatic analyses based on the highly conserved domain in the predicted mature peptides of the CEP family tripled the number of classified CEP peptides in *Arabidopsis* (Delay *et al.,* 2013; Roberts *et al.,* 2013).

A protein family with members that were demonstrated to act as signaling peptides in reproduction was named as EAL (EA1-like) protein family (Dresselhaus *et al.,* 2011). The first identified and name-giving member was ZmEA1 (*Zea mays* Egg Apparatus 1) of *Zea mays*, which represents until now the only identified secreted attractant for pollen tube guidance in grasses. ZmEA1 is produced in the egg apparatus of maize and is secreted towards the micropylar region of the ovule. There it acts in short-range attraction of maize pollen tubes towards the female gametophyte (Márton *et al.,* 2005; Márton et al. 2012) and binds in a very specific manner at the surface of growing maize pollen tube tips (Márton *et al.,* 2012; Uebler *et al.,* 2013). Another EAL protein with demonstrated activity in signaling is ZmEAL1 (*Zea mays* EA1-like 1) of *Zea mays*. Fused to GFP, ZmEAL1 was shown to accumulate in granules at the chalazal pole of the egg cell and is likely secreted towards the chalazal pole of the female gametophyte. RNAi-studies showed that ZmEAL1 is required to suppress gametic cell fate of antipodal cells (Krohn *et al.,* 2012).

As EA1-box containing proteins are widely distributed throughout the plant kingdom, EA1 orthologs were wrongly predicted and EALs from other species misclassified. We therefore introduce here a new classification of EA1-box proteins. We further demonstrate that all analyzed EAL peptides and larger EAC proteins enter the secretory pathway, whereas EAGs localize to the cytoplasm and nucleus. ZmEAL2, the third EAL peptide in *Zea mays* was studied in more detail. Although knock-down plants did not show a significant phenotype, our studies indicate that the peptide is involved in late embryogenic development where it is se-

creted to the extracellular space. Additionally, we introduce EALs of rice representing potential functional orthologues to ZmEA1.

2. 2 Experimental procedures

2. 2. 1 Bioinformatic analysis

Protein sequences of EAL, EAC and EAG proteins were identified by BLASTP searches using the EA1-box of ZmEA1 against the genomes of *Zea mays*, *Sorghum bicolor*, *Oryza sativa ssp. japonica*, *Brachypodium distachyon*, *Arabidopsis thaliana*, *Arabidopsis lyrata*, *Glycine max* and *Populus trichocarpa*, available at www.gramene.de (Monaco *et al.,* 2014) and against protein sequences of the aforementioned plant species available at http://www.ncbi.nlm.nih.gov/. EA1-boxes of identified proteins were used for further BLASTP searches against the above plant species. A list of all identified genes including chromosomal location is attached (Supplement table 1). Protein sequence alignments and phylogenetic tree were created using ClustalX 2.1 (Larkin *et al.,* 2007). The phylogenetic tree was visualized by FigTree v1.4.2 (http://tree.bio.ed.ac.uk/software/figtree/) and protein alignments manually edited with GeneDoc V2.7.000 (Nicholas *et al.,* 1997). Prediction of classical N-terminal signal peptides was performed using SignalP 4.1 (Petersen *et al.,* 2011; http://www.cbs.dtu.dk/services/SignalP/). Proteins entering the non-classical secretory pathway were predicted by SecretomeP 2.0 (Bendtsen *et al.,* 2004, http://www.cbs.dtu.dk/services/SecretomeP/).

2. 2. 2 Generation of constructs for transformation of BMS cells

To generate constructs for transient transformation of BMS cells, the open reading frames (ORFs) of *ZmEA1*, *sEA1*, *AtEAG1*, *OsEAL1* and *OsEAL3* were amplified using the primer pairs EAF-GFP/EAR-GFP (*ZmEA1*), oSU26/oSU27 (*sEA1*), 3f/3r (*AtEAG1*), 2f/2r (*OsEAL1*) and 1f/1r (*OsEAL3*) and digested with *Spe*I/*Bam*HI for ligation into the vector pLNU-GFP (DNA Cloning Service, Hamburg, Germany). The ORFs of *ZmEAL2*, *ZmEAC1* and *ZmEAC2* were amplified using the primer pairs oSU17/oSU19 (*ZmEAL2*), oSU38/oSU39 (*ZmEAC1*) and oSU40/oSU41 (*ZmEAC2*) for directional TOPO® cloning into the pENTR™/D-TOPO® vector (Thermo Fisher Scientific Inc., Waltham, USA) followed by transfer of the ORFs into the destination vector pB7FWG2,0 (Karimi *et al.,* 2002) using Gateway® LR clonase® II enzyme mix (Thermo Fisher Scientific Inc., Waltham, USA). The plasmid PMON30049

(Pang *et al.*, 1996) was used as control for cytoplasmic GFP. To analyze *ZmEAL2* promoter activity in BMS suspension cells, a fragment containing the putative *ZmEAL2* promoter and ORF of *GFP* was cut out from the plasmid p7U-EAL2P-GFP described in 2. 2. 8. 1 using *Sfi*I restriction sites. The fragment was cloned into the pLNU-GFP plasmid (DNA Cloning Service, Hamburg, Germany), after removing its *GFP* cassette with *Sfi*I restriction sites, to generate the plasmid pLG-EAL2P-GFP.

2. 2. 3 Transient transformation of maize BMS suspension cells

Black Mexican Sweet (BMS) maize suspension cells (Sheridan, 1982) were cultivated in liquid MS media (30 g/l sucrose, 4.4 g/l MS-salts [Duchefa Biochemie B.V, Haarlem, Netherlands], 2 mg/l 2,4-Dichlorophenoxyacetic acid, pH 5.8, based on Murashige and Skoog, 1962). For transient transformation via microprojectile bombardement after Klein *et al.*, 1987 and Klein *et al.*, 1988, 2-4 ml of growing culture were harvested and transferred as a thin layer onto solid MS media (liquid MS media solidified with 0.3% Gelrite). Plates were incubated for 2 hours at 26°C. Gold particles (0.6 µM diameter) were washed and dissolved in ethanol (p.a.). 10 µg plasmid DNA (concentration 0.5-1 µg/µl) was precipitated on gold particles by adding 50 µl $CaCl_2$ (2.5 M) and 20 µl spermidine (0.1 M) followed by incubation on ice. Gold particles were washed with absolute ethanol and finally resuspended in 150 µl ethanol (p.a.). 7.5 µl of the suspension was transferred on a macrocarrier for bombardment using the particle delivery system PDS1000/He (BioRad Laboratories, Inc., Hercules, USA) at a vacuum of 28 inch Hg, 1,100 psi rupture discs and a distance of 6 cm. All constructs were co-transformed with a marker for the endoplasmic reticulum (ER) (Nelson *et al.*, 2007), composed of the signal peptide of AtWAK2 at the N-terminus of mCherry and an ER-retention signal at its C-terminus (Gomord *et al.*, 1997). The plate was incubated overnight at 26°C in the dark. Afterwards, cells were transferred into liquid MS media and shaken at 26°C for at least 4 h in the dark. Microscopic analysis was performed using an Axiovert 200M inverted microscope (Carl Zeiss AG, Oberkochen, Germany), equipped with the confocal laser scanning unit LSM 510 META with GFP-excitation at 488 nm and detection using the BP 505-550 filter. Images were processed using the software ImageJ 1.43q (http://imagej.nih.gov/ij/).

2. 2. 4 Extraction of total RNA and generation of cDNA

Total RNA of various plant tissues was extracted as described by Logemann *et al.*, 1987. To generate cDNA, 1 µg total RNA was digested with DNase I (Thermo Fisher Scientific Inc., Waltham, USA) to remove DNA contaminations. cDNA was synthesized by using Super-

Script® III Reverse Transcriptase (Thermo Fisher Scientific Inc., Waltham, USA) and Oligo(dT)$_{18}$ primers (Thermo Fisher Scientific Inc., Waltham, USA) according to the manufacturer's protocol.

2. 2. 5 Semi-quantitative reverse transcriptase-PCR (RT-PCR) and quantitative real–time PCR (qRT-PCR)

For semi-quantitative RT-PCR, rice and maize tissues were isolated and grounded in liquid nitrogen. Approximately 150 mg of the sample powder was used for RNA extraction and cDNA generation. RT-PCR was performed using the primer pairs OsP0493C06-fwd/OsP0493C06-rev (*OsEAL1*), OsEAL2a-fwd/OsEAL2b-rev (*OsEAL2*), OsEAL3-a(fwd-new)/OsEAL3-b(rev-new) (*OsEAL3*), oSU99/oSU100 (*ZmEAL2*), and GAPnew1/GAPnew2 (*ZmGAPDH*, Krohn *et al.*, 2012). Standard PCR reactions were performed applying 1 µl of the cDNA as template and primer concentrations of 0.25 µM for each primer.

For qRT-PCR experiments, 20 to 30 maize embryos were dissected from pollinated maize cobs immediately after removing the cob from the plant. Embryo samples were collected and grounded in liquid nitrogen. Approximately 150 mg of the powder was used for RNA extraction and cDNA generation. The cDNA was diluted 1:10 and directly used as template for qRT-PCR reactions with KAPA SYBR FAST Master Mix Kit (VWR International GmbH, Erlangen, Germany). For each sample, three technical replicate reactions were performed. Primer pair oSU99/oSU100 was used to quantify the *ZmEAL2* transcript level. For analysis of the reference genes, the primer pairs LUGfwd/LUGrev (*LUG*) and CULfwd/CULrev (*CUL*) (both derived from Manoli *et al.*, 2012) were used. Final concentration of all primers was 200 nM. All reactions using the Realplex 2 cycler (Eppendorf, Hamburg, Germany) were performed with 20 s at 54°C for elongation and 10 s at 72°C for synthesis. Data were statistically processed by calculating the $2^{\Delta Ct}$ value with normalization against *LUG* or *CUL*, respectively.

2. 2. 6 Immunoblot analysis and generation of anti-ZmEAL2 antiserum

Proteins smaller than 15 kDa were separated by SDS-PAGE using Tris/Tricine buffer system (Schägger and Jagow, 1987). The Tris/Glycine buffer system (Laemmli, 1970) was used for proteins with a higher molecular weight. Following SDS-PAGE, proteins were transferred for 35 minutes at 300 mAmp onto a nitrocellulose membrane using a tank blotting system. The membrane was blocked in blocking solution (5% milk powder, 50 mM Tris-HCl pH 7.5, 150 mM NaCl, 0.1% Tween-20). The 11 amino acid peptide NH_2-CFLAKKELYFK-$CONH_2$ specific to ZmEAL2 (partially covering the EA1-box with an additional cysteine at the N-

terminus for coupling with a protein carrier) was commercially synthesized (Centic Biotec, Heidelberg, Germany) and used for immunization of rabbits (Pineda Antibody-Service, Berlin, Germany). Unpurified polyclonal anti-ZmEAL2-antiserum was diluted 1:1000 in blocking solution for overnight incubation of the membrane at 4°C. Afterwards, the membrane was washed in washing buffer (50 mM Tris-HCl pH 7.5, 150 mM NaCl, 0.1% Tween-20) and subsequently incubated with anti-rabbit IgG antibody from goat conjugated with horse reddish peroxidase (Sigma-Aldrich, St. Louis, USA) diluted 1:5000 in blocking buffer for 2 hours at room temperature. Commercially available H3-directed antibody was used as loading control. After washing, the membrane was incubated in luminol-based substrate (PJK GmbH, Kleinblittersdorf, Germany). Chemiluminescence was detected using Super RX X-ray films (Fujifilm, Minato, Japan). Estimation of the apparent molecular weight of detected proteins was carried out by comparison to commercially available molecular weight standards.

2. 2. 7 Immunohistochemical detection of ZmEAL2

Immunohistochemical experiments were performed based on a protocol by Stadler and Sauer, 1996, with adaption of incubation times. Embryos 18 DAP and 25 DAP were isolated and manually cut into 2-4 cross sections. Fixation was performed for 6-8 h. After fixation, the samples were washed and placed in 70% ethanol (v/v) containing 1 mM DTT for 2 days. Samples were dehydrated for 1 day in increasing ethanol concentrations. For infiltration with methacrylate, samples were incubated for at least 1 day per step. Sections of 5-10 µm were prepared with a Reichert Om U2 microtome (Leica, Wetzlar, Germany). Unpurified polyclonal ZmEAL2-directed antibody from rabbit was diluted 1:50 for overnight incubation of sections, followed by incubation for at least 2 h with anti-rabbit IgG antibody conjugated with Cy2 from goat (Dianova GmbH, Hamburg, Germany) diluted 1:80. Samples were analyzed microscopically at the Axioskop FL epifluorescence microscope (Carl Zeiss AG, Jena, Germany) using Zeiss filter set no. 46 and at the Eclipse TE2000-S inverted microscope (Nikon Corporation, Tokyo, Japan) using a HC Alexa 488/eGFP filter. Images were processed using the software ImageJ 1.43q (http://imagej.nih.gov/ij/).

2. 2. 8 Generation of stable transgenic maize lines

2. 2. 8. 1 Constructs for Agrobacterium-mediated transformation of maize

For analysis of *ZmEAL2* promoter activity in maize, the putative promoter fragment described in 2. 3. 4 was amplified using primer pairs oSU44/oSU46 and cloned into p7U-GFP (DNA

Cloning Service, Hamburg, Germany) using *Spe*I and *Hind*III restriction sites. To generate the construct for *ZmEAL2* expression under control of its endogenous promoter, the putative promoter fragment and the ORF of *ZmEAL2* was amplified with the primer pair oSU44/oSU47 and ligated into p7U-GFP using *Spe*I and *Hind*III restriction sites. Additionally, two RNAi constructs were generated. For the first RNAi construct, a 219 bp fragment including the 5'-UTR and the N-terminus of the ORF of *ZmEAL2* was amplified with the primer pair oSU48/oSU49 and cloned in antisense direction into the pUBI-IF2 vector (DNA Cloning Service, Hamburg, Germany) using *Eco*RI and *Sbf*I restriction sites. The same fragment was amplified with the primer pair oSU54/oSU55 and cloned in sense-direction into the pUBI-IF2 vector with the antisense fragment by using *Hind*III and *Mlu*I restriction sites. A fragment containing the *UBI* promoter and the RNAi cassette was cut out of the vector using *Sfi*I restriction sites and transferred into the vector p7U (DNA Cloning Service, Hamburg, Germany) to generate the plasmid p7U-RNAi1(EAL2). For the second RNAi construct, a 208 bp fragment including the 3'-UTR and the C-terminus of the *ZmEAL2* ORF was amplified with the primer pair oSU50/oSU51 and cloned in antisense direction into the pUBI-IF2 vector using *Eco*RI and *Sbf*I restriction sites. The same fragment was amplified with the primer pair oSU56/oSU57 and cloned in sense-direction into the pUBI-IF2 vector with the antisense fragment by using *Hind*III and *Mlu*I restriction sites. A fragment containing the *UBI* promoter and the RNAi cassette was cut out of the vector using *Sfi*I restriction sites and transferred into the vector p7U to generate the plasmid p7U-RNAi2(EAL2).

2. 2. 8. 2 Agrobacterium-mediated transformation of maize

Stable transgenic maize lines were generated based on the protocol of Frame *et al.,* 2002. Media were prepared as described for HiII transformation in Frame *et al.,* 2011. HiIIA and HiIIB plants were cross-pollinated and harvested 11-13 DAP for transformation. *Agrobacterium tumefaciens* strain LBA4404 (background TiAch5, Ti plasmid: pAL4404; Hoekema *et al.,* 1983) was transformed with binary plasmids like described in 6. 2. 2. 30 ml overnight culture supplemented with antibiotics was grown at 28°C until OD_{600} = 0.4, washed with 15 ml 10 mM $MgSO_4$ and resuspended to OD_{600} = 0.5 in infection medium (1x infection medium with 100 µM acetosyringone; 2 x infection medium contains per liter: 200 ml 10x N6 macro salts [contains per 1 l: 4.63 g $(NH_4)_2SO_4$, 28.3 g KNO_3, 4 g KH_2PO_4, 1.85 g $MgSO_4$ * 7 H_2O, 1.66 g $CaCl_2$ * 2 H_2O], 2 ml 1000x N6 micro salts [contains per 100 ml: 387 mg $MnSO_4$ * H_2O, 150 mg $ZnSO_4$ * 7 H_2O, 160 mg H_3BO_3, 80 mg KI], 2 ml 1000x N6 vitamins [contains per 100 ml: 200 mg glycine, 100 mg thiamine-HCl, 50 mg pyridoxine-HCl, 50 mg niacin], 4 ml

NaFe-EDTA (50 mM), 1.4 g L-proline, 136.8 g sucrose, 72 g glucose, pH 5.2). Harvesting steps were performed at room temperature. Immature embryos at size of approximately 1.5 mm were dissected under sterile conditions and washed twice with infection medium. Embryos were transferred into *Agrobacterium* suspension containing 15 µl/ml Silwet® L-77 and incubated for 5 min at RT. The embryos were distributed on co-cultivation medium plates (1 x co-cultivation medium [2 x co-cultivation medium contains per 1 l: 200 ml 10x N6 macro salts, 2 ml 1,000x N6 micro salts, 2 ml 1000x N6 vitamins, 4 ml NaFe-EDTA (50 mM), 1.4 g L-proline, 60 g sucrose, pH 5.8], 5 µM $AgNO_3$, 100 µM acetosyringone, 300 mg/l L-cysteine, 1.5 mg/l 2,4-D, 0,3% Gelrite®), excess *Agrobacterium* suspension was removed and the plates were incubated overnight at 21°C in the dark. The day after, embryos were placed onto new co-cultivation plates with reverse orientation and incubated overnight at 21°C in the dark. Subsequently, the embryos were transferred onto resting medium plates (1 x resting medium [2 x resting medium was composed like co-cultivation medium supplemented with 1 g 2-(4-morpholino)-ethanesulfonic acid (MES)], 5 µM AgNO3, 100 mg/l cefotaxime, 100 mg/l vancomycin, 1.5 mg/l 2,4-D, 0.3% Gelrite®) with scutellum side upturned for incubation at 28°C in the dark. After 7 days, the embryos were placed onto selection medium I plates (1 x resting medium, 5 µM $AgNO_3$, 100 mg/l cefotaxime, 100 mg/l vancomycin, 1.5 mg/L glufosinate, 0.3% Gelrite®) and incubated for 14 days at 28°C in the dark, followed by two times incubation for 14 days at the same conditions on selection media II plates (like selection medium I with doubled concentration of glufosinate) to induce embryogenic type II callus formation. Emerging coleoptiles were removed routinely by dissection. For regeneration of the plants, the embryos with callus were placed onto regeneration I medium plates (1 x regeneration medium I, 100 mg/l cefotaxime, 3 mg/ml glufosinate, 0.3% Gelrite®; 2 x regeneration medium I contains per 1 l: 200 ml 10x MS macro salts (contains per 1 l: 16.5 g NH_4NO_3, 19 g KNO_3, 1.7 g KH_2PO_4, 3.7 g $MgSO_4$ * 7 H_2O, 4.4 g $CaCl_2$ * 2 H_2O), 2 ml 1000x MS micro salts (contains per 100 ml: 1.69 g $MnSO_4$ * H_2O, 860 mg $ZnSO_4$ * 7 H_2O, 620 mg H_3BO_3, 83 mg KI, 25 mg Na_2MoO_4 * 2 H_2O, 2.5 mg $CoCl_2$ * 6 H_2O, 2.5 mg $CuSO_4$ * 5 H_2O), 2 ml 1000x MS vitamins (contains per 100 ml: 200 mg glycine, 10 mg thiamine-HCl, 50 mg pyridoxine-HCl, 50 mg niacin), 4 ml NaFe-EDTA (50 mM), 4 ml myo-inositol (50 mg/ml), 120 g sucrose, pH 5.8) for 21 days at 28°C in the dark. Afterwards, they were transferred onto regeneration II medium plates (like regeneration I medium, but without cefotaxime and with half of sugar concentration) for incubation at 28°C in a light chamber with a photoperiod of 16 hours per day. For analysis of regenerated maize plants, genomic DNA was extracted like described in Pallotta *et al.*, 2000 and tested for insertion of the construct by standard PCR (6.

2. 3. 1). Positive plants were grown at greenhouse conditions (6. 2. 1. 1) and either self-pollinated or used for cross-pollination with wild type plants. Seeds were harvested at maturity and analysis of the transgenic maize lines was performed with plants derived from this seed material.

2. 3 Results and discussion

2. 3. 1 EA1-box containing proteins can be separated into three classes

First experimental examinations of the EA1-like protein family were performed about one decade ago, showing that genes homologous to *ZmEA1* exist also in other cereals (Márton *et al.,* 2005). The genes encoding secreted peptides were therefore named as *EA1-like* (*EALs*). Later, all proteins containing the conserved EA1-domain were classified as EALs (Gray-Mitsumune and Matton, 2006), disregarding the fact that many of these proteins are likely not secreted and contain a different overall structure. With respect to the increasing quality of genome-wide sequencing efforts and the appearance of new EA1-box proteins in maize (Chettoor *et al.,* 2014), we now suggest to reclassify EA1-box containing proteins. These proteins were identified by using the sequence of the EA1-box of ZmEA1 (Dresselhaus *et al.,* 2011) as query for BLASTP searches against the genomes of the monocotyledonous species *Zea mays*, *Sorghum bicolor*, *Oryza sativa japonica* and *Brachypodium distachyon* as well as the dicotyledonous plants *Arabidopsis thaliana*, *Arabidopsis lyrata*, *Glycine max* and *Populus trichocarpa*. BLASTP searches were performed on two platforms, the Gramene Database (http://www.gramene.org/) and the National Center for Biotechnology Information (http://www.ncbi.nlm.nih.gov/). Proteins containing the EA1-box were found in all of the analyzed monocotyledonous and dicotyledonous plants. By further classification, these proteins were clustered into three families: EAL, EAG (EA1-box glycine-rich) and EAC (EA1-box containing) (Figure 2.1 A-C). Protein sequences of the three classes were aligned to visualize conserved motives and protein domains.

Class 1 consists of EAL peptide precursors with a length of approximately 100 amino acids (Figure 2.1 A). All EAL proteins exhibit either a “classical” N-terminal signal peptide or an N-terminally located internal signal peptide domain preceding the conserved EA1-domain. The C-terminal region contains an alanine-rich domain (A-box). The predicted N-terminal cleavage sites are located shortly downstream of a conserved motive that was named as P-box, based on a highly conserved proline at its last position. Cleavage of an EAL peptide pre-

cursor behind the P-box creates a peptide of about 50 amino acids starting with a variable sequence of 3-7 amino acids followed by the highly conserved EA1-box and the A-box. GFP-fusion protein experiments previously indicated that EAL peptides are not cleaved at their C-termini (Márton *et al.,* 2005; Krohn *et al.,* 2012; Márton *et al.,* 2012). The only identified EAL protein with a different structure is BdEAL5 with a predicted length of 197 amino acids. The first half of BdEAL5 exhibits high similarity with other EALs, while the second half after the A-box encodes for a different protein. As this region is also annotated as a second exon in the Gramene database, it might have been wrongly annotated or may represent a recent gene fusion event.

The second class of EA1-box proteins was named as EAG proteins and was found to be present in all analyzed species except *Populus trichocarpa* (Figure 2.1 B). All EAGs are short proteins with amino acid sequences ranging between 70 and 120 AS. Besides the highly conserved EA1-box at their C-termini, they possess a glycine content varying from 35.6% to 59.5%, spanning the whole protein outside the EA1-box on both sides. The C-termini of EAGs are very short with a length of maximum 8 amino acids behind the EA1-box and usually end with a lysine. EAGs lack both A- and P-boxes as well as a classical signal peptide domain for targeting to the secretory pathway. Proteins with a high content of glycine have been identified from several eukaryotic species. In insects, for example, they are known to act as antimicrobial peptides. As they are usually directed against fungi, gram-negative bacteria and cancer cells, they play an important role in immunity (Herbinière *et al.,* 2005; Dang *et al.,* 2009). Like insects, plants generate glycine-rich proteins involved in defense mechanisms against bacteria and fungi, but also in a wide variety of other independent physiological processes (Park *et al.,* 2000; Bocca *et al.,* 2005). Glycine-rich proteins (GRPs) can be grouped into different classes based on the nature of the glycine-repeats in combination with additional motives, their expression pattern, their modulation by external factors and their subcellular localization (for review see Mangeon *et al.,* 2010). GRPs of several plants including *Arabidopsis thaliana* act as secreted signaling peptides involved, for example, in pollen hydration or as extracellular ligands in signal transduction processes (Mayfield and Preuss, 2000; Park *et al.,* 2001) or act as cell wall constituents with different functions (Ryser *et al.,* 2004; Ueki and Citovsky, 2005). However, considering that secreted and extracellular proteins usually contain an N-terminal signal peptide, which is lacking in all EAGs, it is unlikely that they are involved in extracellular signaling processes. Cytoplasmic GRPs were demonstrated to act, for example, as RNA-binding proteins involved in flowering time control and stress responses (Kim *et al.,* 2007; Streitner *et al.,* 2008). For some of the GRPs, additional domains, like

RNA-binding domains or cysteine-rich regions, seem to be necessary for their functionality, whereas other proteins contain only glycine-rich domains after processing (Mangeon *et al.*, 2009). It was also speculated that the glycine-repeats are mainly contributing to the structural properties of GRPs (Sachetto-Martins *et al.*, 2000), potentially mediating interactions in multi-protein complexes (Mangeon *et al.*, 2010). Regarding the wide variety of potential GRP functions and the fact that EAGs lack additional conserved domains besides the EA1-box, their function(s) cannot be predicted.

The third class of proteins containing the EA1-box is formed by EAC proteins identified in all analyzed plant species. This class contains all proteins that could not be grouped into the other two classes. As shown in Figure 2.1 C, they range in length between 60 and more than 400 amino acids. In contrast to the EAL and EAG class, there are no conserved features except the EA1-box. Many of the EAC proteins contain an N-terminal signal peptide or one to several transmembrane domains, indicating that they might be secreted or located at membranes. To our knowledge, none of the EAC proteins has been functionally characterized to date.

Figure 2.1 Protein alignment of EA1-box proteins. Amino acid sequences of EA1-box proteins of *Zea mays*, *Sorghum bicolor*, *Oryza sativa Japonica*, *Brachypodium distachyon*, *Arabidopsis thaliana*, *Arabidopsis lyrata*, *Glycine max* and *Populus trichocarpa* were identified by BLAST search and aligned. Based on sequence and structure similarities, they were clustered into the three different families of EAL, EAG and EAC proteins. (**A**) EAL (ZmEA1-like) proteins contain either an N-terminal signal peptide or transmembrane domain, a P-box motive consisting of five amino acids with a conserved proline at the end, the highly conserved EA1-box and a C-terminal alanine-rich motive, the A-box. Predicted cleavage of the signal domain behind the P-box results in small peptides containing the EA1-box and the A-box. All EAL proteins were exclusively detected in grasses. (**B**) EAG (EA1-box glycine-rich) proteins were detected in all analyzed species except *Populus trichocarpa* and are highly glycine-rich up- and downstream of the EA1-box. EAG proteins never contained a signal peptide or transmembrane domain. (**C**) EAC (EA1-box containing) proteins are the most divergent family of EA1-box proteins with the EA1-box representing the only conserved motive and a high variety in length. Several members of the EAC proteins contain a signal peptide or one or more transmembrane domains. All analyzed plant species contained EAC proteins. Protein alignment was performed by the program ClustalX2 (Larkin *et al.*, 2007) and manually edited using GeneDoc 2.7.000 (Nicholas *et al.*, 1997). Signal peptides are shaded in yellow, transmembrane domains in orange, the EA1-box in red, the A-box in blue and glycine-rich regions in green. The P-box is indicated by a light green box.

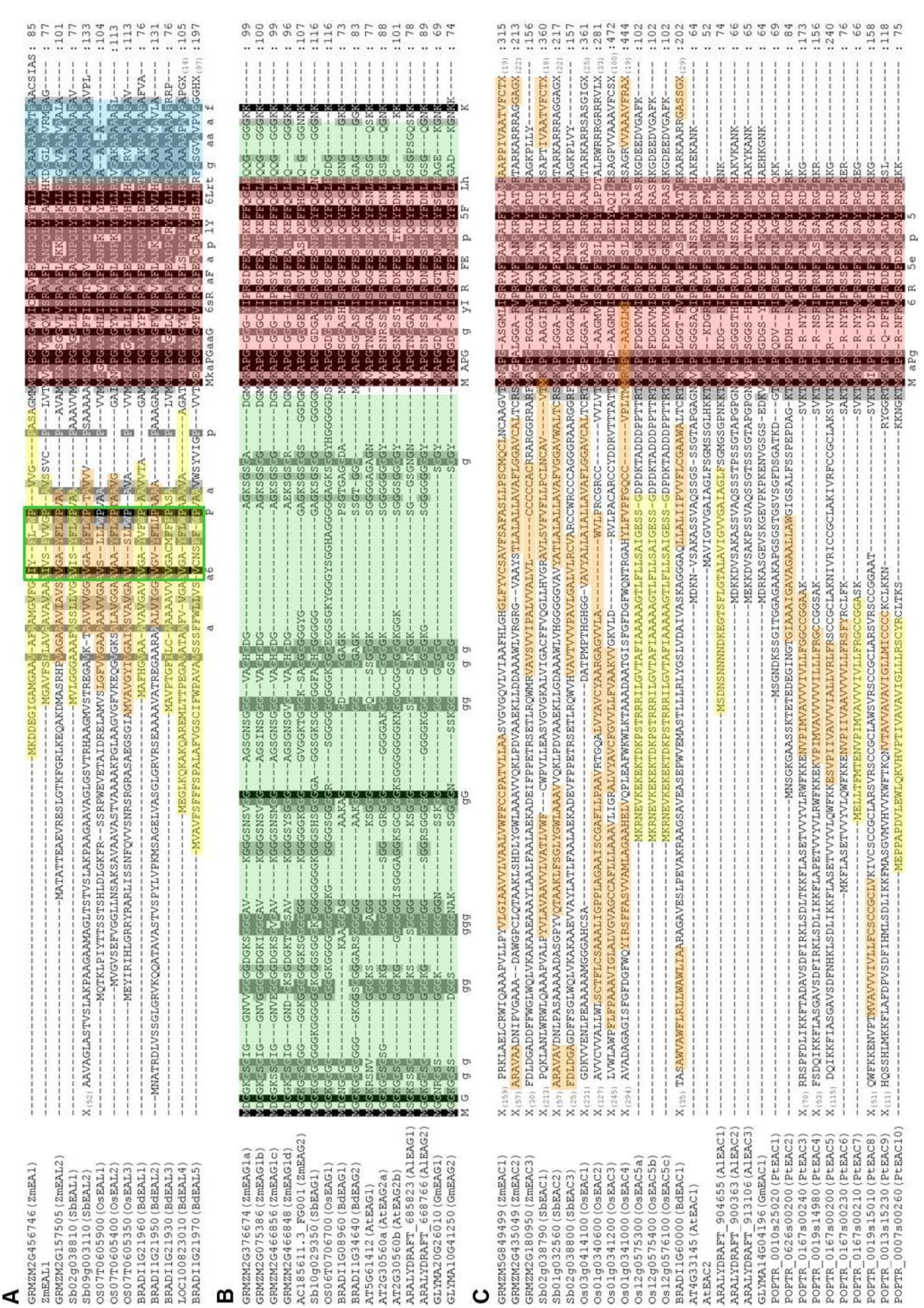

Not all of the listed EA1-box proteins are yet annotated. *ZmEAL1*, for example, was originally identified as a strongly transcribed gene in a cDNA library of maize egg cells (Dresselhaus *et al.*, 1994) and *AtEAL2* was shown to be expressed by RT-PCR (Gray-Mitsumune and Matton, 2006), although official genome annotations do not exist for both genes. Due to their small size, peptide genes are often overlooked in genome annotations by gene-finding computer programs (Lease and Walker, 2006). We therefore cannot rule out that additional EA1-box proteins exist and expect that their number will increase in the future with improved methods for large-scale gene annotations. We now discovered a short sequence closely related to *ZmEAL1* that localizes in close proximity to *ZmEAL1* and was named as the short version of *ZmEAL1* (*ZmEAL1s*: *ZmEAL1 short version*). Both predicted peptides share high sequence similarity until the first half of the EA1-box whereas the following parts strongly differ from each other and ZmEAL1s also lacks the A-box (Figure 2.2). Thus, due to the lack of a complete EA1-box, one cannot classify ZmEAL1s as EA1-box protein in the strict sense. The gene might have resulted from a partial duplication of *ZmEAL1* and it is not known whether it is indeed expressed and functional.

Figure 2.2 Partial protein sequence similarity between ZmEAL1 and ZmEAL1s. Both genes are located closely to each other on chromosome 7. There is a high sequence similarity between both encoded protein sequences until the first half of the EA1-box. ZmEAL1s is lacking the second half of the EA1-box as well as the A-box. Signal peptides are shaded in yellow, the EA1-box in red, the A-box in blue and glycine-rich regions in green. The P-box is indicated by a light green box.

Next, the three classes of EA1-box containing proteins were mapped in an unrooted phylogenetic tree (Figure 2.3 A). Due to the high sequence and structure similarity of EAL as well as EAG peptides, both classes cluster into distinct branches that can be easily distinguished from EAC proteins. Whereas the EAG branch can be divided into sub-branches based on the species, the EAL branch does not exhibit any species-related sub-clustering. EAL proteins of different analyzed grass species seem to be more closely related to each other than within one species, suggesting functional similarity. *Zea mays*, *Sorghum bicolor*, *Brachypodium distachyon* and *Oryza sativa* share a common ancestor which diverged about 50 million years ago (Schnable *et al.*, 2012). *EAL* genes thus might have evolved from the same progenitor gene

and obtained *Gramineae*-specific functions. Notably all *EAL* genes of a single species, except of *Sorghum bicolor*, are located on the same chromosome with varying orientations in close proximity to each other (Figure 2.3 B). The distance between the individual *EAL* genes varies up to several thousand base pairs. Although some genes coding for EAG and EAC proteins, like ZmEAG1a-d and OsEAC5a-c, could also be located closely together on the same chromosomes, this is not a general phenomenon, indicating that EALs likely represent a phylogenetic younger protein group. However, EAC proteins of *Zea mays* and *Sorghum bicolor* were highly similar, as for each of the three maize EACs a corresponding homologous EAC encoding gene could be detected in *Sorghum*. While *ZmEAC1* and *ZmEAC3* are both located on chromosome 2, the corresponding *SbEAC1* and *SbEAC3* genes are also both located on the same chromosome.

2. 3. 2 EA1-box proteins show a highly variable expression pattern

The genes coding for EA1-box proteins show a highly diverse expression pattern. Based on data derived from the Genevestigator V3 database (Hruz *et al.*, 2008), transcripts of *EAL*, *EAG* and *EAC* genes from different plants can be detected in many generative as well as vegetative tissues. *EAL* genes of rice were therefore chosen as a representative group to study the expression pattern of genes located closely together on one chromosome with the ultimate goal to investigate whether orthologous genes of *EA1* and *EAL1* of maize can be predicted based on expression pattern and phylogenetic relationship. We analyzed 13 rice tissues including isolated egg cells. As shown in Figure 2.3 C, *OsEAL1* is exclusively expressed in the mature egg cell, while *OsEAL2* transcript was detected in all analyzed tissues including egg cells, except mature embryos. Expression of *OsEAL3* was not detected in the tissues tested although significant expression levels have been reported previously in leaves and shoot (http://www.ebi.ac.uk/gxa/genes/OS07G0605350). Based on the expression pattern shown, we suggest that OsEAL1 represents the ortholog of EA1 of maize, while other rice EALs possess functions similar to ZmEAL1 and/or ZmEAL2 (see below). Thus, although the structures of predicted mature EALs appears very similar, they show very diverse expression pattern, highly specific binding pattern (Uebler et al. 2013) and therefore functional studies are necessary to ultimately demonstrate similar functions in diverse species.


A
Os12g0575300/5400/6300 (OsEAC5a/b/c)
Os03g0414100 (OsEAC1)
Sb01g032560 (SbEAC2)
GRMZM2G435049 (ZmEAC2)
BRADI1G60000 (BdEAC1)
GRMZM2G180950 (ZmEAC3)
Sb04g038800 (SbEAC3)
POPTR_0010s25020 (PtEAC1)
ARALYDRAFT_904655 (AtEAC1)
POPTR_0626s00200 (PtEAC2)
AtEAC2
ARALYDRAFT_904655 (AtEAC1)
ARALYDRAFT_913106 (AtEAC2)
ARALYDRAFT_900365 (AtEAC3)
GLYMA14G04196 (GmEAC1)
POPTR_0167s00240 (PtEAC3)
POPTR_0019s14980 (PtEAC4)
POPTR_0167s00200 (PtEAC5)
POPTR_0167s00210 (PtEAC7)
POPTR_0019s15010 (PtEAC8)
POPTR_0167s00230 (PtEAC6)
POPTR_0007s00260 (PtEAC10)
POPTR_0013s15230 (PtEAC9)
GRMZM2G466848 (ZmEAG1d)
GRMZM2G466856 (ZmEAG1c)
GRMZM2G075366 (ZmEAG1b)
GRMZM2G376674 (ZmEAG1a)
BRADI1G34640 (BdEAG2)
BRADI1G08960 (BdEAG1)
GLYMA10G41250 (GmEAG2)
GLYMA20G26010 (GmEAG1)
ARALYDRAFT_685823 (AtEAG1)
AT5G61412 (AtEAG1)
AT2G30560b_AtEAG2b
ARALYDRAFT_668766 (AtEAG2)
AT2G30560a (AtEAG2a)
OS06T0706700 (OsEAG1)
Sb10g029350 (SbEAG1)
AC185611.3_FG001 (ZmEAG2)
GRMZM5G849499 (ZmEAC1)
Sb02g038790 (SbEAC1)
Os01g0340600 (OsEAC2)
Os01g0341200 (OsEAC3)
Os01g0341000 (OsEAC4)
GRMZM2G157505 (ZmEAL2)
BRADI1G21950 (BdEAL2)
BRADI1G21960 (BdEAL1)
OS07T0605400 (OsEAL2)
LOC100823010 (BdEAL4)
Sb09g003110 (SbEAL2)
GRMZM2G456746 (ZmEA1)
Sb02g038810 (SbEAL1)
OS07T0605350 (OsEAL3)
BRADI1G21930 (BdEAL3)
OS07T0605900 (OsEAL1)
ZmEAL1
BRADI1G21970 (BdEAL5)
0.05
B
Chr. 7
ZmEAL2
ZmEA1
ZmEAL1
ZmEAL1s
Chr. 7
OsEAL3
OsEAL2
OsEAL1
Chr. 1
BdEAL3
BdEAL2
BdEA1
BdEAL5
BdEAL4
C
CLP LB LP L RT R IN N IF A P EC EM H2O gDNA
OsEAL1
OsEAL2
CLP LB LP L RT R IN N IF A P EC EM H2O gDNA
OsEAL3
OsGAPDH

Figure 2.3 Phylogenetic tree of proteins containing the EA1-box and genomic localization of EAL proteins. (**A**) To compare the phylogenetic distance of all EA1-box proteins, an unrooted tree was generated. EALs and EAGs were clustering in branches distinguishable from the EACs. EALs are shaded in red, EAGs in green and EACs in blue. EAL proteins of maize are underlined. Protein alignment and the phylogenetic tree of the EA1-box proteins were created using ClustalX2 (Larkin *et al.,* 2007). The phylogenetic tree was visualized by the program FigTree v1.4.2 (http://tree.bio.ed.ac.uk/publications/). (**B**) All EAL protein genes are localizing on the same chromosome in *Zea mays* (chromosome 7), *Oryza sativa e* (chromosome 7) and *Brachypodium distachyon* (chromosome 1). The scheme represents the orientation and the position of these genes to each other (not to scale). Genes are marked by red arrows. (**C**) Expression of the rice EAL proteins *OsEAL1*, *OsEAL2* and *OsEAL3* was analyzed in vegetative and generative tissues by RT-PCR. *OsEAL1* transcript was solely detected in the egg cell whereas *OsEAL2* transcript was present in all samples, except the mature embryo one day after germination (DAG). No expression of *OsEAL3* was observed in any of the tissues. Abbreviations: A = anther immature, CLP = coleoptile + primary leaf, EC = egg cell, EM = embryo mature (1 DAG), IF = inflorescence immature, gDNA = genomic DNA, IN = internode, L = leaf, LB = meristematic leaf base, LP = primary leaf, N = node, P = pistil immature, R = root (-tip), RT = root tip.

2. 3. 3 EALs and EACs enter the secretory pathway, while EAGs localize to the cytoplasm and nucleus

EAL peptide precursors contain either an N-terminal signal peptide or a transmembrane domain close to the N-terminus. A high and significant score using the SecretomeP 2.0 server (Bendtsen *et al.,* 2004) was also obtained for EALs lacking a "classical" N-terminal signal peptide, predicting them as secreted peptides. Until now only ZmEA1 and ZmEAL1 were experimentally shown to be secreted (Márton *et al.,* 2005; Krohn *et al.,* 2012). EALs ZmEA1, ZmEAL2, OsEAL1 and OsEAL3 were therefore selected for further analysis to study their subcellular localization after transient transformation as GFP-fusion proteins into maize Black Mexican Sweet (BMS) suspension cells (Figure 2.4). All fusion proteins co-localized with a marker for the endoplasmic reticulum (ER) (Nelson *et al.,* 2007) composed of the signal peptide of AtWAK2 (*Arabidopsis thaliana* wall-associated kinase 2; He *et al.*, 1999) at the N-terminus of mCherry and an ER-retention signal at its C-terminus (Gomord *et al.,* 1997). Quantification of GFP and mCherry signal intensity showed perfect overlap of ZmEA1 (Figure 2.4 A-D), ZmEAL2 (Figure 2.4 I-L), OsEAL1 (Figure 2.4 M-P) and OsEAL3 (Figure 2.4 Q-T) with the ER marker. These findings are comparable with the results showing subcellular localization of ZmEAL1 in BMS suspension cells (Krohn *et al.,* 2012). Control experiments using free GFP in combination with the ER marker showed GFP distribution inside cytoplasmic strands as well as inside the nucleus of the BMS cells. A significant overlap of

both fluorescence channels was not observed (Figure 2.4 U-W). These findings support the hypothesis that all EAL peptides are secreted to the extracellular space.

To confirm that the N-terminus containing the signal peptide is responsible for ER localization of EALs, subcellular localization of the predicted mature form of ZmEA1 (sEA1) lacking the N-terminal signal peptide was fused to GFP and analyzed in BMS suspension cells. Unlike the precursor peptide of ZmEA1, which was shown to localize to the ER (see above), the predicted mature peptide of 49 amino acids fused to GFP was mainly cytoplasmic and accumulated in large aggregates in the cytoplasm and nucleus. Based on the general hydropathy model of Kyte and Doolittle, 1982, mature EALs are highly hydrophobic peptides. ZmEA1 contains only one non-hydrophobic domain of five amino acids and its solubility in an aqueous environment like the cytoplasm is therefore expected to be relatively low. The aggregates observed are evenly distributed throughout the cytoplasm and don't accumulate as aggresomes in vicinity to the Golgi apparatus, which has been described for overexpressed and misfolded proteins (Johnston *et al.,* 1998; García-Mata *et al.,* 1999). This observation indicates that EALs are likely further processed in the ER, for example, by phosphorylation or glycosylation (see below) to increase their water solubility.

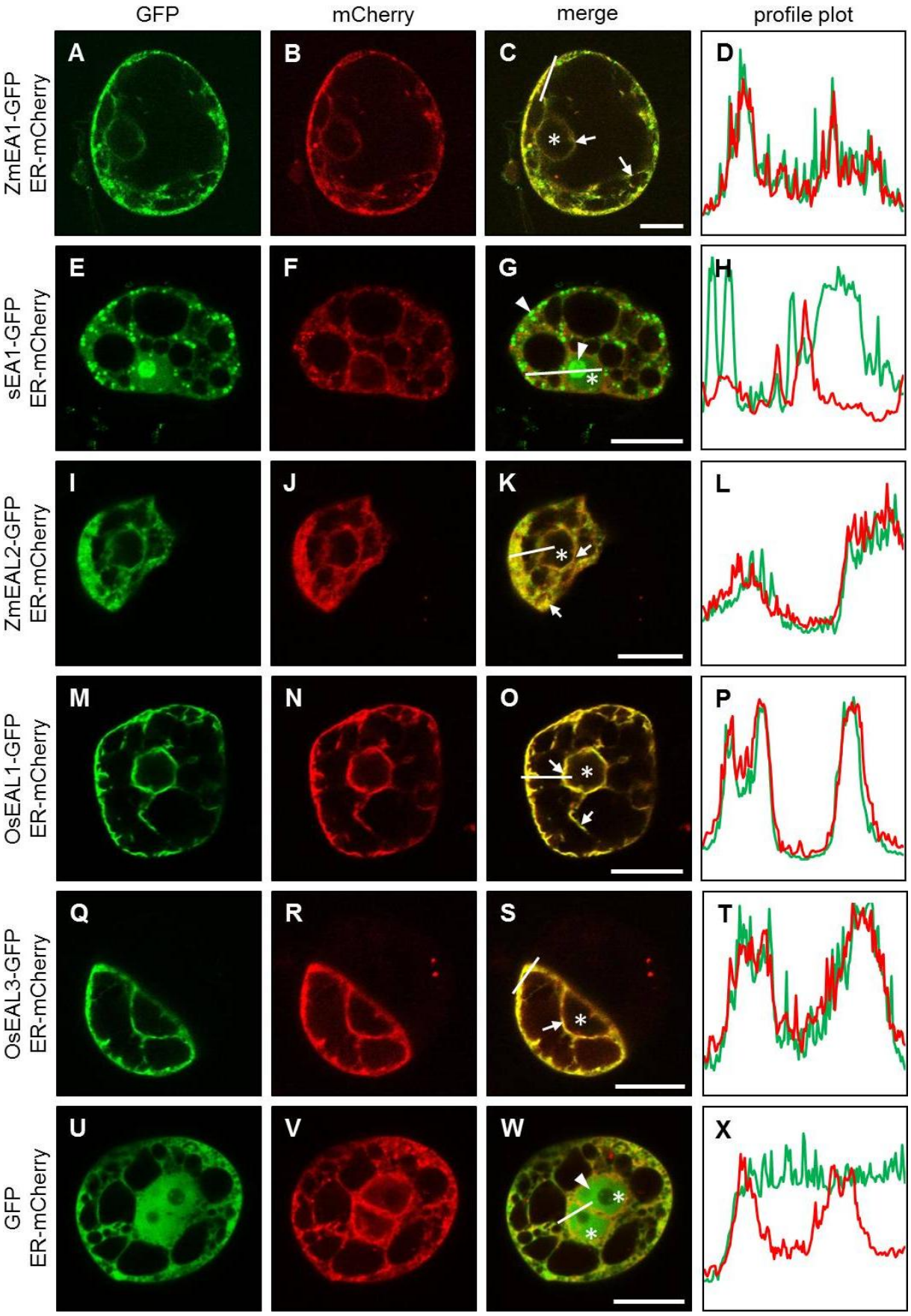
GFP
mCherry
merge
profile plot
ZmEA1-GFP ER-mCherry
sEA1-GFP ER-mCherry
ZmEAL2-GFP ER-mCherry
OsEAL1-GFP ER-mCherry
OsEAL3-GFP ER-mCherry
GFP ER-mCherry
A
B
C
D
E
F
G
H
I
J
K
L
M
N
O
P
Q
R
S
T
U
V
W
X

Figure 2.4 Subcellular localization of EAL proteins in BMS suspension cells. Several EAL proteins fused to GFP were transiently co-transformed with a marker for the endoplasmic reticulum (ER) fused to mCherry (Nelson *et al.*, 2007) into BMS suspension cells via biolistic bombardment: (**A-D**) ZmEA1, (**I-L**) ZmEAL2, (**M-P**) OsEAL1 and (**Q-T**) OsEAL3. All proteins showed co-localization with the ER-marker, indicating that they entered the secretory pathway. (**E-H**) Predicted mature ZmEA1 lacking the N-terminal signal peptide, named sEA1, was detected in the cytoplasm and aggregating in cytoplasmic granules. No co-localization with the ER was observed. (**U-X**) Cytoplasmic GFP was used as control. (**D, H, L, P, T, X**) Profile plot of the single fluorescence channels indicate the extent of signal overlap. Asterisks mark the nucleus. Arrows mark matching overlaps of both fluorescent channels. Arrowheads mark positions without overlay of both fluorescent channels. Scale bar represents 20 µM.

In contrast to EALs, EAGs do not contain any signal peptide or transmembrane domain. Subcellular localization studies using AtEAG1-GFP fusion protein together with the mCherry-coupled ER-marker as an example for EAGs did not show any co-localization with the ER marker (Figure 2.5 A-D). AtEAG1-GFP was detected in the cytoplasm and nucleus of suspension cells, thereby resembling the localization pattern of free GFP (Figure 2.4 U-X).

The third EA1-box containing protein group EAC is less defined in structure (Figure 2.1 C). However, most members are predicted to contain one or more transmembrane domains and/or an N-terminal signal peptide. The two maize proteins ZmEAC1 and ZmEAC2 belonging to different EAC subclades were selected for subcellular localization studies. Both proteins contain several transmembrane domains flanking the EA1-box and consist of 315 and 213 amino acids, respectively. Localization of the fusion proteins ZmEAC1-GFP (Figure 2.5 E-H) and ZmEAC2-GFP (Figure 2.5 I-L) as well as their fluorescence quantification were observed to match perfectly with the ER marker, supporting the predicted localization to the ER and plasma membrane.

In summary, we could show by expressing fusion proteins of several members of all three EA1-box protein classes in maize BMS suspension cells that EALs and EACs localize to the secretory pathway while EAGs are cytoplasmic and also localize to the nucleus. Moreover, using ZmEA1 as an example, it could be demonstrated that the N-terminal signal peptide is required to localize EALs to the ER where the peptides are likely further processed to increase their water solubility. In future experimentation it will now be necessary to extract mature peptides and proteins, respectively, to determine post-translational modifications. Moreover, their localization pattern should be studied in the original tissues preferentially by immunohistochemistry as the relatively large GFP tag may influence the activity, localization and mobility of the proteins.

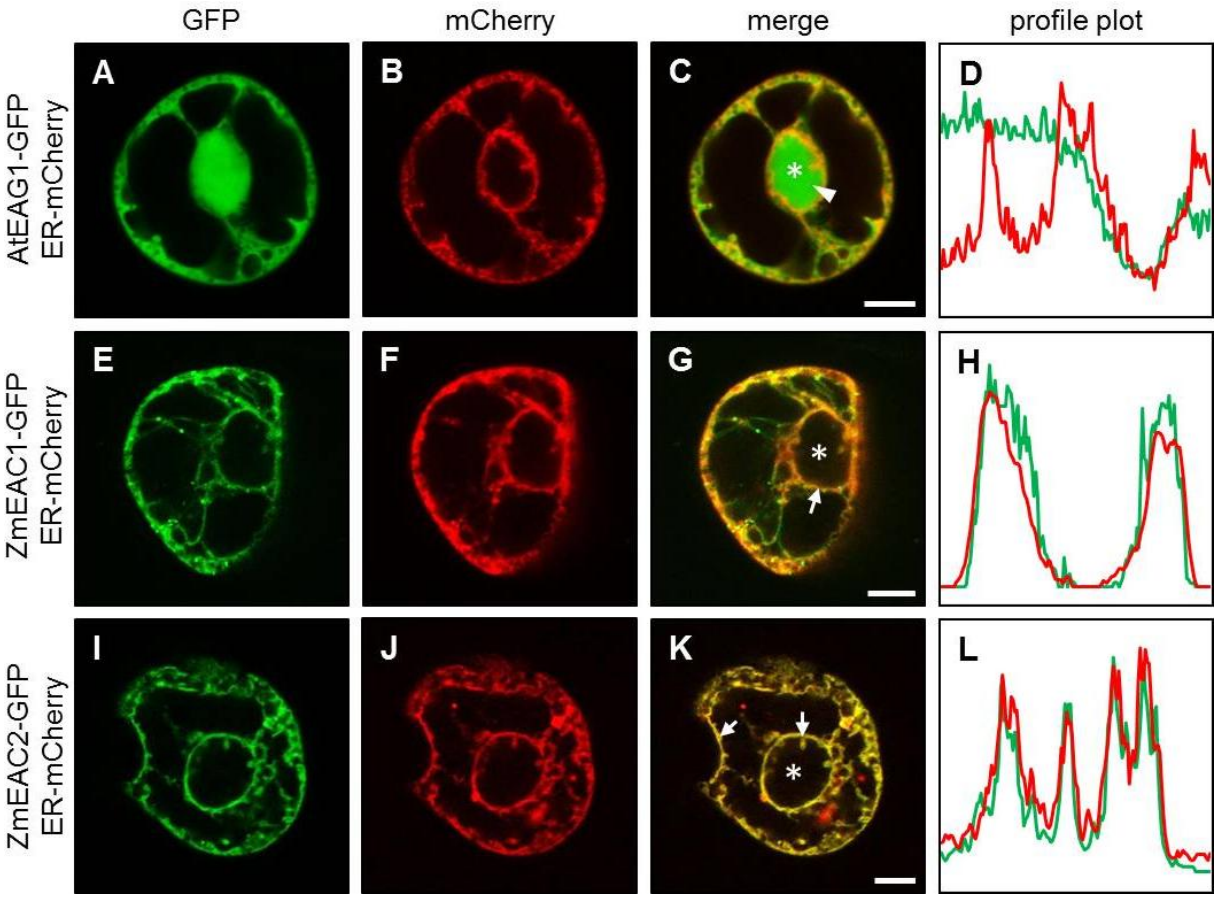

Figure 2.5 Subcellular localization of EAG and EAC proteins in BMS suspension cells. EAG and EAC proteins fused to GFP transiently co-transformed with a marker for the endoplasmic reticulum (ER) fused to mCherry (Nelson *et al.*, 2007) into BMS suspension cells via biolistic bombardment. (**A-D**) ZmEAC1 and (**E-H**) ZmEAC2, both containing predicted transmembrane domains, were observed co-localizing with the ER. (**I-L**) The glycine-rich AtEAG1 did not show co-localization with the ER. (**D, H, L**) Profile plot of the single fluorescence channels indicate the extent of signal overlap. Asterisks mark the nucleus. Arrows mark matching overlaps of both fluorescent channels. Arrowheads mark positions without overlay of both fluorescent channels. Scale bar represents 10 µM.

2. 3. 4 ZmEAL2 potentially plays a role during late embryogenesis

From the small *EAL* gene family of maize until now only *ZmEA1* and *ZmEAL1* have been functionally characterized (Márton *et al.*, 2005; Krohn *et al.*, 2012). Here we report about the gene expression pattern of the third maize *EAL* gene, *ZmEAL2*. Similar to rice *OsEAL1* (Figure 2.3 C), it shows a broad expression pattern (Figure 2.8 A) and transcript levels were especially high in root tips and a mixture of embryo and endosperm six days after pollination (DAP). *In silico* expression analysis based on the data of Sekhon *et al.*, 2011 showed a strong transcription activity of *ZmEAL2* in maize embryos at different stages of development where-

as expression in other tissues was constantly low. We now additionally show that expression in the endosperm is absent (Figure 2.6).

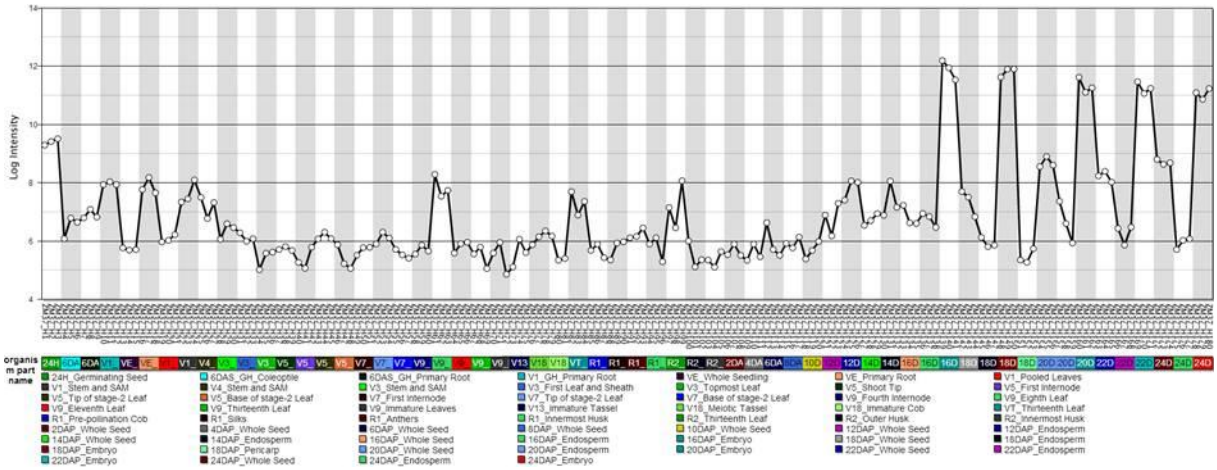

Figure 2.6 ***In silico*** **analysis of the expression profile of *ZmEAL2*.** The expression pattern of the maize EAL protein coding *ZmEAL2* was examined in 60 different maize tissues using the genome-wide transcription atlas of Sekhon *et al.*, 2011. Whereas in most tissues, including the endosperm, transcript was detected on a low level, embryos 16 – 24 DAP showed a slightly decreasing expression of *ZmEAL2*. The data set was created by RNA sequencing and RMA normalization of 3 replicates per tissue, with logarithmic expression intensity of each replicate indicated by a white dot and grouping of the 3 replicates of each tissue in columns with an alternating gray-white color scheme. The expression graph was generated using PLEXdb browser and experiment ZM37 (Dash *et al.*, 2012).

Therefore we examined the expression of *ZmEAL2* during maize embryogenesis in more detail. Embryos were isolated at different time points after pollination, staged (Figure 2.8 B) and the level of *ZmEAL2* transcript determined via quantitative real-time PCR (Figure 2.8 C). The two genes *LUG* (GRMZM2G425377) and *CUL* (GRMZM2G166694) were chosen as reference genes as they show a quite constant expression pattern throughout embryogenesis. As shown in Figure 2.8 C, *ZmEAL2* is not expressed before fertilization and expression strongly increases in embryos 6 DAP. Until 34 DAP, expression constantly decreases to about 5% of the level at 6 DAP with another peak at 18 DAP.

To correlate transcript and protein level, we first generated a ZmEAL2-specific peptide antibody directed against an 11 amino acid sequence of the ZmEAL2 EA1-box. Immunoblot analysis using this antibody and protein extract from different embryo stages exhibited a signal with a molecular weight of approximately 13-14 kDa (Figure 2.8 D). This is more than the expected 10.2 kDa predicted from the amino acid sequence, either resulting from a different

migration behavior of the peptide and/or calibration of the corresponding protein ladder towards uncoupled proteins in a Tris/glycine system, while we had to use a Tris/tricine system to separate the highly hydrophobic peptide. Another explanation would be post-translational modification of ZmEAL2 causing a shift of its migration behavior. Especially glycosylations are high-molecular weight modifications of up to several thousand Daltons which can significantly contribute to the total molecular weight of the protein (Ahmad *et al.,* 2005; Unal *et al.,* 2008; Parker *et al.,* 2010). Glycosylations are common post-translational modifications associated to secreted proteins (for review see Fitchette *et al.,* 2007) and are known to play important roles in the functionality of signaling molecules (for review see Wopereis *et al.,* 2006 and Theillet *et al.,* 2012).

Separation of crude cell debris and lysate revealed an enrichment of ZmEAL2 in the pellet fraction, indicating association of the protein to crude cell wall components. During embryo development, the immunoblot signal derived by the ZmEAL2-directed antibody occurred weak in the pellet of embryo samples until 18 DAP. After 18 DAP, signal intensity increased and remained stable during maturation of the embryo until 34 DAP (Figure 2.8 D). The protein did not undergo any changes in molecular size throughout embryogenesis. The change of ZmEAL2 protein level during embryogenesis is in strong contrast to its gene activity, as expression decreases constantly from 6 DAP until maturity of the embryo. Whether ZmEAL2 mRNA is stored in P-bodies for delayed translation (Parker and Sheth, 2007) or the protein is not secreted until 18 DAP remains a task for future investigations. However, it is important to mention that the occurrence of the ZmEAL2 protein appears embryo-specific since immunoblot analysis of the endosperm during kernel development did not show any presence of the protein (Figure 2.7).

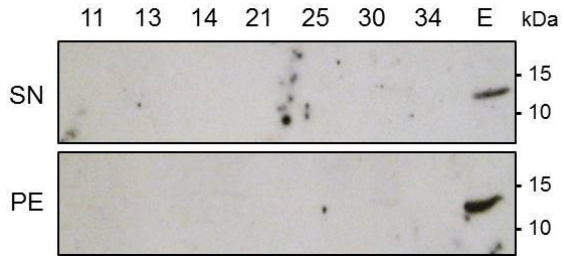

Figure 2.7 ZmEAL2 protein level in maize endosperm was analyzed from 11 to 34 DAP using a ZmEAL2-specific antibody. ZmEAL2 was not detected in the pellet (PE) and the supernatant (SN) of endosperm. Maize embryo (E) was used as positive control.

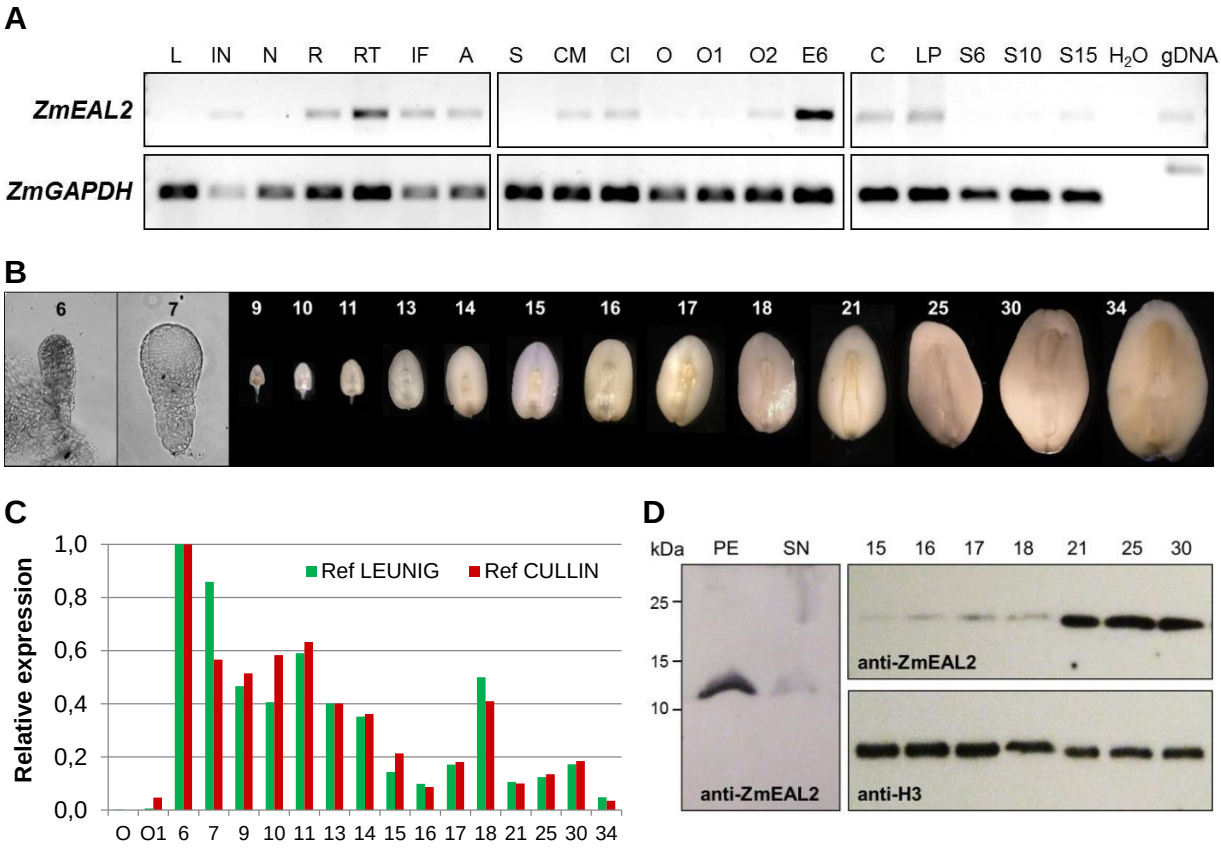

Figure 2.8 Expression analysis of *ZmEAL2*. (**A**) Expression of *ZmEAL2* in several maize tissues was analyzed by RT-PCR. Transcript was detectable in most of the tissues with the strongest signal intensity in the sample containing embryo and endosperm 6 days after pollination (DAP). (**B**) Maize embryos used for qRT-PCR and western blot analysis isolated during embryogenesis. Numbers indicate the time point of harvesting in DAP. (**C**) Quantitative expression profile of *ZmEAL2* during the embryogenesis at several time points ranging from 1 DAP until 34 DAP for *ZmEAL2* transcript. Expression increased after pollination compared to ovules and showed afterwards the tendency to decrease again. *LEUNIG* and *CULLIN* were used as reference genes. (**D**) The ZmEAL2 protein level in maize embryo was analyzed from 15 to 34 DAP using a ZmEAL2-directed antibody. ZmEAL2 was detected in the crude cell fraction (centrifugation at 1000 g) and with less intensity in the supernatant. ZmEAL2 level increased after 18 DAP and remained stable until 34 DAP. Histon H3-directed antibody was used as loading control. Abbreviations: A = anther immature, C = coleoptile, CM = cob meiotic, CI = cob immature (stages FG1-FG5), E6 = embryo + endosperm 6 DAP, gDNA = genomic DNA, IF = inflorescence immature, IN = internode, L = leaf, LP = primary leaf, N = node, O = ovule mature, O1/2 = ovule 1/2 DAP, PE = pellet, S = silk, S6/10/15 = seedling 6/10/15 DAG, SN = supernatant, R = root (-tip), RT = root tip.

Because *ZmEAL2* is strongly expressed during embryogenesis 6-34 DAP and its protein accumulates in embryos from 18 DAP, we performed immunohistochemical localization studies using the ZmEAL2-directed peptide antibody described above. Embryos 18 DAP and 25 DAP were chosen as samples for immunolocalization studies as there was strong difference in pro-

tein level at both time points. Antibody-derived signals were observed in the scutellum of both samples (Figure 2.9 A-B, E-F). The scutellum is attached to the embryo axis and consists of four tissues: the epithelium, the parenchyma, the epidermis and the provascular tissue (Negbi, 1984; excellent drawings are also available from Sargant and Robertson, 1905). ZmEAL2 signal was mainly detected in the outer regions of the scutellar parenchyma and the cells surrounding the provascular tissue. Close-ups of the parenchyma 18 DAP showed that the signal is mainly localized extracellular and accumulates in the intercellular space between parenchyma cells (Figure 2.9 C-D).

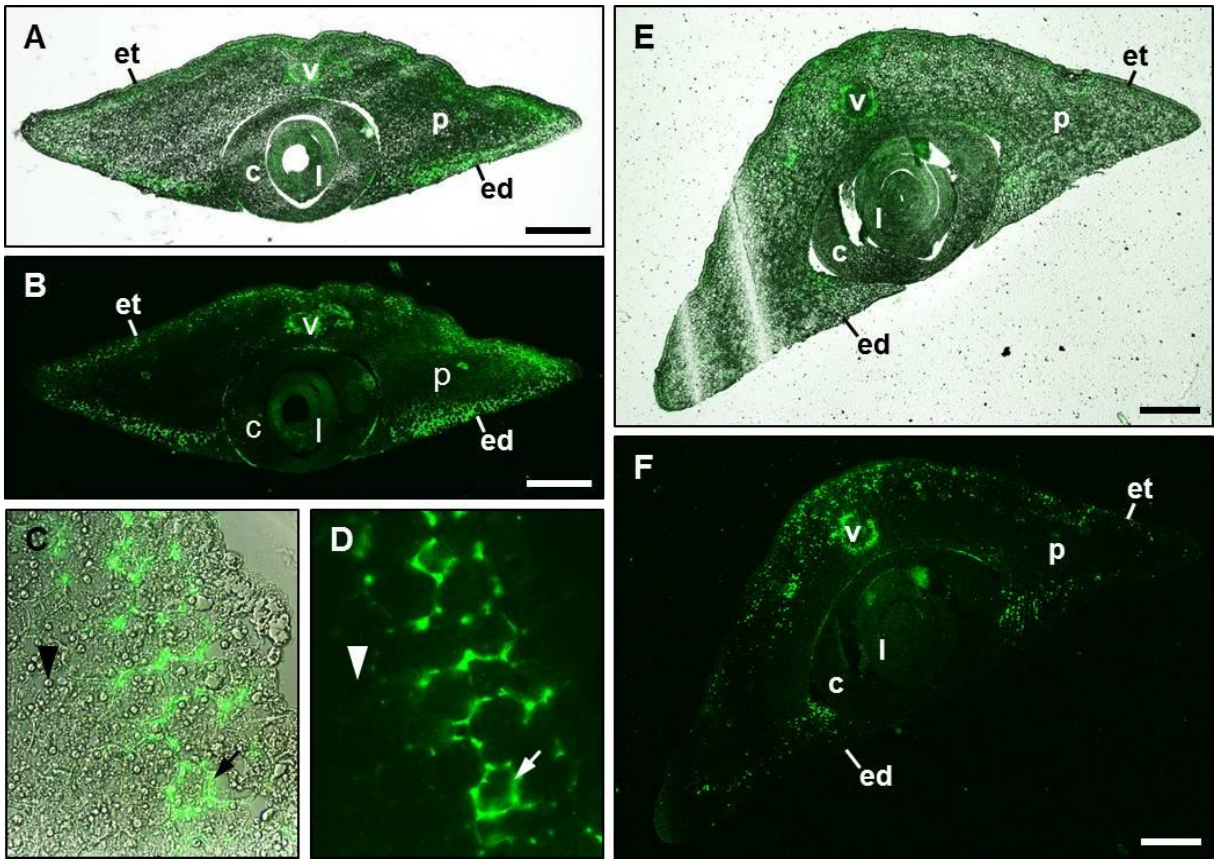

Figure 2.9 Immunolocalization of ZmEAL2 in the maize embryo. Immunolocalization of ZmEAL2 using a ZmEAL2-directed antibody was performed using semi-thin transversal sections of embryos at two different developmental stages. (**A, B**) In the embryo 18 DAP fluorescence signal was observed at the outer regions of the scutellar parenchyma and surrounding the vascular tissue. (**C, D**) Close-up of outer region of the scutellar parenchyma of embryo 18 DAP. Signal was detected surrounding the parenchyma cells (marked by arrow). Arrowhead marks oil body. (**E, F**) In the embryo 25 DAP fluorescence signal was detected in the scutellar parenchyma, less definite than 18 DAP, and surrounding the vascular system. (**A, C, E**) Merged bright field and fluorescene micrographs. (**B, D, F**) Fluorescence micrographs. Abbreviations: c = coleoptile, ed = scutellar epidermis, et = scutellar endothelium, l = leaf primordia, p = scutellar parenchyma, v = vascular tissue. Scale bar represents 200 µM.

Although there was a clear difference in protein level of ZmEAL2 at both embryo stages, immunohistochemical labeling did not show a significant change in protein localization pattern between both stages. Pre-immune serum from the antibody-producing animal before immunization was used as negative control. Sections from the same embryo samples did not show any significant fluorescence (Figure 2.10).

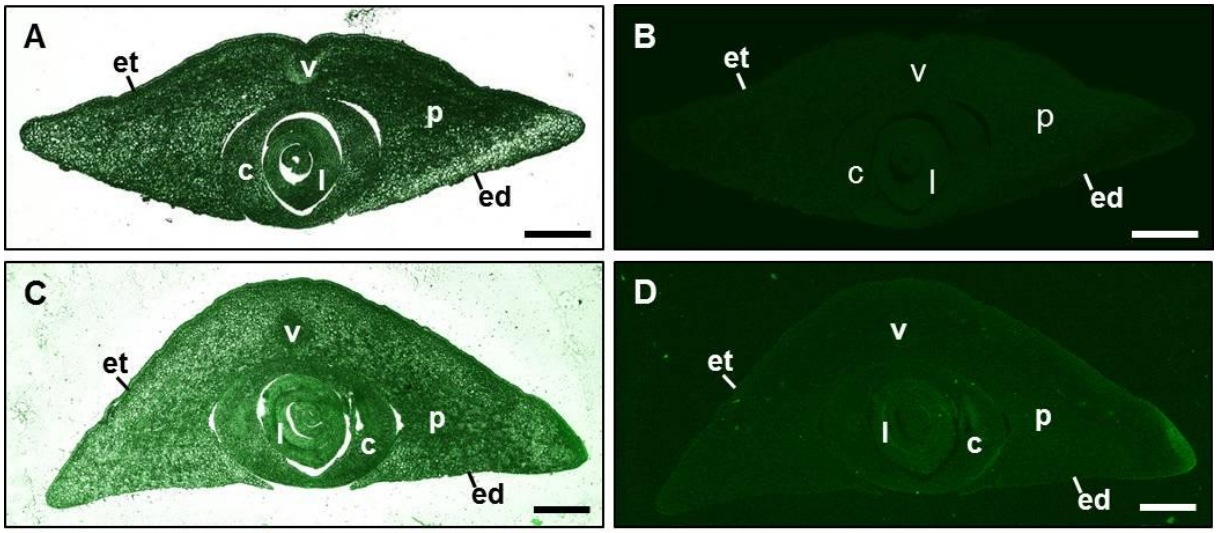

Figure 2.10 Control experiments of immunohistochemically labeling of ZmEAL2 in the maize embryo. Control experiments were performed using sections from embryo (**A**, **B**) 18 DAP and (**C**, **D**) 25 DAP and pre-immune serum isolated before immunization. No signals were detected in the scutellar parenchyma or the vascular system. (**A, C**) Merged bright field and fluorescence micrographs. (**B, D**) Fluorescence micrographs. Abbreviations: c = coleoptile, ed = scutellar epidermis, et = scutellar endothelium, l = leaf primordia, p = scutellar parenchyma, v = vascular tissue. Scale bar represents 200 µM.

The role of ZmEAL2 during late embryogenesis remains unclear. We generated a number of independent *ZmEAL2*-RNAi lines to down-regulate gene activity, but none of the lines showed an obvious phenotype during embryogenesis, although transcript levels in some lines were significantly reduced (data not shown). The observation that ZmEAL2 is not present in the endosperm but strongly in the outer scutellar parenchyma indicates that it might be involved in embryo-endosperm communication. The scutellum plays an important role in storage and transfer of nutrients as it contains high amounts of oil bodies and secretes hydrolytic enzymes into the endosperm for mobilization and uptake of nutrients during the germination (Nomura *et al.*, 1969; Huang, 1992). The major structure of the scutellum is comprised by the parenchyma, which enables the transfer of these nutrients towards the embryo axis (Aoki *et al.*, 2006). Signaling by ZmEAL2 might therefore also be required either for the formation of

structures which are necessary for transport of nutrients during later stages of embryo development until maturity and germination or ZmEAL2 might become activated during germination to induce, for example, the release of scutellar enzymes towards the endosperm. Thus the next important step will be to determine the exact functions of ZmEAL2 by construction of mutant maize lines. The RNAi approach was not sufficient to fully knock-out ZmEAL2 function. Alternative methods such as CRISPR/Cas (Cong *et al.,* 2013) can now be used to generate a full knock-out mutant.

To analyze promoter activity and protein localization of ZmEAL2 in maize embryo *in vivo*, a fragment of 1,937 base pairs upstream of the ORF of *ZmEAL2* was isolated as putative promoter sequence. BMS suspension cells were utilized for verification of the activity of the putative promoter. The presence of *ZmEAL2* transcript in BMS cells could be demonstrated by RT-PCR, indicating an active promoter in these cells (Figure 2.11 A). A vector was constructed with *GFP* under control of the putative *ZmEAL2* promoter and transiently transformed into BMS suspension cells by particle bombardement. Cytosolic GFP was detected in the cells, demonstrating the potential of the 1,937 bp fragment upstream of the *ZmEAL2* ORF to promote *ZmEAL2* expression (Figure 2.11 B). To further examine activity of the putative *ZmEAL2* promoter in the maize embryo, 6 independent stable transgenic maize lines were generated with *GFP* under control of the putative promoter by *Agrobacterium*-mediated transformation. Fertilized cobs of transgenic plants were analyzed for fluorescence at time points ranging from 6 to 30 days after pollination either with wild-type or transgenic pollen, respectively. No fluorescence signal could be detected in any of the lines or time points, indicating the inactivity of the putative promoter sequence in the embryo despite its observed activity in BMS suspension cells described in Figure 2.11 B. It has to be considered that contribution of additional regulatory elements is necessary for the promoter sequence to achieve activity. Generally, *Agrobacterium*-mediated transformation results in a lower construct copy number than biolistical transformation methodologies (Oltmanns *et al.,* 2010). Positive fluorescence signal in biolistically transformed BMS cells might result from an excess of construct fragments circumventing the necessity of regulatory elements. Additionally, to examine the subcellular localization pattern in maize embryos, constructs were created for expression of *ZmEAL2-GFP* in the maize embryo under control of the putative promoter sequence. Only one independent line could be obtained after transformation and was analyzed at various time points during embryogenesis for the presence of the GFP-fusion protein. Like with P_{ZmEAL2}*:GFP* constructs, no signal could be detected in any sample.

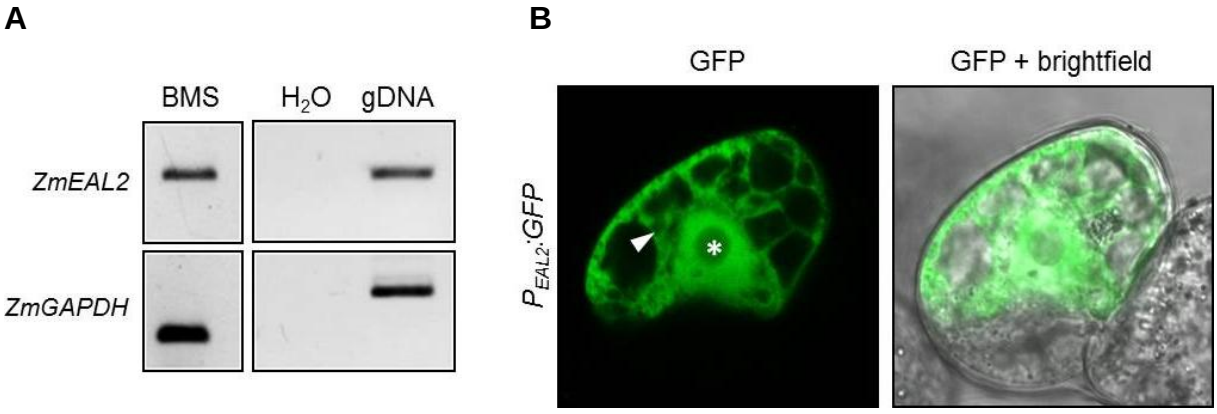

Figure 2.11 Putative *ZmEAL2* promoter shows activity in BMS suspension cells. (**A**) *ZmEAL2* transcript was detectable in BMS suspension cells by semi-quantitative RT-PCR, indicating activity of an associated promoter sequence. (**B**) GFP under control of a fragment of 1,937 bp upstream of the *ZmEAL2* ORF, representing the putative *ZmEAL2* promoter, was transiently transformed into BMS cells. GFP-derived fluorescence was visible in the nucleus (marked with asterisk) and cytoplasmic strands (marked with arrow head), suggesting promoter activity.

2. 4 Conclusions

Our data shows that in spite of the high sequence homology of all three maize EAL proteins, they appear to function in completely different pathways. It cannot be ruled out that ZmEAL2 also plays a role in other processes besides a likely role during embryogenesis and seed development, but it likely does not act redundantly with ZmEA1 as it is not capable to bind to the surface of pollen tubes (Uebler et al. 2013). The described phenotype of *ZmEAL1*-RNAi was very low (Krohn *et al.,* 2012), which indicates that ZmEAL2 might act as a redundant component in this pathway. However, alike *ZmEAL2* a full knock-out could also not be generated for *ZmEAL1*. It is thus more likely that significant amounts of the signaling ligand are still present and moreover, *ZmEAL2* is almost silent in egg cells (J. Chen and T. Dresselhaus, unpublished data).

Taken together, the example of EA1-box proteins shows that *in silico* classification of small proteins and interpretations about orthologous proteins has to be taken with care. We think that the novel classification of EA1-box containing peptides and proteins now helps to shed some light into the jungle of these exciting protein classes and may motivate the research community to study more EALs and first members of the EAG and EAC classes. After their discovery the role of EALs in pollen tube guidance was discussed controversially (McCormick and Yang, 2005) and all EA1-box were classified as EALs widely distributed

throughout the plant kingdom both in monocotyledonous and dicotyledonous plant species (Gray-Mitsumune and Matton, 2006). ZmEAC1 and ZmEAC2, for example, were previously grouped according to their structure in a subclass together with ZmEA1, and *Arabidopsis* EALs were shown to be ubiquitously expressed (Gray-Mitsumune and Matton, 2006). Now, we have clarified that EALs encoding secreted peptides possess a specific peptide-structure lacking in other EA1-box proteins and appear to exist specifically in the grasses. Eudicotyledonous species contain both cytoplasmic/nuclear EAGs and membrane-associated EACs likely including secreted peptides different from EALs. A major question remains: which is the biochemical function of the EA1-box? We suggest that it is simply a protein-protein interaction motif, but this has to be shown in further experimentation and by 3D structure analyses.

CHAPTER 3 - OVERCOMING HYBRIDIZATION BARRIERS BY THE SECRETION OF THE MAIZE POLLEN TUBE ATTRACTANT ZMEA1 FROM *ARABIDOPSIS* OVULES

This CHAPTER is based on the manuscript Márton *et al.,* 2012, in *Current Biology*. S. Uebler performed the immunoblot experiments (Figure 3.4 E) and wrote the corresponding paragraph in the section of experimental design (3. 2. 6).

3. 1 Introduction

A major goal of plant reproduction research is to understand and overcome hybridization barriers so that the gene pool of crop plants can be increased and improved upon. After successful pollen germination on a receptive stigma, the nonmotile sperm cells of flowering plants are transported via the pollen tube (PT) to the egg apparatus for the achievement of double fertilization. The PT path is controlled by various hybridization mechanisms probably involving a larger number of species-specific molecular interactions (Lausser *et al.,* 2010; Dresselhaus *et al.,* 2011). The egg-apparatus-secreted polymorphic peptides ZmEA1 in maize (Márton *et al.,* 2005) and LURE1 and LURE2 in *Torenia fournieri* (Okuda *et al.,* 2009) as well as TcCRP1 in *T. concolor* (Kanaoka *et al.,* 2011) were shown to be required for micropylar PT guidance, the last step of the PT journey. We report here that ZmEA1 attracts maize PTs *in vitro* and arrests their growth at higher concentrations. Furthermore, it binds to the subapical region of maize PT tips in a species-preferential manner. To overcome hybridization barriers at the level of gametophytic PT guidance, we expressed ZmEA1 in *Arabidopsis* synergid cells. Secreted ZmEA1 enabled *Arabidopsis* ovules to guide maize PT *in vitro* in a species-preferential manner to the micropylar opening of the ovule. These results demonstrate that the egg-apparatus-controlled reproductive-isolation barrier of PT guidance can be overcome even between unrelated plant families.

3. 2 Experimental procedures

3. 2. 1 Plant material and growth

Maize (*Zea mays*) inbred line A188, tetraploid and hexaploid accessions of *Tripsacum dactyloides* as well as *Arabidopsis thaliana* (ecotype Columbia-O) and *Nicotiana benthamiana*

plants were applied for various experiments. All Poaceae were kept in the greenhouse under long-day conditions (16 h of light) and a relative air humidity of about 60%. The temperature was kept at 25°C during the light period and at 18°C in the dark. *A. thaliana* seeds were vernalized in growth chambers for 2 days at 4°C without light and an average air humidity of about 55% – 60%. After vernalization, seeds were germinated and grown in growth chambers under short-day conditions and shifted to long-day conditions after 4 weeks. Long- and short-day chambers were kept at 20– 22°C and 70% humidity. Tobacco (*Nicotiana benthamiana*) plants were grown at 22°C with 16 hours light and at 18°C in the dark with a relative air humidity of ~70%. Pollen from *A. thaliana* and from *N. benthamiana* was obtained by harvesting anthers 1 day before or at anthesis. Maize and *T. dactyloides* pollen was obtained by hand shaking tassels containing mature and fresh pollen grains into paper bags between 9.30 and 10.00 a.m. Older pollen was removed from tassels by vigorous shaking tassels the evening before pollen harvest.

3. 2. 2 Generation of constructs and transgenic plants

To clone the binary vector p7N-MYB98-EA1-GFP, an intermediary vector pMYB98-EA1-GFP was generated first. By digesting the plasmid pLG-ZmEA1 (*UBIp::ZmEA1-GFP::NOSt*, [Márton *et al.*, 2005]) with *Sal*I/*Spe*I, the *UBI* promoter was removed and replaced by ligating a 1,498 bp *MYB98* promoter fragment (Kasahara *et al.*, 2005) from a *MYB98p::GUS* containing vector (S. Sprunck, unpublished data) using *Sal*I und *Spe*I restriction sites, and hence generating the vector pMYB98-EA1-GFP. Further on, the whole MYB98-EA1-GFP fragment from pMYB98-EA1-GFP was cloned into p7N-MYB98-GUS (S. Sprunck, unpublished data) by *Sfi*I digest and ligation, and the final binary vector p7N-MYB98-EA1-GFP was constructed. For cloning the binary vector p7N-MYB98-spEA1-GFP, a 248 bp genomic fragment from *ZmEA1*, named as *spEA1* (short peptide encoding *EA1* ORF, Figure 3.4 A) was amplified using ACCUZYME DNA polymerase (Bioline) and the forward and reverse primers spEAF and EAR-GFP, respectively. By digesting the plasmid p7N-UBI-EA1-GFP (M. Márton, unpublished data) with *Spe*I/*Bam*HI, the *ZmEA1* fragment was removed and replaced by ligating the *Spe*I/*Bam*HI digested *spEA1* fragment and, hence, generating the intermediary vector p7N-UBI-spEA1-GFP. The final binary vector p7N-MYB98-spEA1-GFP was generated by replacing the *UBI* promoter from p7N-UBI-spEA1-GFP with the *MYB98* promoter from p7N-MYB98-EA1-GFP through digestion and ligation using *Aat*II and *Spe*I restriction sites. After DNA sequencing generated binary plasmids were delivered into *Agrobacterium tumefaciens* strain GV3101 (pMP90RK) and used for transformation of *Arabidopsis* Col-0 using the floral

dip method, according to Clough and Bent, 1998. Three days after germination, BASTA-resistant seedlings were selected by spraying three times with 200 mg/L BASTA (Bayer Crop Science) supplemented with 0.1% Tween 20. Several BASTA-resistant *Arabidopsis* transgenic lines were generated and analyzed for the presence of transgenes by PCR using EA1-entr or spEA1-entr as forward primers and ZE-GFP2-rev as reverse primer. *MYB98:GFP* (Kasahara *et al.,* 2005) transgenic *Arabidopsis* seeds were kindly provided by G. Drews and used to generate several transgenic plant lines that were here analyzed.

3. 2. 3 Chemical labeling of synthetic ZmEA1 peptide

An N-terminal cleaved predicted mature ZmEA1 protein of 49 amino acids (sEA1, Figure 3.4 A) was chemically synthesized with 80%-90% HPLC-purity by JPT Peptide Technologies GmbH. Successful synthesis of the linear peptide was shown by LC-MS. Chemically labeling of the synthetic ZmEA1 peptide was performed with fluorophore DyLight 488 NHS Ester (Thermo Scientific) according to the manufacturer protocol. Hence, 0.5 mg peptide was each first dissolved together with an aliquot of the fluorophore DyLight 488 NHS Ester in 100% DMSO and then in 1 M Sodium Carbonate buffer (pH 8.3-9) to reach a final concentration of 20% DMSO. After 1.5 h incubation at room temperature, the mixture was dialyzed against 50 mM Tris buffer (pH 8) with a final concentration of DMSO not exceeding 1% using a Slide-A-Lyzer® MINI Dialysis Unit (Thermo Scientific). Trypsin inhibitor from soybean (Sigma-Aldrich) was dissolved and chemically labeled using the same method described above.

3. 2. 4 *In vitro* pollen tube guidance and competition assays and ZmEA1 bioassay

In order to perform *in vitro* pollen tube (PT) guidance assays, fresh pollen was collected from A188 WT maize plants and germinated onto a solid maize pollen germination medium (PGM, [Schreiber *et al.,* 2004]). Once germinated PTs reached a minimum length of about 200-1,000 µm, a chemotropism assay was performed using PTs showing intense cytoplasmic activity. Using the Nanoject II Auto-Nanoliter Microinjection Pipet (Drummond Scientific Company) and the InjectMan NI 2 Micromanipulator (Eppendorf), a small droplet with 10 µM solution of ZmEA1 or Trypsin inhibitor (in 50 mM Tris buffer, pH 8 and with 1% DMSO) that were either unlabeled or chemically labeled with fluorophore DyLight 488 NHS Ester or mixed with Alexa Fluor 488 Dye (Invitrogen, 1:10 dilution) was placed by micromanipulation very close (less than 100 µm distance) to the tip of single actively growing PTs, which were then each monitored for more than two hours.

Several *in vitro* pollen tube competition assays (PTCAs) have been performed with both dissected WT and transgenic *Arabidopsis* ovules expressing ZmEA1-GFP. Ovules were placed very close (less than 100 µm distance) onto solid PGM to the tips of actively growing maize, *Tripsacum dactyloides* or *Arabidopsis thaliana* PTs, respectively, using PGM as described (Palanivelu *et al.,* 2003; Schreiber and Dresselhaus, 2003). PT behavior was monitored over the time. *Arabidopsis* PTs were grown by a semi-*in vivo* method (Palanivelu and Preuss, 2006), where the upper portion of a pollinated pistil (stigma and style) was excised and placed horizontally on PGM close (~2 mm) to dissected ovules. At 4 h after pollination, PTs started to emerge from the cut pistil and grew further onto the solid PGM and were monitored over time.

The ZmEA1 bioassay was conducted as follows: fresh pollen grains of maize were shaken directly onto 10 µl drops of 1xPGM placed in a 35 mm plastic Petri dish. Pollen of *N. benthamiana* was transferred directly from a fresh opened anther onto drops of 1xPGM using forceps. Germination was performed at room temperature for 30 to 45 min. Further on, 1xPGM with 1% DMSO and chemically labeled ZmEA1 or control Trypsin inhibitor (1:10 dilution) were added to each droplet with germinated pollen to reach a 20 µl volume. 60 minutes after incubation the content of each droplet was transferred very carefully using a cut pipette tip to an Eppendorf tube, to which 1xPGM with 1% DMSO was added to a final volume of 200 µl. Samples were then washed very carefully 3 times each using 200 µl 1xPGM with 1% DMSO by allowing pollen tubes to sink at the bottom of Eppendorf tubes. Finally, for each sample PTs were resuspended very carefully into 100 µl 1xPGM with 1% DMSO. Microscopy analysis was started directly after, using either the Nikon Eclipse TE2000-S inverted microscope or Zeiss Axiovert 200M LSM 510 META confocal laser scanning microscope. In general germinated PTs were subjected to biological assays only if germination rates exceeded 75% and if most of PTs remained intact during the described procedures. To check integrity and behavior, PTs were initially always observed using an Eclipse TE2000-S inverted microscope (Nikon).

3. 2. 5 Microscopy

Arabidopsis pistils were dissected on a glass slide in 100 mM sodium phosphate buffer (pH 7.0). To visualize cell borders and nuclei, ovules were counterstained with 15 µg/ml propidium iodide (Invitrogen) for 10 to 30 min on a glass slide before microscopy. Bright-field and fluorescent specimens were observed using an Eclipse TE2000-S inverted microscope (Nikon) 6 equipped with a HC Alexa 488/eGFP filter (excitation at 472-495 nm, emission at 520

nm), a 1.4 Megapixel digital AxioCam MRm camera and AxioVision digital image processing software (both Zeiss). Samples were excited with UV-light produced by an Intensilight C-HGFI (Nikon). Confocal laser scanning microscopy (CLSM) was performed using the Zeiss Axiovert 200M inverted microscope equipped with a LSM 510 META module. For detection of GFP samples, an Argon laser (488 nm) and a BP 505-550 nm filter were used. For propidium-iodide stained samples a Helium/Neon laser (543 nm) and LP 560 nm filter were used. Image capture and processing were performed using the AxioCam HRc camera, the Zeiss LSM 510 META software, and the Zeiss LSM image browser version 4.2.0.121.

3. 2. 6 Immunoblot analysis

One hundred pistils for each sample type were collected from *Arabidopsis* wild type and heterozygous transgenic plants expressing either ZmEA1-GFP or spEA1-GFP fusion proteins, respectively, and then frozen at -80°C. Protein extraction buffer [50 mM Tris/0.05 % MES, pH 7.5, 330 mM Saccharose, 100 mM KCl, 1 mM EDTA, DTT 5 mM and protease inhibitor cocktail for plant cell and tissue extracts (Sigma-Aldrich)] was added to ground samples. Suspensions were centrifuged at 1,000 g for 15 min at 4°C. Resulting cell debris samples were solubilized by boiling in SDS sample buffer at 95°C and used for SDS-PAGE analysis. The corresponding lysates were further on centrifuged at 10,000 g for 15 min at 4°C and separated into soluble (supernatant, SN1) and insoluble (pellet, P1) protein fractions, respectively. Half of the SN1 and all of P1 protein fractions were solubilized by boiling in SDS sample buffer at 95°C and then used for SDS-PAGE. Each other half of SN1 protein fractions was submitted to ultracentrifugation at 63,000 g for 1 hour at 4°C and corresponding soluble (supernatant, SN2) and membrane (pellet, P2) protein fractions were solubilized by boiling in SDS sample buffer at 95°C for the SDS-PAGE. Protein samples were separated on a 12% SDS-PAGE and transferred onto Hybond ECL nitrocellulose membranes (0.2 µm, GE Healthcare) by wet electroblotting. For detection of GFP, a mouse IgG monoclonal GFP antibody (Roche) and an anti-mouse IgG (whole molecule) antibody conjugated with HRP (horseradish peroxidase) from goat (Sigma-Aldrich) were used at 1:5,000 dilutions as primary and secondary antibodies, respectively. Signals were detected using the SuperSignal West Femto Chemiluminescent Substrate Kit (Thermo Scientific).

3. 3 Results and discussion

3. 3. 1 Mature ZmEA1 attracts and arrests maize pollen tubes *in vitro* and binds to the subapical region of their tips

The last phase of pollen tube (PT) growth and guidance is controlled by the female gametophyte in angiosperms and requires species-preferential chemotropic guidance molecules (Lausser *et al.,* 2010; Shimizu and Okada, 2000; Higashiyama *et al.,* 2001; Márton and Dresselhaus, 2010). Maize ZmEA1 was the first identified signaling molecule accomplishing the properties of a female-gametophyte-derived PT attractant. ZmEA1 (*Zea mays* egg apparatus 1) is an intronless single gene specifically expressed in the egg apparatus (egg and synergid cells) of maize and encodes a hydrophobic precursor protein of 94 amino acids (of which 47 are hydrophobic) with a predicted N-terminal transmembrane domain. It has been shown that ZmEA1 is a member of a novel class of polymorphic small proteins; it is secreted from the egg apparatus toward the cell walls of micropylar nucellar cells, and its knockdown impairs micropylar PT guidance in maize (Dresselhaus *et al.,* 2011; Márton *et al.,* 2005). Studying female-gametophyte-controlled PT attraction *in planta* is very difficult because the cells of the egg apparatus are deeply embedded in the maternal tissues of the ovule. Therefore, an *in vitro* PT guidance assay was established with a synthetic ZmEA1 peptide. An N-terminal-cleaved, 49 amino acid oligopeptide predicted to represent the mature ZmEA1 was chemically synthesized and was used unlabeled or labeled with fluorophore DyLight 488 NHS Ester or mixed with Alexa Fluor 488 Dye so that its tropism effect on *in vitro* germinated and grown maize PTs could be studied. The usage of a semi-*in-vivo* guidance assay that has been previously used for visualizing micropylar PT growth in *Arabidopsis* (Palanivelu and Preuss, 2006) could not be used for maize PTs, which ceased to grow around 1 mm before cut silk ends (data not shown). This finding is similar to earlier observations made by Booy *et al.,* 1992, which shows that injured transmitting tracts lead to the inability of PTs to pass their destroyed tissue. Moreover, we have tried several published methods, including the bead method such as in Okuda *et al.,* 2009 and the chemotropism assay such as in Kim *et al.,* 2003, for the *in vitro* attraction assay. None of these methods worked because the hydrophobic ZmEA1 synthetic peptide of 49 amino acids (of which 26 are hydrophobic) precipitated in beads and was therefore probably unable to diffuse in sufficient amounts into the medium and to build the gradient necessary for PT attraction (data not shown). Hence, we developed an *in vitro* PT guidance assay in which ZmEA1-containing droplets were placed in front of PT tips

by micromanipulation. An experiment was considered successful when the droplet was deposited at a distance less than 100 mM away from the PT tip. This was the maximum distance observed for maize PT attraction *in vitro* (Márton *et al.*, 2005; Márton and Dresselhaus, 2010). As shown in Figure 3.1, synthetic ZmEA1 was capable of directly attracting *in vitro* germinated and grown maize PTs at a concentration of <10 mM. In general, we found that fluorescence signals derived from ZmEA1 labeled with DyLight were visible up to 5 min after application. ZmEA1 formed aggregates after droplet release, indicating that the amount diffusing from the droplet into the medium and thus the true concentration of the attraction signal was probably significantly lower than 10 mM of the droplet. PT growth behavior was monitored for at least 2 hr. A total of 26.6% (n = 8) of monitored PTs (n = 30) changed growth direction toward the region containing ZmEA1 droplet placement (Figure 3.1 A and B). PTs were counted as positive when they changed growth direction by at least 20° and grew into the area of droplet placement. On average, PTs required between 10 and 29 min before a clear change in growth direction was visible, as shown in Figure 3.1 C and D. PTs continued to grow (Figure 3.1 E) and stopped growing after reaching the area of ZmEA1 droplet placement (Figure 3.1 F). They remained intact for more than 60 min (data not shown), which was visible by active cytoplasmic streaming. Thus, in addition to its known role as an attractant (Márton *et al.*, 2005), ZmEA1 might possess an additional function, namely to arrest PT growth at high concentrations (up to 10 mM in our experiments). None of the monitored maize PTs (n = 12) was attracted or arrested by other small proteins such as chemically labeled trypsin inhibitor (TI) from soybean (Figure 3.2 A-C). To prove ZmEA1 binding to PTs and to study their localization at the PT surface, we incubated maize PTs with the same chemically labelled ZmEA1. ZmEA1 mainly accumulated behind the PT apex - at the apical flank and subapical membrane domains - but not at the very tip of maize PTs (Figure 3.1 G and H). PTs follow chemical gradients by rapidly reorienting their growth. They achieve this change by the reorganization of the motion pattern of vesicles and of the actin cytoskeleton at the subapical region (Bou Daher and Geitmann, 2011), where ZmEA1 was also found to bind. This behavior was species preferential given that ZmEA1 binding has not been observed when PTs of *Nicotiana benthamiana* were incubated with a labeled ZmEA1 peptide with the same concentration and conditions (Figure 3.1 I). In contrast, labeled TI was found to bind rather nonspecifically to the whole surface of *Nicotiana benthamiana* PTs (Figure 3.2 E and F) but was unable to bind to maize PTs (Figure 3.2 D).

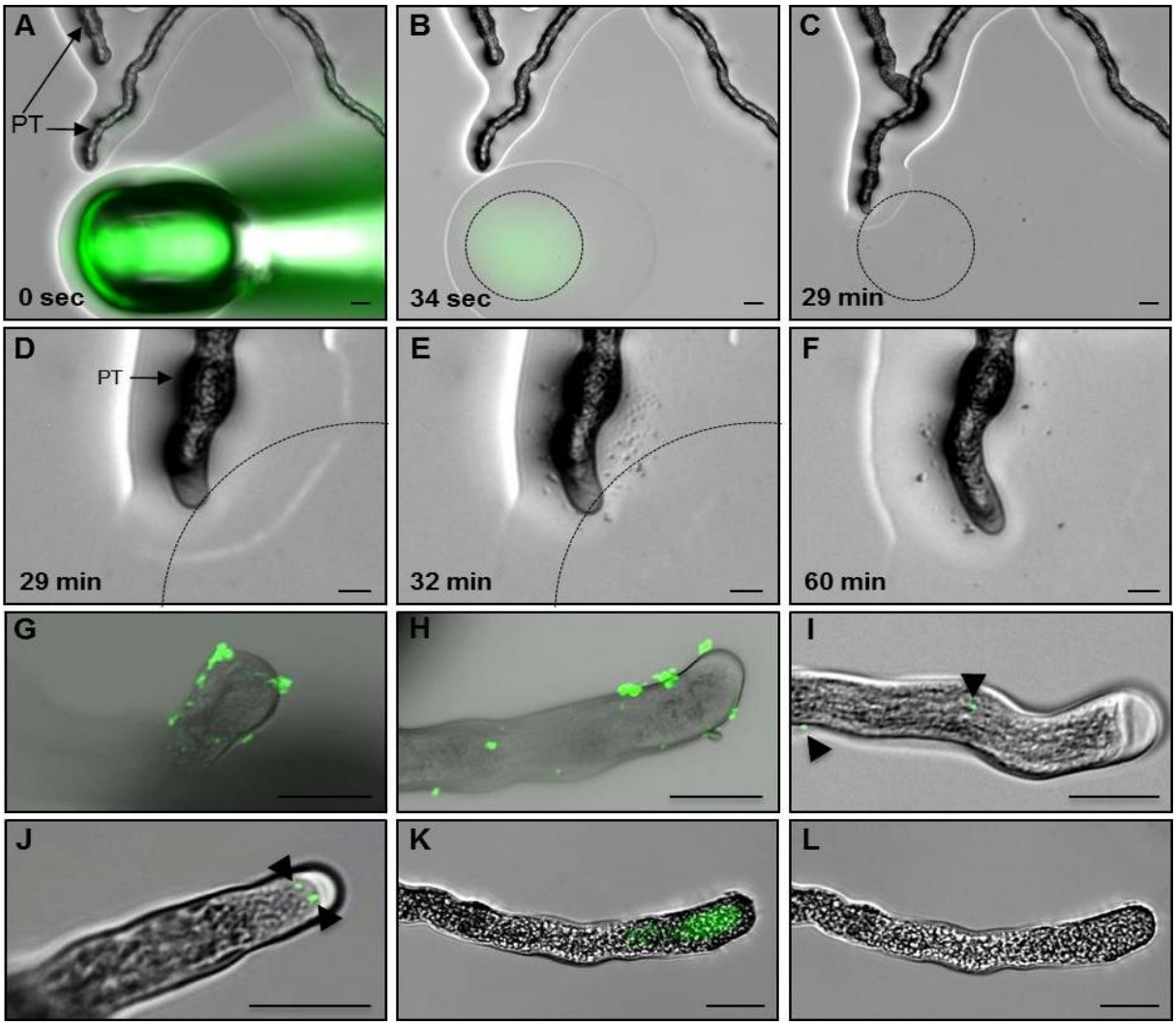

Figure 3.1 Predicted mature ZmEA1 attracts and arrests maize pollen tubes *in vitro* and binds in a species-preferential manner to the subapical region of the PT tip. *In vitro* PT guidance and binding assays with a synthetic predicted mature 49 amino acid ZmEA1 labeled with green fluorophore DyLight 488 NHS Ester. (**A**-**F**) A time series showing PT growth behavior after peptide application. Time points after the start of the experiment are indicated. (**A**) A microcapillary was used for the release of ZmEA1 less than 100 mm from an active maize PT. (**B**) 34 s after application, fluorescence signals were still detectable in the released droplet before complete invisibility 5 min after application. (**C**) 29 min after application, PT tip growth was reoriented toward the region containing ZmEA1 droplet placement. (**D**) A close-up image of (**C**). (**E**) The PT continued to grow toward the droplet, and 1 hr after droplet application, it reached its target, stopped growing (**F**), and remained intact and viable for more than 1 hr (data not shown). (**G**, **H**) One hour after incubation of PTs with labeled ZmEA1 and a subsequent series of washing steps, fluorescent signals were observed to accumulate mostly behind the apex at the apical flank and subapical membrane domains of maize PTs. (**I**) In contrast, with the same peptide concentration and conditions, *Nicotiana benthamiana* PTs did not interact with the peptide and displayed only a few randomly distributed signals over the whole PT surface (arrow heads). (**J**, **K**) Maize PTs displaying internalized labeled ZmEA1 in vesicles at the PT tip (arrow heads in **J**) and in larger amounts in the center of the PT (**K**). (**L**) 30 min after further observation of the PT shown in (**K**), fluorescence signals were no longer detectable; this indicates rapid degradation of the labeled peptide. Scale bars represent 20 mm.

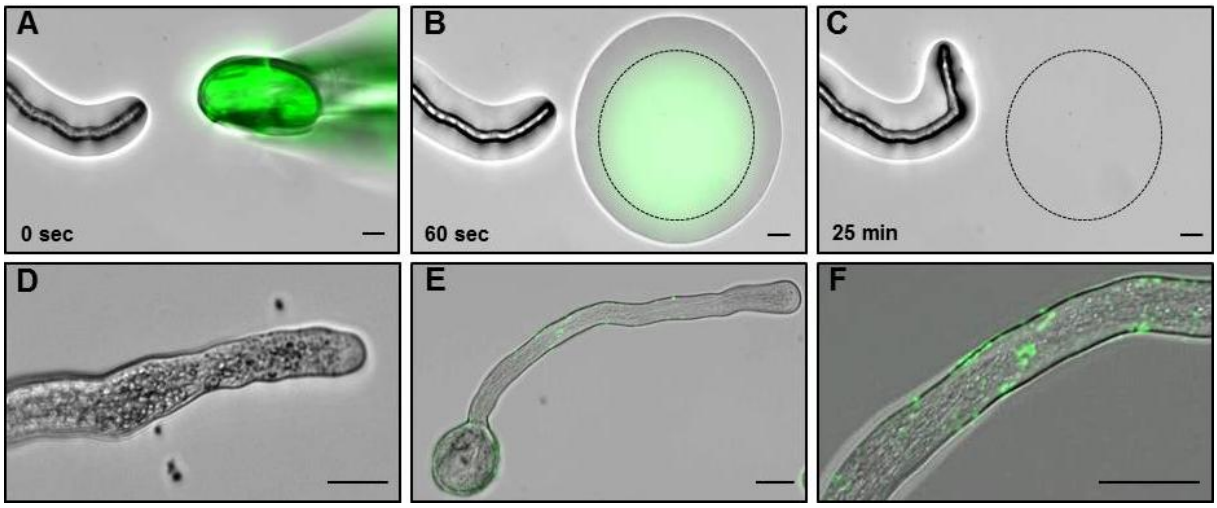

Figure 3.2 Unspecific proteins are unable to attract and bind maize pollen tubes *in vitro* (related to Figure 3.1). Trypsin inhibitor was used as an unspecific small protein to elucidate whether maize pollen tubes (PTs) are generally attracted by small proteins and whether PTs surfaces are capable to bind proteins unspecifically under the conditions applied. Scale bars represent 20 µm. (**A**-**C**) *In vitro* PT guidance assay using trypsin inhibitor (TI) that was chemically labeled with the fluorophore DyLight 488 NHS Ester. Time points after start of the experiment are indicated. (**A**) TI was released using a microcapillary at less than 100 µm distance from an active maize PT. (**B**) One minute after application, fluorescence signals of the labeled TI protein could be still detected on the medium. The signals were no longer visible 5 minutes later on (data not shown). (**C**) 25 minutes after application PT grows away from the droplet placement indicating that TI does not attract maize PTs *in vitro*. (**D**–**F**) *In vitro* incubation of maize and *Nicotiana benthamiana* PTs with the same chemically labeled TI protein. (**D**) One hour after incubation and washing fluorescence signals could not be detected at the tip or inside the maize PT. (**E**) In contrast, using the same labeled TI protein concentration and conditions, labeled TI protein could be detected randomly distributed at the surface of *Nicotiana benthamiana* PT and grain, respectively. (**F**) Close-up of a middle PT area shown in (**E**).

After binding, ZmEA1 most likely becomes internalized, as shown by the occurrence of internal granules containing DyLight-labeled ZmEA1 at the tip of maize PTs (Figure 3.1 J) or in larger amounts in the center of PTs (Figure 3.1 K). Thirty minutes later, after internalization, the fact that fluorescence signals could no longer be detected indicated that ZmEA1 had probably been rapidly degraded (Figure 3.1 L). This finding is similar to other reproductive proteins, such as *Nicotiana* S-RNase and lily SCA (stigma/stylar cysteine-rich adhesin), that are secreted from female tissues of plants and that have been shown to be internalized by PTs and sometimes sequestered into storage or degradative organelles (Goldraij *et al.*, 2006; Kim *et al.*, 2006). Although the exocytic and endocytic events during PT growth are still not precisely understood and described, the common view is that the prominent endocytic activity occurs

at the subapical membrane domain (Derksen *et al.*, 1995; Cheung and Wu, 2008). ZmEA1 might be internalized as a signal molecule by receptor-mediated endocytosis.

3. 3. 2 ZmEA1-GFP fusion proteins are predominantly localized to the filiform apparatus, the secretory zone of synergid cells in *Arabidopsis* ovules

Because of the technical difficulties associated with the above-described experimental *in vitro* system and the low number of PTs that could be observed and with the additional aim of attracting maize PTs by using ovules of an unrelated plant species, we first studied whether it would be possible to secrete ZmEA1 from the female gametophyte cells of the model plant *Arabidopsis thaliana*. Several *Arabidopsis* plant lines were generated to express a ZmEA1-GFP fusion protein under the control of the synergid-, egg-, and central-cell specific promoters *MYB98* (Kasahara *et al.*, 2005), EC1 (Ingouff *et al.*, 2010), and DD65 (Steffen *et al.*, 2007), respectively. Although transcripts were detected in all transgenic lines generated independently of the promoters used (data not shown), fluorescence signals could be detected only in the lines in which the ZmEA1-GFP fusion protein was expressed under the synergid-cell-specific promoter *MYB98*. Here, microscopy analysis of 18 independent lines showed fluorescence signals most strongly in the filiform apparatus (Figure 3.3 A–D), a thickened extracellular structure generated by cell-wall invaginations of both synergid cells. This apoplastic structure seems to play an important role in PT guidance and reception because it can take up and export vesicle contents - such as PT attractant(s) - secreted by the synergid cells (Kasahara *et al.*, 2005; Punwani and Drews, 2008). Thus, the ZmEA1-GFP fusion protein seems to be secreted via the secretory pathway. Inside synergid cells, the fusion protein was mainly visible in small vesicles of unfertilized *Arabidopsis* ovules (Figure 3.3 C). Expression of free *GFP* under the control of the *MYB98* promoter showed fluorescence signals exclusively in the cytoplasm and nuclei of synergid cells (Figure 3.3 E-F and Figure 3.4 D). This result supports a previous presumption that, similar to follicle cells in mammals, synergid cells might contain cell-type-specific secretion machinery and function as the “glandular cells” of the female gametophyte (Márton and Dresselhaus, 2008). The rapid loss of GFP signal already 24 hr after *in vitro* pollination in maize ovules suggests that proteolysis might be a regulatory pathway for degrading ZmEA1 after fertilization so that, most likely, polyspermy can be avoided. This feature is considered a major characteristic of a PT attractant derived from the female gametophyte (Márton *et al.*, 2005; Higashiyama and Hamamura, 2008). In *Arabidopsis*, ZmEA1-GFP fluorescence signals could be detected at the micropylar region in de-

veloping seeds at least 2 days after fertilization until signals disappeared (data not shown), indicating that ZmEA1 is not actively degraded in this species.

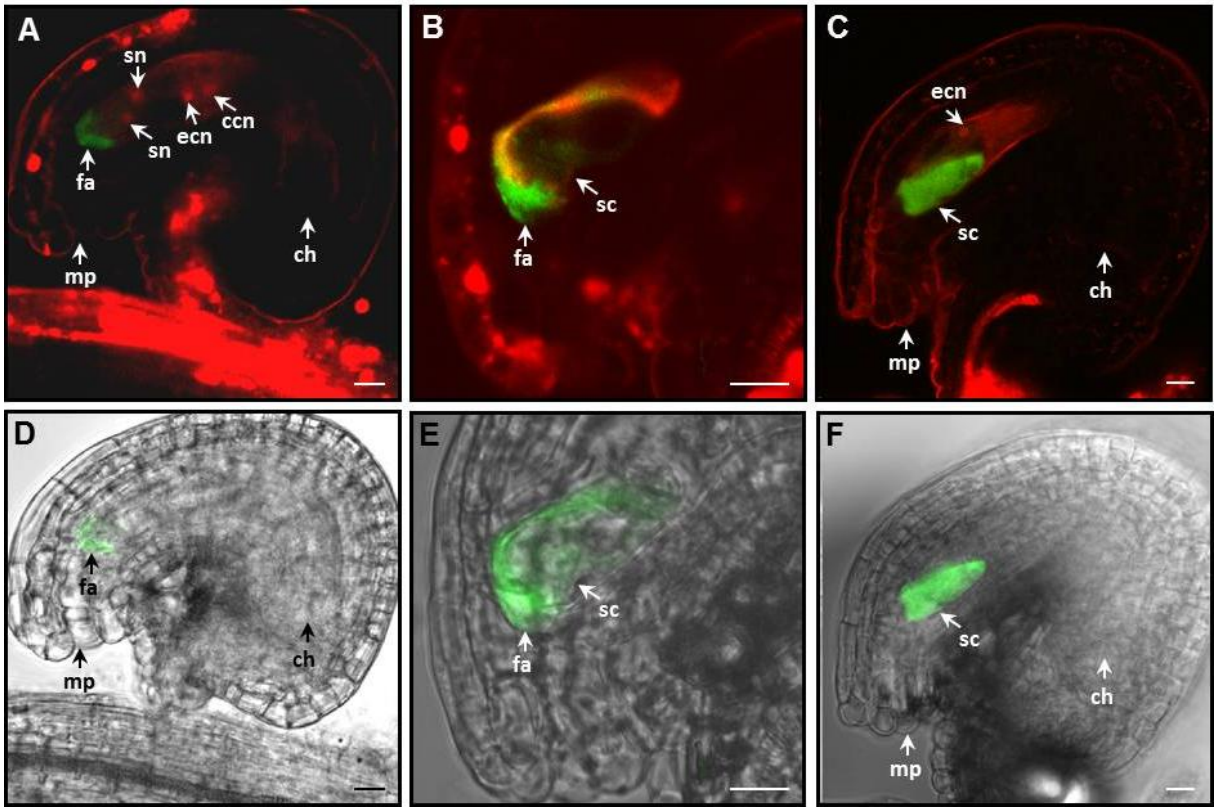

Figure 3.3 ZmEA1-GFP fusion protein is secreted to the filiform apparatus of *Arabidopsis* ovules. A maize ZmEA1-GFP precursor protein was expressed in *Arabidopsis* ovules under the control of the synergid-cell-specific promoter *MYB98*. Propidium iodide was used for counterstaining so that nuclei and cell structures could be visualized. Two examples (**A**, **D** and **B**, **E**) show ZmEA1-GFP localization within the cytoplasm and small vesicles in the synergid cells; the strongest signals are in the filiform apparatus. The corresponding control (**C**, **F**) with free GFP is expressed in the cytoplasm under the control of the synergid-cell-specific promoter *MYB98*. The overlay between green and red channels is shown in (**A**-**C**), and the overlay between green and bright-field channels is shown in (**D**-**F**). The following abbreviations are used: ccn, central-cell nucleus; ch, chalazal region of the ovule; ecn, egg-cell nucleus; fa, filiform apparatus; mp, micropyle; sc, synergid cell; sn, synergid nucleus. Scale bars represent 10 mm. See also Figure 3.4.

We have previously mapped the transcription start point of ZmEA1 (Márton *et al.*, 2005) and indicated that the predicted mature 49 amino acid peptide (sEA1, Figure 3.4 A) is generated from a 94 amino acid precursor protein containing a hydrophobic transmembrane region that probably represents an internal signal recognition motif. However, grass genome annotations have predicted shorter EA1 precursor proteins, such as a 76 amino acid protein (spEA1) with an N-terminal signal sequence (Figure 3.4 A).

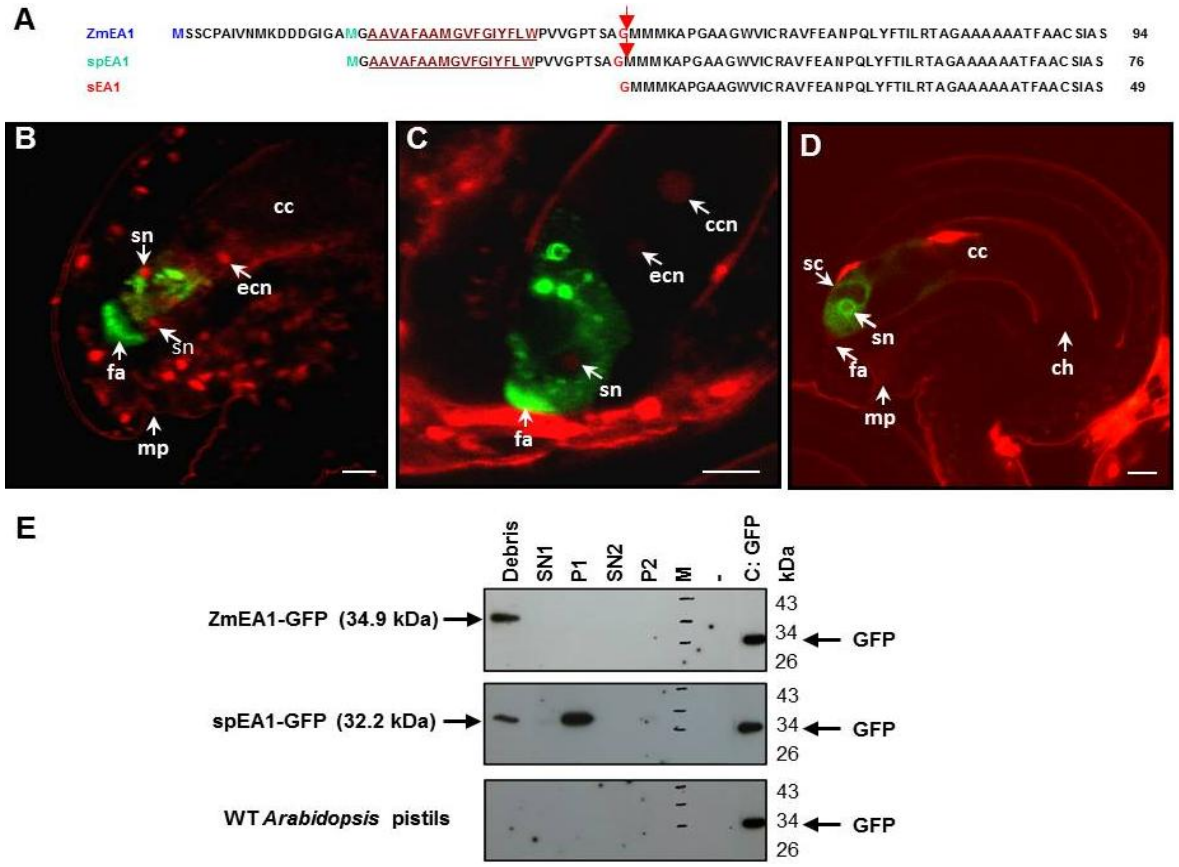

Figure 3.4 ZmEA1 variants containing an internal or N-terminal signal recognition motif are secreted to the filiform apparatus of *Arabidopsis* ovules (related to Figure 3.3). (**A**) ZmEA1 precursor proteins are either predicted to consist of 94 amino acids (ZmEA1) containing an internal signal recognition motif or as a shorter protein of 76 amino acids (spEA1) containing an N-terminal signal sequence. Signal motifs are underlined and indicated in dark red. Arrows point toward the predicted cleavage site generating a mature peptide of 49 amino acids (sEA1). (**B**, **C**) Similar to the longer ZmEA1-GFP fusion protein (shown in Figure 3.3), the shorter GFP fusion protein (spEA1-GFP) is secreted to the filiform apparatus of *Arabidopsis* ovules using the synergid cell-specific promoter *MYB98*. Note that in contrast to the longer protein shown in Figure 3.3, stronger signals and large vesicles are visible in the cytoplasm. The following abbreviations are used: cc, central cell; ccn, central cell nucleus; ecn, egg cell nucleus; fa, filiform apparatus; mp, micropyle; and sn, synergid nucleus. Scale bars represent 10 µm. (**D**) Free GFP under control of the same *MYB98* promoter is visible in the cytoplasm and nucleus of synergid cells, but not in the filiform apparatus. To visualize cell borders and nuclei, ovules were counterstained with propidium iodide (red color). The following abbreviations are used: cc, central cell; ch, chalazal region of the ovule; fa, filiform apparatus; mp, micropyle; sc, synergid cell; and sn, synergid nucleus. Scale bars represent 10 µm. (**E**) Immunoblot analysis with protein extracts from *Arabidopsis* pistils expressing either ZmEA1-GFP or spEA1-GFP. Non-transgenic wild type pistils are used as a control. Free GFP (26.9 kDa) was used as a positive control. Proteins were detected using an anti-GFP antibody. ZmEA1-GFP was only detected in the cell debris sample, while the shorter protein spEA1-GFP was detected in cell debris, most strongly in pellet 1 (P1), and weekly in supernatant 1 (SN1) and in pellet 2 (P2). Note that the size of spEA1-GFP protein band matches with the predicted processed sEA1-GFP fusion protein (32.2 kDa) indicating that spEA1-GFP was likely processed at the predicted cleavage site shown in (**A**).

We have therefore also expressed and localized the shorter ZmEA1 variant (spEA1) in *Arabidopsis* ovules and detected its GFP-fusion protein mainly in the filiform apparatus as well as inside synergid cells in small vesicles (Figure 3.4 B and C) similar to the longer version of the protein. However, in contrast to the ZmEA1-GFP fusion protein, a number of larger aggregates were formed in spEA1-GFP-expressing synergid cells. The presence of ZmEA1-GFP or spEA1-GFP fusion proteins in *Arabidopsis* ovules has been confirmed by immunoblot analyses (Figure 3.4 E).

3. 3. 3 Maize PTs are attracted *in vitro* by *Arabidopsis* ovules expressing ZmEA1-GFP fusion protein in synergid cells

In order to compare attraction of maize PTs by unfertilized wild-type (WT) *Arabidopsis* ovules and ovules expressing a ZmEA1-GFP fusion protein driven by the synergid-specific *MYB98* promoter, we established a PT competition assay (PTCA). For each experiment, one WT and one ZmEA1-GFP-expressing *Arabidopsis* ovule were placed close to each other and at the same distance (up to 100 mm) from an actively growing maize PT. PT growth behavior was monitored for at least 2 hr.

Remarkably, more than 51% (n = 17) of all monitored maize PTs (n = 33) changed their growth direction and were attracted by ZmEA1-GFP-expressing *Arabidopsis* ovules as shown in Figure 3.5 A-D. Growth of PTs was arrested after guidance at (33.3% [n = 11]) or close to (18.2% [n = 6]) the micropylar opening of ovules (Figure 3.5 D and I). Only these two categories were considered as guided PTs. A total of 33.3% of PTs (n = 11) were not attracted by transgenic ovules, and only a few of them (n = 3 [9% of total analyzed PTs]) grew toward WT ovules without being arrested. Moreover, 15.2% (n = 5) of the total monitored PTs changed direction toward transgenic ovules but did not cease growing (Figure 3.5 I). Because of the small size of the micropylar opening (around half of the diameter of a maize PT) of *Arabidopsis* ovules, tubes might not have been capable of entering the ovule. However, the observed growth arrest might also have occurred as a result of the highest concentration of ZmEA1-GFP at the micropyle phenocopying the effect that has been found for the synthetic ZmEA1 (Figure 3.1 A-F). WT or free-GFP expressing *Arabidopsis* ovules were not capable of attracting maize PTs (Figure 3.5 E-I). None of the maize PTs was attracted by *Arabidopsis* ovules and ceased to grow. Only a few maize PTs seemed to grow toward the micropyle of WT (n = 4 [15.4%]) or free-GFP-expressing (n = 2 [18.2%]) *Arabidopsis* ovules, but they continued to grow without arrest (Figure 3.5 I).

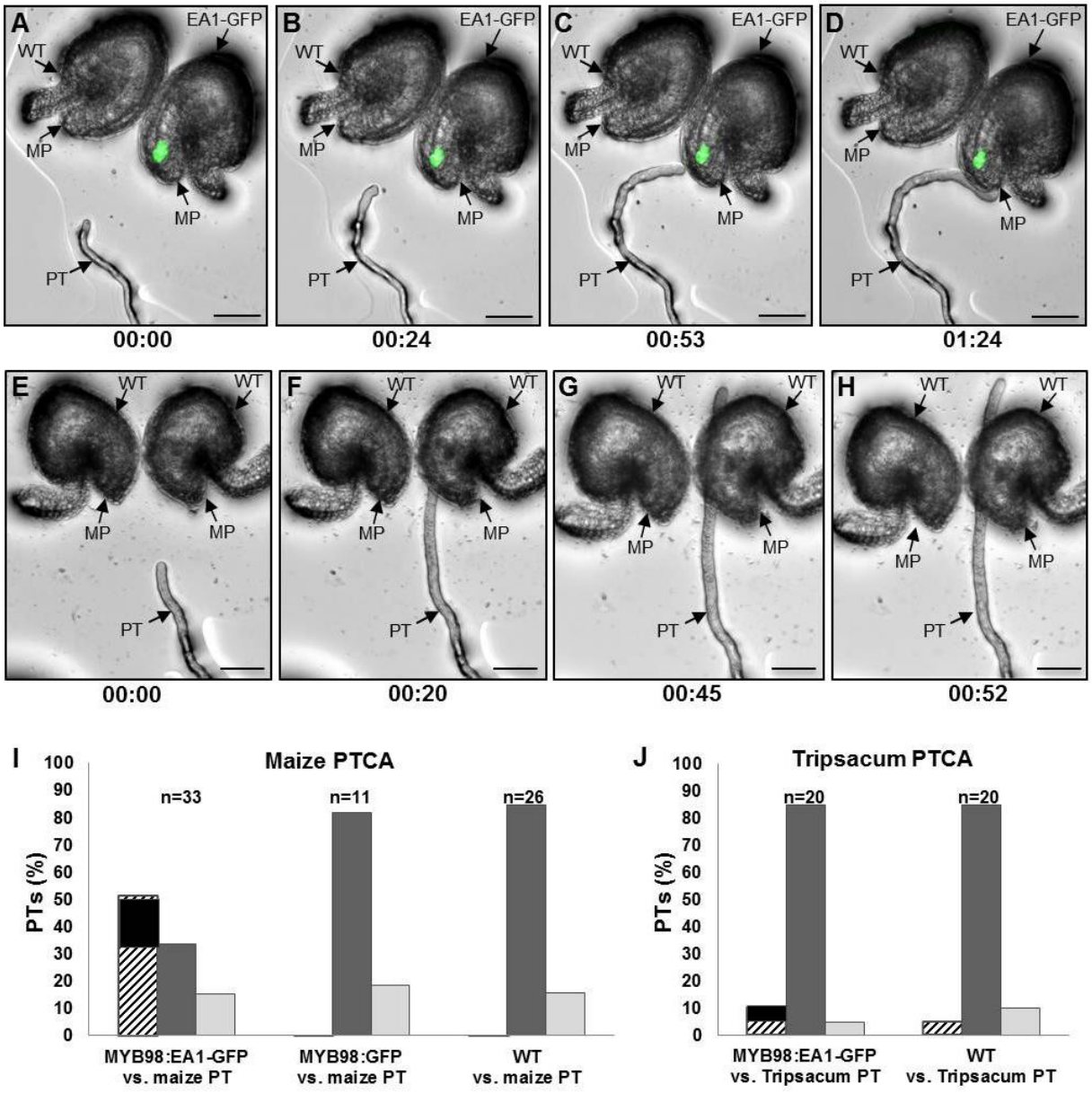

Figure 3.5 ***In vitro*** **PT competition assay showing ZmEA1-mediated attraction of maize PTs by** ***Arabidopsis*** **ovules.** The ZmEA1-GFP fusion protein was expressed in *Arabidopsis* ovules under the control of the synergid-cell-specific promoter *MYB98*. A PTCA was established for the comparison of attraction by WT with attraction by the ZmEA1-GFP-expressing *Arabidopsis* ovules indicated by green synergid cells. The time frame (hr:min) of each experiment in (**A**-**H**) is indicated below each image. (**A**-**D**) A maize PT is guided to the micropylar region of a ZmEA1-GFP-expressing ovule. (**B**) 24 min after ovule exposure, PT tip growth was already reoriented toward the transgenic ovule, (**C**) grew toward the micropylar tip, and (**D**) ceased to grow at the micropylar opening without penetration. (**E**-**H**) *Arabidopsis* ovules are not capable of attracting maize PTs. (**I**) Statistical analysis of the maize PTCA shows that in contrast to free-GFP-expressing *Arabidopsis* ovules (*MYB98*:*GFP*) and to WT *Arabidopsis* ovules, >50% of maize PTs are attracted by the ZmEA1-GFP-expressing *Arabidopsis* ovules (*MYB98:EA1-GFP*). (**J**) Statistical results from a PTCA with PTs of the maize relative *Tripsacum dactyloides*. Only 10% of monitored PTs were attracted and stopped at *Arabidopsis* ovules expressing the ZmEA1-GFP fusion protein, whereas 5% of PTs grew and stopped at the micropylar region of WT ovules. Striped and

black columns show maize and *Tripsacum* PTs that stopped at or close to, respectively, the micropylar opening of *Arabidopsis* ovules. Dark-gray columns indicate PTs that were not attracted, whereas light-gray columns show PTs that grew toward the micropylar region but did not stop growing. The following abbreviations are used: EA1-GFP, ZmEA1-GFP expressing *Arabidopsis* ovule; MP, micropyle; PT, pollen tube; PTCA, PT competition assay; and WT, wild-type *Arabidopsis* ovule. Scale bars represent 50 mm. See also Figure 3.6.

We performed semi-*in-vivo* PT guidance assays as controls to show that competent *Arabidopsis* PTs were attracted by both WT and ZmEA1-GFP-expressing *Arabidopsis* ovules; the fact that the PTs were attracted by both ovules indicates that there was neither an obvious morphological difference nor a functional difference between both types of ovules (Figure 3.6 A-D).

We further used the *Arabidopsis* PTCA to study the species specificity of the maize PT attractant ZmEA1. PT growth behavior of the closest maize relative, *Tripsacum dactyloides*, was monitored in the presence of WT and ZmEA1-GFP expressing *Arabidopsis* ovules. In the two types of assays, the majority of PTs were not attracted by either the transgenic ovules (85% of PTs [n = 17]) or the WT ovules (85% of PTs [n = 17]) within a distance of less than 100 mm (Figure 3.5 J and Figure 3.6 E-L). Fifteen percent of PTs (n = 3) changed growth direction toward the micropyle of ZmEA1-GFP expressing ovules, but only 10% ceased to grow at or close to the micropylar opening, whereas 5% continued to grow. When only WT ovules were used, 5% of *T. dactyloides* PTs seemed to be attracted and stopped growing at the micropylar opening of ovules, whereas 10% continued to grow. These observations indicate that micropylar guidance and growth arrest of *T. dactyloides* PTs are not notably influenced by ZmEA1-GFP secretion from *Arabidopsis* ovules. These observations support findings in dicotyledonous species with excised *Arabidopsis* and *Torenia* ovules as well as with LURE peptides, suggesting that micropylar or short-range PT guidance is species preferential (Okuda *et al.*, 2009; Kanaoka *et al.*, 2011; Palanivelu and Preuss, 2006). However, the finding that *Tripsacum* PTs are able to fertilize maize ovules at a high frequency *in vivo* (Mangelsdorf and Reeves, 1931) might indicate that PTs of this species require a growth phase during the transmitting tract to become competent to recognize female-derived signals similar to reports from *Torenia*, *Arabidopsis*, and other wild dicot plant species (Higashiyama *et al.*, 2006; Qin *et al.*, 2009). Cultivated species such as maize have been selected for hundreds of years for inbreeding and might have lost this prerequisite, as shown by the finding that >50% of maize PTs fully germinated and grown *in vitro* were capable of finding the *Arabidopsis* source of ZmEA1.

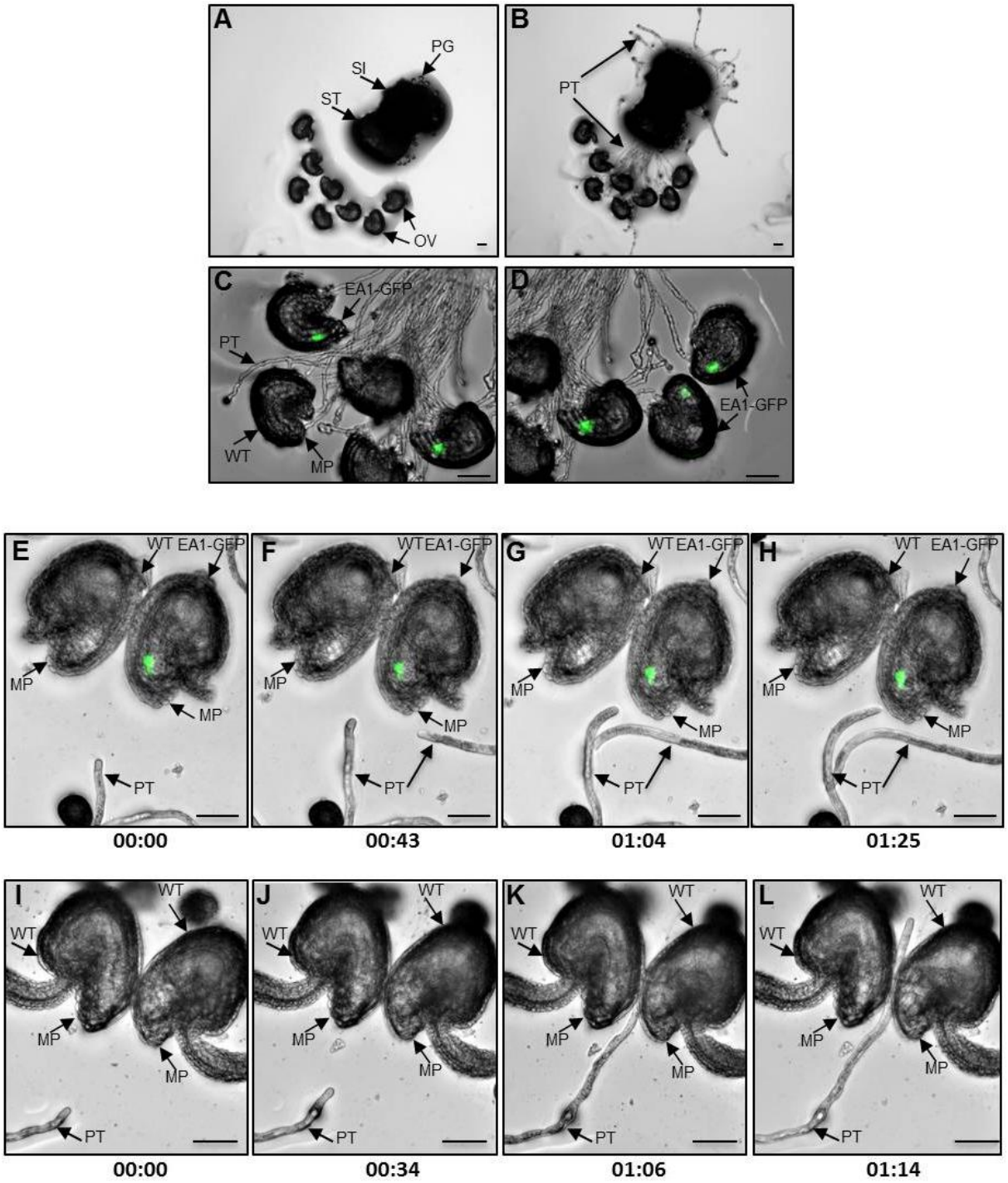

Figure 3.6 Secretion of ZmEA1-GFP fusion protein from *Arabidopsis* synergid cells enables *Arabidopsis* ovules to attract own competent pollen tubes and shows no significant influence on micropylar guidance and growth arrest of *Tripsacum dactyloides* pollen tubes (related to Figure 3.5). (**A-D**) Merged fluorescent and bright field images show heterozygous *Arabidopsis* ovules containing the construct *MYB98*:*ZmEA1-GFP* expressing the ZmEA1 precursor protein in synergid cells. The following abbreviations are used: EA1-GFP, ZmEA1-GFP expressing ovule; MP, micropyle; OV, ovule; PG, pollen grain; PT, pollen tube; SI, stigma; ST, style; WT, wild-type *Arabidopsis* ovule. Scale bars represent 50 µm. (**A**) A pollinated *Arabidopsis* pistil was cut at the junction between the style and the ovary and placed horizontally on pollen growth medium closely (~2 mm) to dissected *Arabidopsis* ovules. Note pollen grains at the surface of stigmatic papillae cells. (**B**) 20 hr after

pollination the majority of pollen tubes (PTs) emerged from the cut portion of the pistil and grew on the agarose medium before entering excised wild type or ZmEA1-GFP expressing *Arabidopsis* ovules. (**C**, **D**) Enlarged regions of (**B**) where *Arabidopsis* PTs are visible penetrating both WT and transgenic *Arabidopsis* ovules, respectively. (**E**-**L**) The PT competition assay (PTCA) was used to compare attraction of PTs from the maize relative *Tripsacum dactyloides* between wild-type (WT) and ZmEA1-GFP fusion protein expressing *Arabidopsis* ovules indicated by green synergid cells. The time frame of the experiments (h:min) is indicated below images. The following abbreviations are used: EA1-GFP, ZmEA1-GFP expressing ovule; MP, micropyle; PT, pollen tube; WT, wild type *Arabidopsis* ovule. Scale bars represent 50 μm. (**E**-**H**) 43 min after starting the experiment, the tip of the first monitored PT was reoriented (**F**) and grew straight toward the micropylar region and stopped growing (**H**). Note that at the same time a second PT grew closely to the micropyle, but it did not change direction and instead continued to grow. (**I**-**L**) Wild-type *Arabidopsis* ovules were not capable to attract *T. dactyloides* PTs.

3. 4 Conclusions

In summary, we present evidence that ZmEA1 is a species-preferential direct attractant of PTs in maize. It binds to the subapical region of PT tips and arrests their growth at higher concentrations. Moreover, we show that secreting ZmEA1 from *Arabidopsis* synergid cells enabled *Arabidopsis* ovules to attract maize PTs *in vitro*, indicating that it is generally possible to overcome wide crossing barriers by combining genetic engineering with the tools currently being developed in plant reproduction research. Once the ZmEA1-ligand-receptor complex is identified, it might be possible for the research community to introduce the whole complex into various grass species for usage as a tool for future plant breeding programs to overcome species-specific micropylar prezygotic crossing barriers and to enable hybridization between plant genera that cannot be crossed today.

CHAPTER 4 - SPECIES-SPECIFIC INTERACTION OF EA1 WITH THE MAIZE POLLEN TUBE APEX

This CHAPTER is based on the manuscript Uebler *et al.,* 2013, in *Plant Signaling & Behavior*. S. Uebler performed all experiments and wrote the manuscript except the introduction paragraph. The manuscript was edited by T. Dresselhaus and M. Márton.

4. 1 Introduction

After successful adhesion, hydration and germination on a receptive stigma, flowering plants (angiosperms) transport and deliver the two non-motile sperm cells to the female gametophyte via a highly specialized cell type, the pollen tube, for the achievement of double fertilization. Genetic studies have shown that the pollen tube path is controlled by various cross-incompatible (interspecific) and self-incompatible (intraspecific) hybridization mechanisms likely involving a larger number of species-specific molecular players (Lausser *et al.,* 2010; Dresselhaus *et al.,* 2011; Palanivelu and Tsukamoto, 2012). Among the molecules involved, maize EA1 (Egg Apparatus 1) was the first female gametophyte expressed signaling molecule identified to be required for pollen tube guidance during the last step of the journey (Márton *et al.,* 2005). The egg apparatus specifically expressed *EA1* is encoding a 94 amino acids hydrophobic precursor protein with a predicted N-terminal transmembrane domain. We have previously shown that a GFP fusion protein of EA1 is secreted from the egg apparatus and accumulates in the cell walls of micropylar nucellar cells, and that its knockdown triggers loss of micropylar pollen tube guidance (Márton *et al.,* 2005). EA1 belongs to a novel class of hydrophobic and polymorphic peptides, of which until now only one additional member, EAL1 (EA1-like1) has been functionally characterized in maize and was shown to be involved in regulating cell fate of female gametophyte cells (Krohn *et al.,* 2012).

EA1-like peptides do not exist in eudicotyledonous plant species. In the eudicot model plant *Torenia fournieri* cysteine-rich defensin-like proteins were identified as LUREs to attract own pollen tubes in a species-preferential manner (Okuda *et al.,* 2009). LUREs have been identified recently also in *Torenia concolor* (TcCRP1) and in *Arabidopsis* species (AtLURE1 and AlLURE1) (Kanaoka *et al.,* 2011; Takeuchi and Higashiyama, 2012). In a recent publication we could show that EA1 acts as a species-preferential direct attractant of maize pollen tubes

in vitro. *Arabidopsis* ovules secreting the peptide are capable to guide maize pollen tubes in a species-preferential manner toward the micropylar opening of the ovule (Márton *et al.*, 2012).

4. 2 Experimental procedures

4. 2. 1 Chemical labeling of synthetic peptides

Predicted mature EA1 peptide of 49 amino acids (Márton and Dresselhaus, 2010) was chemically synthesized with 80%-90% HPLC-purity by Centic Biotec. Successful synthesis of the linear peptide was shown by LC-MS. Chemically labeling of the synthetic EA1 peptide was performed with fluorophore DyLight 488 NHS Ester (Thermo Scientific) according to the manufacturer's protocol with a number of modifications. 0.5 mg peptide was first dissolved in 100% DMSO and then diluted stepwise in 0.1 M sodium phosphate, 0.15 NaCl (pH 7.4) to a final concentration of 1% DMSO. The protein solution was mixed with an aliquot of the fluorophore DyLight 488 NHS Ester. After 1.5 h incubation at room temperature the mixture was dialyzed against 0.1 M sodium phosphate, 0.15 NaCl (pH 7.4) with a final concentration of DMSO not exceeding 1% using a Slide-A-Lyzer® MINI Dialysis Unit (Thermo Scientific). Precipitates were removed by centrifugation at 10.000 g. Predicted mature EAL2 consisting of 52 amino acids (Dresselhaus *et al.*, 2011) was chemically synthesized with 80%-90% HPLC-purity by Centic Biotec. The chemical labeling of the peptide was performed using the same method described above.

4. 2. 2 Pollen tube binding assay

The pollen tube binding assay was conducted as follows: in order to obtain pollen tubes, pollen grains of maize inbred lines or *Tripsacum dactyloides* were shaken shortly after anthesis directly onto 10 µl droplets of 1xPGM (Schreiber and Dresselhaus, 2003) containing a final concentration of 1% DMSO placed in a 35 mm plastic Petri dish. Pollen of *Nicotiana benthamiana* was transferred directly from a freshly opened anther onto drops of 1xPGM with 1% DMSO using forceps. Pollen of lily was directly taken one day after anthesis, dried at room temperature for at least 1 day and transferred directly into 1.5 ml of 1xPGM containing 1% DMSO in a 25 mm plastic Petri dish using forceps. Germination of maize and *T. dactyloides* pollen was performed for 30 to 45 min, while *N. benthamiana* pollen was germinated for 60 to 90 minutes and lily pollen over night for 14-15 hours. All incubations were performed at room temperature. Further on, 1 µl of chemically labeled EA1 or EAL2 were added

to each droplet containing germinated pollen of maize, *T. dactyloides* or *N. benthamiana*. Germinated lily pollen were transferred step by step onto an object slide using a cut pipette tip and the media was removed to concentrate pollen into a final volume of 100 µl. Subsequently, 10 µl of chemically labeled peptide were added. After incubation of germinated pollen of maize, *T. dactyloides* and *N. benthamiana*, the content of each droplet was transferred carefully using a cut pipette tip onto an object slide, to which 1xPGM containing 1% DMSO was added to a final volume of 200 µl. Samples were then washed on the object slide very carefully 3 times, using each time 200 µl 1xPGM with 1% DMSO, and resuspended in 500 µl 1xPGM with 1% DMSO. Microscopic analysis was initiated immediately after washing using a Zeiss Axiovert 200M LSM 510 META confocal laser scanning microscope.

4. 3 Results and discussion

In addition to the above work, we have now visualized the interaction of EA1 peptide derived from the maize inbred line A188 with pollen tubes of various maize inbred lines, a maize relative and two non-grass species *in vitro*. Therefore we performed several modified *in vitro* pollen tube binding assays based on Márton *et al.*, 2012. For each experiment we used freshly germinated pollen of the maize inbred lines B73, A188 and HiIIA, of *Tripsacum dactyloides*, *Lilium* "Stargazer" and *Nicotiana benthamiana*, respectively. Pollen tubes were incubated either with synthetic predicted mature EA1 or its homologous peptide EAL2 (EA1-like2) (Dresselhaus *et al.*, 2011) that were both labeled with the green fluorophore DyLight 488 NHS Ester. Binding of labeled EA1 could be observed at the pollen tube apex for all maize lines (Figure 4.1 A–H), but was weaker with HiIIA pollen compared with the other inbred lines (see also Table 4.1).

Table 4.1 Summary of *in vitro* pollen tube binding assays of three maize inbred lines, *Tripsacum dactyloides*, *Lilium* "Stargazer" and *Nicotiana benthamiana*, respectively.

Peptide vs. PTs	+ DyLight 488-labeled sEA1	+ DyLight 488-labeled EAL2
Zea mays A188	++	-
Zea mays B73	++	-
Zea mays HiIIA	+	-
Tripsacum dactyloides	-	-
Lilium "Stargazer"	-	-
Nicotiana benthamiana	-	-

Experiments were either performed with synthetic predicted mature EA1 or EAL2 peptides both labeled with the green fluorophore DyLight 488 NH S Ester. PT, pollen tubes; vs.,vs.; +, interaction; -, no interaction.

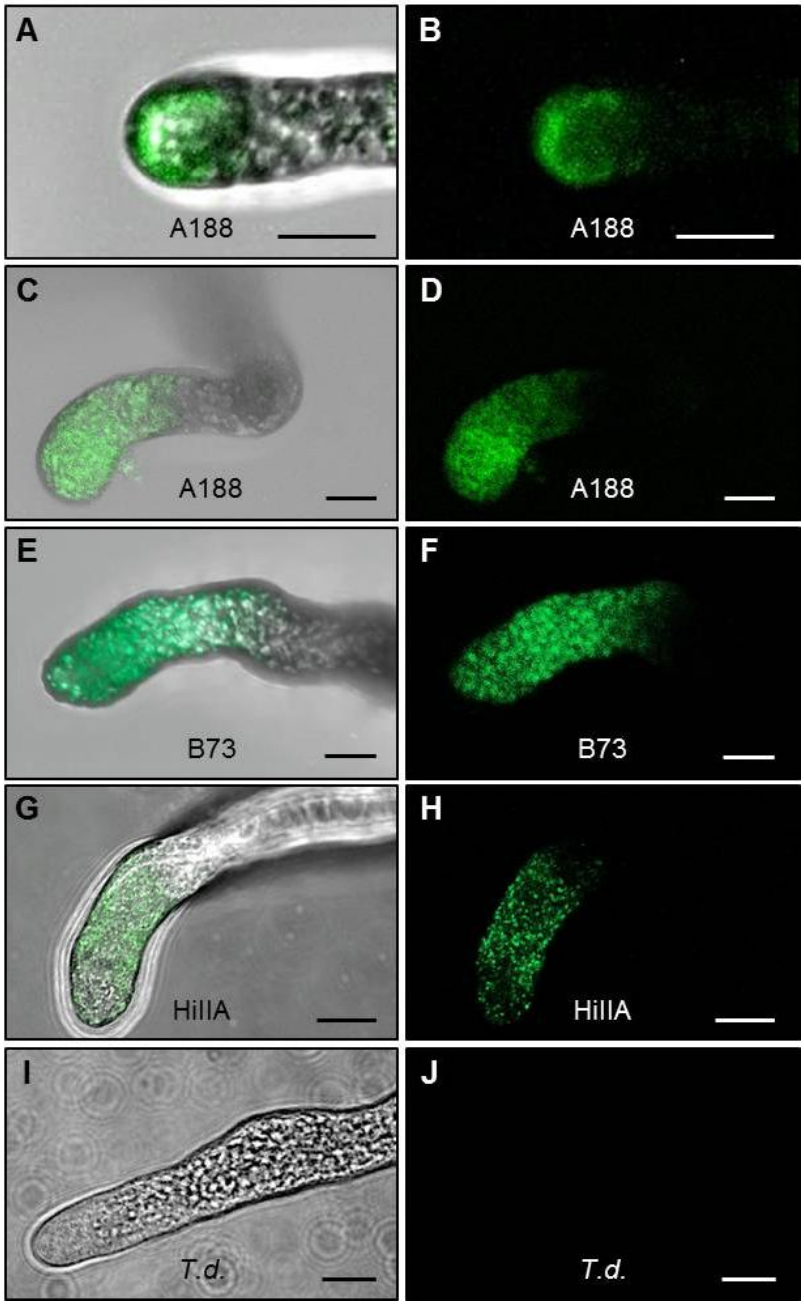

Figure 4.1 EA1 peptide interacts with the maize pollen tube apex in a species-specific manner. *In vitro* tube binding assays of three maize inbred lines and the maize relative *Tripsacum dactyloides* (*T.d.*) were performed with synthetic predicted mature EA1 peptide labeled with the green fluorophore DyLight 488 NHS Ester. Z-projections of confocal image stacks of 6 to 20 µm thick sections are shown in each panel. (**A, C, E, G, I**) Merged bright field and fluorescence micrographs. (**B, D, F, H, J**) UV-fluorescence images. (**A, B**) Labeled EA1 fluorescence is visible at the apical membrane region of a A188 pollen tube tip. (**C-H**) Pollen tubes of A188, B73, and HiIIA, respectively, displaying fluorescence at their apical region in vesicle-like structures, whereas (**I, J**) fluorescence is not detectable from *T. d.* pollen tubes. Scale bars represent 10 µm.

The peptide could also be detected inside vesicles within the pollen tube apex region. These data indicate that the peptide is recognized specifically at the pollen tube membrane and gets immediately internalized. Binding events could not be observed with the related EAL2 control peptide (Figure 4.2), demonstrating a highly specific interaction of EA1 with its receptor.

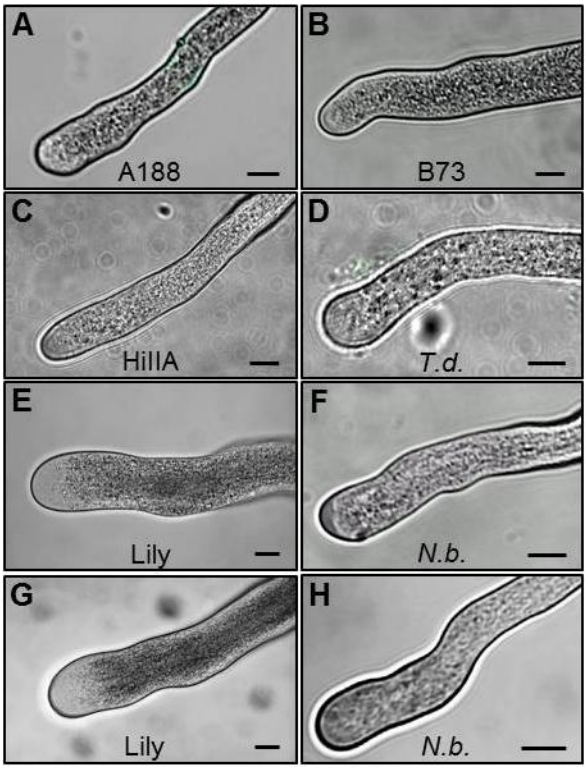

Figure 4.2 EA1-related EAL2 peptide does not interact with maize and *Tripsacum dactyloides* pollen tube tips. Moreover, lily (*Lilium longiflorum* "Stargazer") and tobacco (*N. benthamiana*) pollen tubes are neither bound by EA1 nor EAL2, respectively. *In vitro* pollen tube binding assays of the maize inbred lines A188, B73 and HiIIA, *Tripsacum dactyloides* (*T.d.*), lily and *Nicotiana benthamiana* (*N.b.*) were performed as controls at the same concentration and condition like in Figure 3.1 either with synthetic predicted mature EAL2 (**A**, **B**, **C**, **D**, **E**, **F**) or EA1 (**G**, **H**) peptides both labeled with the green fluorophore DyLight 488 NHS-ester. Each panel shows merged micrographs of bright field and fluorescence Z-projections of confocal image stacks of 10 to 20 µm thick sections, respectively. Scale bars represent 10 µm.

Until now only few ligand-receptor pairs for cell-to-cell communication are described in plants and they mainly involve receptor-like kinases (RLKs). One of the best characterized RLKs is CLAVATA1 (CLV1) which is bound by the signaling peptide CLAVATA3 (CLV3) to control stem cell fate in the shoot apical meristem (Ogawa *et al.,* 2008). Other signaling peptides include EPIDERMAL PATTERNING FACTOR 1/2 (EPF1/2), which are regulating stomatal patterning via interaction with the ERECTA family RLKs (Lee *et al.,* 2012), and INFLORESCENCE DEFICIENT IN ABSCISSION (IDA), which is signaling through the RLKs HAESA (HAE) and HAESA-LIKE2 (HSL2) during floral abscission and lateral root emergence (Butenko *et al.,* 2003; Kumpf *et al.,* 2013). In the Brassicacea binding of the pollen-coat protein S-Locus Cysteine-Rich/SProtein-11 (SCR/SP11) to the stigma-specific S-locus Receptor Kinase (SRK) regulates sporophytic self-incompatibility, which is a reproductive strategy for preventing self-fertilization and allowing genetic diversity to be maintained (Iwano and Takayama, 2012).

Although it still has to be shown whether the EA1 peptide also acts through a proteinaceous membrane receptor, it is conceivable that it may be recognized either by a tip-localized transmembrane RLK protein or an ion channel. The RLK superfamily forms a large receptor group in plants with more than 100 RLKs expressed in pollen of *Arabidopsis* (Shiu and Bleecker, 2001; Qin and Yang, 2011). A subsequent signal transduction pathway could lead to reorientation of the polar tip growth toward the source of the attractant, since the direction of pollen tube growth is controlled at its tip involving Rho GTPase signaling (Qin and Yang, 2011). The receptor might also represent an ion channel, which have been shown to be involved in pollen tube growth and guidance (Dresselhaus and Franklin-Tong, 2013). To avoid circular tube growth, one would expect such a reorientation signal to be transient and short for fine-tuning of the growth direction. A ligand-receptor complex thus must be inactivated, dissociated, degraded or internalized shortly after signal transduction pathway(s) are initiated.

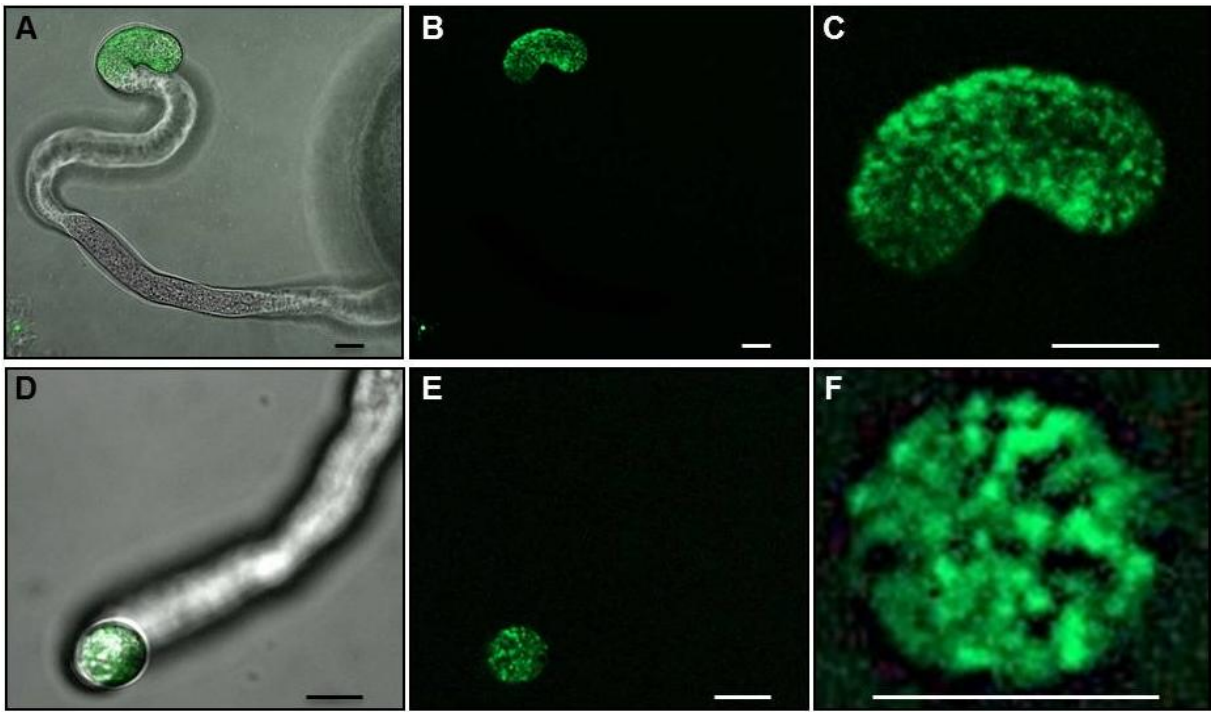

Figure 4.3 DyLight-labeled synthetic EA1 peptide gets internalized in vesicles at the apical region of the maize pollen tube tip. (**A**, **D**) Merged bright field and fluorescence micrographs. (**B**, **C**, **E**, **F**) UV-fluorescence micrographs. (**A**, **B**) Side-view of a pollen tube interacting with labeled EA1 peptide at its apical and sub-apical region. (**C**) Close-up of (**B**) displaying labeled EA1 in vesicle-like structures inside the pollen tube tip region. (**D**, **E**) A pollen tube tip facing towards the observer displays labeled EA1 peptide in the tube tip. (**F**) Close-up of (**E**) displaying labeled EA1 in vesicles inside the pollen tube tip. Single optical sections are shown in (**B**, **C**, **E**, **F**). Scale bars represent 10 µm.

Usually disassociation and inactivation of peptide ligands occurs in endosomes (Reyes *et al.*, 2011; Geldner and Robatzek, 2008; Irani and Russinova, 2009). As the fluorophore Dylight 488 is stable from pH 4 to pH 9, its insensitivity against the acid environment inside endosomal vesicles is consistent with the remaining strong signal inside the pollen tube apex after removing excess of labeled peptide from the pollen tubes (Figure 4.3).

Within many plant species, several reproductive crossing barriers have evolved to avoid fertilization by undesirable or alien pollen tubes and sperm cells, respectively (Dresselhaus *et al.*, 2011; Wheeler *et al.*, 2009). EA1 as a short-range pollen tube attractor is a candidate for being involved in such a control mechanism. To examine whether EA1 acts species-specific, we investigated its ability to bind to pollen tubes of other plant species than maize. Neither germinated pollen of the eudicot model plant *Nicotiana benthamiana* nor of the monocot plant lily "Stargazer" was able to recognize EA1 in the assay (Figure 4.2 ; Table 4.1). *Tripsacum dactyloides* was chosen as a grass model to analyze species-specificity of EA1 interaction. Based on ribosomal ITS sequences, *Zea* and *Tripsacum* are closely related and form a clade that is clearly differentiated from other Poacea (Buckler and Holtsford, 1996). Despite this close relationship, EA1 as well as the control peptide EAL2 are not capable to bind to pollen tube tips of *T. dactyloides* (Figure 4.1 I–J, Figure 4.2). This result is substantiated by the finding that pollen tubes of *T. dactyloides* were not attracted by EA1 secreted from *Arabidopsis* ovules (Márton *et al.*, 2012). Regarding the fact that *in vivo* pollination of shortened *Z. mays* silks with *T. dactyloides* pollen results in fertilization and seed set (Lausser *et al.*, 2010, Mangelsdorf and Reeves, 1931), these pollen tubes might need to grow through the sporophytic tissue of the transmitting tract in order to become competent for attraction, as it was reported for *Arabidopsis* and *Torenia* (Higashiyama *et al.*, 1998; Qin *et al.*, 2009).

4. 4 Conclusions

Taken together, we presented a method for visualizing the specific interaction of a peptide ligand with its unknown receptor at the apex of a growing pollen tube. Recently, Okuda et al. reported an alternative method for displaying the binding activity of LURE2, a pollen tube attractor of *Torenia fournieri* (Okuda *et al.*, 2009; Okuda *et al.*, 2013). After incubation with pollen tubes, LURE2 could be detected via crosslinking and immunostaining at the pollen tube tip region. Both methods demonstrate the binding of a pollen tube attractor to the pollen tube tip. The usage of a fluorophore coupled peptide for *in vitro* binding assays with non-fixed pollen tubes additionally allows the detection of the internalized peptide after being

bound to the tip. It will now be the major future challenge to identify and characterize the exact binding mechanism, to identify the receptor and the corresponding signal pathway that leads to a reorientation of the pollen tube growth.

CHAPTER 5 - IDENTIFYING PLANT CELL-SURFACE RECEPTORS: COMBINING "CLASSICAL" TECHNIQUES WITH NOVEL METHODS.

The following CHAPTER is based on the manuscript of Uebler and Dresselhaus, 2014, in *Biochemical Society Transactions* and surveys several methods to identify plant surface receptors of known ligands. It introduces CHAPTER 6, which covers the identification of putative interaction partners of EA1 since a focus of CHAPTER 6 will be on experimental procedures mentioned in paragraph 5. 3. The manuscript was written by S. Uebler and edited by T. Dresselhaus.

5. 1 Introduction

Cell-to-cell communication events play a key role during developmental processes and reproduction of multicellular organisms. To decipher the underlying signaling network in plants, researchers mainly studied non-peptide plant hormones (phytohormones) such as auxin, cytokinin and gibberellin and their interplay (for review see Vanstraelen and Benková, 2012). The diverse roles of these hormone classes in plant growth, development and reproduction were investigated since more than 50 years (Went and Thimann, 1937). However, it becomes more and more obvious that numerous signaling events in plants are carried out by small polymorphic secreted peptides. These peptides are thought to act mainly through interaction(s) with membrane-located receptors located at the surface of recipient cells and in most cases represent either receptor-like kinases (RLKs) or ion channels. RLKs represent a large family of transmembrane kinases in plants with an extracellular ligand-binding domain, encoded by more than 400 genes in the *Arabidopsis* genome (Shiu and Bleecker, 2001). RLKs have been shown to play important roles in numerous signaling processes, from defence (Gómez-Gómez and Boller, 2000; Heese *et al.,* 2007) to vegetative development (Clark *et al.,* 1997), but also during reproduction such as self-incompatibility (Takayama *et al.,* 2001), pollen tube discharge (Boisson-Dernier *et al.,* 2009) and fertilization (Escobar-Restrepo *et al.,* 2007), respectively. Surprisingly, only few interactions of a receptor with its ligand(s) have been shown to date. Considering the finding that higher plant genomes contain more than 1000 genes encoding for putative secreted peptides (Lease and Walker, 2010), it becomes obvious that major research efforts have to be undertaken to elucidate the underlying plant signaling processes. Many approaches have failed to date to identify membrane-bound peptide receptors due to

technical problems. This short review article provides an overview about the most frequently and novel biochemical methods used for unveiling interaction partners of secreted peptides at the cell surface.

5. 2 Genetic and bioinformatic approaches are limited to identify peptide ligand interaction partners

A "classical" method to identify a receptor protein is the use of a genetic screen. In *Arabidopsis*, the CRP (cysteine-rich putative secreted peptide) TAPETUM DETERMINANT 1 (TPD1) was identified in such a phenotypic screen (Yang *et al.,* 2003) and could be demonstrated to act as ligand of the leucin-rich-repeat (LRR)-RLK EXCESS MICROSPOROCYTES 1 (EMS1), which is required for determination of anther cell fate (Zhao *et al.,* 2002; Canales *et al.,* 2002). Mutants of both components displayed the lack of anther tapetal cells and excess production of microspores. Genetically, ligands and their receptors are expected to act in the same signaling pathway and thus are expected to generate similar mutant phenotypes. However, many receptors such as the RLK FERONIA or the ion channel KZM1 display a very broad expression pattern (Escobar-Restrepo *et al.,* 2007; Philippar *et al.,* 2003) and function in various biological processes (Kessler *et al.,* 2010). Specificity seems to be provided by the peptide ligand, which often is expressed only in few cells (Amien *et al.,* 2010; Sprunck *et al.,* 2012). Another drawback is gene redundancy, as single mutants of peptide ligand genes often don't show any phenotype (Sprunck *et al.,* 2012). Furthermore, for an effective genetic screen it is necessary to examine a fairly large quantity of plants. This demand for greenhouse capacity often limits the possibilities for extensive screens, especially if transgenic plants and crop plants such as maize are involved.

Another genetic approach to screen for interaction partners is the yeast-two-hybrid system. The usability of this method could be demonstrated by the identification of a ligand of the pollen-specific LRR-RLK LePRK2 (*Lycopersicon esculentum* pollen receptor kinase 2) of tomato, which is thought to play a role in pollen-pistil communication. The extracellular domain of LePRK2 was used as bait in a yeast-two-hybrid screen and revealed the secreted cysteine-rich protein LAT52 as peptide ligand (Tang *et al.,* 2002). LAT52 is involved in pollen hydration and pollen tube growth (Muschietti *et al.,* 1994) and like LePRK2 it is produced in pollen, suggesting an autocrine signaling pathway. However, yeast-two-hybrid screens with membrane proteins face several difficulties as their extracellular domains might not exhibit

the correct post-translational modifications such as glycosylation and phosphorylation and might not be folded correctly in yeast.

Fortunately, resources for bioinformatics-based approaches to identify protein-protein interactions develop rapidly and allow user-friendly *in silico* screenings. The increasing number of confirmed entries in different databases, more and more reliable *in silico* prediction methods and the availability of genome sequencing data of many species allows the interconnection of data. The cell-targeting peptide TP H2009.1, for example, was isolated by phage display bio-opanning of a lung cancer cell line and shows a high selectivity for the discrimination between normal and cancerous cell (Oyama *et al.,* 2003). It is also able to deliver a chemotherapeutic agent, resulting in the death of the target cell (Zhou *et al.,* 2004). The peptide sequence sequence of TP H2009.1 is similar to a component of the foot-and-mouth-disease virus (FMDV) and contains the known tri-peptide integrin-binding motif RGD (Hynes, 1992). As FMDV was postulated to bind four integrins (Jackson *et al.,* 1997; Jackson *et al.,* 2000a; Jackson *et al.,* 2000b; Jackson *et al.,* 2002), these ones were tested for interaction with the peptide and the integrin $\alpha_v\beta_6$ could be demonstrated to represent the corresponding binding partner (Elayadi *et al.,* 2007). However these success stories are rare and depend on large amounts of pre-existing knowledge.

5. 3 Cross-linking: Panacea for receptor-fishing?

In respect to the limited success of above described approaches, could a biochemical cross-linking approach represent the Panacea (Greek goddess of universal remedy) for receptor identification in plants? Beside the hydrophobicity as well as the low abundancy of membrane proteins, one of the major challenging problems for the identification of a receptor protein via classical affinity purification is the transient binding nature of many ligands (Helbig *et al.,* 2010; Elschenbroich *et al.,* 2010). Therefore only very few affinity purifications of cell surface receptors are published to date. One example is the identification of the LRR-RLK phytosulfokine receptor PSKR1 (PSK receptor 1) from *Daucus carota* that binds the sulphated pentapeptide phytosulfokine (PSK) (Matsubayashi *et al.,* 2002). The PSK receptor was isolated from the solubilized microsomal fraction of carrot cells by ligand-based affinity purification using a PSK-coupled-column. The technique applied requires stable binding of the ligand to its receptor that must not be disturbed by the solubilizing agents. However, as these interactions are often only transient, most promising approaches include chemical cross-linking by covalently coupling the ligand to its surface interaction partner. The interaction is thus stabi-

lized and the binding partner can be identified by mass spectrometry (MS). A broad range of cross-linking reagents of various lengths and with different reactive groups, like the amine-reactive *N*-hydroxysuccinimide esters or the photo-reactive diazirines, provides a source for a wide variety of experiments (Sinz, 2006). Although cross-linking reactions between proteins are often unspecific and therefore have to be confirmed by additional methods, they have been successfully applied already by several labs. The LRR-RLK AtPepR1, for example, could be isolated using this approach by applying photoaffinity labeling with the endogenous peptide elicitor of *Arabidopsis* leaves named as AtPep1 (Yamaguchi *et al.*, 2006). By carrying an UV-light activatable cross-linker, the peptide was bound by the membranous AtPepR1 receptor in *Arabidopsis* cell suspension culture. Additional experiments verified this interaction.

But not only receptors of peptide ligands can be identified using cross-linking approaches. Using a cell suspension culture of rice cells, the binding of biotinlylated *N*-acetylchitooctaose to the chitin binding elicitor (CEBiP) was successfully demonstrated by this method (Kaku *et al.*, 2006; Shinya *et al.*, 2010). Prerequisite for the application of this method is always the availability of enough receptor proteins, which are normally distributed at low amounts at the cell surface. In contrast to CEBiP, the affinity of the RLK FLS2 (FLAGELLINE SENSITIVE 2) to its peptide ligand flg22, a fragment of bacterial flagellin (Gómez-Gómez and Boller, 2000), could not be verified in *Arabidopsis* cultured cells. Only when the rice orthologous protein OsFLS2 (Takai *et al.*, 2008) was overexpressed in rice cells, binding to biotinylated flg22 could be detected, suggesting that an appropriate amount of the receptor is necessary to apply this method.

Extensive cell-cell communication events occur during the pollen tube pathway towards the female gametes (Dresselhaus and Franklin-Tong, 2013). During its journey, the growing pollen tube communicates with many cell types including the sporophytic papillae cells, transmitting tract and ovule cells and finally cells of the female gametophyte. The whole path requires precise guiding, growth support and recognition of self- and non-self identity. Different peptide classes are secreted from the maternal sporophytic tissues including the plantacyanin chemocyanin that acts as a directional cue for reorienting lily pollen tubes and the lily lipid transfer protein SCA (stigma stylar cysteine-rich adhesion), which functions in pollen tube tip growth (for review see Chae and Lord, 2011). The only egg apparatus peptides with the ability to attract pollen tubes discovered up to date are the CRPs called LUREs in the eudicot species *Torenia fournieri*, *Torenia concolor* and *Arabidopsis thaliana* (Okuda *et al.*, 2009; Kanaoka *et al.*, 2011; Takeuchi and Higashiyama, 2012). LUREs are secreted by the synergid

cells as short-range pollen tube attractors. In the grasses, until now only ZmEA1 (*Zea mays* EGG APPARATUS 1) of maize has been shown to represent a short distance pollen tube attractor (Márton *et al.*, 2005; Márton *et al.*, 2012). The predicted mature form of ZmEA1 can bind to the tip of growing maize pollen tubes (Figure 5.1) (Uebler *et al.*, 2013). The peptide seems to get internalised in vesicles and to be degraded at the pollen tube apex likely shortly after binding to its receptor(s). Experiments with immunolocalisation of LUREs using fixed pollen tubes also showed a binding of these peptides to the pollen tube tip (Okuda *et al.*, 2013). A challenge is now the identification of the corresponding membrane targets of these pollen tube attractors and the internalised peptide-receptor complexes. As pollen tubes are fast growing cells (Franklin-Tong, 1999), the above mentioned signaling events for growth redirection should occur only short and transiently to allow a fine-tuned regulation. As a consequence, the interaction between signaling ligand and receptor is supposed to be unstable and likely dissolves quickly. Therefore cross-linking of such peptide ligands to their cell surface partner(s) may stabilize this transient interaction and allow its identification after affinity purification.

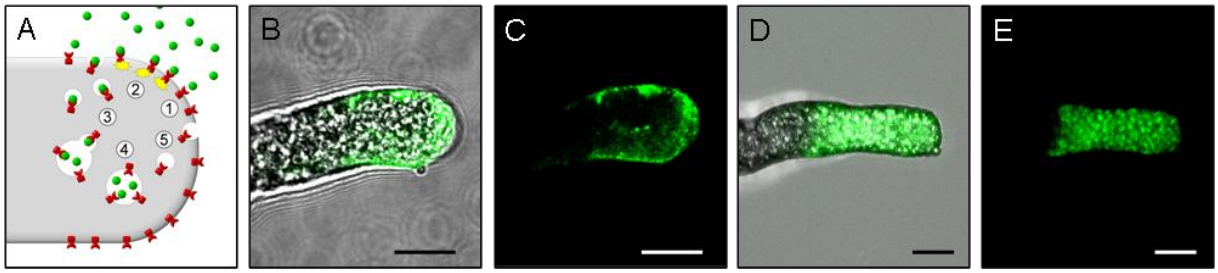

Figure 5.1 Pollen tube attractor EA1 binds to an unknown interaction partner at the apical maize pollen tube cell surface. (**A**) Model of EA1 interaction with the maize pollen tube tip. (1) Secreted EA1 peptide (indicated in green) binds to the extracellular domain of an unknown interaction partner (indicated in red) localised at the cell surface of the pollen tube tip, inducing (2) intracellular signaling events (indicated in yellow) to redirect pollen tube growth. (3) Receptor-ligand complexes are internalized by vesicle-mediated endocytosis and (4) appear in primary endosomal compartments. Here the complex dissociates, EA1 is degraded and (5) the unknown receptor recycled and exposed again at the cell surface after exocytosis. (**B-E**) *In vitro* pollen tube binding assay of maize using predicted mature EA1 peptide labelled with the fluorescent dye DyLight 488 NHS Ester. (**B, D**) Merged bright field and fluorescence micrographs. (**C, E**) UV-fluorescence micrographs. (**B, C**) EA1-fluorescence could be detected initially at the apical membrane region of the pollen tube tip and later (**D, E**) in vesicle-like structures inside the pollen tube. Scale bar represents 10 µm.

5. 4 Innovative novel method: Ligand-based receptor-capture technology

One of the most exciting innovations in ligand-receptor identification is the ligand-based receptor-capture technology (LRC) that was published recently (Frei *et al.,* 2012; Frei *et al.,* 2013). Most cell surface proteins are known or predicted to contain glycosylations, one of the most common posttranslational modifications existing in all domains of life (Wollscheid *et al.,* 2009; Schwarz and Aebi, 2011). Therefore the new reagent TRICEPS was designed for selective capture of cell surface glycoproteins. TRICEPS is composed of three components: an *N*-hydroxysuccinimide ester (Mädler *et al.,* 2009) for covalently linking the ligand to TRICEPS, a hydrazine that binds induced carbohydrate aldehydes of the cell interacting receptor and biotin for affinity purification of the ligand-receptor complex, followed by MS analysis (Figure 5.2). Thereby, among others, the binding of human insulin to the low abundance insulin receptor on cultured murine adipocytes could be successfully demonstrated (Frei *et al.,* 2012). An alternative to overcome the necessity of cell cultures was also demonstrated. On U251 human glioblastoma cells the therapeutic antibody trastuzumab is known to bind to the transmembrane tyrosine kinase ErbB2, a member of the epidermal growth factor family, which is involved in tumorigenesis of breast cancer (Yarden, 2001). Primary breast cancer tissue was cut in small slices (Steu *et al.,* 2008) and used directly for LRC to investigate the binding of trastuzumab to ErbB2 in a more complex target tissue. The interaction could be unambiguously confirmed, although ErbB2 was very low abundant in the primary tissue (Frei *et al.,* 2012). Furthermore, several additional interaction partners could be detected, which were not present in the U251 cells, highlighting the potential of the LRC technology to unveil complex interaction networks directly in tissues. To date, this method was not performed with samples of plant origin and it will be interesting whether TRICEPS is also suitable for large-scale LRC in plants.

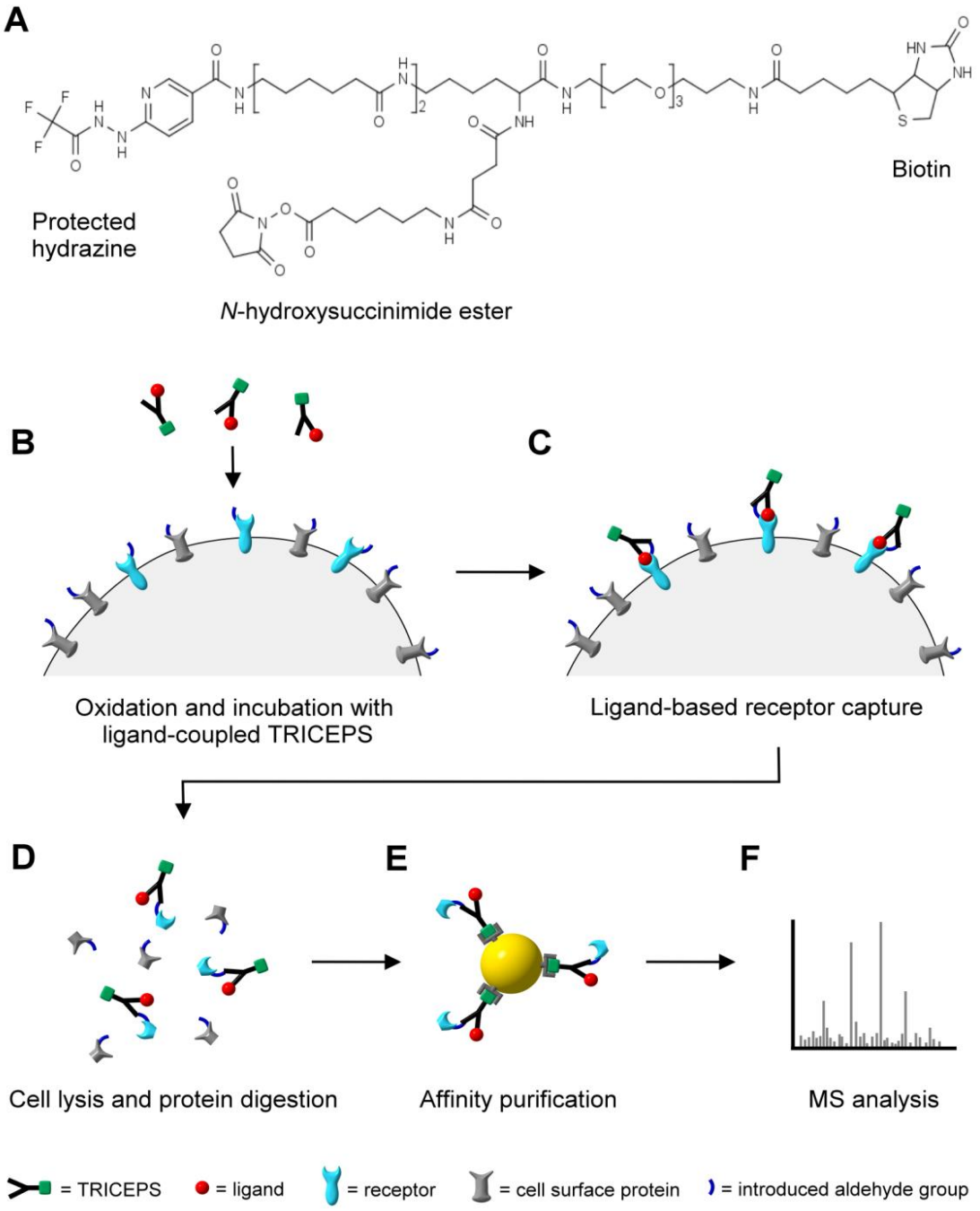

Figure 5.2 Ligand-based receptor-capture technology (LRC) after Frei *et al.*, 2013. This method is especially suited for glycosylated cell surface proteins and is enabled by the reagent TRICEPS. (**A**) TRICEPS is composed of an *N*-hydroxysuccinimide ester for coupling TRICEPS to the ligand, a protected hydrazine group that reacts with aldehydes introduced into carbohydrates by oxidation and a biotin group for affinity purification of the captured glycopeptides. (**B**) Aldehydes are introduced into carbohydrates of cell surface proteins by gentle oxidation and the oxidised sample is incubated with ligand-coupled TRICEPS. (**C**) The ligand binds to its receptor and due to the resulting proximity the protected hydrazine group of TRICEPS can be covalently linked to the carbohydrate aldehyde. (**D**) The complex of ligand, receptor and TRICEPS is released after cell lysis and protein digestion. (**E**) Affinity purification using the biotin group of TRICEPS results in enrichment of receptor fragments. (**F**) The identity of targeted glycoproteins can be determined by mass spectrometry.

5. 5 Alternative "classical" method: mRNA-display libraries

mRNA-display represents an *in vitro* method designed especially for the identification of interaction partners that are present at low abundance. The major idea is to synthesize protein pools by *in vitro* transcription and *in vitro* translation using a cDNA library and to link these proteins covalently to their own coding mRNA using a puromycin linker (Roberts and Szostak, 1997), resulting in an mRNA display library. Now the peptide ligand can be immobilised at a matrix for incubation with the mRNA display library in order to purify its binding partner. The purified sample can then be used as a PCR template to generate a ligand-binding library. This method allows the strong enrichment of interaction partners and can be applied to any ligand that can be immobilised without losing its functionality (McPherson *et al.,* 2002). Unfortunately, there are several limitations to this *in vitro* system, which can hamper the application of cell surface receptors. *In vitro* translation of membrane proteins is still a very difficult task and requires optimization for each individual protein. Many membrane proteins need to be embedded in their natural cellular environment to maintain their binding characteristics (Lee, 2004) and proper folding. Moreover, the lack of posttranslational modifications may affect their functionality. However, as membrane proteins are of great importance, they are investigated intensively and impressive advances were achieved during the last years in expressing membrane proteins in cell-free systems, especially by using lipids and detergents (Rajesh *et al.,* 2011). Therefore it is conceivable that these improvements can be combined soon with the *in vitro* translation of cDNA libraries for mRNA-displays to screen for membrane localised interaction partners.

5. 6 Concluding remarks

Numerous cell-to-cell communication events occur in plants that are achieved by signaling events triggered by the activity of large families of secreted peptide classes and their various receptors. Thus identifying the cell surface interaction partners of secreted peptide ligands is one of the emerging fields in plant research and of increasing importance to understand cellular cross-talk both during vegetative and reproductive development as well as during interactions of plants cells with their biotic environment. The appearance of innovative methodologies and the rediscovery of established techniques offer a broad field of approaches to elucidate many more components of peptide triggered signal transduction pathways in plants. Nevertheless, several limitations are attributable to the biochemical nature of these interac-

tions, of which many appear transient and occur only in few cell types within complex tissues. Routine and high-throughput analyses will remain another technical challenge, as ligand-receptor binding have to be verified individually by additional methods. It is also likely that there may be a large network as individual ligands or receptors may interact with several different partners of various families at certain conditions. Therefore large-scale approaches, like the use of the recent developed reagent TRICEPS, combinations of affinity purification with cross-linking and mRNA-displays, will move into the spotlight of interest and it will be exciting to see future methodological developments and innovations.

CHAPTER 6 - IDENTIFICATION OF CANDIDATE INTERACTION PARTNERS OF THE POLLEN TUBE ATTRACTOR ZMEA1

The following CHAPTER contains unpublished data and conclusions.

6. 1 Introduction

Communication between different cells by peptide signaling requires the secretion of peptides from source cells and perception by the target cells. Although hundreds of peptides seem to be involved in plant signaling processes, only few interaction partners could be unveiled, mainly due to experimental obstacles (see CHAPTER 5). As knowledge about members of single pathways is elementary to understand signaling networks, identification of interaction partners represents recently one of the most challenging tasks in plant signaling research.

Several small molecules were demonstrated to be involved in growth and guidance of pollen-tubes towards the female gametophyte (Figure 6.1; for review see Higashiyama and Takeuchi, 2015). The peptides ZmEA1 from maize and LUREs derived from *Torenia fournieri*, *Torenia concolor* and *Arabidopsis thaliana* are secreted from cells of the egg apparatus and act as micropylar pollen tube guidance cues. They are expected to bind corresponding proteins localized at the surface of the attracted pollen tube for mediating tube growth direction (Okuda *et al.*, 2013; Uebler *et al.*, 2013), but yet no interaction partners could be identified. To date, few membrane-associated male factors were demonstrated to be involved in pollen tube guidance (Hafidh *et al.*, 2014). The glycosylphosphatidylinositol (GPI)-anchored protein COBRA-LIKE 10 (COBL10) from *Arabidopsis* localizes at the pollen tube tip surface and is necessary for proper pollen tube growth. *COBL10* mutants show abnormal cell wall organization and impaired sensitivity against ovule-derived guidance cues, although it cannot be excluded that defective tube attraction is an indirect result of improper cell wall formation (Li *et al.*, 2013). As described in paragraph 5. 1, binding of a secreted ligand on the surface of the perceptive cell and introduction of a signaling cascade for response is commonly achieved in plants by receptor-like kinases (RLK). They are involved, among others, in formation and maintenance of meristems, disease resistance, self-incompatibility and anther tissue development (for review see de Smet *et al.*, 2009). In *Arabidopsis*, more than 100 RLKs are described to be expressed in pollen (Shiu and Bleecker, 2001; Qin and Yang, 2011) and regarding their widespread occurrence and functionality in plants, it is easily conceivable that they are also in-

volved in recognition of pollen tube attractants secreted from the female gametophyte. The pollen-specific tomato RLKs LePRK1 and LePRK2, forming a complex on the membrane of pollen tubes, were reported to interact with extracellular ligands derived from the pistil, the CRP LeSTIG (Tang *et al.,* 2004) and a small molecule called STIL (Wengier *et al.,* 2010), both promoting pollen tube growth *in vitro*. In *Arabidopsis*, double mutants lacking the two pollen RLKs LOST IN POLLEN TUBE GUIDANCE 1 and 2 (LIP 1/2) showed impaired micropylar pollen tube guidance as well as reduced attraction by LURE1 (Liu *et al.,* 2013; Takeuchi and Higashiyama, 2012). This indicates that these RLKs are members of the signaling pathway through which LURE1 controls pollen tube growth towards the female gametophyte. Although anchoring of the two RLKs to the plasma membrane of the tube tip via palmitoylation was essential for their functionality, both proteins lack an extracellular domain for interaction with signaling peptides. Therefore they are thought to act as components of a receptor complex perceiving LURE1 signaling (Liu *et al.,* 2013).

Although membranous RLKs initiating signaling cascades represent very frequently the corresponding binding partner of secreted peptide ligands, other ways of perception have to be considered. Animal peptide toxins acting as ion channel antagonists were demonstrated to bind directly to their target channels (Swartz and MacKinnon, 1997; Imredy *et al.,* 1998; Gui *et al.,* 2014). Their modes of operation includes modifying channel open mechanisms, blocking the channel pore and influencing their conductance properties (Quintero-Hernández *et al.,* 2013), as for examples scorpion venoms related to defensins exhibit potassium channel blocking activity (Diego-García *et al.,* 2007). In plants, the defensin MsDef1 from alfalfa is expected to interact with the extracellular region of the calcium channel $Ca_v1.2$ (Spelbrink *et al.,* 2004). Furthermore, the maize defensin ZmES4 binding the pollen tube surface (Woriedh *et al.*, 2015) was shown to introduce bursting of the pollen tube after entering the receptive synergid cell by opening the potassium channel KZM1 (Amien *et al.,* 2010), indicating that it might directly bind towards the extracellular domains of the channel.

Additionally, ions and ion transporters in plants seem to be involved in mechanisms for pollen tube attraction in *Arabidopsis*. Reorientation of pollen tubes towards the micropyle of ovules was observed to induce increase of cytoplasmic calcium at the tube tip, indicating that perception of ovule secreted guidance cues might modulate calcium dynamics of the pollen tubes (Iwano *et al.,* 2012). It is thus assumed, that influx of extracellular calcium is the primary source of tip-focused cytoplasmic calcium gradient (Zhou *et al.,* 2015). γ-Aminobutyric acid (GABA) derived from pistil tissue, which was demonstrated to be involved in pollen tube

guidance (Palanivelu *et al.*, 2003), is modulating the activity of calcium and potassium channels after binding to the pollen tube surface (Yu *et al.*, 2014). Nevertheless, pollen tube attraction capability was not observed for GABA. Taken together, this indicates that ion channel activity is elementary for micropylar pollen tube attraction, although it is not clear until now how transporters respond to attraction cues (Higashiyama and Takeuchi, 2015). As ion flow plays an important role for proper pollen tube growth, it is conceivable that pollen tube attractants might bind ion channels directly and inducing a change in ion flow and concentration for quick response to the attractor.

After perception of the secreted attractant, other male factors were demonstrated to be involved in controlling redirected growth of the pollen tube towards the ovule. *Arabidopsis* double mutant pollen tubes lacking the ER-localized potassium transporters CHX21 and CHX23 are able to grow through the transmitting tract, but fail to orient towards ovules and show impaired micropylar pollen tube guidance (Lu *et al.*, 2011).

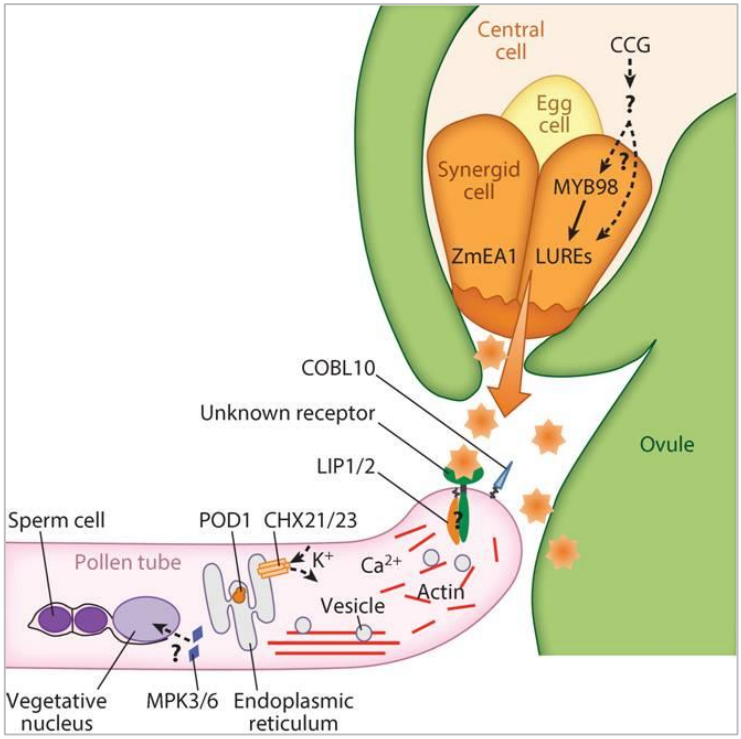

Figure 6.1 Male and female factors for ovular pollen tube guidance. The model illustrates male and female factors involved in ovular pollen tube guidance from different plant species. Signaling peptides are secreted from the female gametophyte of maize (ZmEA1) or *Arabidopsis* and *Torenia* (LUREs, under control of female gametophytic factors) for attraction of the pollen tube. Several male factors discussed in the text are involved in perception of the attraction cues and reorientation of pollen tube growth towards the micropyle of the female gametophyte. Adapted from Higashiyama and Takeuchi, 2015.

Another ER-localized protein, POLLEN DEFECTIVE IN GUIDANCE (POD1), is also necessary for successful pollen tube attraction but not for pollen tube growth. It interacts with the ER chaperone CALRETICULIN 3 (CRT3), suggesting that it is involved in folding and quality control of membrane proteins like receptors, mediating perception of female guidance cues (Li *et al.,* 2011). The signaling pathway in pollen tubes downstream of attractant binding seems to be dependent of the kind of ovular guidance. The two mitogen-activated protein kinases MPK3 and MPK6 of *Arabidopsis* mediate pollen tube response to funicular guidance cues, but are not involved in micropylar guidance events, supporting the idea that funicular and micropylar guidance require distinct signaling pathways (Guan *et al.*, 2014).

The following CHAPTER 6 focuses on the identification and characterization of interaction partners of ZmEA1. A biochemical pull-down approach using predicted mature ZmEA1 as bait protein was applied to isolate pollen tube derived binding partners. Three potential candidate proteins strongly expressed in maize pollen are presented and first characterizations were performed.

6. 2 Experimental procedures

6. 2. 1 Cultivation of organisms

6. 2. 1. 1 Plant material and growth conditions

Maize inbred line A188, the partial inbred lines HiII A and HiII B, derived from crossing of A188 and B73 (Armstrong *et al.,* 1991) and *Nicotiana benthamiana* were kept under greenhouse conditions like described in 3. 2. 1.

6. 2. 1. 2 Bacterial strains and culture conditions

The *Escherichia coli* strain DH5α was used for standard cloning procedures and DB3.1 for cloning and replication of Gateway® Destination vectors with preservation of the lethal *ccdB* gene. Expression of transgenes for protein production was performed with the strains Lemo21(DE3) and Rosetta™(DE3). Transient transformation of *Nicotiana benthamiana* leaves was mediated by the *Agrobacterium tumefaciens* strain GV3101. Information about all bacterial strains is listed in table Table 6.1. Bacteria were grown under sterile conditions in liquid or on solid media supplemented with appropriated antibiotics, if required. For long-time storage at -80°C, bacteria were grown overnight at appropriate temperature, harvested by centrifugation and resuspended in 15% glycerol.

Table 6.1 Bacterial strains used in this study.

Species	Strain	Genotype / Information	Reference / Supplier
E. coli	DH5α™	F⁻ Φ80*lac*ZΔM15 Δ(*lac*ZYA-*arg*F) U169 *rec*A1 *end*A1 *hsd*R17(r_k^-, m_k^+) *pho*A *sup*E44 *thi*-1 *gyr*A96 *rel*A1 λ⁻	Thermo Fisher Scientific Inc., Waltham, USA
	DB3.1™	F⁻ *gyr*A462 *end*A1 Δ(sr1-*rec*A) *mcr*B *mrr hsd*S20(r_B^-, m_B^-) *sup*E44 *ara*⁻14 *gal*K2 *lac*Y1 *pro*A2 *rps*L20(SmR) *xyl*-5 λ⁻ *leu mtl*1	Thermo Fisher Scientific Inc., Waltham, USA
	Lemo21(DE3)	*fhuA2 [lon] ompT gal (λ DE3) [dcm] ΔhsdS/ pLemo*(Cam^R) *λ DE3 = λ sBamHIo ΔEcoRI-B int::(lacI::PlacUV5::T7 gene1) i21 Δnin5* pLemo = pACYC184-*PrhaBAD-lysY*	Wagner *et al.,* 2008
	Rosetta™(DE3)	F⁻ *ompT hsd*S_B(r_B^- m_B^-) *gal dcm* (DE3) pRARE (Cam^R)	Merck KGaA, Darmstadt, Germany
A. tumefaciens	GV3101	Background: C58 (marker: rif); helper plasmid: pMK90	Holsters *et al.,* 1980

6. 2. 2 Transformation of bacteria

Preparation of competent *E. coli* and heat-shock transformation with plasmids was performed after Inoue *et al.*, 1990 and positive transformed cells were selected using appropriate antibiotics. Competent cells of *A. tumefaciens* were prepared and transformed with plasmids according to the protocol of Chen *et al.*, 1994. All bacterial clones were tested by plasmid isolation using High-Speed Plasmid Mini Kit (Geneaid Biotech Ltd., New Taipei City, Taiwan) according to the manufacturer's protocol, followed by restriction enzyme digestion and Sanger sequencing, if required. If plasmid yield of *A. tumefaciens* was not enough for restriction enzyme analysis, the isolated plasmid was transformed into *E. coli* strain DH5α, followed by plasmid preparation and analysis of several *E. coli* clones. Sanger sequencing reactions were carried out by the companies GATC Biotech AG (Konstanz, Germany) and LGC (Teddington, UK).

6. 2. 3 Molecular cloning and PCR

Standard molecular work was performed according to Sambrook and Russell, 2001 using reagents at molecular grades.

6. 2. 3. 1 PCR and quantitative real-time PCR (qRT-PCR)

Standard polymerase chain reactions (PCR) were executed using the KAPA HiFi™ PCR Kit (VWR International GmbH, Erlangen, Germany) with proofreading activity, according to the manufacturer's protocol. For comparative quantification of *WSL1a/b*, *WSL3* and *WSL4* ex-

pression levels, qRT-PCR was performed using cDNA of *in vitro* germinated pollen derived from three HiIIAB (HiIIA x HiIIB) maize plants (cDNA kindly provided by L. Zhou, University of Regensburg). Experiments were conducted as described in 2. 2. 5 using the primer pairs oSU175/oSU176 (*WSL1a*), oSU154/oSU155 (*WSL1b*), oSU156/oSU157 (*WSL3*) and oSU158/oSU159 (*WSL4*). For qRT-PCR of the reference genes, the primer pairs LUGfwd/LUGrev (*LUG*), MEPfwd/MEPrev (*MEP*) and FPGSfwd/FPGSrev (*FPGS*) (all derived from Manoli *et al.*, 2012) were used.

6. 2. 3. 2 Determination of UTR sequences

To analyze 5'- and 3'-UTRs of the candidate genes *WSL1a*, *WSL3* and *WSL4*, a cDNA library of maize pollen ligated into the lambda Uni-ZAP XR vector (kindly provided by T. Dresselhaus) was analyzed. To amplify the 5'-UTR, the forward primer ER I (Dresselhaus *et al.*, 1994) was combined with reverse primer oSU146 (*WSL1a*), oSU148 (*WSL3*) or oSU150 (*WSL4*), respectively, for standard PCR reactions like described in 6. 2. 3. 1. To amplify the 3'-UTR, the forward primer oSU147 (*WSL1a*), oSU149 (*WSL3*) or oSU151 (*WSL4*) was combined with reverse primer X I (Dresselhaus *et al.*, 1994) for standard PCR reaction. ER I and X I were derived from the vector polylinker up- or downstream of the insert. The other primer binding sites were located in the ORF of the analyzed cDNA. The PCR products were examined by gel electrophoresis and Sanger sequencing.

6. 2. 3. 3 Constructs for heterologous expression in E. coli

For Gateway® cloning, the coding sequence of predicted mature *ZmEA1* (*sEA1*) was amplified using primer pair sEA1-fwd/EA1-entr-rev and cloned into the vector pENTR™/D-TOPO® using DNA topoisomerase II of the pENTR™/D-TOPO® Cloning Kit (Thermo Fisher Scientific Inc., Waltham, USA), creating pENTR-sEA1. A recombination reaction was performed using the Gateway® LR Clonase® II enzyme mix (Thermo Fisher Scientific Inc., Waltham, USA) to transfer *sEA1* from pENTR-sEA1 into the destination vector pET-53-DEST (Merck Millipore, Billerica, USA), containing the Gateway™ cassette with C-terminal *6xHis*-tag and N-terminal *StrepII*-tag under control of the T7 promoter. Constructs for production of GST-sEA1 and 6xHis-MBP-sEA1 fusion proteins were constructed by LR Clonase® recombination reaction of pENTR-sEA1 with destination vectors pGEX-2-GW and pDEST-HisMBP (Nallamsetty *et al.*, 2005), respectively. The vector pGEX-2-GW is derived from pGEX-2T (Smith and Johnson, 1988; GE Healthcare, Buckinghamshire, UK) with introduced Gateway™ cassette at the 3'-end of *GST* and thrombin site, under control of the *tac*

promoter. The destination vector pDEST-HisMBP harbors C-terminal *6xHis-MBP*-tag followed by the Gateway™ cassette under control of the *tac* promoter. Cloning reactions were performed according to the manufacturer's protocol.

6. 2. 3. 4 Constructs for transient expression in N. benthamiana

The constructs for *Agrobacterium*-mediated transient transformation of GFP-fusion (Cormack *et al.*, 1996) proteins into tobacco were generated by Gateway® cloning. The coding sequences *sEA1* (primer sEA1-fwd/EA1-entr-rev), *WSL1a/b* (primer oSU104/oSU105), *WSL3* (primer oSU109/oSU110) and *WSL4* (primer oSU112/113) were amplified and cloned into pENTR™/D-TOPO® vector by TOPO® cloning to create the entry vectors pENTR-sEA1, pENTR-WSL1a/b, pENTR-WSL3 and pENTR-WSL4. The entry vectors pENTR-ZmEA1 and pENTR-spEA1 were kindly provided by A. Fastner, University of Regensburg. As destination vectors, pB7FWG2 and pB7WGF2 (Karimi *et al.*, 2002) were used for LR Clonase® II-mediated recombination. In both vectors, expression is triggered by the *35S* promoter and they contain a Gateway™ cassette with either a C-terminal (pB7FWG2) or N-terminal (pB7WGF2) *GFP*-tag. To transiently express the before mentioned genes with N-terminal *HA*- or *Myc*-tag in tobacco, Gateway™ recombination reaction was performed with the corresponding entry vectors and pEarleyGate 201 (N-terminal HA-tag) or pEarleyGate 203 (N-terminal Myc-tag) (Earley *et al.*, 2006, no vector sequence available). Both vectors contain the *35S* promoter and an N-terminal tag upstream of the Gateway™ cassette followed by the *OCS* terminator.

6. 2. 3. 5 Constructs for in vitro transcription/translation (IVT/T)

A variety of vectors was constructed for IVT/T with different systems. To express *ZmEA1*, *sEA1*, *WSL1a/b*, *WSL3* and *WSL4* with C-terminal *HA*- or *Myc*-fusion tag using TNT® Coupled Wheat Germ Extract System (Promega GmbH, Mannheim, Germany), *Drosophila* embryo translation extract and Human In Vitro Glycoprotein Expression Kit (formerly Pierce, now Thermo Fisher Scientific Inc., Waltham, MA, USA), the coding sequences were amplified using primer pairs oSU123/oSU124 (*ZmEA1*), oSU125/oSU126 (*sEA1*), oSU117/oSU118 (*WSL1a/b*), oSU119/oSU120 (*WSL3*) and oSU121/oSU122 (*WSL4*). The PCR fragments and goal vectors were digested using restriction enzymes *Eco*RI/*Sac*I and ligated into the vectors pT7CFE1-CHA and pT7CFE1-CMyc (Thermo Fisher Scientific Inc., Waltham, MA, USA). Both vectors contain the T7 promoter and an internal ribosome entry site (IRES) of the encephalomyocarditis virus (EMCV) upstream of the insert, followed by C-terminal *HA*- or

Myc-tag, polyA-tail and T7 terminator. To generate constructs without IRES for expression in the wheat germ system, the plasmids pT7CFE1-CHA/CMyc containing the above mentioned genes were digested with the restriction enzymes *Eco*RI/*Sac*I to cut out the insert including the tag. This fragment was blunted and cloned into pJet1.2/blunt vector (Thermo Fisher Scientific Inc., Waltham, MA, USA) containing T7 promoter. The plasmid was linearized with *Nco*I prior to IVT/T reactions.

6. 2. 4 Heterologous expression in *E. coli* and protein purification

To heterologously express *sEA1* fused to affinity tags, the coding sequence of *sEA1* was cloned into appropriate vectors like described in 6. 2. 3. 3 and transformed into *Escherichia coli*. 6xHis-sEA1-StrepII, 6xHis-MBP-sEA1 and GST-sEA1 fusion proteins were synthesized in the strains Rosetta™(DE3) and 6xHis-sEA1-StrepII additionally in Lemo21(DE3). A single colony was grown overnight in 5 ml LB media (1% tryptone, 0.5% yeast extract, 1% NaCl) supplemented with antibiotics and was used for inoculation of 50 - 500 ml fresh media. The culture was grown at temperatures from 25 – 37°C, depending on optimal expression temperature, until OD_{600} = 0.4 - 0.8 and a pre-induction sample was taken. IPTG was added to a final concentration of 1 mM (Rosetta™(DE3)) or 400 µM (Lemo21(DE3)) to induce expression and the culture was grown for 3 – 5 h. If Lemo21(DE3) was used, L-rhamnose was added different concentrations ranging from 0 – 2 mM for fine-tuning of expression intensity. A post-induction sample was saved for verification of protein production by SDS-PAGE. The remaining cells were harvested and frozen for protein purification.

6. 2. 4. 1 Purification of His-tagged protein

For purification of 6xHis-sEA1-StrepII and 6xHis-MBP-sEA1 under native conditions, induced harvested cells were resuspended in lysis buffer (50 mM NaPi pH 8.0, 300 mM NaCl). To extract proteins, cells were supplemented with 1 mg/ml lysozyme, incubated on ice for 30 min and sonificated. The extract was cleared by centrifugation (20 min, 10,000 g, 4°C) and samples from the soluble and insoluble fraction were analyzed to determine solubility of the recombinant protein by immunoblot. Recombinant His-tagged protein was purified using gravity flow columns with TALON® Metal Affinity agarose resin (Takara Bio Inc., Otsu, Japan) according to the manufacturer's protocol for native protein purification without column centrifugation. Resin was equilibrated using lysis buffer before application of the cleared lysate onto the resin and incubation for 20 min at room temperature. Afterwards, the resin was washed using 10fold resin volume lysis buffer followed by 5fold resin volume wash buffer

(50 mM NaPi pH 7.0, 300 mM NaCl, 7.5 mM imidazole). Bound recombinant protein was eluted with 5fold resin volume elution buffer (50 mM NaPi pH 7.0, 300 mM NaCl, 150 mM imidazole) and collected in 500 µl fractions. Samples were analyzed by immunoblot using primary sEA1-directed antibody described in 6. 2. 6. 1 and secondary anti-rabbit IgG antibody from goat conjugated with horse reddish peroxidase (Sigma-Aldrich, St. Louis, USA) diluted 1:5,000. To purify proteins under denaturing conditions, cells were lysed by resuspension in lysis buffer supplemented with 8 M urea. The following procedure was performed as described for native conditions with addition of 8 M urea to each buffer.

6. 2. 4. 2 On-column refolding of His-tagged protein

To refold heterologously produced 6xHis-sEA1-StrepII protein purified under denaturing conditions, purification procedure until washing step with 8 M urea was performed following the protocol for purification of denatured protein described in 6. 2. 4. 1 . Afterwards, additional washing steps with decreasing urea concentration (6 M – 4 M – 2 M – 0 M) were applied for stepwise refolding of the denatured protein. Additives to enhance solubility and refolding of the purified protein were supplemented to all washing steps and are listed in Table 6.3. The final elution step was performed with elution buffer lacking urea but containing additives. The samples were analyzed by SDS-PAGE.

6. 2. 4. 3 Native protein purification of GST-tagged protein

Native purification of GST-sEA1 was performed like described in 6. 2. 4. 1 with following adjustments: Glutathione-loaded cellulose beads (Carl Roth GmbH & Co. KG, Karlsruhe, Germany) were used as binding resin and compositions were changed for lysis/wash buffer (10 mM Na_2HPO_4, 1.8 mM KH_2PO_4, 137 mM NaCl, 2.7 KCl, adjusted to pH 7.2) and elution buffer (50 mM Tris-HCl pH 8.0, 10 mM reduced glutathione). These conditions are according to the protocol provided by the resin supplier. The samples were analyzed by SDS-PAGE.

6. 2. 5 Heterologous expression in *N. benthamiana* leaves and protein purification

6. 2. 5. 1 Transient transgene expression in tobacco

Agrobacterium tumefaciens-mediated transformation of *Nicotiana benthamiana* for transient expression of transgenes was based on the leave infiltration protocol of Sparkes *et al.*, 2006. 2 ml of liquid YEP media (1% yeast extract, 1% Bacto peptone, 0.5% NaCl, pH 7.0) were inoculated with a single colony of *Agrobacterium tumefaciens* transformed with the transgene for overnight incubation at 28°C. This culture was diluted with fresh YEP supplemented with

antibiotics and 20 µM acetosyringone (1M stock in DMSO) for growth at 28°C until approximately OD_{600}=1.0. Cells were harvested via centrifugation (10 min, 1,000 g, RT) and resuspended in appropriate volume of infiltration buffer (10 mM MES-KOH pH 5.7, 10 mM $MgCl_2$, 100 µM acetosyringone) to adjust the bacteria suspension to OD_{600}=1.0. This suspension was stored up to several hours at room temperature until infiltration of young tobacco plants with at least 2 big leaves. Infiltration was performed using disposable 1 ml syringes (B. Braun Syringes Melsungen AG, Melsungen, Germany) without needle by gently pressing the syringe towards the underside of a leaf and slowly infiltrating the suspension into the leaf tissue. The transformed plants were kept for 2-8 days at room temperature under natural light conditions, depending on the appearance of the heterologously produced protein. For confocal microscopic analysis, pieces of the leaves were cut with a scalpel and were mounted in water on glass slides with coverslips. Microscopic analysis was performed using an Axiovert 200M inverted microscope (Carl Zeiss AG, Oberkochen, Germany) equipped with the confocal laser scanning unit LSM 510 META with GFP-excitation at 488 nm and detection using the BP 505-550 filter. Images were processed using the software ImageJ 1.43q (http://imagej.nih.gov/ij/).

6. 2. 5. 2 Extraction of recombinant protein produced in tobacco

Tobacco leaves transiently expressing fusion proteins were grounded in liquid nitrogen, weighted and suspended in extraction buffer (137 mM NaCl, 2.7 mM KCl, 10 mM Na_2HPO_4, 1.8 mM KH_2PO_4, adjusted to pH 7.4) supplemented with 1:100 Protease Inhibitor Cocktail (Sigma-Aldrich, St. Louis, USA), using 5 ml buffer for 1 g plant material. Crude cell fragments were separated from the lysate by centrifugation at 1,000 g and both samples were analyzed by immunoblot using either anti-GFP antibody (Roche Diagnostics International AG, Rotkreuz, Swiss), anti-c-Myc antibody or anti-HA antibody (both Sigma-Aldrich, St. Louis, USA) diluted 1:1,000, and secondary anti-mouse IgG antibody from goat conjugated with horse reddish peroxidase (Sigma-Aldrich, St. Louis, USA) diluted 1:5,000.

6. 2. 5. 3 Purification of sEA1-GFP produced in tobacco

To extract plant material from tobacco transiently expressing *sEA1-EGFP*, pieces of leaves were grounded in liquid nitrogen, weighted and suspended in extraction buffer (10 mM Tris-HCl pH 7.5, 150 mM NaCl, 0.5 mM EDTA) supplemented with 1:100 Protease Inhibitor Cocktail (Sigma-Aldrich, St. Louis, USA), using 5 ml buffer for 1 g plant material. Cell debris was separated from the lysate by centrifugation at 10,000 g and discarded. The lysate was

used for protein purification with GFP-binding GFP-Trap®_A agarose beads (ChromoTek GmbH, Planegg-Martinsried, Germany) according to the manufacturer's protocol. 25 µl equilibrated beads were added to 500-1,000 µl lysate, incubated for 1 h at 4°C and washed three times with 500 µl equilibration buffer. The beads were heated in SDS sample buffer to dissociate bound proteins and all samples were analyzed by immunoblot using anti-GFP antibody (Roche Diagnostics International AG, Rotkreuz, Swiss) diluted 1:1,000 and secondary anti-mouse IgG antibody from goat conjugated with horse reddish peroxidase (Sigma-Aldrich, St. Louis, USA) diluted 1:5,000.

6. 2. 5. 4 Pull-down of recombinant Myc-WSL3 with sEA1-biotin

Tobacco leaves transiently producing Myc-WSL3 were harvested 4 days after infiltration, grounded in liquid nitrogen and suspended in extraction buffer (50 mM HEPES-KOH pH 7.5, 5% glycerol, 50 mM $Na_4O_7P_2$, 1 mM Na_2MoO_4, 25 mM NaF, 10 mM EDTA, 0.5% polyvinylpyrrolidone, 20 mM sucrose, 3 mM DTT) supplemented with 1:100 Protease Inhibitor Cocktail (Sigma-Aldrich, St. Louis, USA), using 5 ml buffer for 1 g plant material. Crude cell debris was separated from the lysate by centrifugation at 1,000 g and discarded. The microsomal fraction containing Myc-WSL3 was isolated by ultracentrifugation of the lysate (100,000 g, 45 min, 4°C), the supernatant was discarded. The microsomal fraction was resuspended in solubilization buffer (137 mM NaCl, 2.7 mM KCl, 10 mM Na_2HPO_4, 1.8 mM KH_2PO_4, 10% glycerol, adjusted to pH 7.4) with protease inhibitor and solubilized by stepwise addition of Triton™ X-100 until final concentration of 0.5%. The synthetic peptide sEA1-biotin as well as biotin control were dissolved in DMSO and diluted with solubilization buffer without detergent to stock concentration of 1 mg/ml. Peptide or biotin were added to the microsomal fraction to a final concentration of 5 µg/ml and subsequently incubated (20 min, RT) with constant shaking. Equalized NeutrAvidin™ Agarose beads (Thermo Fisher Scientific Inc., Waltham, USA) were added for additional 30 min incubation at room temperature. Six washing steps were performed with 20fold bead volume, twice with wash buffer A (solubilization buffer with 0.05% Triton™ X-100), wash buffer B (solubilization buffer with 0.01% Triton™ X-100) or wash buffer C (solubilization buffer without detergent), respectively. The beads were collected and boiled in SDS sample buffer for immunoblot analysis using primary anti-c-Myc antibody (Sigma-Aldrich, St. Louis, USA) diluted 1:1,000, and secondary anti-mouse IgG antibody from goat conjugated with horse reddish peroxidase (Sigma-Aldrich, St. Louis, USA) diluted 1:5,000.

6. 2. 5. 5 Pull-down of candidate proteins fused to GFP with sEA1-biotin

To perform a pull-down with sEA1-biotin and WSL1a/b, WSL3 or WSL4 C-terminally fused to GFP, the fusion proteins were transiently transformed into tobacco leaves. Leave samples were grounded in liquid nitrogen and suspended in extraction buffer (137 mM NaCl, 2.7 mM KCl, 10 mM Na_2HPO_4, 1.8 mM KH_2PO_4, 10% glycerol, adjusted to pH 7.4), supplemented with 1:100 Protease Inhibitor Cocktail (Sigma-Aldrich, St. Louis, USA), using 5 ml buffer for 1 g plant material. Crude cell debris was separated from the lysate by centrifugation at 1,000 g and discarded. The synthetic peptide sEA1-biotin as well as biotin as control were dissolved in DMSO and diluted with extraction buffer without detergent to stock concentration of 1 mg/ml. Peptide or biotin were added to a final concentration of 5 µg/ml and subsequently incubated (15 min, RT) with constant shaking. Equalized NeutrAvidin™ Agarose beads (Thermo Fisher Scientific Inc., Waltham, USA) were added for 30 min incubation at room temperature. Six washing steps with extraction buffer were performed with 20fold bead volume. The beads were collected and boiled in SDS sample buffer for immunoblot analysis using primary anti-GFP antibody (Roche Diagnostics International AG, Rotkreuz, Swiss) diluted 1:1,000, and secondary anti-mouse IgG antibody from goat conjugated with horse reddish peroxidase (Sigma-Aldrich, St. Louis, USA) diluted 1:5,000.

6. 2. 6 Protein analysis

6. 2. 6. 1 Generation of polyclonal peptide antibodies against EA1, WSL1a/b and WSL3

The peptides CRAVFEANPQLYFT specific to the protein sequence of ZmEA1 (synthesized by JPT Peptide Technologies, Berlin, Germany) as well as CAKEKNPRLSENCKRS fully specific to WSL1a/b (synthesized by Centic Biotec, Heidelberg, Germany) and partially specific to WSL3 were used for immunization of three rabbits each (carried out by Pineda Antikörper-Service, Berlin, Germany). Binding availability of the unpurified serum was tested by dot blot analysis with a dilution series of the peptide used for immunization. Specificity against the full-length proteins was demonstrated by immunoblot analysis of recombinant 6xHis-MBP-sEA1 (produced in *E. coli*) or WSL1a/b-GFP and WSL3-GFP (produced in *Nicotiana benthamiana*), respectively. Pre-immune serum was used as negative control.

6. 2. 6. 2 SDS-PAGE, gel staining and immunoblot analysis

SDS-PAGE and immunoblot analysis were performed as described in 2. 2. 6. SDS polyacrylamide gels were stained using either Coomassie based InstantBlue (Expedeon Inc., San

Diego, USA) or mass spectrometric compatible Pierce™ Silver Stain Kit (Thermo Fisher Scientific Inc., Waltham, USA) according to the manufacturer's protocol.

6. 2. 7 *In vitro* transcription/translation (IVT/T) of proteins

To produce HA- and Myc-tagged versions of EA1, sEA1 as well as the interaction candidates WSL1, WSL3 and WSL4, several *in vitro* transcription/translation systems were used. The five protein sequences cloned into the vectors pT7CFE1-CHA and pT7CFE1-CMyc served as templates for the TNT ® Coupled Wheat Germ Extract System (Promega GmbH, Mannheim, Germany), for the Human In Vitro Glycoprotein Expression Kit (formerly Pierce, now Thermo Fisher Scientific Inc., Waltham, MA, USA) and a *Drosophila* embryo extract system. As all plasmids contained a T7 terminator, they were not linearized. Experiments using the commercially available systems were performed according to the manufacturer's protocol. IVT/T using the *Drosophila* embryo extract was conducted based on Medenbach *et al.*, 2011. Plasmid templates were transcribed using 3'-O-Me-m^7(5')Gppp(5')G ("anti-reverse") cap analog (New England Biolabs GmbH, Frankfurt am Main, Germany) and T7 RNA polymerase (Agilent Technologies, Santa Clara, USA) and transcript was analyzed by gel electrophoresis. *Drosophila* embryo translation extract was kindly provided ready-to-use by J. Medenbach, University of Regensburg. The extract was produced from overnight embryos collected and dechorionated using 3% sodium hypochlorite solution. The embryos were washed and disrupted by 20 strokes of a Potter-Elvehjem homogenizer at 1,500 rpm in buffer (10 mM HEPES-KOH pH 7.4, 5 mM DTT, and complete protease inhibitor [Roche Diagnostics International AG, Rotkreuz, Swiss]). The clear phase was collected by centrifugation (20 min, 40,000 g, 4°C) and supplemented with 10 % glycerole. Translation reaction was performed in 10 µl volume using 1 µl transcript, 24 mM HEPES-KOH pH 7.4, 100 mM KOAc, 0.6 mM $Mg(OAc)_2$, 60 µM amino acid mix, 20 mM creatine phosphate, 800 ng creatine kinase and 40% *Drosophila* embryo extract for 90 min at 25°C. Additionally, IVT/T was performed using the wheat germ extract system and the five sequences cloned into the pJet1.2/blunt vector (Thermo Fisher Scientific Inc., Waltham, MA, USA) serving as templates. As this vector does not contain T7 promoter, all constructs were linearized prior to IVT/T. Translation products were examined by detection of the fusion tags via immunoblot using primary anti-c-Myc antibody or anti-HA antibody (both Sigma-Aldrich, St. Louis, USA) diluted 1:1,000, and secondary anti-mouse IgG antibody from goat conjugated with horse reddish peroxidase (Sigma-Aldrich, St. Louis, USA) diluted 1:5,000.

6. 2. 8 Protein extraction from maize pollen tubes

Male maize flowers of the maize inbred line A188 were shaken to remove old pollen and fresh pollen was collected 3-4 h later by shaking pollen from the anthers into petri dishes filled with a thin layer of liquid PGM media for maize (Schreiber and Dresselhaus, 2003). The petri dishes were kept at room temperature for 45-60 min and germination rate was analyzed. Pollen with a germination rate of at least 80% was collected by centrifugation (2 min, 500 g, RT) and grounded in liquid nitrogen. Sample powder was suspended in extraction buffer (137 mM NaCl, 2.7 mM KCl, 10 mM Na_2HPO_4, 1.8 mM KH_2PO_4, adjusted to pH 7.4) supplemented with 1:100 Protease Inhibitor Cocktail (Sigma-Aldrich, St. Louis, USA), using 5 ml buffer for 1 g plant material. Crude insoluble cell fragments were separated from the lysate by centrifugation at 1,000 g and both samples were analyzed by immunoblot using polyclonal primary anti-WSL1 antibody and secondary anti-rabbit IgG antibody from goat conjugated with horse reddish peroxidase (Sigma-Aldrich, St. Louis, USA) diluted 1:5,000.

6. 2. 9 Pull-down with sEA1-biotin and germinated maize pollen

6. 2. 9. 1 With crosslinking, analysis by immunoblot

Freshly collected maize pollen were collected in a petri dish covered with a thin layer of 1xPGM for maize (Schreiber and Dresselhaus, 2003) and pollen exhibiting a germination rate of at least 80% were collected and concentrated in three 50 ml plastic tubes by centrifugation (5 min, 500 g, RT). Synthetic sEA1-biotin peptide or biotin as negative control was dissolved in DMSO and diluted with 1xPGM to a stock concentration 1 mg/ml. Peptide was added to two tubes of the concentrated pollen suspension and biotin to the third tube to a final concentration of 5 µg/ml and shaken at room temperature for 20 min. The crosslinker Sulfo-LC-SDA (Thermo Fisher Scientific Inc., Waltham, USA) was dissolved in 1xPBS buffer and added to the pollen suspension containing biotin and to one of the two suspensions containing peptide to a final concentration of 0.1 mg/ml. Sulfo-LC-SDA represents a membrane-impermeable non-cleavable and heterobifunctional crosslinker with length of 12.5 Å containing an amine-reactive and a photo-reactive moiety. The three samples were shaken at RT for additional 20 min for amine-reactive crosslinking. Subsequently, the suspensions were transferred into petri dishes without lid and placed for 20 min under a UV lamp emitting at 345 nm with distance of 5 cm to induce photo-reactive crosslinking reaction. Pollen was collected by centrifugation (5 min, 500 g, RT) and 1xPGM was completely removed. The pellets were grounded in liquid nitrogen and suspended in extraction buffer (50 mM HEPES-KOH pH 7.5, 5% glycerol, 50

mM $Na_4O_7P_2$, 1 mM Na_2MoO_4, 25 mM NaF, 10 mM EDTA, 0.5% polyvinylpyrrolidone, 20 mM sucrose, 3 mM DTT) supplemented with 1:100 Protease Inhibitor Cocktail (Sigma-Aldrich, St. Louis, USA), using 5 ml buffer for 1 g plant material. Crude cell debris was separated from the lysate by centrifugation at 1,000 g and discarded. The microsomal fraction was isolated by ultracentrifugation of the lysate (100,000 g, 45 min, 4°C). The supernatant was discarded and the microsomal fraction was resuspended in solubilization buffer (137 mM NaCl, 2.7 mM KCl, 10 mM Na_2HPO_4, 1.8 mM KH_2PO_4, 10% glycerol, adjusted to pH 7.4) with protease inhibitor and solubilized by stepwise addition of Triton™ X-100 until final concentration of 0.5%. Equalized NeutrAvidin™ Agarose beads (Thermo Fisher Scientific Inc., Waltham, USA) were added to the samples and shaken at room temperature for 30 min. Four washing steps with solubilization buffer without detergent were performed with 10fold bead volume. The beads were collected and boiled in SDS sample buffer for immunoblot analysis using either polyclonal anti-sEA1 antibody or monoclonal anti-biotin antibody (Thermo Fisher Scientific Inc., Waltham, USA), and secondary anti-mouse or anti-rabbit IgG antibody from goat conjugated with horse reddish peroxidase (Sigma-Aldrich, St. Louis, USA), diluted 1:5,000.

6. 2. 9. 2 No crosslinking, analysis by mass spectrometry

Freshly collected maize pollen were germinated in a thin layer of 1xPGM in a petri dish and pollen exhibiting a germination rate of at least 80% were collected by centrifugation (2 min, 500 g, RT). They were grounded in liquid nitrogen and used for pull-down experiment with the aim to identify interaction partners of sEA1 on the surface of germinated maize pollen. Experimental procedure was performed like described for tobacco leaves in 6. 2. 5. 4, but with pollen instead of tobacco leave material. The experiment was conducted with three replicates to avoid experimental biases. These steps included microsomal fractionation, solubilization, incubation with peptide or biotin and purification with NeutrAvidin™ beads. Please note that in contrast to the procedure described in 6. 2. 5. 4, the beads were not boiled in SDS sample buffer but were collected and frozen in liquid nitrogen. These frozen triplicate samples were sent for Orbitrap LC-MS analysis by Dr. Igor Paron at the MPI of Biochemistry, Martinsried, Germany, using a Thermo Fisher™ Q Exactive™ Plus.

6. 2. 10 Bioinformatic analysis

To identify protein sequences similar to WSL1a/b, WSL3 and WSL4, TBLASTN search, using the whole protein sequences as templates, was performed against the genomes of *Zea*

mays, *Sorghum bicolor*, *Oryza sativa ssp. japonica*, *Brachypodium distachyon*, *Triticum aestivum*, *Arabidopsis thaliana*, *Glycine max* and *Populus trichocarpa*, available at www.gramene.de (Monaco *et al.*, 2014). Protein sequence alignments and prediction of classical N-terminal signal peptides was performed like described in 2. 2. 1. Amino acid similarity was calculated using the SIAS server (http://imed.med.ucm.es/Tools/sias.html). *In silico* expression data were derived from the Genevestigator V3 database (Hruz *et al.*, 2008) and the genome-wide transcription atlas of Sekhon *et al.*, 2011 provided by the PLEXdb browser (experiment ZM37) (Dash *et al.*, 2012).

6. 3 Results

6. 3. 1 Heterologous expression of predicted mature *ZmEA1* (*sEA1*)

As biochemical studies of ZmEA1 and the identification of its interaction partner(s) require availability of sufficient protein, *ZmEA1* was expressed full-length as well as in its predicted mature form (*sEA1*). This truncated form consists of 49 amino acids lacking the N-terminal signal sequence and is supposed to be the active form of the protein (Márton *et al.*, 2012).

6. 3. 1. 1 Expression of sEA1 in Escherichia coli

Escherichia coli is one of the most commonly used heterologous expression systems for the production of recombinant protein (Rosano and Ceccarelli, 2014). In former experiments the full-length EA1 could not be obtained in a soluble form for purification (Fastner, 2010; Márton, personal communication), therefore the predicted mature ZmEA1 was chosen for recombinant protein expression. The sequence was cloned into the pGEX-2-GW Gateway® destination vector with an N-terminal glutathione-S-transferase-tag. The resulting plasmid was used for heterologous expression in the *E. coli* strains Rosetta™(DE) (Merck KGaA, Darmstadt, Germany). Regarding the amino acid sequence of sEA1, a high level of hydrophobicity is expected based on the model of Kyte and Doolittle, 1982. But although the GST-affinity tag is frequently utilized to enhance solubility of poor soluble proteins (Esposito and Chatterjee, 2006), the fusion of GST to sEA1 was found to be enhanced in the insoluble fraction of the cell lysate along with GST. Free GST was also detectable in the soluble sample, probably due to protein degradation (Figure 6.2 B). This was contrary to free GST of the control experiment, which was mainly detected in the soluble fraction (Figure 6.2 A). In both cases just protein corresponding to the molecular weight of GST could be purified from the soluble fraction, indicating that no soluble GST-sEA1 fusion protein was produced.

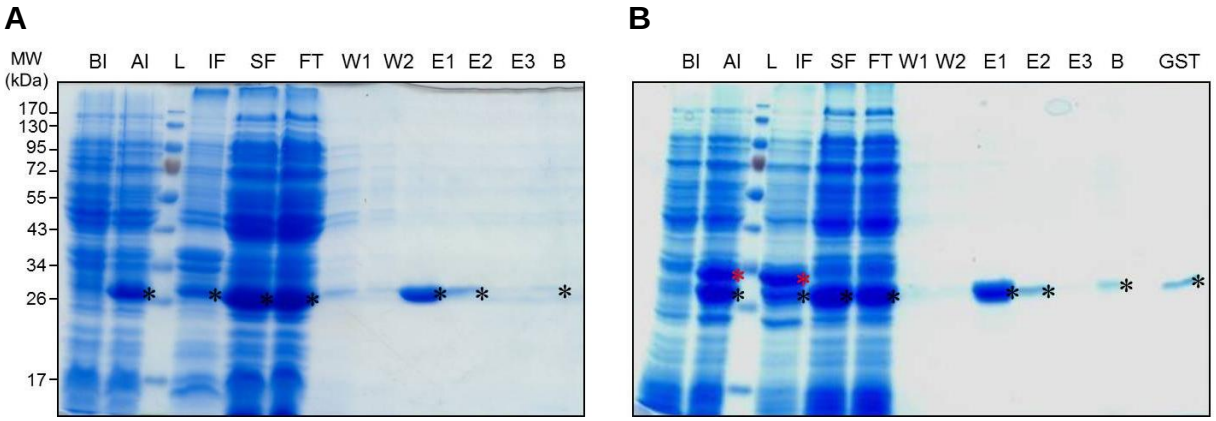

Figure 6.2 Production and purification of GST and GST-sEA1 in Rosetta™ (Coomassie stained gel). Expression of (**A**) *GST* as control and (**B**) *GST-sEA1*, respectively, was induced in the *E. coli* strain Rosetta™. Both bacterial protein lysates showed bands of appropriate molecular weight (MW) for GST (expected MW: 26.0 kDa, marked with black asterisks) and GST-sEA1 (expected MW: 30.9 kDa, marked with red asterisks) after induction (AI). The soluble fraction (SF) of the lysate was used for purification against GST. (**A**) As expected, major part of GST was detected in the SF of the induced lysate and could be purified successfully. (**B**) GST-sEA1 fusion protein was just visible in the insoluble fraction (IF) together with a band corresponding to free GST, which was also detected in the SF. GST-sEA1 was not present in the SI, as only bands corresponding to the size of GST were detected in the eluted fractions (E1-3) after purification. GST was loaded as size control. Abbreviations: B = beads, BI = before induction, FT = flow through, L = protein ladder, W1-2 = wash fractions.

In parallel, *sEA1* was cloned into the pET-53-DEST™ Gateway® destination vector with an N-terminal 6xHis-Tag and a C-terminal Strep-Tag II for T7 promoter based heterologous expression using the *E. coli* strains Rosetta™ and Lemo21(DE3) (NEB) and His-Tag purification of the recombinant protein. Lemo21(DE3) contains an additional plasmid compared to the original strain BL21(DE3), with a gene encoding for the T7 lysozyme, a T7 RNA polymerase inhibitor, under control of the inducible rhamnose promoter (Wagner *et al.*, 2008). This allows fine-tuning of the expression intensity by variation of rhamnose concentration and therefore potentially the reduction of toxic recombinant protein level and inclusion bodies. Inclusion bodies consist of insoluble, denatured and/or wrongly folded proteins packed into particles inside of the cytoplasm during over-expression of recombinant protein, which can harm the cells (for review see Kopito, 2000).

Induction of expression of the *6xHis-sEA1-StrepII* construct was successful, but separation of the bacterial lysate into soluble and insoluble fraction revealed that recombinant protein was solely present in the insoluble fraction (Figure 6.3). Increasing the concentration of rhamnose up to 1,000 µM led to reduction of the recombinant protein until no protein bands of corre-

sponding size were detected on Coomassie-stained SDS-gels, but no enrichment of recombinant protein in the soluble fraction could be observed.

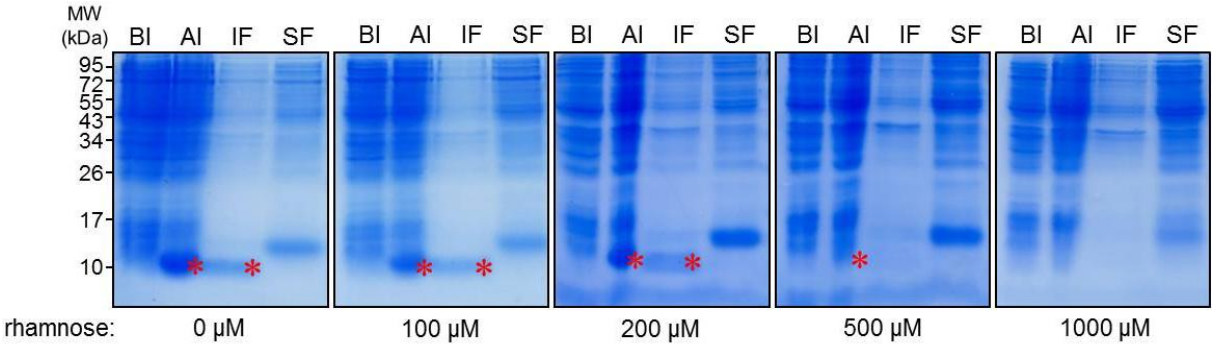

Figure 6.3 Production of 6xHis-sEA1-StrepII in Lemo21(DE3) (Coomassie stained gel). The production of recombinant 6xHis-sEA1-StrepII protein was induced in the *E. coli* strain Lemo21(DE3). SDS-PAGE analysis revealed protein bands of appropriate size for 6xHis-sEA1-StrepII (expected molecular weight [MW]: 10.1 kDa, marked with red asterisks) in the bacterial lysate after induction (AI) and the insoluble fraction (IF) of the lysate, which was not present before induction (BI). Down-regulation of the expression intensity by increasing the rhamnose concentration in the media from 0 to 1,000 µM did not result in notable accumulation of the recombinant protein in the soluble fraction (SF).

The 6xHis-sEA1-StrepII fusion protein was also produced using the *E. coli* strain Rosetta™ and like observed in Lemo21(DE3), fusion protein was detected exclusively in the insoluble fraction (Figure 6.4 A). As 1% sodium lauroyl sarcosinate is known to improve solubility of recombinant protein (Tao *et al.*, 2010), the detergent was used for solubilization of 6xHis-sEA1-StrepII containing inclusion bodies, which were enriched from bacteria lysate by centrifugation and washing steps based on Mukhopadhyay, 1997. Despite the effectiveness of this method to solubilize the protein, it could not be purified using TALON® cobalt resin (data not shown). Therefore it was decided to perform purification under denaturing conditions using 8M urea. Purification of the denaturated 6xHis-sEA1-StrepII yielded high levels of the recombinant protein (Figure 6.4 B).

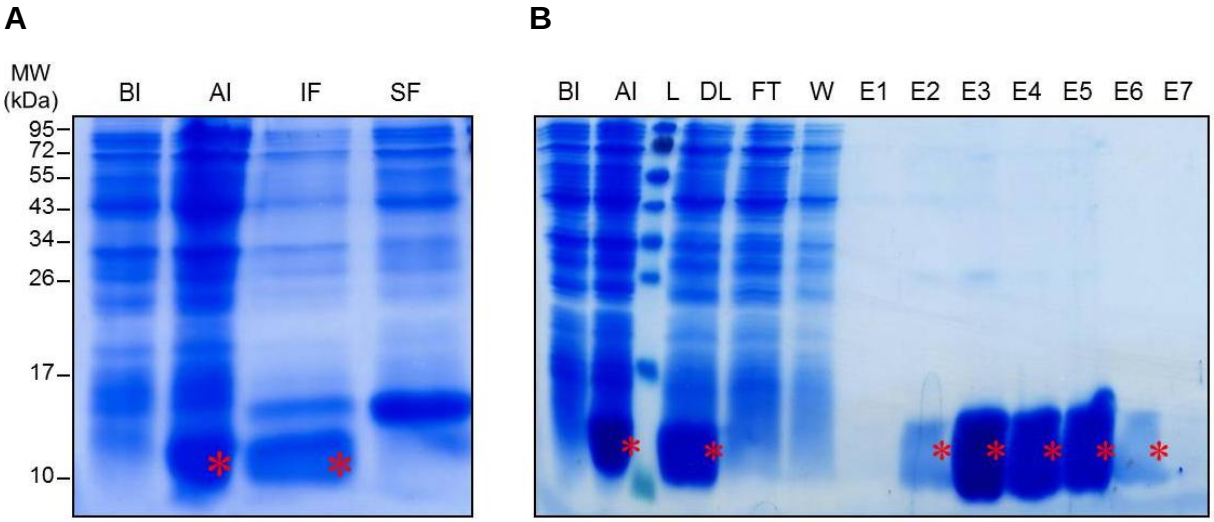

Figure 6.4 Production and purification of 6xHis-sEA1-StrepII in Rosetta™ (Coomassie stained gel). Production of 6xHis-sEA1-StrepII fusion protein was induced in the *E. coli* strain Rosetta™. (**A**) Analysis via SDS-PAGE showed protein bands with corresponding size of the fusion protein (expected molecular weight [MW]: 10.1 kDa, marked with red asterisks) after induction and in the insoluble fraction of the bacterial lysate. (**B**) Purification of the recombinant protein with denaturing buffers containing 8 M urea allowed the enrichment of 6xHis-sEA1-StrepII in the eluted fractions. Abbreviations: AI = after induction, BI = before induction, DL = denatured bacterial lysate, E1-7 = eluted fractions, FT = flow through, IF = insoluble fraction, L = protein ladder, SF = soluble fraction, W = wash fraction.

To remove the urea from the elution samples and to refold the recombinant protein to its native state, several dialysis steps with decreasing concentrations of urea were performed using SnakeSkin™ Dialysis Tubing (Thermo Fisher Scientific Inc., Waltham, USA) with 3.5 K molecular weight cut-off. As this method led to the complete precipitation of the recombinant protein, a urea gradient from 6 to 0 M urea was applied directly onto the beads inside of the purifcation column, with the recombinant protein still bound to the beads, to minimize aggregation of precipitating protein. Analysis of the eluted fractions without urea did not reveal any recombinant protein in the samples (data not shown).

To improve efficiency of the refolding processes during renaturation, several agents were added to the buffers, which are known to promote solubility and improve stability of proteins (Table 6.2). This included chaotropes, like $CaCl_2$, which interact with the peptide group and thereby replace or prevent intermolecular interactions between the protein that promote aggregations (Baldwin, 1996; Bondos and Bicknell, 2003). Another strategy included the use of kosmotropes, which are known to stabilize the native state of proteins and out-compete intramolecular interactions leading to aggregation by raising the entropic costs of hydrating inter-

mediate or denatured states (Baldwin, 1996; Timasheff, 1998; Bondos and Bicknell, 2003). $MgSO_4$ was chosen as representative agent for kosmotropes. Like kosmotropes, also sugars, like sucrose, and polyhydric alcohols, like glycerol, are excluded from the surface of proteins in solution and therefore stabilize the conformational state with the smallest surface area of the protein, which is normally the native state (Arakawa and Timasheff, 1982a, 1982b; Bondos and Bicknell, 2003).

Purification of 6xHis-sEA1-StrepII including renaturing steps with decreasing urea gradient was successful after the addition of 0.5% Tween®-20, Triton™-X-100 and n-Dodecyl-β-D-maltoside, respectively, to the renaturing buffers (Figure 6.5). Usage of all other additives, including n-Octyl-β-D-glucopyranoside, did not show any purified recombinant protein.

Table 6.2 Additives used to stabilize recombinant protein and to prevent aggregation. Buffers for refolding of recombinant protein purified under denaturing conditions were supplemented with various additives. The table lists all used agents, their concentration (Conc.) and substance class. The agents as well as the concentrations were chosen from a list of different substance classes investigated by Bondos and Bicknell, 2003, except n-Octyl-β-D-glucopyranoside, n-Dodecyl-β-D-maltoside and Triton™ X-100.

Agent	Conc.	Substance class	Reference
$MgSO_4$	0.2 M	Kosmotrope	Neagu *et al.,* 2001; Bondos and Bicknell, 2003
$CaCl_2$	0.1 M	Chaotrope	Neagu *et al.,* 2001; Bondos and Bicknell, 2003
Sucrose	0.5 M	Sugar	Kerwin *et al.,* 1998; Webb *et al.,* 2001
Glycerole	20%	Polyhydric alcohol	Gekko and Timasheff, 1981; Bondos and Bicknell, 2003; Arakawa and Timasheff, 1982a; Bondos and Bicknell, 2003
n-Octyl-β-D-glucopyranoside	0,5%	Non-ionic detergent	Rogl *et al.,* 1998; Chang *et al.,* 2001
Tween®-20	0,5%	Non-ionic detergent	Kreilgaard *et al.,* 1998; Bondos and Bicknell, 2003
Triton™ X-100	0,5%	Non-ionic detergent	Leibly *et al.,* 2012
n-Dodecyl-β-D-maltoside	0,5%	Non-ionic detergent	Zardeneta and Horowitz, 1992; Haji Abdolvahab *et al.,* 2014

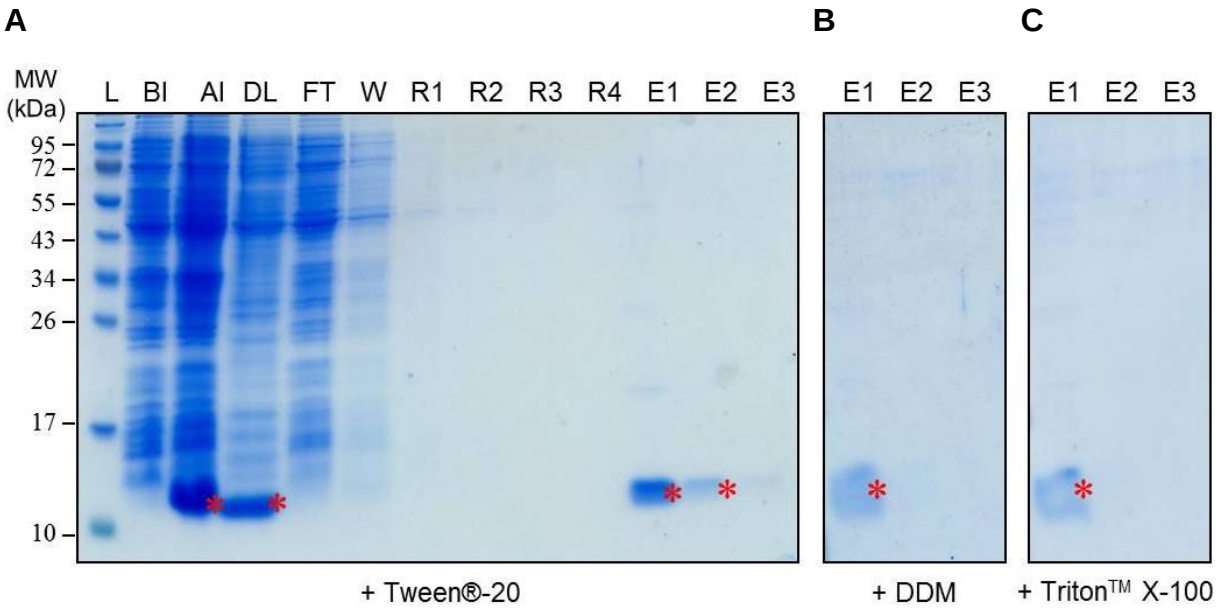

Figure 6.5 Denaturing purification of 6xHis-sEA1-StrepII and refolding including agents for prevention of protein aggregation (Coomassie stained gel). (**A**) Production of 6xHis-sEA1-StrepII was induced in the *E. coli* strain Rosetta™ and protein bands with molecular weight (MW) corresponding to the size of the recombinant protein were detected (expected MW: 10.1 kDa, marked with red asterisks). Denaturing urea-based lysis of the bacteria was followed by purification including refolding steps (R1-4) using buffers with decreasing urea concentration and supplementation of 0.5% Tween®-20. Recombinant protein was enriched in the eluted fractions (E1-3). (**B, C**) The experimental procedure was performed like in (**A**), except the usage of (**B**) 0.5% n-Dodecyl-β-D-maltoside or (**C**) Triton™ X-100, respectively, instead of Tween®-20. With all three detergents, recombinant protein could be purified successfully. Abbreviations: AI = after induction, BI = before induction, DL = denatured bacterial lysate, FT = flow through, L = protein ladder, W = wash fraction.

The critical micelle concentration (CMC) of n-Octyl-β-D-glucopyranoside is 25 mM or 0.73% w/v (Shinoda *et al.*, 1961) and therefore it was the only one of the used detergents with a concentration below its CMC (Table 6.3), probably weakening its ability for increasing protein solubility. It is likely that the recombinant protein was enclosed by micelles formed by the other detergents which allowed its purification. Hence one has to expect that removing the detergents would result in the precipitation of the protein. Downstream applications of the recombinant pollen tube attracting protein should mainly focus on interaction studies with living maize pollen tubes. Presence of detergents would be supposed to disturb the cell integrity and additionally, the mature signaling peptide would be expected to be trapped inside of the micelles as it does not contain transmembrane domains. Interactions of the recombinant protein with binding partners outside of the micelles can therefore not be anticipated.

Table 6.3 Critical micellar concentrations (CMCs) of detergents utilized for refolding of denatured purified 6xHis-sEA1-StrepII. Comparison of CMCs of various detergents demonstrates that n-Octyl-β-D-glucopyranoside features the highest CMC.

Detergent	CMC	Reference
n-Octyl-β-D-glucopyranoside	25 mM / 0.73% w/v	Shinoda *et al.*, 1961
Tween®-20	0.059 mM / 0.0072% w/v	Helenius *et al.*, 1979
Triton™ X-100	0.27 mM / 0.017% w/v	Holloway and Katz, 1972
n-Dodecyl-β-D-maltoside	0.16 mM / 0.081% w/v	DeGrip and Bovee-Geurts, 1979

To increase the solubility of recombinant predicted mature ZmEA1, *sEA1* was cloned into the pDEST-HisMBP Gateway® destination vector with an N-terminal 6xHis-Tag followed by an N-terminal maltose-binding protein (MBP)-tag (Nallamsetty *et al.*, 2005) for heterologous expression using the *E. coli* strains Rosetta™, followed by His-Tag purification via TALON® cobalt resin (Takara Bio Inc., Otsu, Japan). The MBP fusion tag is known to enhance the solubility of recombinant proteins more effectively than GST and can also promote correct folding of the attached proteins (Kapust and Waugh, 1999). His-MBP-sEA1 fusion protein could be detected in the soluble fraction after induction of expression by immunoblot, using a ZmEA1-specific antibody (Figure 6.6 B). Although notable amounts of the protein remained in the flow-through after purification, it was possible to enrich the recombinant protein in the eluted fraction (Figure 6.6 B). Nevertheless, one has to consider that the entire fusion protein exhibit a molecular weight of about 44 kDa with sEA1 having a small proportion of 4.9 kDa. It is possible that this large N-terminal fusion impairs the functionality of the signaling peptide, especially as its ability to diffuse and to bind to its interaction partners on the surface of pollen tubes might be affected due to the size and the changed steric properties. Attraction or binding tests like described in Uebler *et al.*, 2013, or Márton *et al.*, 2012, would be necessary to proof the functionality of the recombinant protein.

Before these results were obtained, a commercially ordered synthetic version of the 49 amino acid sEA1-peptide was successfully synthesized (Centic Biotec, Heidelberg, Germany) with and without biotin labeling. As the unlabeled peptide was already demonstrated to bind on the surface of the pollen tube tip (see 4. 3) the biotin-labeled peptide was used for further biochemical experiments for identification of the binding partner(s) of ZmEA1.

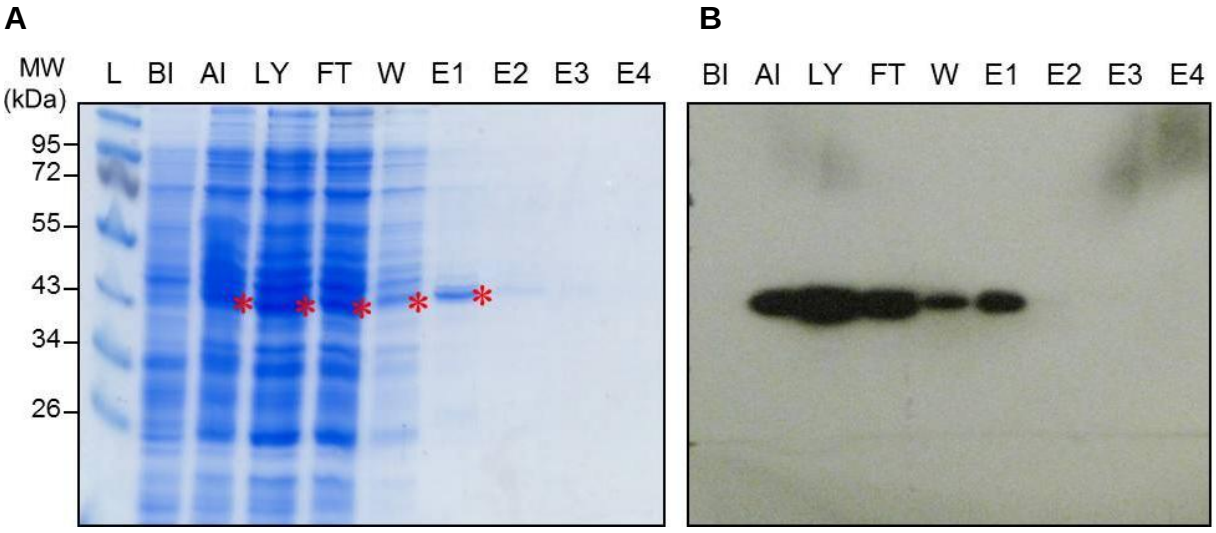

Figure 6.6 Purification of 6xHis-MBP-sEA1 in RosettaTM under native conditions. Expression of 6xHis-MBP-sEA1 was induced in the *E. coli* strain Rosetta^{TM} and (**A**) SDS-PAGE analysis as well as (**B**) immunoblot analysis using a polyclonal antibody against ZmEA1 revealed protein bands of the corresponding size (expected molecular weight [MW]: 44 kDa, marked with red asterisks) in the soluble fraction (SF). The recombinant protein could be purified under native conditions utilizing the 6xHis-tag. Weak protein bands visible in the background of the eluted fractions (E1-4) demonstrate that the eluate was not highly pure and additional purification steps would be necessary for further downstream applications. Abbreviations: AI = after induction, BI = before induction, FT = flow through, L = protein ladder, W = wash fraction.

6. 3. 1. 2 Expression of sEA1 in Nicotiana benthamiana leaves

As recombinant expression of *sEA1* in *E. coli* was problematic due to the insolubility of the protein, another host system was chosen for protein production. *Nicotiana benthamiana* plants are a very common system to study subcellular localization of recombinantly produced plant proteins. As transient transformation of the leaves can be performed very easily and quickly by agroinfiltration, notable amount of fusion-tagged proteins can be obtained *in planta* for purification. Plant cells are unique regarding protein folding pathways (Onda, 2013) and tobacco leaves in particular have a high yield of biomass and provide high levels of soluble proteins (Rymerson *et al.,* 2002). Therefore tobacco was considered as an alternative expression system for production of sEA1 and ZmEA1 fusion proteins. Additionally, a shortened form of ZmEA1 (spEA1, Márton *et al.,* 2012) was included. Although the transcription start of ZmEA1 was mapped by Márton *et al.,* 2005, a shorter form is predicted in the maize genome (Márton *et al.,* 2012). As spEA1 still contains a computationally predicted classical N-terminal signal peptide, it was used in this study. For amino acid sequences of the three EA1 forms, see Figure 3.4. The sequences of *sEA1*, *spEA1* and full-length *ZmEA1* were cloned into

the pB7FWG2,0 vector (Karimi *et al.*, 2002) for expression with C-terminal GFP fusion under control of the constitutively active *35S* promoter of the cauliflower mosaic virus (Odell *et al.*, 1985). Protein localization was analyzed in transiently transformed *Nicotiana benthamiana* leaves (Figure 6.7). In accordance with the subcellular localization pattern in BMS suspension cells described in 2. 3. 3, the full-length ZmEA1-GFP could be detected surrounding the nucleus and localizing in strains throughout the cells, resembling the endoplasmic reticulum (Figure 6.7 A-B), whereas free GFP was detected solely in the cytoplasm (Figure 6.7 G-H). Aggregation of granular structures in the cell indicated that the fusion protein is packed into aggresomes, probably due to misfolding of the protein after overexpression (Johnston *et al.*, 1998). No difference could be detected compared to the localization pattern of spEA1-GFP (Figure 6.7 C-D). In contrast to these two proteins but according to the results of CHAPTER 2 (see Figure 2.4), sEA1-GFP was distributed throughout the cytoplasm, including the nucleus (Figure 6.7 E-F). Scattered aggregations of the sEA1-GFP were also observed inside of the tobacco epidermis cells.

The leave samples were analyzed via immunoblot to estimate their suitability for native purification of the recombinant proteins. For detection, a GFP-directed antibody (Roche Diagnostics International AG) was used. The protein lysates were separated from the crude cell extract and SDS-PAGE was performed. Protein bands corresponding to the expected size of EA1-GFP, spEA1-GFP and sEA1-GFP could be detected, with sEA1-GFP exhibiting the strongest intensity (Figure 6.8 A). All three samples showed protein bands with molecular weight of free GFP, probably by degradation of the fusion protein. Additional bands with a molecular weight of double size of the fusion-proteins were observed in each sample. It is supposed that these bands are the results of aggregated fusion proteins which were not sufficiently denatured during SDS-PAGE analysis.

Due to its signal intensity and cytoplasmic localization, sEA1-GFP was chosen for further purification against the GFP-tag using the GFP-Trap system (ChromoTek GmbH, Planegg, Germany) with agarose beads. Although the fusion protein was bound by the GFP-Trap resin and successfully eluted from the beads (Figure 6.8 B), silver staining of the protein gels demonstrated extremely low levels of the recombinant sEA1-GFP in the eluted fractions (data not shown). Additionally, most of the protein was degraded during the purification process, noticeable by the increase of free GFP in the eluted fraction compared to the lysate. These small amounts of protein were not considered to be used for further biochemical experiments.

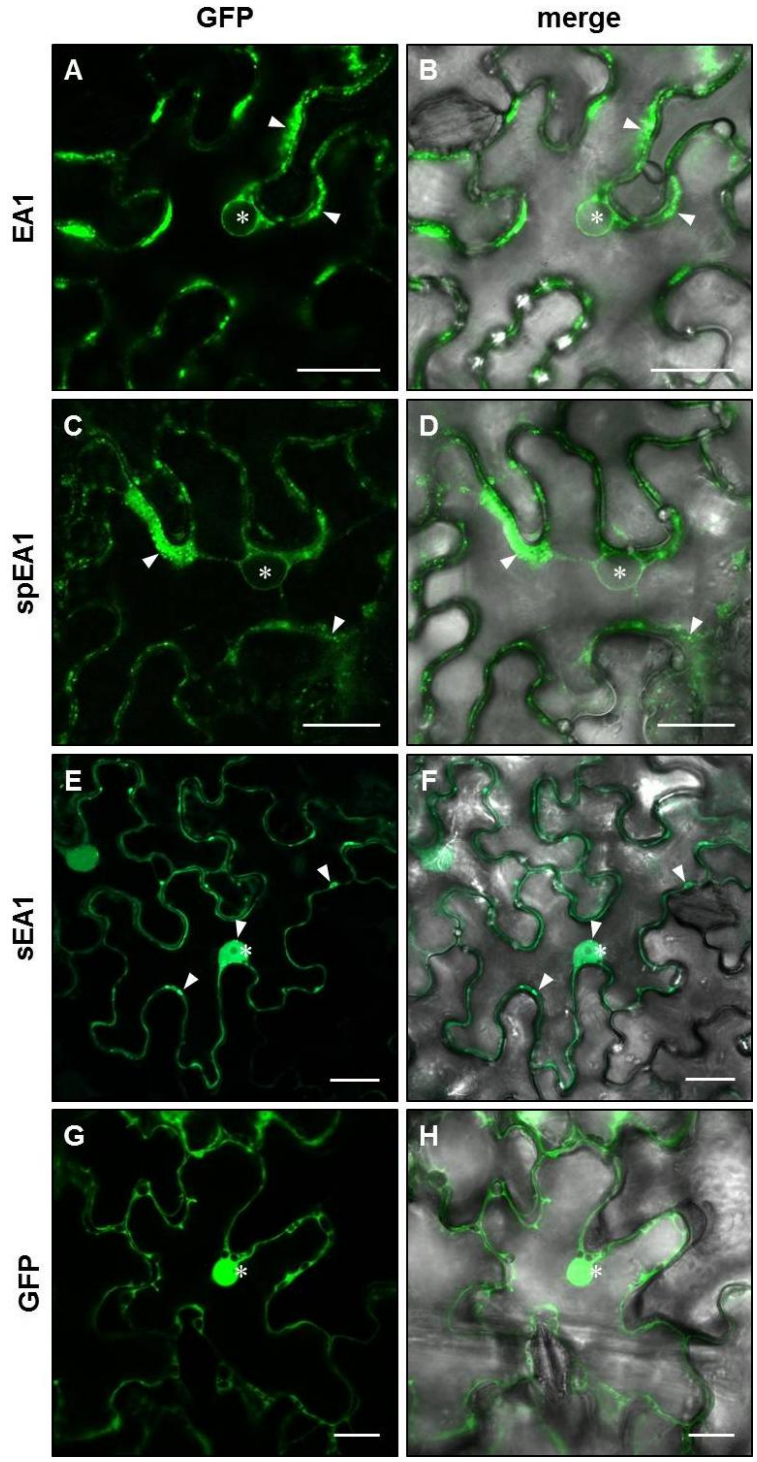

Figure 6.7 Subcellular localization of ZmEA1, spEA1 and sEA1 fused to GFP in leave epidermis cells of tobacco. ZmEA1, spEA1 and sEA1, respectively, fused to GFP were transiently expressed in *Nicotiana benthamiana* leaves and analyzed for their subcellular localization pattern. (**A**, **B**) ZmEA1-GFP and (**C**, **D**) spEA1-GFP were localized surrounding the cell nucleus (marked with asterisks) and aggregating inside of the cells (marked with arrowheads), reflecting the localization pattern of the endoplasmic reticulum. (**E**, **F**) sEA1-GFP could be detected inside of the cytoplasm with few aggregations (marked with arrowheads) and the nucleus (marked with asterisk), comparable to free GFP (**G**, **H**). (**A**, **C**, **E**, **G**) Fluorescence micrographs. (**B**, **D**, **F**, **H**) Merged bright field and fluorescence micrographs. Scale bar represents 20 µm.

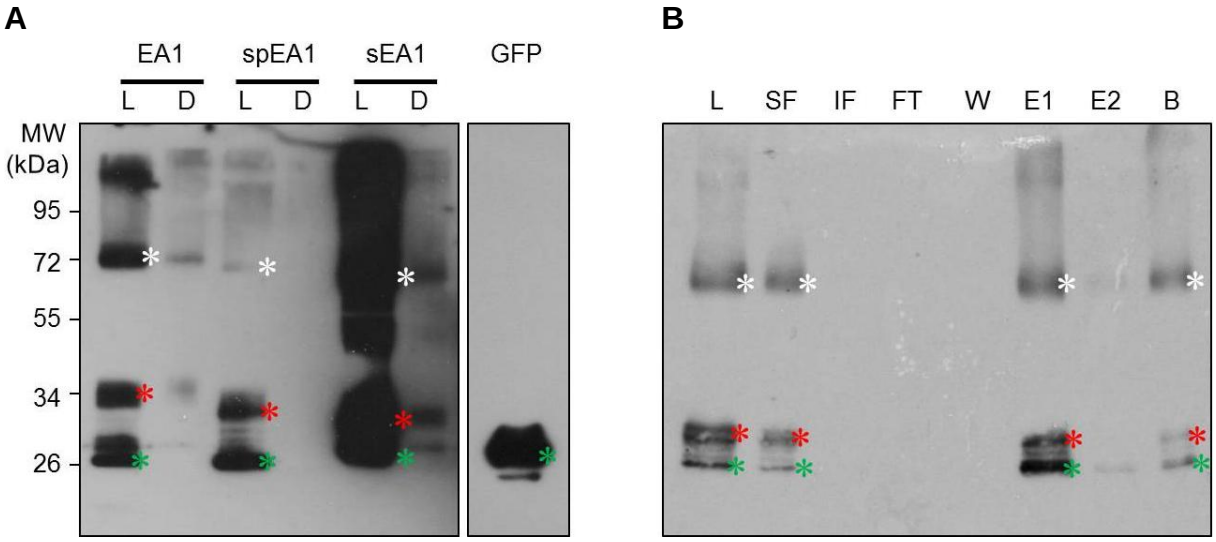

Figure 6.8 Detection and purification of GFP-tagged ZmEA1, spEA1 and sEA1 produced in *Nicotiana benthamiana*. (**A**) ZmEA1, spEA1 and sEA1, respectively, were transiently expressed as GFP-fusion proteins in tobacco leaves. Crude cell debris (D) and lysate (L) were separated and analyzed via immunoblot using a GFP-directed antibody. For each of the fusion proteins, corresponding bands were detectable in the lysate (expected molecular weights [MW]: ZmEA1-GFP = 38.3 kDa, spEA1-GFP = 36.4 kDa, sEA1-GFP = 33.7 kDa; all marked with red asterisks) as well as bands of free GFP (expected MW: 26.9 kDa, marked with green asterisks), probably due to degraded fusion protein. Additional bands of MW approximately twice as much as the fusion proteins could be observed in each sample (marked with white asterisks), likely representing aggregated fusion protein that could not be sufficiently denatured during SDS-PAGE. (**B**) With sEA1-GFP showing the strongest signal intensity and cytoplasmic localization, it was chosen for purification with the GFP-binding resin GFP-Trap. The lysate (L) was separated into soluble (SF) and insoluble fractions (IF), demonstrating the solubility of sEA1-GFP. The fusion protein (marked with red asterisks) was purified from the SF and detected in the eluted fractions (E1-2) and after heating the resin (B), including the additional signals of doubled MW like already observed in (**A**) (marked with white asterisks). During the purification process, remarkable parts of the recombinant protein were degraded to free GFP (marked with green asterisks), indicated by the increasing ration of GFP to sEA1-GFP in the eluted fraction. Abbreviations: FT = flow through, W = wash fraction.

6. 3. 2 Potential interaction partners of sEA1

6. 3. 2. 1 Visualization of sEA1 binding to other proteins

As synthetic biotinylated sEA1 was available, it was used for biochemical approaches to identify binding partners of sEA1. It was observed that sEA1, coupled to a fluorophore, is able to bind the pollen tube tip in a very specific manner (see CHAPTER 4, Uebler *et al.*, 2013). Therefore, it was supposed that pollen tube surface localized proteins can form a complex with sEA1 to initiate a signal transduction. To visualize potential binding partners of sEA1 by im-

munoblot, *in vitro* growing maize pollen tubes were incubated with biotinylated sEA1, followed by crosslinking using Sulfo-LC-SDA (Thermo Fisher Scientific Inc., Waltham, MA, USA) to covalently couple sEA1 to its binding partner(s). Sulfo-LC-SDA represents a non-cleavable, membrane-impermeable and heterobifunctional crosslinker containing an N-hydroxysuccinimide ester and a diazirine-based photoreaction moiety as functional groups. As negative control, biotin instead of biotinylated sEA1 was chosen. The microsomal fraction was isolated and the complete fraction was applied for denaturing immunoblot analysis using either anti-biotin antibody or anti-sEA1 antibody. Covalent binding of sEA1 to its interaction partner(s) should result in a signal of molecular weight larger than sEA1 alone (4.9 kDa), depending on the molecular weight of the coupled binding partner.

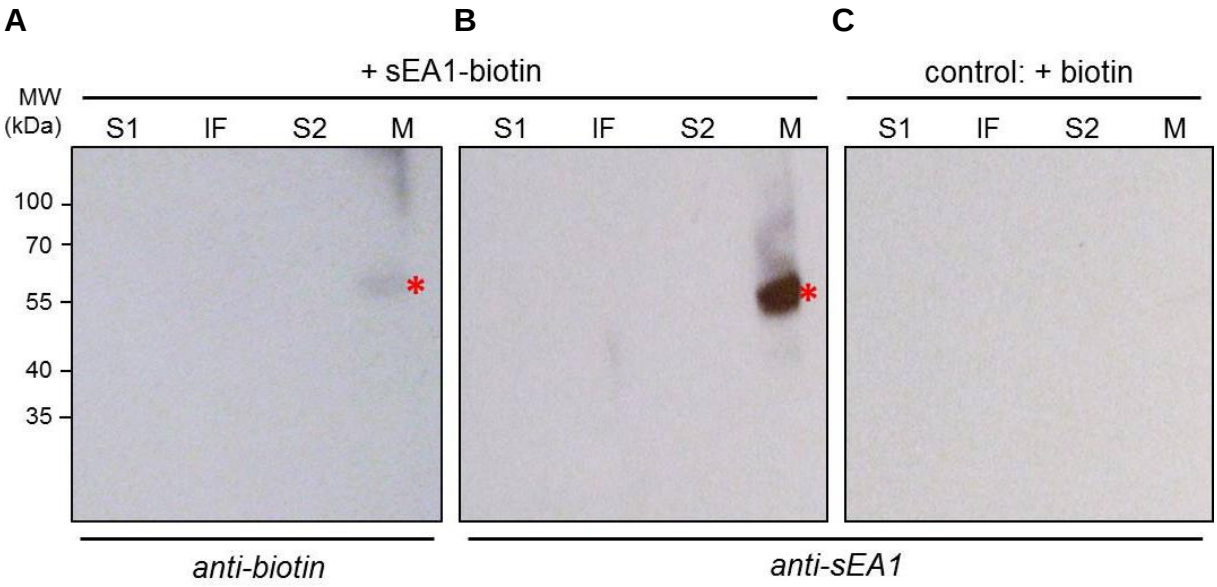

Figure 6.9 Visualization of a putative interaction partner of sEA1. *In vitro* germinated maize pollen tubes were incubated with either biotinylated sEA1 or biotin for control reaction and crosslinked using the non-cleavable crosslinker Sulfo-LC-SDA to covalently couple sEA1 to putative binding partner(s) on the pollen tube surface. The pollen were harvested and separated into soluble fraction (S1) and insoluble cell debris fraction (IF). S1 was used to isolate the microsomal fraction (M) and all samples were analyzed by immunoblot. Pollen samples incubated with sEA1-biotin analyzed using (**A**) biotin-directed primary antibody or (**B**) sEA1-directed antibody showed both a signal in the microsomal fraction (marked with red asterisks). Molecular weight (MW) of the signal was between 55 and 70 kDa, indicating a potential interaction partner crosslinked to the small sEA1 (MW 4.9 kDa). (**C**) Control experiment using biotin instead of biotinylated sEA1 analyzed using sEA1-directed antibody did not show any signal.

The addition of biotinylated sEA1 resulted in a signal between 55 – 70 kDa in the microsomal fraction which could be detected with both antibodies, indicating a complex of sEA1-biotin with an interaction partner(s) sizing between 50 – 65 kDa (Figure 6.9 A, B). It could be excluded that formation of this complex was mediated by binding of the biotin conjugate, as the biotin-only control did not show any signal (Figure 6.9 C). Please note, that detection with anti-biotin antibody was much weaker than with anti-sEA1 antibody, due to less sensitivity of this antibody (Figure 6.9 A).

To figure out whether this binding partner can be isolated, the experiment was repeated and the microsomal fraction was solubilized using 0.5 % Triton-X 100. It was used for affinity purification against the conjugated biotin to isolate this putative complex (Figure 6.10 A) for further analysis by SDS-PAGE and immunoblot, using anti-sEA1 antibody (Figure 6.10 C). Parallel to the addition of peptide and crosslinker (*+peptide/+CL*), two negative controls were performed, the first one with supplementation of biotin instead of peptide (*+biotin/+CL*), the second one with peptide and no crosslinker (*+peptide/-CL*). Analysis of +peptide/+CL revealed a double band signal in between 55 - 70 kDa in the solubilized microsomal fraction and the eluted fraction. No signal was obtained regarding *+biotin/+CL*, coinciding with the results of Figure 6.9. Surprisingly, immunoblot of *+peptide/-CL* showed the same double band in the eluted fraction but lacking in the solubilized microsomal fraction. The biotinylated peptide alone without germinated pollen did not form any bands of larger molecular weight than 4.9 kDa (Figure 6.10 D). Although silver-stained SDS-PAGE gels of the same samples were difficult to analyze as there was strong background staining, they resembled the immunoblot results by indicating an additional band in the eluted fractions of *+peptide/+CL* and *+peptide/-CL*, which was lacking in *+biotin/+CL* (Figure 6.10 C).

To summarize, there was a clear hint that incubation of germinated maize pollen tubes with biotinylated sEA1 caused a strong shift of sEA1 derived immunoblot signal, likely induced by coupling to binding partners to the peptide. Nevertheless, the appearance of the same signal in different fractions of *+peptide/+CL* and *+peptide/-CL* cannot be clearly interpreted, especially as any interaction between sEA1 and its putative receptor should be dissolved during SDS-PAGE, if it is not stabilized by covalent crosslinking. It is possible that the signals in the eluted fraction of *+peptide/-CL* are the result of insufficient denaturation of a very strong binding between sEA1-biotin and its interaction partner after solubilization of the microsomal fraction. Due to its high hydrophobicity, free synthetic sEA1-biotin enriches in the microsomal fraction and could therefore gain access to solubilized pollen tube receptors.

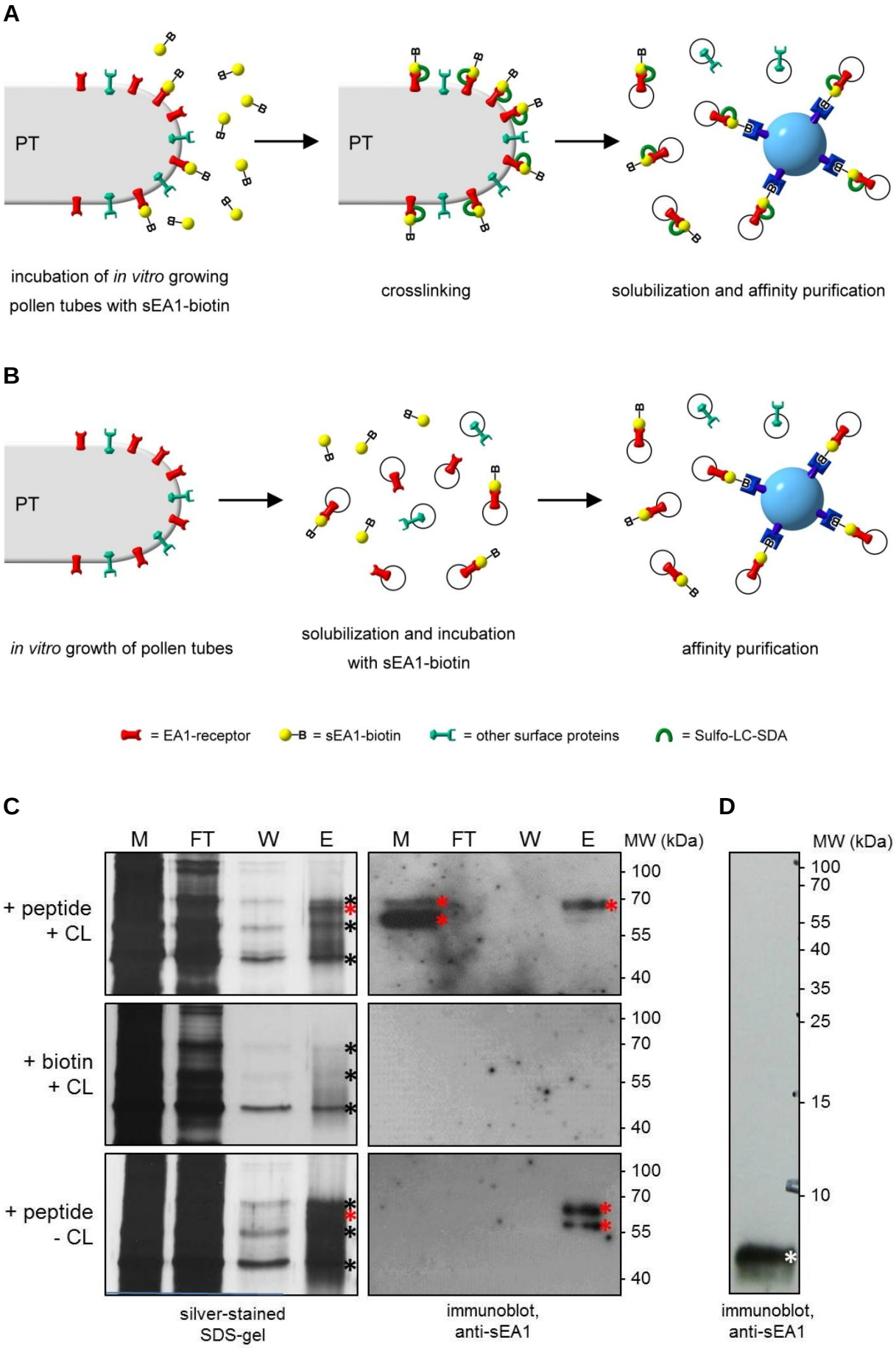
A
PT
PT
incubation of *in vitro* growing pollen tubes with sEA1-biotin
crosslinking
solubilization and affinity purification
B
PT
in vitro growth of pollen tubes
solubilization and incubation with sEA1-biotin
affinity purification
= EA1-receptor
= sEA1-biotin
= other surface proteins
= Sulfo-LC-SDA
C
M FT W E M FT W E MW (kDa)
+ peptide + CL
+ biotin + CL
+ peptide - CL
100
70
55
40
silver-stained SDS-gel
immunoblot, anti-sEA1
D
MW (kDa)
100
70
55
40
35
25
15
10
immunoblot, anti-sEA1

Figure 6.10 Affinity purification of sEA1 binding partners. (**A**) Model illustrating the experimental procedure to visualize whether sEA1 is binding other proteins derived from germinated maize pollen. *In vitro* growing pollen tubes (PT) were incubated with synthetic biotinylated sEA1 to bind putative interaction partners on the tube surface. The protein complexes were crosslinked using non-cleavable Sulfo-LC-SDA and the microsomal fraction was isolated and solubilized for biotin-directed affinity purification, in order to isolate the complex for SDS-PAGE and immunoblot analysis. For results see (**C**, **D**). (**B**) Model illustrating the experimental procedure to identify putative interaction partners of sEA1 without crosslinking. The microsomal fraction of *in vitro* grown maize PTs was solubilized and incubated with sEA1-biotin in order to bind the solubilized interaction partners. The complex was affinity-purified using biotin-binding beads and the isolated proteins were analyzed by mass spectrometry. No crosslinking reaction was performed. (**C**) Visualization of putative sEA1-binding proteins by SDS-PAGE (left) and immunoblot (right) after experimental procedure illustrated in (**A**). Silver stained SDS protein gels of crosslinked sEA1-biotin (*+peptide/+CL*) and control experiments with crosslinked biotin (*+biotin/+CL*) and non-crosslinked sEA1-biotin (*+peptide/-CL*) showed several unspecific bands in the eluted fraction (E) (marked with black asterisks). Both *+peptide/+CL* and *+peptide/-CL* showed an additional band lacking in *+biotin/+CL* (marked with red asterisks). Immunoblot analysis using polyclonal anti-sEA1 antibody revealed a double band of approximately corresponding size (marked with red asterisks) in the microsomal (M) and the eluted fraction of *+peptide/+CL*, but only in the eluted fraction of *+peptide/-CL*. (**D**) Synthetic sEA1-biotin without PT extract did not exhibit formation of aggregates of higher molecular weight (MW) in immunoblot analysis using anti-sEA1 antibody. The only detectable band represented the expected molecular weight of sEA1-biotin (4.9 kDa, marked with white asterisk). Abbreviations: CL = crosslinker, FT = flow through, W = wash fraction.

6. 3. 2. 2 Identification of potential interaction partners of sEA1

The next step was to identify the protein(s) causing the change in molecular size of sEA1-biotin. As the first approach (Figure 6.10 A) did not gain material of enough quantity or quality for successful MS analysis of the isolated proteins, another experimental design was created to increase the efficiency. Instead of incubating the intact pollen tubes with biotinylated sEA1, the microsomal fraction of pollen tubes was isolated and solubilized prior to the incubation with sEA1-biotin and biotin-directed affinity purification (Figure 6.10 B). As MS-analysis of the isolated proteins after crosslinking has to challenge several obstacles, like an altered fragmentation behavior of proteins (for review see Petrotchenko and Borchers, 2010, chapter IV), no crosslinker was used in this approach. To reduce experimental variations, the purification step was performed with three technical replicates. Protein sequences were analyzed by Orbitrap mass spectrometry (cooperation with I. Paron, MPI of Biochemistriy, Martinsried) and identified by comparison of the data with the UniProt protein database (The UniProt Consortium, 2015). All detected proteins with at least 2 unique peptides after diges-

tion are listed in Table 6.4. The bait protein sEA1 was identified with sequence coverage of 100 % in the samples and approximately 50 % in two of the negative controls. As sEA1 protein can be detected with only 4 peptides in mass spectrometry, the identification of only 2 of these peptides was enough to reach this high sequence coverage in the negative control without supplementation with sEA1. Nevertheless, the LFQ intensity in the samples was up to 200fold lower in the negative controls, indicating that this might be only background signal. To select putative interaction candidates, only proteins with sequence coverage of at least 30 % in the samples and less than 15 % in the negative controls were considered. It could be demonstrated that three protein groups were enriched in the samples compared to the negative control. The first group was composed of the proteins B6SKG2, B6TDW3 and B6T7E9. B6TDW3 could be excluded, as closer examination of the corresponding regions of the maize genome revealed that B6TDW3 was the result of wrong annotation of B6SKG2, introducing a frame shift. The protein sequences of B6SKG2 and B6T7E9 were identical, but only B6SKG2 featured corresponding genome annotations (GRMZM2G419209 and GRMZM2G319875). The other two protein groups consisted of only one protein, B4FM84 (genome annotation: AC189771.3) and B6TP27 (genome annotation: GRMZM2G703173), respectively. All of the candidates were identified with sequence coverage of at least 35 % and less than 10 % in the negative controls. The LFQ intensities of the candidates was very low by ranging from 50 to 1700 fold less compared to the LFQ intensity of the positive sEA1 signal. Although one could assume these intensities to be background signals, they were treated as real candidates, as the negative controls of B6SKG2 and B6TP27 did not display any LFQ intensity at all and LFQ intensities of B4FM84 negative controls were at least 10 fold lower than in the samples with sEA1-biotin.

Table 6.4 Protein groups identified in biotin-directed pull-down of pollen tubes after incubation with sEA1. Three technical replicates were analyzed for interaction with sEA1-biotin (S1-3) or biotin (B1-3), respectively. Candidates for further examinations are shaded in green; sEA1-biotin is shaded in red. LFQ: label-free quantification value [*10^6]; ∑ Pep: sum of unique peptides; Pep: number of identified unique peptides; SeqC: sequence coverage [%].

UniProt ID	LFQ B1	LFQ B2	LFQ B3	LFQ S1	LFQ S2	LFQ S3	∑ Pep	Pep B1	Pep B2	Pep B3	Pep S1	Pep S2	Pep S3	SeqC B1	SeqC B2	SeqC B3	SeqC S1	SeqC S2	SeqC S3
B6SKG2; B6TDW3; B6T7E9	0	0	0	206.86	292.52	437.78	11	0	0	0	10	10	10	0	0	0	65.1	65.1	65.1
B4FM84	9.49	10.34	0	88.30	54.56	109.85	9	1	2	0	6	8	6	6.9	8.3	0	36.1	44.4	38.2
B6TP27	0	0	0	13.39	12.76	18.84	5	0	0	0	3	4	5	0	0	0	37.5	38.9	38.9
Q5G8Z3 (sEA1-biotin)	98.89	0	348.25	22607.00	15676.00	13173.00	4	2	0	2	4	4	4	53.1	0	53.1	100	100	100
K7UAP0; B6UE01; B6SMC7; C0HHN5; B6T0H3; B6U2I7; B6TIE3; B6T147	18.90	22.93	22.55	210.13	770.00	220.87	4	2	2	2	4	4	3	38.5	38.5	38.5	44.2	44.2	42.3
B6T249	74.43	65.32	133.52	838.78	526.32	771.42	3	2	3	2	3	3	3	32.9	32.9	32.9	32.9	32.9	32.9
K7URN4	65.47	62.79	57.79	152.28	95.10	195.57	3	1	1	2	3	3	3	8.6	8.6	10.3	17.3	17.3	17.3
B6TQ08; B6SI11; C0HHR4; K7VYB9; P93637; P93635; P93639; P93636; P93634; B6SZ83; K7VII1; B4FV86; K7W273; K7V693; P02582; B6T5K6; B4FPG2; P93633; P93638; Q19R76; C7F8N7; Q84QI1; K7UH70	7001.30	6892.10	7616.10	4436.10	3649.30	5854.40	2	2	2	2	1	1	1	21.2	21.2	21.2	24.4	24.4	24.4
C0HDZ6; B4FVB1; B4FRH8; K7V663; K7VYC4; K7VB13; K7UJB6; B4F989; K7V2I3	224.19	255.15	258.52	82.28	60.41	85.47	2	2	2	2	1	1	2	21.2	21.2	21.2	24.4	24.4	24.4
Q1ZYQ8; B4FIV7; Q1ZYQ9; B4FFK8	10.26	7.36	0	235.74	147.17	211.59	2	1	1	0	2	1	1	4.8	4.8	0	12.2	4.8	4.8
B4FY93	28.04	35.16	21.06	90.67	38.18	66.13	2	1	1	1	2	2	2	3.3	3.3	3.3	5.5	5.5	5.5
B6T3G4; B4FP25; B4FD90; K7VYV0; K7WCY2	20.32	22.50	0	31.43	61.59	88.93	2	1	1	0	2	2	2	8.3	5.5	0	13.8	13.8	13.8
Q9ZQX9; B6TFY4; K7U5V7; B6TUY0	30.93	42.85	41.67	28.00	22.93	23.28	2	2	2	1	2	2	2	31.4	31.4	9.3	31.4	31.4	31.4
C4IYA0	0	8.72	18.53	26.33	18.16	65.74	2	0	1	1	2	2	2	0	12.8	6.7	12.8	12.8	12.8
C4IY28	13.55	10.93	9.82	14.52	19.55	17.23	2	1	1	2	2	1	2	3.2	3.2	3.2	3.2	3.2	3.2
K7V5R7; B6TUA2; Q9SWR9	22.68	24.63	29.01	13.64	12.26	25.42	2	2	2	2	2	2	2	8.4	8.4	8.4	8.4	8.4	8.4
K7U545	0	0	0	12.17	0	0	2	1	1	1	2	1	1	1.4	1.4	1.4	1.7	1.4	1.4
K7UYG2; K7UFF5; B4FJ48; P19950; P19951; B6UHC8; B6UH09; B6T522; B4FBS3; B4FKA4; K7UYG7; K7U4U0; K7UW87; C0PK42; K7VW88; B6T281; B6UE59; K7VDG3	11.19	10.83	11.52	11.91	11.16	12.74	2	2	2	2	2	2	1	27.2	27.2	27.2	27.2	27.2	15.2
B4FC75; Q6QU83; O22424; B4FMI5; O22453	4.77	0	0	7.24	8.75	14.85	2	1	0	0	2	1	1	9.8	0	0	17.6	9.8	9.8
C0HDU7	6.90	7.22	0	5.11	6.80	6.80	2	1	1	0	2	1	2	4.9	4.9	0	12.1	4.9	12.1
K7U845; C0HFW0; K7UB12; K7V1V1; K7TWC7; K7TI47	0	0	0	3.91	3.73	3.37	2	0	0	0	2	1	1	0	0	0	2.3	1.1	1.1
K7V5U2; B4FZ74; Q43861	26.49	24.16	22.30	47.97	27.72	44.55	2	1	1	1	1	1	2	2.9	2.9	2.9	2.9	2.9	5.2
K7UXN8	26.65	20.38	11.23	39.22	20.04	44.49	2	1	1	2	1	1	1	2.8	2.8	5.9	3.1	3.1	3.1
B6U2P6; B6TV30	0	0	0	30.74	1.35	6.09	2	0	0	0	1	1	2	0	0	0	12.6	12.6	43.7
B4FFF8; B6TMY6; B6UGL6; B6SHZ1	0	5.10	0	27.47	34.40	46.76	2	0	1	0	1	2	2	0	9.2	0	9.2	12.5	12.5
B6TA75; B4FM79	0	8.88	0	14.26	22.89	20.82	2	0	1	0	1	2	2	0	4.3	0	4.3	11.2	11.2
B6TI54; B6T4D2; B6SGI4; B6TLT4; B6UF11	14.64	0	0	13.06	19.70	16.09	2	1	0	1	1	2	2	38.7	0	38.7	38.7	45.2	45.2
K7U4U1	0	0	0	1.62	0.79	1.45	2	0	0	0	1	1	2	0	0	0	9	9	24.2
C0PK19; B4FLR4; K7UV45; B6UGU1; B6UE26; B6U6W1; B6T8R5; B6T098; B6SIF8; B4FXX2; B4FGQ6; K7TZZ7; B6UH15	0	0	0	0	14.34	25.41	2	0	0	0	1	1	1	0	0	0	11.3	15.5	15.5
B4F8K1; K7TNC3; K7TW45; K7VHA1; B4FQ03	0	0	0	0	8.90	13.59	2	0	0	0	0	2	1	0	0	0	0	6.1	6.1

6. 3. 2. 3 Sequence analysis of the potential interaction partners

To get more information about the candidate interaction partners of sEA1, their nucleotide and amino acid sequences were analyzed. All candidates obtained the working title WHY SO LATE (WSL). The first candidate B6SKG2 was encoded by two genes, which were named WSL1a (GRMZM2G419209) and WSL1b (GRMZM2G319875). They are located closely to each other on chromosome 4 (WSL1a: 239,363,789 - 239,364,641 reverse strand; WSL1b: 239,338,677 - 239,339,463 reverse strand) and exhibit different untranslated region (UTR) sequences, probably resulting from a very recent gene duplication. Comparison of the WSL1a/b amino acid sequence with the other two candidates demonstrated that it showed high similarity of 83.9 % with AC189771.3_FG001 (named WSL3; located on chromosome 5). With similarity values of 18.75% (WSL1a/b) and 20.8% (WSL3), no remarkable relationship could be detected to the fourth candidate, GRMZM2G703173 (named WSL4; located on chromosome 2). All of four candidates were proteins of a relatively small molecular weight of 14.9 kDa (WSL1a/b), 14.4 kDa (WSL3) and 7.8 kDa (WSL4), respectively. They all contained a predicted signal peptide at their N-terminus and processing of the full-length proteins at the corresponding cleavage site would result in mature peptides of 12.83 kDa (WSL1a/b), 12.85 kDa (WSL3) and 5.49 kDa (WSL4), respectively. The sequence similarity between mature WSL1a/b and WSL3 even increases in comparison to their full-length forms from 83.9 % to 87.4 %. Another noticeable feature was the high ratio of cysteine residues, with WSL1a/b containing 12 and WSL3 containing 13 and WSL4 containing cysteine residues. One has to consider that the first cysteine residue of WSL3 was located within the N-terminal signal peptide, which would result in a mature peptide containing 12 cysteine residues after processing, comparable to WSL1a/b. The cysteine residues are arranged in a repetitive pattern of cysteine pairs separated by three other amino acids and 10 to 15 amino acids in between those paired cysteine residues (-CXXXC-$X_{(10\text{-}15)}$-CXXXC-).

Taken together, these data indicate that all of the candidates represent small secreted cysteine rich peptides (CRPs). Since high sequence similarity between different proteins imply that these proteins are homologous to each other (Pearson, 2013), the highly similar WSL1a/b and WSL3 might belong to a yet uncharacterized protein family involved in plant signaling. Protein BLAST searches of these proteins against the maize genome did not reveal any additional comparable sequences, indicating that they might be the only members of this family.

A

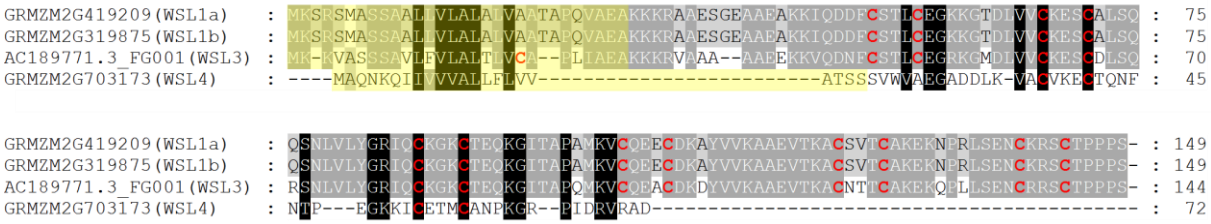

B

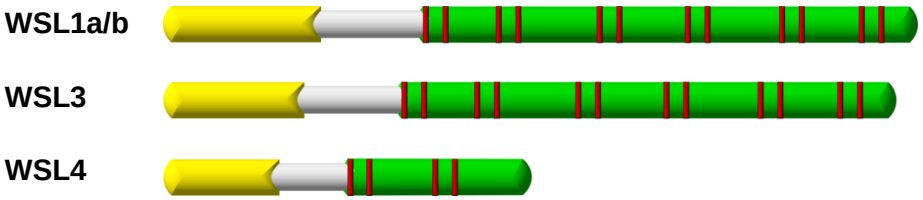

Figure 6.11 Protein sequences and domain structure of WSL peptides, which were identified candidates for interaction with sEA1. (**A**) The protein sequences were aligned for comparison. All of the candidates are predicted to contain an N-terminal signal peptide (shaded in yellow). The amino acid sequences of WSL1a and WSL1b are identical to each other and also highly similar to WSL3. The fourth candidate, WSL4, does not share notable sequence similarities with the other WSL peptides. All proteins are cysteine-rich by containing 12 (WSL1a/b), 13 (WSL3) or 4 (WSL4) cysteine residues, respectively (marked in red). The sequences were aligned using the software ClustalX 2.1 (Larkin *et al.*, 2007) and manually edited using GeneDoc 2.7.000 (Nicholas *et al.*, 1997). Prediction of signal peptides and corresponding cleavage sites was performed by SignalP 4.1 server (Petersen *et al.*, 2011). Sequence similarity of (**A**) is indicated by nuanced shading in grayscale (black = complete similarity, white = no similarity). (**B**) A scheme true to scale representing the domains of the candidate interaction partners was generated. Yellow shading = signal peptide, grey shading = variable region, green shading = cysteine-rich region with cysteine positions marked as red bars.

Based on former results (see 6. 3. 2. 1 and Uebler *et al.*, 2013), membrane-associated proteins of higher molecular weight were expected to interact with sEA1. The candidate genes *WSL1a*, *WSL3* and *WSL4* were therefore further examined to find out whether they might represent wrongly annotated parts of genes coding for larger proteins. In plants, for example cysteine-rich receptor-like kinases form a superfamily with highly conserved cysteine-rich domains (Chen, 2001). As all of the candidates are expressed in pollen (see following results in paragraph 6. 3. 5. 1), a pollen cDNA library ligated into the lambda Uni-ZAP XR vector (kindly provided by T. Dresselhaus) was analyzed according to Dresselhaus *et al.*, 1994. Primers binding in the lambda vector, in combination with *WSL*-specific primers, allowed amplification of the *WSL* transcripts to determine whether they are of the expected size (Figure 6.12 A).

The identity of all PCR products was verified by Sanger sequencing. The size of the *WSL1a* PCR products was corresponding with the annotation available at the data resource Gramene (Monaco *et al.,* 2014) (Figure 6.12 B). The PCR of the 3'-end of *WSL3* was running 300 bp higher than the expected 402 bp based on the annotation. There are no UTRs annotated in the Gramene database for *WSL3* and it is likely that this additional sequence length represent un-annotated UTRs. Lengths of the *WSL4* PCR products are in accordance with the expected sizes regarding the annotated sequences. Please note that the additional lower band in the sample amplifying the 3' part of *WSL4* was identified to represent a shorter form of the annotated *WSL4*. These data support the idea of the candidates representing small secreted CRPs instead of parts of larger proteins.

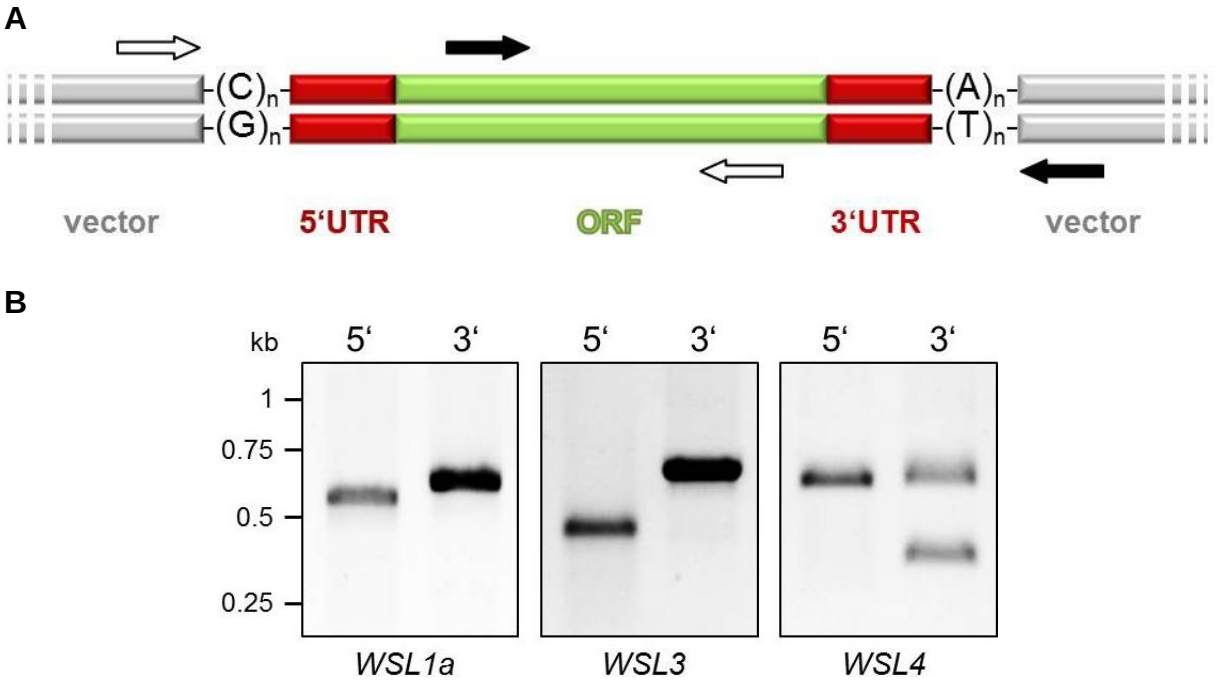

Figure 6.12 Analysis of 5'- and 3'-UTRs of WSL peptides. (**A**) Scheme illustrating the analysis of 5'- and 3'-UTRs (marked in red) of *WSL* genes using a pollen cDNA library ligated into the Uni-ZAP XR vector (marked in light grey). A primer pair binding upstream of the insert and reverse in the ORF (ORF marked in green; primers marked in white) was used to amplify the 5'-UTR. A primer pair binding forward in the ORF and reverse downstream of the insert (primers marked in black) was used to amplify the 3'-UTR. (**B**) PCR products from amplifications described in (**A**). The expected sizes for *WSL1a* were 568 bp (5') and 602 bp (3'), for *WSL3* 422 bp (5') and 406 bp (3') and for *WSL4* 669 bp (5') and 656 bp (3'). *WSL1a*, *WSL3* (5') and *WSL4* PCR products exhibited the expected sizes (please note that the lower band for *WSL4* 3'UTR represents a shortened form of *WSL4*). WSL3 (3') PCR product is running approximately 300 bp higher than expected, potentially due to unannotated 3'-UTR sequence.

6. 3. 3 WSL1a/b and WSL3 exhibit structural similarities to DEFLs

CRPs are involved in a variety of cell-cell communication events in plants (Marshall *et al.*, 2011). They play divers roles in developmental processes like root development (Pearce *et al.*, 2001) and stomatal patterning (Hara *et al.*, 2009; Kondo *et al.*, 2010; Niwa *et al.*, 2013), mediate signaling for nodulation in plant-bacteria symbiosis (Scheres *et al.*, 1990; Mergaert *et al.*, 2003) and act as antimicrobial peptides against a broad range of pathogens (Marshall *et al.*, 2011). In plant reproduction, CRPs act, among others, as self-incompatibility factors (Suzuki *et al.*, 1999; Wheeler *et al.*, 2009) and pollen-tube attractants (Okuda *et al.*, 2009; Kanaoka *et al.*, 2011; Takeuchi and Higashiyama, 2012). CRPs can be classified into different subclasses, like lipid transfer proteins (Molina *et al.*, 1993), snakin/GASA proteins (Nahirñak *et al.*, 2012) and defensins (Silverstein *et al.*, 2007). Plant defensins exhibit a conserved protein structure stabilized by disulfide bridges formed by typically eight conserved cysteine residues (Cornet *et al.*, 1995; Lacerda *et al.*, 2014). Interestingly, defensins contain the amino acid motive CXXXC twice, at position C_3/C_4 and C_7/C_8 (Lay and Anderson, 2005). As previously mentioned, all cysteine residues of the candidates are embedded in this motive. Therefore, a potential structural relationship between defensins and the candidates was examined. Defensins and defensin-like proteins (DEFL) contain the γ-core motive, which was defined as $GXC(X_{3-9})C$ (Yount and Yeaman, 2004). A comparable motive could be identified in the candidates WSL1a/b and WSL3, with the glycine residue located in between C_5 and C_6 (excluding the cysteine residue of WSL3 located in the N-terminal signal peptide) (Figure 6.13). As distance of the glycine residue to C_5 and C_6 is identical, the γ-core motive could be oriented into both directions. The number of variable residues between both cysteine residues of the γ-core motive was initially defined as 3-9 (Yount and Yeaman, 2004) and WSL1a/b / WSL3 exhibit 13 or 15 residues at this position, depending on the direction of the γ-core. But despite this deviation, this motive should be classified as γ-core since it is comparable with the CRPs LURE1 and LURE2 which also contain 12 residues in between the cysteine residues of the γ-core and were classified as DEFLs (Okuda *et al.*, 2009). The second characteristic motive of defensins/DEFLs is the CSα/β motive, originally defined as an α-helix followed by an anti-parallel β-sheet with stabilization by disulfide bridges. The γ-core motive is interposed between these β-strands (Cornet *et al.*, 1995), although more recent publications describe an additional β-strand upstream of the α-helix as characteristic (Lay and Anderson, 2005; Lacerda *et al.*, 2014). Based on secondary structure prediction, both WSL1a/b and WSL3 contain an α-helical structures flanking two β-strands, potentially forming a β-sheet and with WSL3

containing an additional β-strand at the C-terminus. The inverted γ-core C(X_{15})CXG is largely overlapping with the β-strands, indicating that this protein part might represent the CSα/β motive. Based on these structure homologies, and regarding the fact that WSL1a/b and WSL3 exhibit another cysteine-residue arrangement than the classical defensins, it is advisable to classify both proteins as DEFLs. The last candidate, WSL4, does not fulfill the structural requirements for this classification, but still it has to be considered that it might be related to DEFLs, as it also exhibits the CXXXC motive.

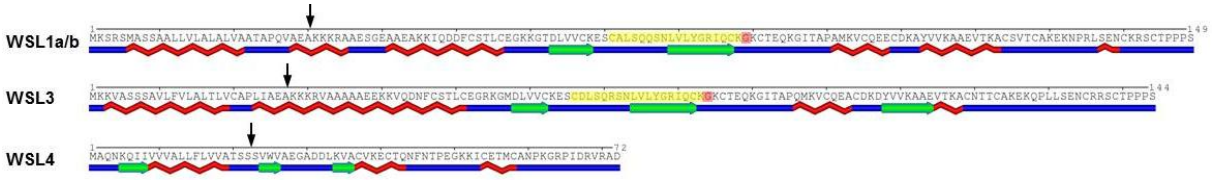

Figure 6.13 Secondary structure prediction of WSL peptides. Amino acid sequence of the WSL peptides was analyzed for γ-core and CSα/β motives characteristic for DEFL proteins. WSL1a/b and WSL3 contain a sequence part highly similar to the γ-core motive GXC(X_{3-9})C in inverse direction (marked in yellow, glycine-residue marked in red). Predicted mature forms of these proteins exhibit C-terminal and N-terminal α-helices (red jagged line) flanking two β-strands (green arrows). The γ-core motive partially overlaps with the β-strands. No such structures could be identified in WSL4. Black arrows mark predicted positions of signal peptide cleavage. Secondary structure prediction and visualization was performed using the SABLE server (Adamczak *et al.*, 2005).

6. 3. 4 Interaction studies with sEA1 and WSLs

As WSL1a/b, WSL3 and WSL4 were assumed to represent interaction partners of sEA1, the interactions should be verified by an additional pull-down of sEA1 and WSL peptides.

6. 3. 4. 1 Expression of WSLs and ZmEA1/sEA1 in IVT/T systems

A very quick way to obtain recombinant protein for interaction studies is the usage of cell-free *in vitro* transcription and translation (IVT/T) systems. A wide variety of systems is available with different features depending on the cell-types and species they are derived from. Origin and properties of the recombinant protein should be considered for choosing the optimal system. To examine the potential interaction of the candidate proteins WSL1/3/4 with ZmEA1 or sEA1, all five sequences were used for *in vitro* translation as Myc- or HA-tagged proteins in a plant, a human and a *Drosophila* IVT/T system.

ZmEA1 as well as its potential interaction partners are plant proteins. Therefore the logical assumption would be that a plant expression system reflects the natural environment of these proteins and offers the best conditions for translation and correct folding. Especially regarding the cysteine-rich sequences of the candidate interaction partners, efficiently working folding machinery is necessary to ensure proper function of the proteins. Cysteine-rich proteins are known to exhibit very specific folding by forming covalent disulfide bridges and this tertiary structure is essential for their functionality (Bulaj, 2005). The commercially available TNT® Coupled Wheat Germ Extract System (Promega GmbH, Mannheim, Germany) was chosen, as it was already demonstrated to successfully produce the EA1-box protein ZmEAL1 (Lausser, 2012). Additionally, the Human In Vitro Glycoprotein Expression Kit (formerly Pierce, now Thermo Fisher Scientific Inc., Waltham, MA, USA) was used, a mammalia system which was optimized for *in vitro* translation of glycosylated proteins. All of the analyzed proteins are predicted to represent secreted peptides. Post-translational modifications like glycosylations influence protein structure and they are frequently necessary to enable interaction of the peptides with their binding partners (Arey, 2012). The third *in vitro* translation system was based on *Drosophila* cell extract (cooperation with J. Medenbach, University of Regensburg). The three candidates WSL1/3/4 as well as ZmEA1 and sEA1 were cloned into the vectors pT7CFE1-CHA (C-terminal HA-tag) and pT7CFE1-CMyc (C-terminal Myc-tag), respectively, and pT7CFE1-NHis-GST-HA was used as positive control (all vectors from Thermo Fisher Scientific Inc., Waltham, MA, USA). These vectors contain a T7 promoter, an internal ribosome entry site (IRES) of encephalomyocarditis virus (EMCV) for cap-independent translation, a polyA-tail and a T7 terminator and were recommended by the manufacturer for the use with the Human In Vitro Glycoprotein Expression Kit. No vectors recommended by the manufacturer of the TNT® Coupled Wheat Germ Extract System were available with the necessary protein tags. No protein could be produced in the human system except the control fusion protein His-GST-HA and kit-derived positive control (Figure 6.14 A), indicating that the vector system was compatible with the system, but the proteins of interest could not be produced in detectable amounts. No protein at all was detected using the wheat germ system. Regarding the fact, that the wheat germ system was functional based on a kit-derived positive light reaction according to the manufacturer's protocol, is was likely that the vector set was not compatible with this system. Although the functionality of the IRES of EMCV, an animal virus, was reported in plant tissue like transgenic tobacco leaves (Urwin *et al.,* 2000), literature search revealed that this IRES was inactive in wheat germ extract (Woolaway *et al.,* 2001; Dorokhov *et al.,* 2002), indicating that vectors containing the EMCV IRES should not

be used for wheat germ extract. Additionally, despite reported moderate activity of the EMCV IRES in *Drosophila* embryo translation extract (Woolaway *et al.*, 2001), no protein at all was detected, including His-GST-HA control (data not shown). This indicates that both the human as well as the *Drosophila* system are not usable for translation of these proteins and this vector system.

To avoid the negative effects of the EMCV IRES in the wheat germ extract, all five genes including the fusion tag were cloned into the pJet1.2/blunt vector (Thermo Fisher Scientific Inc., Waltham, MA, USA). A weak signal was detected for WSL3-HA and ZmEA1-HA, but no Myc-fusion protein could be obtained (Figure 6.14 B). As the protein level was extremely low using the wheat germ system, no interaction studies could be performed successfully.

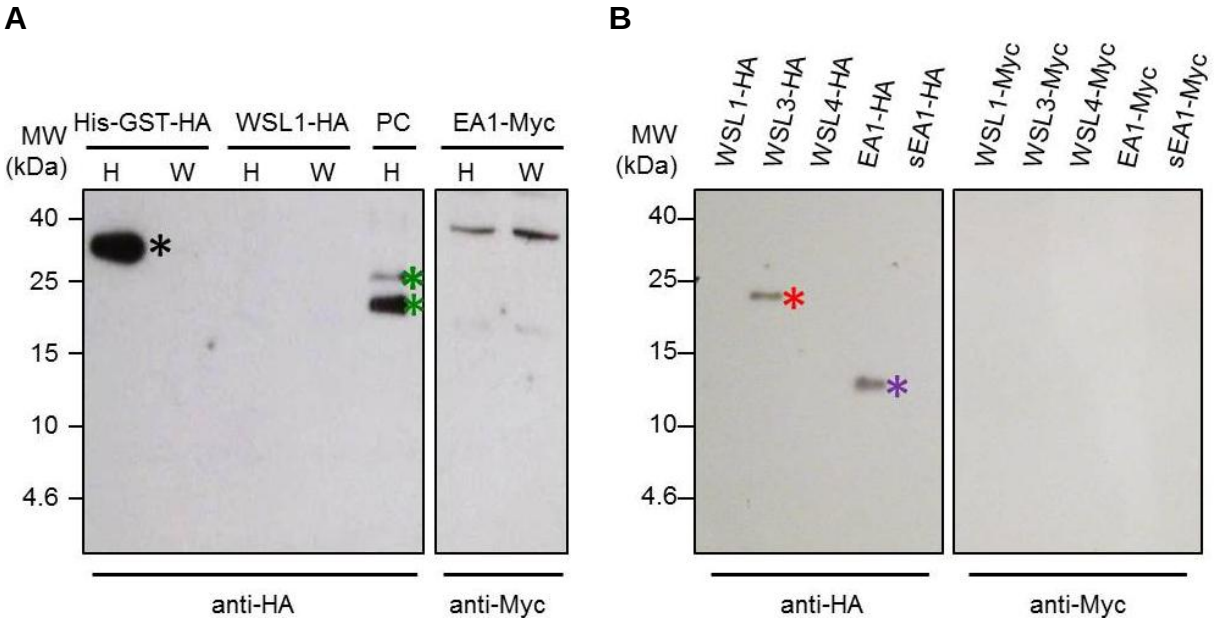

Figure 6.14 ***In vitro*** **transcription and translation (IVT/T) of ZmEA1/sEA1 and WSL peptides fused to affinity tags.** Products of IVT/T were analyzed by immunoblot using primary antibody detecting affinity tags. (**A**) IVT using the Human In Vitro Glycoprotein Expression Kit (H) or TNT® Coupled Wheat Germ Extract System (W) with pT7-CFE1 vectors did not show translation of WSL1-HA, ZmEA1-Myc (see figure) or other combinations of fusion tags and proteins (data not shown). According to the molecular weight (MW), controls using His-GST-HA (marked with black asterisk) and kit-derived positive control (PC; marked with green asterisks) exhibited signal using the human system, indicating that the kit was functional and compatible with the vectors. His-GST-HA control did not exhibit signal using wheat germ system, whereas a positive reaction of the kit-derived control was observed (data not shown). This indicated that the kit was functional but not compatible with the vector. (**B**) IVT using TNT® Coupled Wheat Germ Extract System with pJet1.2/blunt vector showed weak signals for WSL3-HA (marked with red asterisk) and EA1-HA (marked with purple asterisk), but not for any other of the tagged protein.

6. 3. 4. 2 Expression in Nicotiana benthamiana leaves

Another possibility to gain protein material for binding studies is the ectopic expression of putative interaction partners in living plant systems like tobacco leaves. To transiently produce ZmEA1 or sEA1 with the candidates fused to different affinity tags, the ORFs of all sequences were cloned into the vectors pEarleyGate 201 (N-terminal HA-tag) and pEarleyGate 203 (N-terminal Myc-tag) (Earley *et al.*, 2006). To analyze the solubility of the recombinant protein, the samples were separated into soluble and insoluble fraction and analyzed via immunoblot. Only Myc-WSL3 could be detected and was exclusively found in the insoluble fraction (Figure 6.15 A). The insoluble fraction of Myc-WSL3 was solubilized and used for pull-down experiments with synthetic biotinylated sEA1. The experimental procedure was based on the procedure which was applied to identify the candidates (see 6. 3. 2. 2). No interaction could be demonstrated using this approach (Figure 6.15 B).

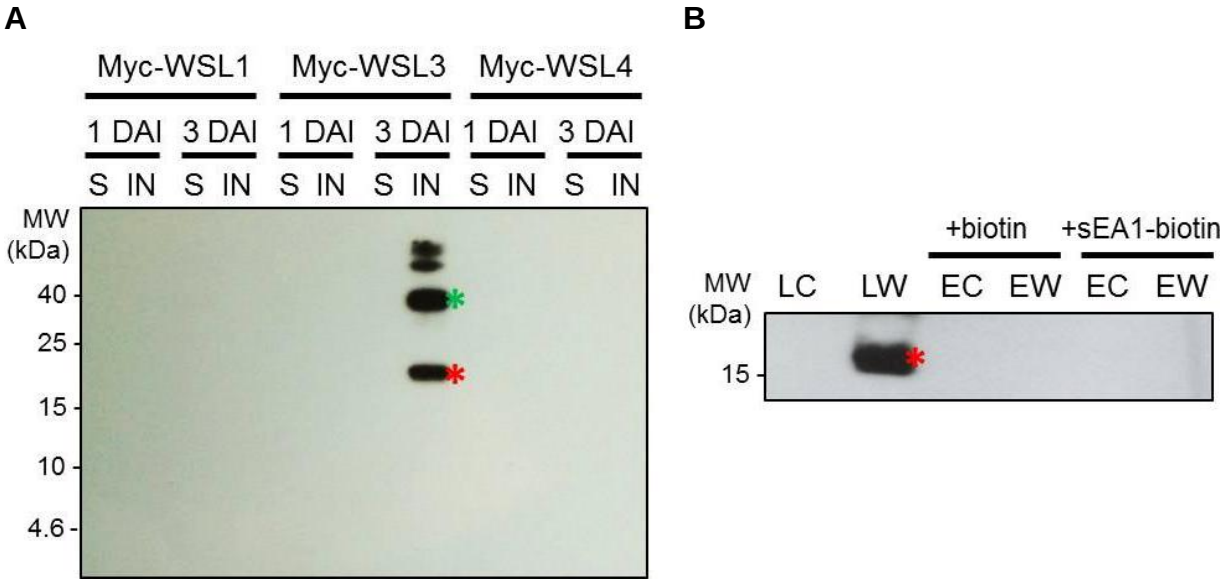

Figure 6.15 Heterologous production of Myc-WSL in tobacco and test for interaction with sEA1. (**A**) *WSL* with N-terminal *Myc*-tag was transiently expressed in *N. benthamiana* leaves. Samples were separated into soluble (S) and insoluble (IN) fraction and analyzed 1 or 3 days after infiltration (DAI) by immunoblot using antibody directed against the affinity tag. Only Myc-WSL3 was detectable in the insoluble fraction with the expected molecular weight (MW) of 17.7 kDa (marked with red asterisk). An additional signal potentially represents dimerized Myc-WSL3 (marked with green asterisk). (**B**) A Pulldown assay was performed to test for interaction of synthetic biotinylated sEA1 with Myc-WSL3 from (**A**), which was solubilized with Triton™ X-100 (LW). To exclude unspecific background signaling, experiments were performed in parallel with solubilized wild type tobacco lysate (LC). Biotin instead of sEA1-biotin was used as negative control. No interaction was shown, as no Myc-derived signal could be detected in the eluted fractions of wild type (EC) or Myc-WSL3 plants (EW), regardless of whether biotin or sEA1-biotin was used as bait.

Regarding the fact that the Myc-tag is N-terminally fused to the putative secreted WSL3, it is possible that the fusion protein was still attached in the ER membrane without cleavage of the signal peptide. This might have hampered correct folding of the cysteine-rich protein, resulting in non-functional protein.

Additionally, *WSL1*-, *WSL3*- and *WSL4-GFP* constructs were transiently co-expressed with a marker for the ER fused to mCherry (Nelson *et al.*, 2007) into tobacco leaf epidermis cells. All of the three proteins were detectable in both soluble and insoluble fraction of the leave extract with WSL4-GFP showing the strongest intensity (Figure 6.16 A). The soluble fraction of all candidates was used for pull-down experiments with synthetic biotinylated sEA1. As the WSL peptides were already soluble, no additional solubilization step had to be performed. For negative control, biotin was used. No interaction was observed with this approach (Figure 6.16 B). Taken together, it was not possible to verify the interaction between sEA1 and WSL1/3/4.

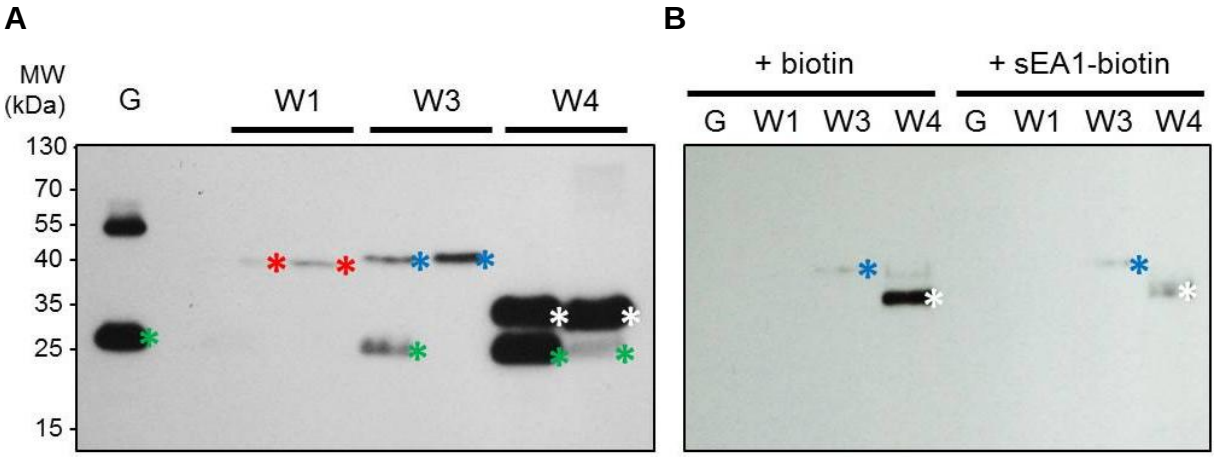

Figure 6.16 Heterologous production of WSL peptides fused to GFP in tobacco leaves and test for interaction with sEA1. (**A**) *WSL1/3/4-GFP* were transiently expressed in *N. benthamiana* leaves and fusion proteins were analyzed by immunoblot using GFP-directed antibody. Signals corresponding to the expected molecular weight (MW) were detected for WSL1-GFP (W1, 42.6 kDa, marked with red asterisk), WSL3-GFP (W3, 42.5 kDa, marked with blue asterisk) and WSL4-GFP (W4, 34.7 kDa, marked with white asterisk) in both soluble fraction (S) and insoluble cell debris (IN). Free GFP was detected in the soluble fractions, probably due to protein degradation; GFP (G) was used as positive control (26.9 kDa; marked with green asterisk). (**B**) Pulldown assay with biotin-binding beads was performed to test for interaction of biotinylated sEA1 with the WSLs and GFP in the soluble fractions shown in (**A**). Biotin was used as control. Fractions eluted from the beads are shown. No interaction could be verified as signals for WSL3-GFP and WSL4-GFP were detected with use of both sEA1-biotin and biotin.

6. 3. 5 Characterization of WSL peptides

6. 3. 5. 1 Expression profile of WSL peptides

To characterize the candidates for interaction with sEA1 more detailed, their expression profile was examined. Initially, the expression profile of *WSL1a*, *WSL1b*, *WSL3* and *WSL4* was analyzed *in silico* using the atlas of transcription during maize development of Sekhon *et al.*, 2011. This atlas comprises RNA sequencing data of 60 different tissues and organs covering various reproductive and vegetative stages of the maize inbred line B73. The data set did not contain any information about the candidate gene *WSL4*, but included expression intensities of *WSL1a*, *WSL1b* and *WSL3*, with all of these 3 candidate genes sharing a highly similar expression profile (Figure 6.17). Logarithmic expression intensities with RMA normalization were constantly low with values ranging around 6 in nearly all tissues except in the anthers. All three anther replicates showed logarithmic expression intensities of more than 14. Although the samples of the maize anthers are pooling all of the anther components (e. g. tapetum, pollen, etc.) and do not distinguish between them, ungerminated pollen are forming a major part of mature anthers. Therefore these data indicate that expression of the candidate genes may be pollen-specific. This and the highly similar expression profiles would support the assumption that WSL1a, WSL1b and WSL3 are male factors involved in perception and/or transduction of EA1-derived signals for short-range guidance of the pollen-tube growth.

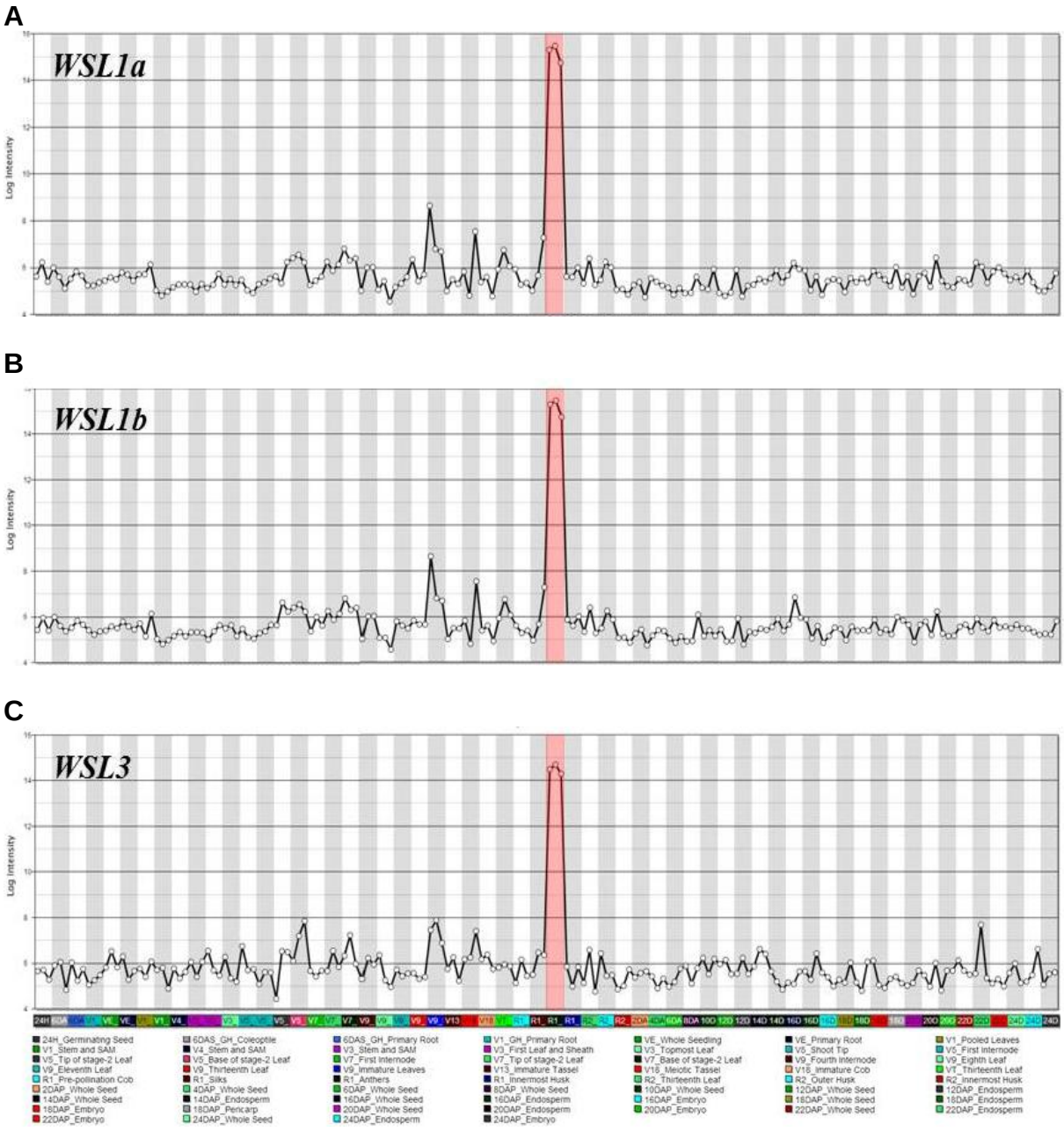

Figure 6.17 ***In silico*** **analysis of the expression profile of** ***WSL*** **genes.** The expression profiles of the genes coding for the identified candidate interaction partners of predicted mature EA1, (**A**) *WSL1a* (GRMZM2G419209_T01), (**B**) WSL1b (GRMZM2G319875_T01) and (**C**) WSL3 (AC189771.3_FGT001), respectively, were examined in 60 different maize tissues based on the genome-wide transcription atlas of Sekhon *et al.*, 2011. In most tissues, expression is on a constant low level, with exception of the anthers (sample "R1_Anthers", column colored in red). No data were available for the fourth candidate gene, *WSL4*. The data set was created by RNA sequencing of 3 replicates of each tissue and RMA normalization, with logarithmic expression intensity of each replicate indicated by a white dot and grouping of the 3 replicates of each tissue in columns with an alternating gray-white color scheme. The expression graph was generated using PLEXdb browser and experiment ZM37 (Dash *et al.*, 2012).

Regarding the fact that, based on these data, the *WSL* genes are strongly expressed in the anthers but not necessarily in pollen, the database Genevestigator V3 (Hruz *et al.*, 2008) was searched for a more detailed expression pattern. Whereas no expression data were available for *WSL1b* and *WSL3*, several experiments published on the database indicated a dominant expression of *WSL1a* and *WSL4* in maize pollen. Furthermore, qRT-PCR was performed to analyze germinated maize pollen for transcript of the candidates as well as to compare their expression intensity (Figure 6.18). *FPGS*, *LUG* and *MEP* were chosen as reference genes (Manoli *et al.*, 2012). To distinguish *WSL1a* and *WSL1b*, primer pairs binding in the variable UTRs of both genes were chosen. Based on the qRT-PCR results, all candidates are expressed in germinated pollen. *WSL1a* and *WSL1b* are the strongest expressed candidates, followed by *WSL3* with approximately 5fold lower transcript level than *WSL1a/b*. The fourth candidate, *WSL4*, was the weakest expressed gene with expression 100fold lower than *WSL1a/b* and 20fold lower than *WSL3*. Please note, that *WSL3* is set into relation with *WSL1a* in Figure 6.18 A and *WSL4* is set into relation to WSL3 in Figure 6.18 B.

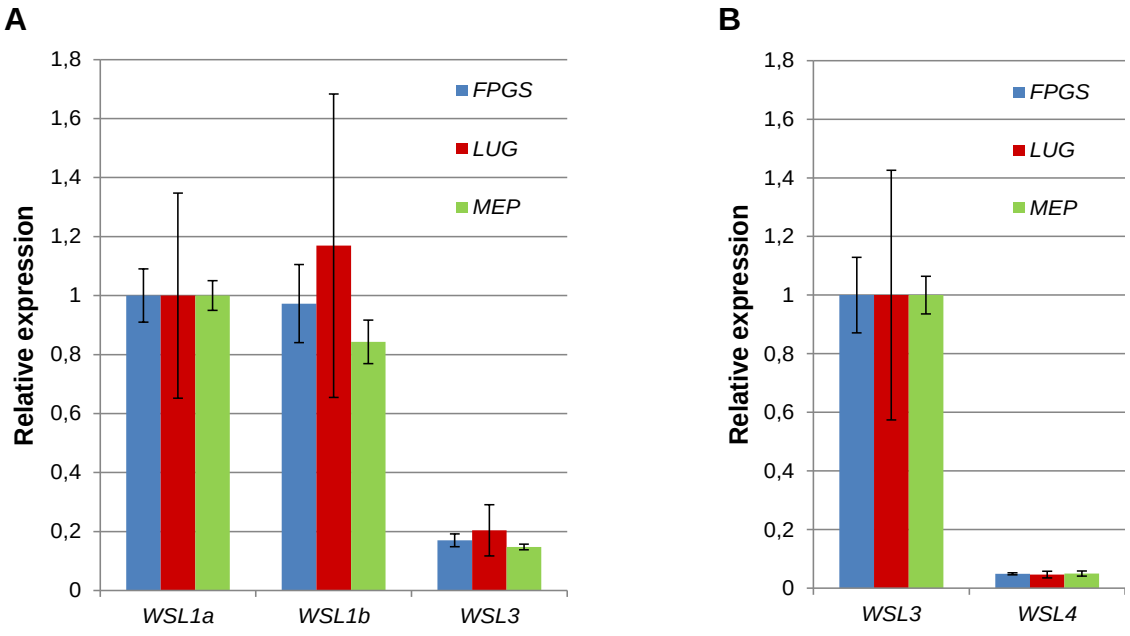

Figure 6.18 Quantitative expression profile of *WSL* genes in *in vitro* germinated maize pollen tubes. (**A**) Expression intensity of the highly related *WSL1a* and *WSL1b* was comparable, whereas *WSL3* was expressed 5fold weaker than *WSL1a*. (**B**) *WSL4* was expressed 20fold weaker than *WSL3* and therefore approximately 100fold weaker than *WSL1a*. Please note, that *WSL1a* expression was set as value 1 in (**A**) and *WSL3* expression was set as value 1 in (**B**). Three biological and three technical replicates were used to determine expression intensity for each gene. *FPGS*, *LUG* and *MEP* were used as reference genes based on Manoli *et al.*, 2012.

6. 3. 5. 2 WSL1 is highly abundant in maize pollen

To analyze WSL1a/b on its protein level, a polyclonal peptide antibody against a 16 amino acid peptide sequence of WSL1a/b was generated by immunization of three rabbits (Pineda Antikörper-Service, Berlin, Germany). Since WSL1a and WSL1b share the same amino acid sequence, they will be treated in this paragraph as one protein. Regarding the high sequence homology of WSL1 and WSL3, it is possible that WSL3 acts redundantly to WSL1 in the same pathway. To detect both proteins with the same antibody, the amino acid sequence of the peptide used for immunization was designed to match for 100% with WSL1 and for 87.5% with WSL3, which was the highest possible sequence coverage. To test the binding capacity of the antibody against WSL1 as well as WSL3, both proteins were transiently expressed into *Nicotiana benthamiana* leaves as GFP-fusion proteins, with WSL4-GFP and GFP as negative controls. Immunoblot analysis using anti-GFP antibody demonstrated that all proteins were successfully produced in tobacco with the expected molecular weights (Figure 6.19 D).

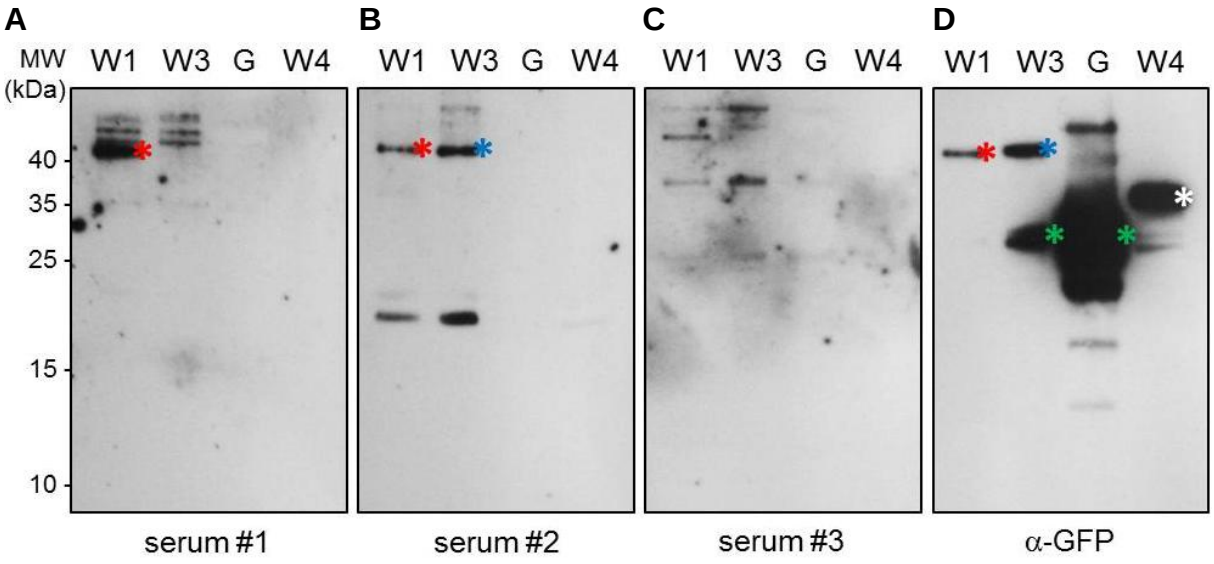

Figure 6.19 Detection of tobacco-produced WSL peptides fused to GFP with anti-WSL1 antibody. WSL1-GFP (W1), WSL3-GFP (W3), WSL4-GFP (W4) and GFP were expressed in *N. benthamiana* leaves. Leave samples were used to test specificity of immune serums directed fully against WSL1 and partially against WSL3 by immunoblot. (**A**) Serum #1 only exhibited a signal of corresponding molecular weight (MW) of WSL1-GFP (42.6 kDa; marked with red asterisk), whereas (**B**) serum #2 could detect both WSL1-GFP and WSL3-GFP (42.5 kDa; marked with blue asterisk). (**C**) Serum #3 did not detect any of these fusion proteins. (**D**) Control experiment using GFP-directed antibody verified the identity of the detected proteins from (**A-C**). None of the immune serums recognized WSL4-GFP (34.7 kDa; marked with white asterisk) and GFP (26.9 kDa; marked with green asterisk).

Detection with anti-WSL1 antibody showed variable signals depending on the source of the serum. Serum derived from rabbit #1 did only detect WSL1-GFP, but not WSL3-GFP (Figure 6.19 A). Both proteins were recognized by serum #2 (Figure 6.19 B) and no clearly distinguishable signal of WSL1-GFP or WSL3-GFP was detected with serum derived from rabbit #3 (Figure 6.19 C). Taken together, serum #1 can be applied to detect only WSL1, whereas serum #2 seems to be usable for analysis of both proteins together.

Since all candidates are strongly expressed in germinated maize pollen, with *WSL1* transcript being the most abundant, it was interesting whether WSL peptides are also detectable on protein level in germinated pollen. For testing the functionality and specificity of the antibody in pollen, *in vitro* germinated pollen was harvested, separated into soluble fraction and insoluble cell debris and analyzed by immunoblot using unpurified serums and pre-immunization serums. An intensive signal of approximately 15 kDa was detected, representing expected size of WSL1 and WSL3 (Figure 6.20 A).

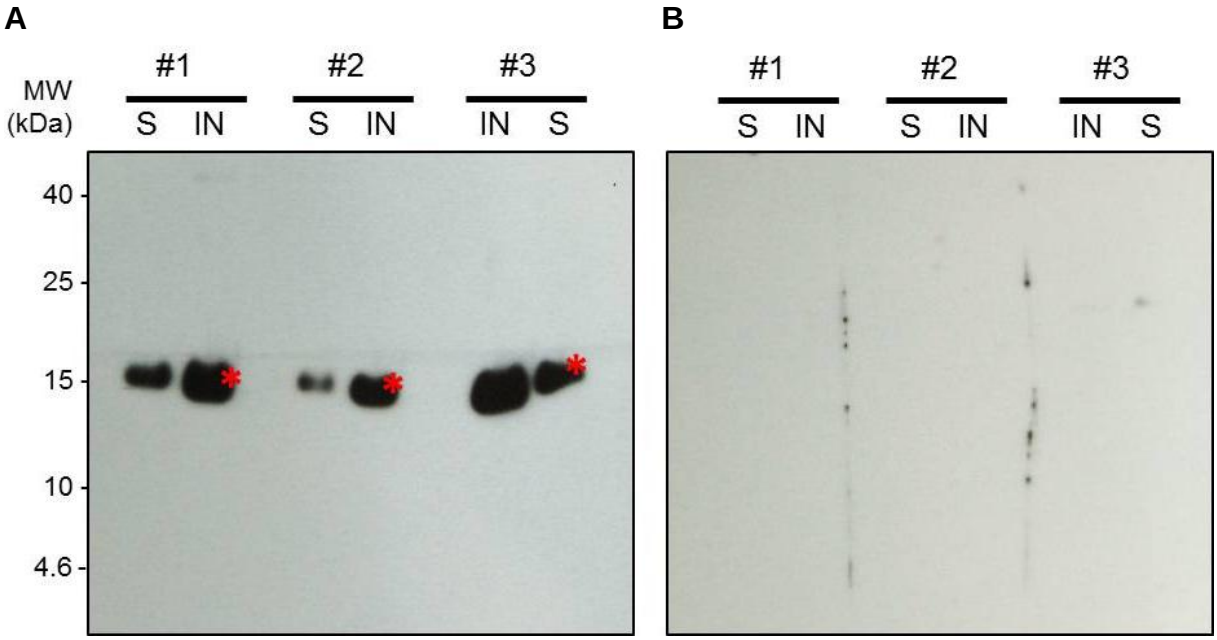

Figure 6.20 WSL1 peptide in germinated maize pollen. (**A**) To detect WSL peptides, a polyclonal antibody fully directed against WSL1 and partially directed against WSL3 was generated. *In vitro* germinated maize pollen were collected, separated into soluble (S) and insoluble (IN) cell debris fraction and analyzed for WSL peptides by immunoblot using three unpurified rabbit immune serums (#1 - #3). With all three serums, signal was detected in both soluble and insoluble fraction at molecular weight (MW) coinciding with WSL1 (14.9 kDa) and WSL3 (14.4 kDa), both marked with red asterisks. (**B**) Control immunoblot using corresponding pre-immune serums did not show any signals, demonstrating specificity of the signals shown in (**A**).

As already demonstrated, serum #2 is able to detect both WSL1 and WSL3, but as they share nearly the same molecular weight it was not possible to distinguish whether signal is derived from one or both proteins. Protein was detected in both soluble fraction and cell debris, indicating that the protein might be associated with cell wall structures. Nevertheless, no processed form of lower molecular weight could be detected, which one would expect for a secreted protein cleaved at its N-terminus. Control immunoblot analysis using the pre-immune serums did not show any unspecific background signal (Figure 6.20 B).

The availability of a polyclonal antibody directed against WSL1 and probably WSL3 offers opportunities for future research. Nevertheless, several aspects have to be handled with care. The antibody was produced by the immunization against a short peptide of WSL1 containing two cysteine residues. This implies that sequence might be involved in disulfide-bridge formation, causing secondary structure which might sterically interfere with the binding of the antibody to the native protein. Applications based on the preservation of the secondary structure, like immunohistochemically labeling or immunoprecipitation experiments might therefore be limited. But despite these potential obstacles, it is worth to test the antibodies for immunolocalization as it could be a powerful instrument to track the way of the WSLs through the pollen tube, like described for LURE protein in Okuda *et al.,* 2013.

6. 3. 5. 3 WSL peptides enter the secretory pathway

To further investigate the WSL proteins as putative secreted peptides, their subcellular localization behavior was analyzed. WSL1, WSL3 and WSL4 wit C- or N-terminal GFP were transiently co-expressed with a marker for the ER fused to mCherry (Nelson *et al.,* 2007) into *N. benthamiana* leaf epidermis cells via *Agrobacterium tumefaciens*-mediated transformation. All three candidates were co-localizing with the ER, regardless of the position of the GFP fusion. Whereas GFP-WSL1/3/4 were strongly present and easy to detect, the proteins with C-terminal fusion could only be detected after co-transformation with an *Agrobacterium*-strain inducing expression of p19 protein of tomato bushy stunt virus, which prevents post-transcriptional gene silencing (Voinnet *et al.,* 2003).

Assuming that all of the candidate proteins are secreted after cleavage of the C-terminal signal peptide, the fusion of GFP upstream of the signal peptide should result in anchoring of the protein into the ER membrane via the signal peptide. GFP-WSL3 strongly aggregates in the transformed cells. This aggregation seems to cause a disorganization of the ER into globular structures. Whereas unaffected ER normally does not allow distinguishing between ER membrane and ER lumen by confocal microscopy, this is possible with the globular structures. It

could be demonstrated that the fluorescence signal is retained in the ER membrane and can't be detected inside of the lumen, supporting the hypothesis that WSL3 is a classically secreted peptide.

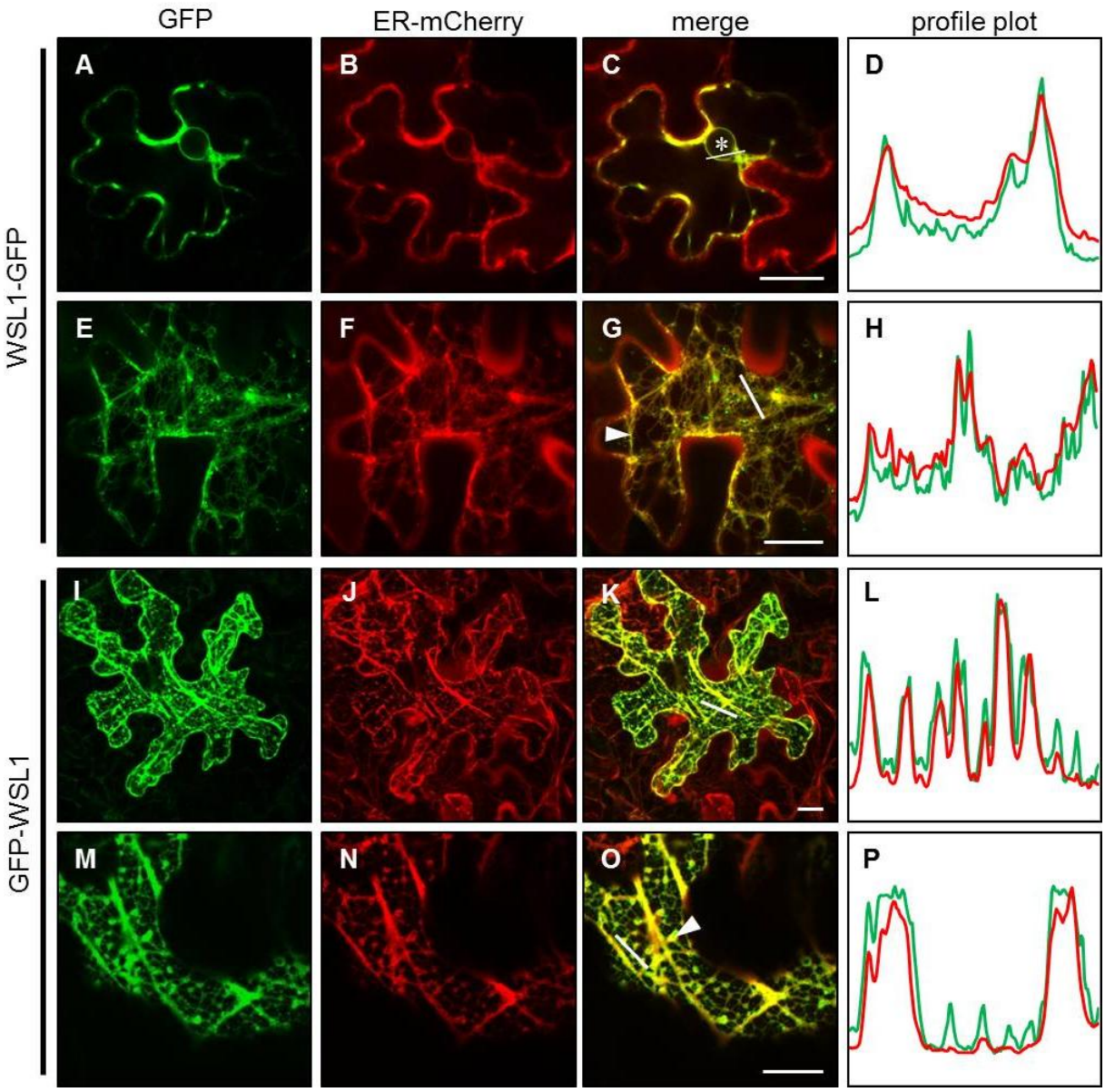

Figure 6.21 Subcellular localization of WSL1 in *Nicotiana benthamiana* leaf cells. The ZmEA1 interaction candidate WSL1 fused to (**A**-**H**) C-terminal or (**I**-**P**) N-terminal GFP was transiently co-expressed with a marker for the ER fused to mCherry (Nelson *et al.*, 2007) into tobacco leaf epidermis cells. Both fusion proteins showed co-localization with the ER-marker, indicating that they entered the secretory pathway. (**A**-**C**) Optical section through the cell. (**E**-**G**, **I**-**K**, **M**-**O**) Z-projections of confocal image stacks of 2 to 10 µm. (**D**, **H**, **L**, **P)** Profile plot for signal quantification of single fluorescence channels. White lines in merged pictures mark the region for fluorescence quantification. Asterisks mark the nucleus. Arrowheads mark matching overlaps of both fluorescent channels. Scale bar represents 20 µM.

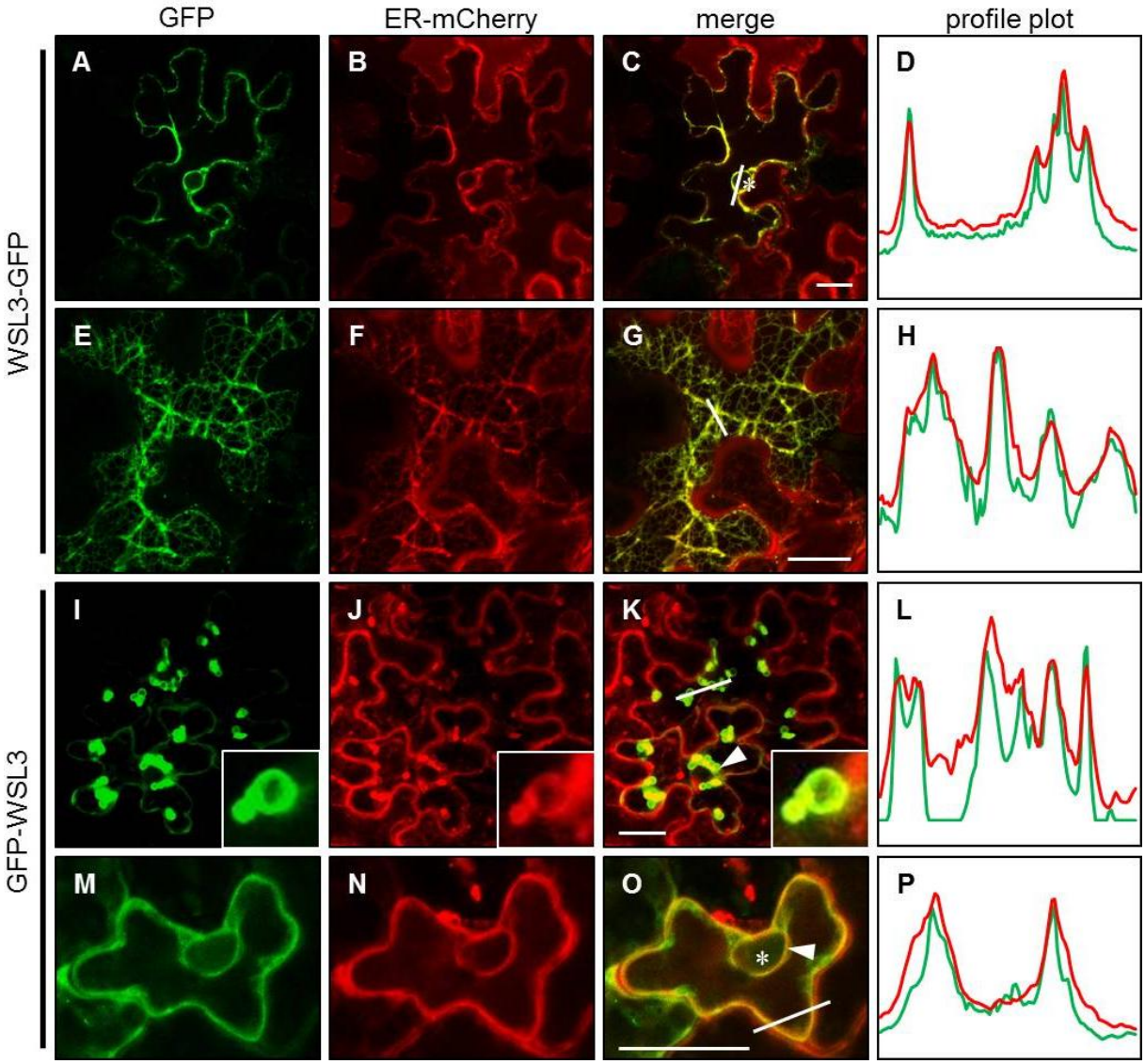

Figure 6.22 Subcellular localization of WSL3 in *Nicotiana benthamiana* leaf cells. The ZmEA1 interaction candidate WSL3 fused to (**A**-**H**) C-terminal or (**I**-**P**) N-terminal GFP was transiently co-expressed with a marker for the ER fused to mCherry (Nelson *et al.*, 2007) into tobacco leaf epidermis cells. Both fusion proteins showed co-localization with the ER-marker, indicating that they entered the secretory pathway. Note that GFP-WSL3 is accumulating in globular structures (**I**-**K**, small picture) and leads to disorganization of the ER. (**A**-**C**, **M**-**O**) Optical section through the cell. (**E**-**G**, **I**-**K**) Z-projections of confocal image stacks of 7 to 10 µm. (**D**, **H**, **L**, **P)** Profile plot for signal quantification of single fluorescence channels. White lines in merged pictures mark the region for fluorescence quantification. Asterisks mark the nucleus. Arrowheads mark matching overlaps of both fluorescent channels. Scale bar represents 20 µM.

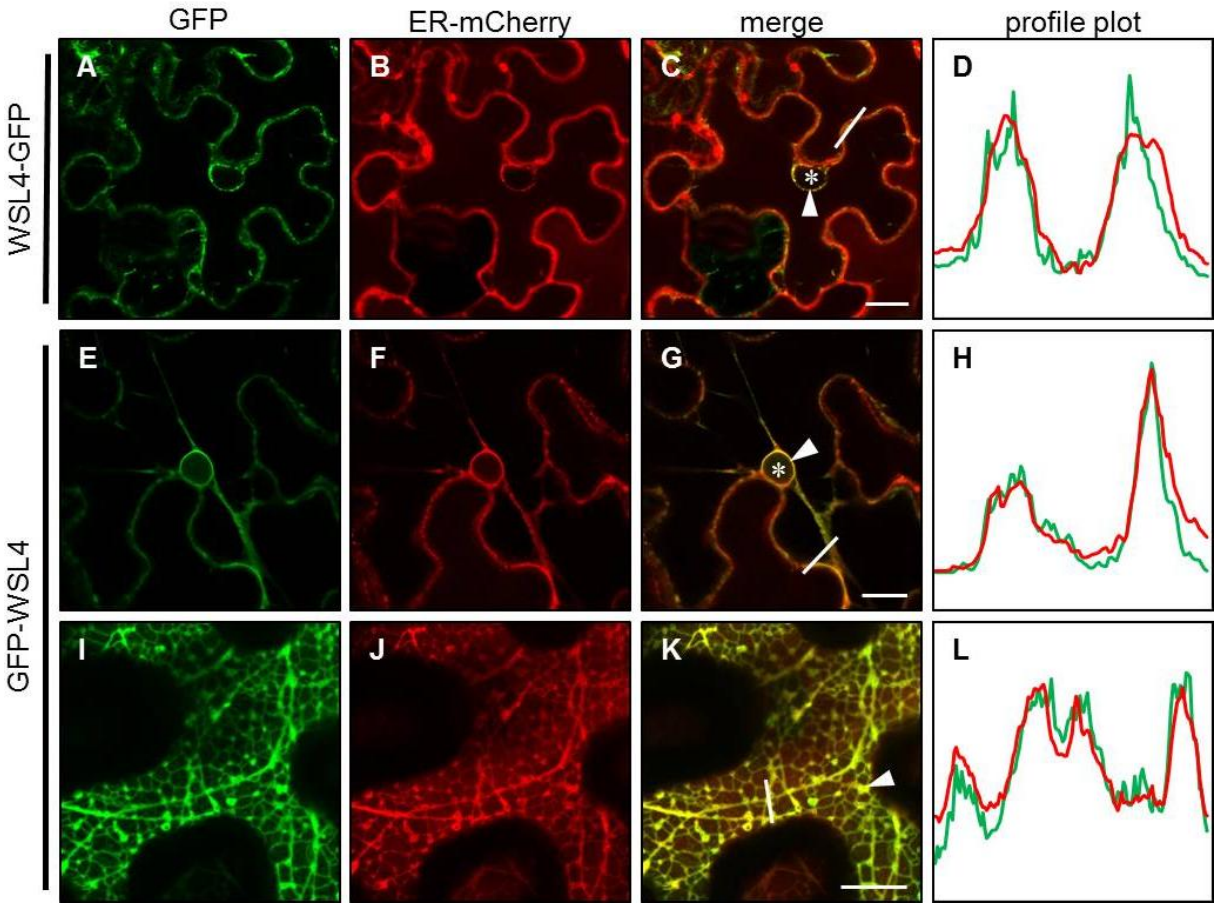

Figure 6.23 Subcellular localization of WSL4 in *Nicotiana benthamiana* leaf cells. The ZmEA1 interaction candidate WSL4 fused to (**A**-**D**) C-terminal or (**E**-**L**) N-terminal GFP was transiently co-expressed with a marker for the ER fused to mCherry (Nelson *et al.*, 2007) into tobacco leaf epidermis cells. Both fusion proteins showed co-localization with the ER-marker, indicating that they entered the secretory pathway. (**A**-**C**, **E**-**G**) Optical section through the cell. (**I**-**K**) Z-projections of confocal image stacks of 2 to 10 µm. (**D**, **H**, **L)** Profile plot for signal quantification of single fluorescence channels. White lines in merged pictures mark the region for fluorescence quantification. Asterisks mark the nucleus. Arrowheads mark matching overlaps of both fluorescent channels. Scale bar represents 20 µM.

6. 3. 5. 4 WSL peptides are exclusively found in maize and Sorghum bicolor

As BLASTP search in several plant genomes provided by the Gramene database (Monaco *et al.*, 2014) did not reveal any protein sequences homologous to the WSLs, TBLASTN search was performed based on translation of genomic sequences. Regarding WSL1a/b and WSL3, no homologous sequences could be detected in the genomes of the grasses *Oryza sativa*, *Hordeum vulgare* and *Brachypodium distachyon*, as well as of the dicots *Arabidopsis thaliana*, *Glycine max* and *Populus trichocarpa*. In *Sorghum bicolor*, a genomic region (2,046,699-2,047,001) with 80.2% identity to WSL1a/b (E-value: 3.4 E^{-54}) and 83.0% identity

to WSL3 (E-value: $3.5E^{-60}$) was identified by TBLASTN in an unannotated region on chromosome 4. Although official bioinformatically predicted annotations lack for this position, it is conceivable that it encodes for a protein orthologous to WSL1a/b and WSL3. No sequences comparable to WSL4 were found in any of the analyzed genomes.

6. 4 Conclusions

6. 4. 1 Candidates for interaction with predicted mature ZmEA1 are secreted CRPs related to defensins

The short-range pollen tube attractor ZmEA1 of maize is known to interact with the tip of *in vitro* growing pollen tubes (Uebler *et al.,* 2013). To identify interaction partners mediating this binding pattern, a biochemical approach was chosen with predicted mature ZmEA1 (sEA1) acting as bait protein for isolation of binding partners. Pull-down experiments using the microsomal fraction of germinated pollen tubes and synthetic biotinylated sEA1 as bait protein indicated binding to an interaction partner enriched to the microsomal fraction. This led to the MS based identification of three proteins as candidate interaction partners, which were named WSL1a/b, WSL3 and WSL4. WSL1a and WSL1b share the same protein sequence and are encoded by two genes closely located on chromosome 4, only differing in their UTR sequences, indicating that they are derived from recent gene duplication. WSL3 protein is highly similar to WSL1a/b, suggesting that these proteins are members of the same protein family, whereas WSL4 does not exhibit remarkable similarity to the other candidates.

The three candidates are predicted to represent small secreted CRP with 12 (WSL1a/b, WSL3) or 4 (WSL4) cysteine residues in the putative mature form. These cysteine residues are arranged in the repeated motive CXXXC. Other proteins known to contain this motive are defensins and DEFLs, both representing CRPs with a complex secondary structure (Lay and Anderson, 2005). WSL1a/b and WSL3 exhibit structural similarities with defensins/DEFL proteins by containing the characteristic γ-core motive and the cysteine-stabilized CSα/β motive, whereas WSL4 lacks these motives. Defensins and DEFL proteins are involved in various signaling processes in plants. They mainly function in defense responses against different pathogens, biotic and abiotic stress response (for review see de Conink *et al.,* 2013; Mirouze *et al.,* 2006) and symbiotic interactions (Johansson *et al.,* 2004; Hanks *et al.,* 2005). Besides these roles of interaction with environmental cues, accumulating evidence demonstrates that defensins/DEFLs are also contributing to developmental processes like root development

(Allen *et al.,* 2008) and are necessary for successful fertilization. The *Zea mays* defensin EMBRYO SAC 4 (ZmES4), for example, induced pollen tube burst for sperm cell release, additionally to its inhibitory effect on pathogens (Cordts *et al.,* 2001; Amien *et al.,* 2010; Woriedh *et al.,* 2015). Other DEFLs function in pollen tube attraction of *Arabidopsis* and *Torenia* (Okuda *et al.,* 2009; Takeuchi and Higashiyama, 2012) or self-incompatibility, like the pollen coat located SCR/SP11, which is the male determinant of self-incompatibility of *Brassica* (Takayama *et al.,* 2000). With WSL1a/b and WSL3 being classified as DEFL proteins potentially contributing to the ZmEA1-dependent pollen tube attraction, they might represent additional members of this class involved in reproduction processes.

Quantitative expression analysis of germinated maize pollen revealed that *WSL1a* and *WSL1b* are expressed on a comparable level, with expression approximately 5fold stronger than *WSL3* and 100fold stronger than *WSL4*. These data coincide with preliminary RNAseq data of germinated maize pollen (T. Dresselhaus and co-workers, personal communication). According to this data set, *WSL1a/b* and *WSL3* rank among the strongest expressed genes in pollen with *WSL4* being expressed much weaker. It would be interesting to compare the absolute expression value of the candidates in ungerminated pollen with germinated pollen and at different stages of growth through the stigma of maize. Although it was demonstrated that transcript of all candidates is present in *in vitro* germinated pollen, their precise expression pattern might be additionally controlled by sporophytic factors derived by the style tissue.

6. 4. 2 Future tasks to verify WSL peptides as interaction partners of ZmEA1

It is important to mention that further experiments are indispensable to verify the candidates as real interaction partners of sEA1. The production of the WSL peptides for first pull-down experiments turned out to be challenging as *in vitro* translation with several different systems failed or did not deliver enough material for further research. Additionally, success in recombinant expression in tobacco leaves was strongly depending on the used affinity tag. Pull-down experiments using recombinant tobacco-derived WSL proteins in combination with the synthetic biotinylated sEA1 peptide could not verify the interaction. It has to be considered that WSL peptides are rich in cysteine residues, implying that they form several disulfide bridges and exhibit a complex secondary structure. In general, the correct folding is essential for protein functionality (Bulaj, 2005) and heterologous overexpression of cysteine-rich proteins is challenging in particular, as formation of wrong disulfide bridges can impair this functionality (de Marco, 2009). It can be speculated, that verification of the interaction failed due to wrongly folded and inactive WSL peptides.

Furthermore, secreted peptides translocated into the ER are often post-translationally modified. These modifications, particularly N-glycosylation, are promoting functional protein conformations by destabilizing unfolded forms (Hanson *et al.*, 2009). They contribute to the conformational stability of the protein by thermodynamically favoring correct folding processes as well as through external effects like the recruitment of carbohydrate-binding factors involved in protein maturation and sorting, like chaperones (for review see Braakman and Hebert, 2013). Chaperones are proteins supporting the folding of other proteins into their native conformation without being part of the final protein structure or impart steric information (Ellis and Van der Vies, 1991). Whereas classical chaperones like heat-shock proteins are found in most cellular localizations including the cytoplasm (Vabulas *et al.*, 2010), carbohydrate-binding chaperones are exclusive for the ER. By binding the carbohydrate chains of proteins translated into the ER, they promote stabilization and formation of disulfide bonds (Braakman and Hebert, 2013). Based on this importance of ER-derived factors, interaction studies of the candidates were performed using full-length WSLs produced in tobacco, to ensure their translocation into the ER. As already mentioned, these pull-down experiments did not verify the interaction with sEA1 and alternative approaches should also be considered for future research, like Y2H assays modified for interaction between secreted proteins (for review see Stynen *et al.*, 2012). Using the screening method SCINEX-P, bait and prey proteins have to be N-terminally fused with two different mutant forms of the membrane-bound sensor Ire1. Interaction leads to dimerization of these mutant Ire1 proteins, forming an active state which initiates expression of reporter gens (Urech *et al.*, 2003). Another method is the Golgi complex two-hybrid system, in which bait and prey protein are fused to the two modular domains of the Golgi complex-resident mannosyltransferase Och1. A complementation of Och1 by the interaction of bait and prey protein increases temperature resistance of the temperature-sensitive yeast strain (Dube *et al.*, 2010). For both methods, interaction between bait and prey protein has to occur in the ER, therefore the full-length unprocessed protein sequences of both ZmEA1 and the WSLs have to be used to trigger translation into the ER.

Despite the advantages of the ER located proteins, direct use of the predicted mature WSL peptides could also offer some opportunities. In contrast to the ER-localized unprocessed ZmEA1, its predicted mature form sEA1 was found to be cytoplasmic. It is possible that this might also be true for the processed forms of the candidates. With both interaction partners being available as cytoplasmic proteins, other methods could be applied, like a classical yeast-two-hybrid (Y2H) assay, which can report interaction of cytoplasmic proteins. Additionally, both interaction partners could be co-translated with different affinity tags in the cytoplasm of

tobacco leave cells for a direct pull-down, instead of applying synthetic sEA1 like it was performed in this study. Furthermore, mature WSL peptides could be used for microscopic analysis by intermolecular Förster resonance energy transfer (FRET) or bimolecular fluorescence complementation (BiFC) might. FRET is based on energy transfer from an excited donor chromophore (fused to the bait protein) to an acceptor chromophore (fused to the prey protein) resulting in light emission from the acceptor at different wavelength than from the donor (Truong and Ikura, 2001). In BiFC analysis, bait and prey protein are fused to fragments of a fluorescent reporter protein, which is complemented by interaction of bait and prey and emits detectable signal (Walter *et al.,* 2004). As demonstrated in this work, all three full-length WSLs and ZmEA1 are ER-localized. Since these signals were very weak, FRET and BiFC were not considered. But it is conceivable, that mature forms of the WSL peptides are expressed more intensively in the cytoplasm, enabling FRET and BiFC analysis.

It is important to note, that also *in vitro* transcription and translation was performed using unprocessed candidate sequences including the N-terminal signal peptide. If IVT/T systems are considered for future research, there are some aspects one has to pay attention to. The only cell-free expression system successfully synthesizing a candidate was wheat germ extract and it is reported that wheat germ extract does not exhibit N-terminal signal peptide cleavage (Jackson and Blobel, 1977). In general, it is possible to trigger signal sequence cleavage in IVT/T systems by supplementation of canine microsomal membranes derived from disintegrated ER (Jackson and Blobel, 1977; Bocco *et al.,* 1988; MacDonald *et al.,* 1988), but the signal recognition particle was removed from the TNT® Coupled Wheat Germ Extract System of Promega. Therefore, addition of microsomal membranes will not work. IVT/T systems exhibiting a high level of post-translational modifications are human HeLa cells and insect cells. For example the microsomal membrane fraction of *Drosophila* embryo cells shows signal peptide cleavage activity (Brennan *et al.*, 1980). Insect cell lysates in general are known to exhibit a high glycosylation rate and to retain their capability for translocation and signal peptide cleavage (Kubick *et al.,* 2009; Carlson *et al.,* 2012), although this cleavage might be specific for signal sequences derived from organisms related to the host system (Tessier *et al.,* 1991). Unfortunately, both of these systems could not synthesize the WSLs. But since cell-free protein synthesis has developed into one of the most powerful methodologies for simple and efficient protein production, many systems are currently improved to face challenging syntheses, like production of disulfide-bridge containing proteins (Merk *et al.,* 2012). Additionally, other expression systems like the baculovirus system could be used to overcome the obstacles of WSL and ZmEA1 synthesis. Proteins synthesized in baculovirus-infected insect

cell culture were demonstrated to exhibit a high level of posttranslational modifications, including signal peptide cleavage, and correct formation of intramolecular interactions was reported in several cases (for review see O'Reilly *et al.*, 1992, chapter 15).

6. 4. 3 Model for interaction of WSL peptides with ZmEA1

Taken together, small secreted CRPs strongly present in germinated maize pollen were identified as potential candidates for interaction with the predicted mature form of the short-range pollen tube attractor ZmEA1. This was surprising, as ZmEA1 also represents a gametophyte-derived secreted peptide. Therefore, membranous proteins like receptor-like kinases or ion channels located on the surface of the growing pollen tube tip were expected to interact with secreted ZmEA1, inducing signal transduction cascades or ion flow, but no such proteins could be identified in this study. The strong sequence similarity between WSL1a/b and WSL3 is of particular interest, since both proteins seem to represent the sole members of a yet uncharacterized protein family. The fact that both of these proteins were identified in the pull-down approach indicates that they possess very similar functions, potentially by both interacting with mature ZmEA1. A model was hypothesized in which the maize pollen tube secretes WSL peptides during its growth towards the female gametophyte, whereas ZmEA1 is secreted from the egg apparatus towards the micropylar region (Figure 6.24). When the pollen tube comes into close proximity to the female gametophyte, mature ZmEA1 and WSLs bind each other to form a peptide complex. This complex is recognized by a membranous receptor or receptor complex on the pollen tube surface, triggering a signal transduction cascade. This leads to redirection of pollen tube growth towards the source of the peptide complex, which corresponds to the source of the ZmEA1 peptide.

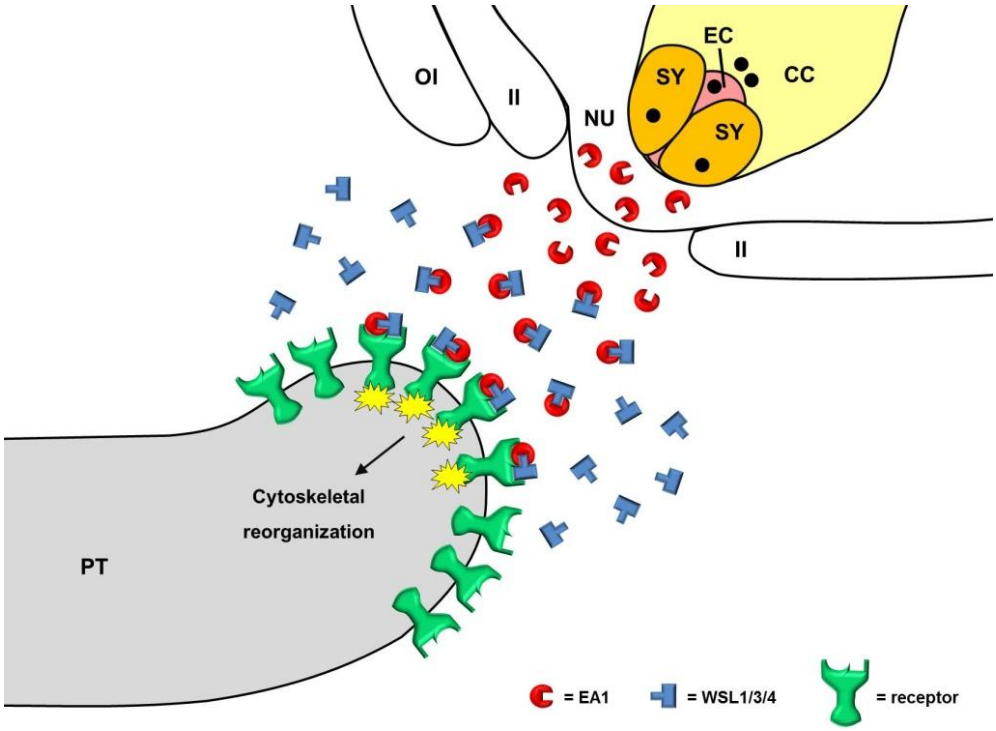

Figure 6.24 Model for involvement of WSL peptides in micropylar pollen tube attraction of maize. The EA1 peptide is secreted from the egg apparatus consisting of the synergids (SY) and the egg cell (EC) through the nucellus cells (NU) covering the female gametophyte. The growing pollen tube (PT) secretes WSL peptides, which are bound by EA1. The peptide-peptide complex is recognized by PT surface localized receptors. Binding of the complex induces a signaling cascade leading to cytoskeletal reorganization and change of the PT growth direction towards the source of the EA1 peptide. Figures are not drawn to scale. Abbreviations: CC = central cell, EC = egg cell, II = inner integument, OI = outer integument.

This model would require the capability of the involved signaling peptides to interact with each other instead of directly binding to a cell-surface protein. Secreted peptides are already known to interact with chitin (Folders *et al.*, 2000), heparin (Tomomura *et al.*, 1990) or exhibit collagen-binding activity (Crouch and Longmore, 1987). The secreted seed storage protein Ginkbilobin2 (Gnk2) of gymnosperms inhibits fungi growth by a defense mechanism depending on its mannose-binding ability (Miyakawa *et al.*, 2014). Furthermore, Sf9 cell cultures derived from the moth *Spodoptera frugiperda* were demonstrated to secret a 27 kDa protein that is able to directly bind insulin-like peptides, a group of secreted peptide hormones (Doverskog *et al.*, 1999). Other prominent examples are the Wnt proteins, representing a large family of extracellular signaling glycoproteins containing several conserved cysteine residues. They are involved in a wide variety of cellular processes in animals like cell fate determination, cell movement and tissue polarity. They interact with a set of secreted peptides acting as

inhibitors for local and temporal control of Wnt activity (for review see Katoh and Katoh, 2007 and Kakumanu *et al.,* 2012). These peptides are summarized as the functional sFRP class, composed of the sFRP family (Jones and Jomary, 2002), Cerberus (Piccolo *et al.,* 1999) and WIF-1 (Hsieh *et al.,* 1999), and they are all directly binding the secreted ligand Wnt to prevent interaction of Wnt with its receptor. Taken together, these data demonstrate that extracellular peptides can exhibit more kinds of action than just being bound by a membranous protein to induce a signaling cascade, but can also interact with extracellular sugars and other secreted peptides.

BLASTP search of other plant species genomes did not reveal any proteins homologous to WSLs, except a potential sequence in *Sorghum bicolor*. A yet unannotated region on chromosome 4 of the *S. bicolor* genome displayed more than 80% identity with WSL1a/b and WSL3 after TBLASTN search, indicating that this position might represent a gene coding for a orthologous protein of the two candidates. *Zea mays*, *Sorghum bicolor*, *Brachypodium distachyon* and *Oryza sativa* share a common ancestor that diverged about 50 million years ago (Schnable *et al.*, 2012) with *Zea mays* an *Sorghum bicolor* representing the most related of the grass species (Springer *et al.,* 1989). The lack of homologous sequences of maize WSLs in other grasses except *S. bicolor* and their potential involvement in the ZmEA1 pathway suggests that they could represent components of a reproductive barrier to avoid cross-pollination of different plant species.

CHAPTER 7 - COMPREHENSIVE DISCUSSION AND OUTLOOK

7. 1 EA1-box as potential protein-protein interaction motive

In plants, a variety of factors are involved in orchestrating the communication between different cells and tissues. Beside the "classical" plant hormones, secreted peptides appear to play an elementary role in mediating signaling during reproductive processes (Simon and Dresselhaus, 2015). In maize, secreted grass-specific EAL signaling peptides (Dresselhaus *et al.,* 2011) containing the conserved EA1-box motif are known to be involved in processes like pollen tube guidance (Márton *et al.,* 2005) and cell fate determination (Krohn *et al.,* 2012). In this study, a new classification of EA1-box containing proteins in different plant species was presented, grouping them into EAL, EAG and EAC proteins based on *in silico* analysis of conserved motives of the protein sequence and subcellular localization behavior (Uebler *et al.*, under review).

The only similarity between all three groups is the shared EA1-box. This raises the question about the function of the EA1-box in different groups of proteins. The extracellular signaling CLE proteins in *Arabidopsis,* for example, act in a tissue-specific manner by interaction with different receptors (Wang and Fiers, 2010). They exhibit the CLE motif as conserved motif and it is supposed that this domain mainly determines the functional tissue-specificity by dictating direct interaction with specifically located receptors, whereas sequences outside of the CLE motif contribute to correct processing of the peptide (Meng *et al.,* 2010). It is conceivable that the EA1-box in the putative secreted EAL proteins shares a comparable function by directly interacting with the corresponding receptor and/or other binding partner(s). This hypothesis is supported by the observed interaction of synthetic predicted mature ZmEA1 (sEA1) with the pollen tube tip (Uebler *et al.,* 2013). sEA1 consists only of the EA1-box and the short C-terminal A-box. Still, it cannot be excluded that the alanine-rich C-terminus also contributes to this direct interaction. In *Streptococcus mutans,* which is the major causative agent of human dental caries, attachment of the bacterium to the tooth surface is mediated by the bacterial surface protein Pac that contains an alanine-rich region (Seifert *et al.,* 2004; Matsumoto-Nakano *et al.,* 2008). This region is supposed to trigger intramolecular interactions between different domains of the antigen and adhesion of the antigen to the tooth surface by enhancing interaction with salivary glycoproteins (Demuth and Irvine, 2002). The alanine-rich A-box of EAL proteins might thus also mediate the interaction with glycosylated binding partners, especially if one considers that likely most cell surface proteins are glyco-

sylated (Wollscheid *et al.,* 2009). Conducting the pollen tube binding assay with sEA1 lacking the A-box or containing a mutated EA1-box would help to determine the peptide domain mediating interaction at the pollen tube tip.

It also has to be taken into consideration that not all EA1-box proteins act as secreted signaling peptides. Especially the glycine-rich EAGs, which can be allocated to the heterogeneous group of glycine-rich proteins (GRPs), are expected to be generally cytoplasmic (Uebler *et al.*, under review). In EAGs, the EA1-box is the only domain besides the glycine-rich regions. Some GRPs contain only the glycine-rich region as conserved motif and were demonstrated to act as structural cell-wall proteins (Ryser *et al.,* 2004) or are involved in cell-elongation by accumulating in the vacuole (Mangeon *et al.,* 2009). This indicates that the glycine-rich domains can also autonomously mediate functional activity without the EA1-box. It is also possible that the EA1-box of EAGs mediates cytoplasmic protein-protein interaction with downstream acting components whereas the glycine-rich domains contribute to other processes, like influencing the structural conformation of the interaction partner. However, speculations about the function(s) of EAGs are difficult, as not a single member of this family has been functionally studied and GRPs are involved in a wide variety of different processes as discussed in CHAPTER 2 (see also Mangeon *et al.,* 2010). But the fact that they are present in nearly all of the analyzed plant species makes them an interesting protein group for future research.

EA1-box proteins that could not be classified either as EALs or EAGs were grouped as EAC proteins, including mainly proteins containing an N-terminal signal sequence and/or several transmembrane domains. Based on subcellular localization studies, longer EACs with several transmembrane domains are expected to enter the secretory pathway, potentially representing cell surface proteins. Due to the lack of other conserved domains, predicting the function of EAC proteins is difficult. A closer look at *in silico* expression data of the three maize EAC encoding genes using the transcription atlas of Sekhon *et al.,* 2011, shows an equal expression intensity in all analyzed tissues. This might indicate that maize EACs contribute to more general processes compared to EALs, or, on the contrary, that they exhibit a very specialized expression pattern in cells or tissues not covered by the atlas. This is for example the case of ZmEA1, which is only expressed in the three-celled egg apparatus. Further analysis of some EACs is inevitable to obtain a clue about their function. As generation of stable transgenic lines of most of the plants, especially crops, is highly time-consuming, it is recommended to first identify the detailed expression pattern of EACs. Besides quantifying the expression val-

ue by qRT-PCR, a spatiotemporal expression pattern of different EACs or plant tissues can be obtained by *in situ* hybridization (see for example Javelle *et al.*, 2011). EAC proteins exhibiting an interesting expression pattern should then be selected for functional analysis.

Based on the widespread existence of EA1-box proteins in the plant kingdom and their structural differences, it is obvious that we only know little about these proteins. Regarding EAL proteins, nothing is known about their function in other grasses than maize. However, sequence similarity and expression pattern indicate that they might act as orthologs of maize EALs. Therefore, research should now be extended to EALs of other species as well as EAGs and EACs to complete our understanding of this exciting protein class. With *Oryza sativa*, another prominent crop of enormous economic importance exhibits several genes encoding EAL, EAG and EAC proteins, respectively. Like for maize, a great number of molecular techniques are available, including the generation of transgenic plants (Hiei and Komari, 2008). These now enable to study the localization and function of some interesting candidates also in an additional important plant species.

7. 2 Structure and posttranslational modifications of EALs: Open questions that need to be answered

Besides increasing the knowledge about the EA1-box proteins in general, it should also be an elementary part of future research to focus on single members. Therefore, one of the main tasks of this study was to unveil the detailed mode of function of the pollen tube attractor ZmEA1. It was demonstrated that ZmEA1 can act as secreted diffusing factor which is able to induce reorientation of the maize pollen tube growth by direct interaction with the pollen tube surface. It is expected that ZmEA1 is proteolytically processed into its putative mature form sEA1 to mediate this function. The amino acid sequence of sEA1 was predicted bioinformatically and the mature peptide was successfully used to attract pollen tubes *in vitro* (Márton and Dresselhaus, 2010) and to visualize interaction with the pollen tube (Uebler *et al.*, 2013). During previous work, immunoblot analysis of dissected unfertilized maize ovules using an EA1-directed polyclonal antibody showed a signal corresponding to the molecular weight of the ZmEA1 propeptide and an additional signal corresponding to the expected mature sEA1 form, supporting the idea that sEA1 represents the processed form (M. L. Márton, personal communication). Nevertheless, experimental evidence of the mature peptide sequence still has to be provided. One possibility to identify the mature ZmEA1 form would be to incubate recombi-

nant propeptide ZmEA1 with maize ovule extract to induce proteolytic processing like described for the secreted CLAVATA3 (CLV3) protein processed by cauliflower extract (Ni and Clark, 2006). However, this method has several obstacles as processing enzymes might only be present in the egg apparatus and therefore at a concentration insufficient to cleave and process detectable amount of peptides. Furthermore unspecific protease activity might cause false positive results. Thus, isolation and enrichment of the protein derived from maize ovules would be the best method, not only to clarify the question about the mature ZmEA1 peptide but also to unveil and quantify potential post-translational attachment of functional groups by mass spectrometry (MS) (Farley and Link, 2009). In plants, most of the secreted signaling peptides are proteolytically processed and contain additional posttranslational modifications critical for their biological function and receptor specificity (for review see Matsubayashi, 2014). For example, tyrosine sulfation, which is also present in the secreted plant peptides PSK and PSY, was implicated to function as determinant of protein-protein interaction (Kehoe and Bertozzi, 2000; Yang *et al.,* 2015). Additionally, glycosylation can contribute to the ability of secreted peptides to diffuse towards their target cell or tissue, as the addition of carbohydrates increases solubility of proteins (Welinder and Tams, 1995; Rudd and Dwek, 1997). Another posttranslational modification that can increase the solubility of a protein is the introduction of a phosphate group by phosphorylation. Increasing evidence indicates, that phosphorylation is not limited to the cytoplasmic compartment but can also occur at extracellular proteins (for review see Yalak and Vogel, 2012). While performing experiments using synthetically produced sEA1, a low solubility of the peptide and its tendency to aggregate were observed. On the one hand, this might be due to the functionality of ZmEA1, which was demonstrated to act as pollen tube attracting factor in concentrations of up to 10 µm (Márton and Dresselhaus, 2010). Low solubility might then be the result of using peptide concentrations that do not occur naturally. The pollen tube attracting LUREs, for example, show a maximum of attraction at concentrations of 40 nM (LURE1) and 4 nM (LURE2), respectively (Okuda *et al.,* 2009). On the other hand, this might also be caused by a lack of posttranslational glycosylation and/or phosphorylation after synthesis. The lack of such potential modifications might impair the function of the synthetic peptide and could weaken the interaction with its binding partners.

The identification of WSL peptides as potential interaction partners of synthetic sEA1 was only achieved after using highly sensitive mass spectrometry as signal intensity was relatively weak. Following biochemical experiments to verify this interaction included the use of synthetic sEA1 and heterologously expressed WSLs. However, with the various methods applied,

binding could not be observed. For the case that sEA1 doesn't represent the correct mature peptide sequence or that important post-translational modifications are missing, this might affect the binding efficiency of sEA1. Surely, ZmEA1 protein isolated from its original source tissue would be the best material for such experiments as it exhibits the highest probability of representing the correctly processed peptide. But as ZmEA1 is only expressed in the three-celled egg apparatus of maize, it is unlikely to gain sufficient peptide amounts. Expression of recombinant sEA1 in systems supporting post-translational modifications of proteins in higher organisms might help to obtain sEA1 with enhanced ability to bind its interaction partners and could therefore be used to verify interaction with WSL peptides. *In vitro* translation using wheat germ extract, for example, surely represents one of the best systems to express plant proteins. Nevertheless, first attempts did not deliver any sEA1 or ZmEA1 peptide. Optimization of the used vector system, for example, by extending the poly(A) tail to increase mRNA stability, could help to increase protein production (J. Medenbach, personal communication). Additionally, other *in vitro* systems with a high level of post-translational modification, like the baculovirus infected insect cell system or CHO (Chinese hamster ovary) cell lines, could be used to gain sEA1 protein with higher activity.

Obtaining sufficient amounts of purified, post-translationally modified mature ZmEA1 protein might not only help to increase efficiency of interaction studies, but could also be used to determine its structural properties by NMR spectroscopy or X-ray cristallography. First attempts to analyze the structure of synthetic sEA1 by NMR in this study failed due to the low solubility of the peptide and might be more successful using a recombinant protein generated in a higher eukaryote system. But why is information about the structure of the mature ZmEA1 peptide useful? The ZmEA1 interaction candidates WSL1/3/4 are predicted to represent secreted cysteine-rich peptides. Cysteine-rich peptides are expected to exhibit a complex folding pattern crucial for their functionality (Okuda *et al.*, 2009). Provided that binding to the WSL peptides can be verified, unveiling the three-dimensional (3D) structure of sEA1 could help to understand the mode of interaction between these peptides. All WSLs as well as sEA1 contains an even number of cysteine residues. Generally, one would expect these residues to form intramolecular disulfide-bridges to receive their structural integrity. However, putative solvent-exposed cysteine residues in other proteins are also known to contribute to intermolecular protein-protein interactions, especially for dimerization (van der Wijk *et al.*, 2004; Nagahara, 2011; Meitzler *et al.*, 2013). Determining the position of the two cysteine residues of sEA1 could help to increase the knowledge about the potential interaction with WSLs, which might in turn also provide cysteine residues for formation of disulfide bonds with

sEA1. Additionally, solvent-exposed cysteine-residues might contribute to dimerization of the sEA1 peptide. Dimerization of secreted peptides can be essential for their functionality, as it was shown already for some secreted plant defensins (Song *et al.,* 2011; Lay *et al.,* 2012). In this study, immunoblot analysis of purified synthetic sEA1 after incubation of pollen tube extract showed bands of a MW higher than it would be expected only from interaction of sEA1 with one of the WSLs. These results were obtained with and without crosslinking and using reducing SDS-PAGE. The reducing conditions should normally lead to a breakup of potential disulfide bridges and dissociation of any protein complex without crosslinking. It is still unclear why these bands of higher MW were obtained and it can be speculated whether it represents an artefact or whether the reducing agents were not sufficient to breakup all protein-protein interactions. However, if these bands represent sEA1 bound to its natural interaction partners, the immunoblot results indicate a binding partner of a higher MW or a multiprotein complex. Such a complex could contain one or more sEA1 molecules and structural analysis by NMR could thus unveil the question whether the peptide functions as monomer or dimer, or eventually uncover the composition of the whole multiprotein complex. Additionally, directed mutagenesis of cysteine residues would help to clarify whether the interactions are mediated by these residues.

Determination of the 3D structure should thus represent a future task of high priority and should also be extended to other members of the EAL protein family to find out whether they share structural similarities. Like plant defensins, EAL proteins might exhibit a conserved folding pattern with a specific 3D structure (Lacerda *et al.,* 2014). This structure could help to figure out functional relationships between EAL proteins of different plant species or to other protein families. ZmEAL2 would represent a good candidate for this. The third member of the small maize EAL family is likely involved in embryogenesis during later developmental stages. ZmEAL2 protein was demonstrated to accumulate in the maize embryo, which can reach a size of up to one centimeter. This provides a valuable protein source which could be purified and used for structure analysis. Nevertheless, although ZmEAL2 is highly abundant in the embryo, its function could not yet be determined as RNAi lines did not exhibit a visible phenotype. As already discussed in CHAPTER 2, one should strive for the use of alternative methods like CRISPR/Cas (Dong *et al.,* 2005) to unveil its mode of function. Additionally, the availability of maize lines mutated by insertions is constantly increasing and can be searched by different tools like the POPcorn database (Cannon *et al.,* 2011). However, to date, an *eal2* insertion line is not available, but the mutant collection is steadily increasing and should be regularly checked for insertions of EA1-box genes.

7. 3 WSL-EA1 interaction – a novel reproductive isolation mechanism?

There is still a lot to be done to understand the potential interaction of sEA1 with WSLs. Although protein production by *in vitro* systems and heterologous expression systems delivered so far poor results for biochemical interaction studies, first pull-down experiments were performed to proof direct interaction of the candidates with sEA1. Until now it was not possible to verify the MS results in this study by biochemical methods using recombinant peptides produced in heterologous expression systems. Expression of the peptides in the maize BMS suspension system (Sheridan, 1982) would be a solution especially for the production of proteins rich in cysteine residues, whose expression often results in wrong folded and inactive protein, which is not suitable for interaction studies. Other options to test the binding behavior are discussed in the concluding remarks of CHAPTER 6. Especially the use of the predicted mature sequence of WSLs should be examined further. If they also show cytoplasmic subcellular localization like mature sEA1 expressed without N-terminal signal motif, it can be used for Y2H experiments or direct pull-down after co-expression with cytoplasmic sEA1 in plant cells. In case the direct binding between one or more WSLs with ZmEA1 can be proven, it still would have to be examined whether this interaction is involved in the function of ZmEA1 as micropylar pollen tube attractor or contributes to other yet unknown signaling processes. Therefore *WSL* mutant maize plants have to be generated and to be studied whether downregulation of *WSLs* results in a comparable phenotype like the loss of micropylar pollen tube guidance as described for *ea1*-RNAi lines (Márton *et al.*, 2005). This genetic study would strongly support the hypothesis that these proteins are acting in the same pathway and would open a highly interesting field of additional research directions. One would expect, for example, that binding of fluorophore labelled sEA1 like described in CHAPTER 4 could not be observed with *wsl* mutant pollen tubes. Nevertheless, one has to consider that *WSL1a*, *WSL1b* and *WSL3* might act redundantly due to their high sequence similarity. Additionally, the phenotype of *wsl* mutants might be much milder than in *ea1* mutants. If binding of ZmEA1 to WSL peptides is an enhancement instead of a prerequisite for perception, for example by increasing the solubility of secreted ZmEA1, then their downregulation might only result in a slightly reduced pollen tube attraction capability. These aspects have to be taken into consideration for generation and analysis of transgenic *wsl* mutant lines.

To date, reports about the contribution of peptide-peptide interaction in reproductive processes of plants are lacking. A signaling pathway mediated by a physical interaction of different secreted mobile non-membranous factors derived from both female and male reproductive

cells would represent a novel signaling mechanism and a highly specific reproductive fertilization barrier. Regarding the fact that sequences homologous to the WSL peptides could only be identified in the genome of the very closely related grass *Sorghum bicolor*, WSLs would represent good candidates for components participating in reproductive isolation barriers. Still, this is a model, which has not been proven yet. Future research should therefore focus on the verification of WSL-EA1 interaction and the study of *wls* pollen tube mutants. However, the identification of a cell surface receptor of ZmEA1 remains the most important step towards a deeper understanding of EA1-induced signaling at the pollen tube apex resulting in its directional growth. This receptor would be expected to trigger a signaling cascade resulting in reorganization of the tube cytoskeleton to modify growth direction. This might be conducted for example by influencing the Armadillo repeat protein ARMADILLO REPEAT ONLY 1 (ARO1), which is expected to play a role in the signaling network regulating tip growth by actin reorganization (Gebert *et al.*, 2008).

REFERENCES

Adamczak, R., Porollo, A. and Meller, J. (2005). Combining prediction of secondary structure and solvent accessibility in proteins. *Proteins* **59**, 467–475.

Ahmad, R., Nguyen, D. H., Wingerd, M. A., Church, G. M. and Steffen, M. A. (2005). Molecular weight assessment of proteins in total proteome profiles using 1D-PAGE and LC/MS/MS. *Proteome Science* **3**, 6.

Allen, A., Snyder, A. K., Preuss, M., Nielsen, E. E., Shah, D. M. and Smith, T. J. (2008). Plant defensins and virally encoded fungal toxin KP4 inhibit plant root growth. *Planta* **227**, 331–339.

Amien, S., Kliwer, I., Márton, M. L., Debener, T., Geiger, D., Becker, D. and Dresselhaus, T. (2010). Defensin-like ZmES4 mediates pollen tube burst in maize via opening of the potassium channel KZM1. *PLoS Biology* **8**, e1000388.

Aoki, N., Scofield, G. N., Wang, X.-D., Offler, C. E., Patrick, J. W. and Furbank, R. T. (2006). Pathway of sugar transport in germinating wheat seeds. *Plant Physiology* **141**, 1255–1263.

Arakawa, T. and Timasheff, S. N. (1982a). Mechanism of stabilization of proteins by glycerol and sucrose. *The Journal of Japanese Biochemical Society* **54**, 1255–1259.

Arakawa, T. and Timasheff, S. N. (1982b). Stabilization of protein structure by sugars. *Biochemistry* **21**, 6536–6544.

Arey, B. J. (2012). The role of glycosylation in receptor signaling. In: Petrescu, S.: *Glycosylation*, 273–286. InTech.

Armstrong, C. L., Green, C. E. and Phillips, R. L. (1991). Development and availability of germplasm with high type II culture formation response. *Maize Genet Cooperation Newsletter* **65**, 92–93.

Baldwin, R. L. (1996). How Hofmeister ion interactions affect protein stability. *Biophysical Journal* **71**, 2056–2063.

Bayer, M., Nawy, T., Giglione, C., Galli, M., Meinnel, T. and Lukowitz, W. (2009). Paternal control of embryonic patterning in Arabidopsis thaliana. *Science* **323**, 1485–1488.

Bedinger, P. A. and Fowler, J. E. (2009). The maize male gametophyte. In: Bennetzen, J. L. and Hake, S.: *Handbook of maize - It's biology*, 57–77. Springer.

Bendtsen, J. D., Jensen, L. J., Blom, N., Heijne, G. von and Brunak, S. (2004). Feature-based prediction of non-classical and leaderless protein secretion. *Protein Engineering, Design & Selection* **17**, 349–356.

Blanvillain, R., Young, B., Cai, Y.-m., Hecht, V., Varoquaux, F., Delorme, V., Lancelin, J.-M., Delseny, M. and Gallois, P. (2011). The Arabidopsis peptide kiss of death is an inducer of programmed cell death. *The EMBO Journal* **30**, 1173–1183.

Boavida, L. C., Vieira, A. M., Becker, J. D. and Feijó, J. A. (2005). Gametophyte interaction and sexual reproduction: how plants make a zygote. *The International Journal of Developmental Biology* **49**, 615–632.

Bocca, S. N., Magioli, C., Mangeon, A., Junqueira, R. M., Cardeal, V., Margis, R. and Sachetto-Martins, G. (2005). Survey of glycine-rich proteins (GRPs) in the Eucalyptus expressed sequence tag database (ForEST). *Genetics and Molecular Biology* **28**, 608–624.

Bocco, J. L., Panzetta, G. M., Flury, A. and Patrito, L. C. (1988). Processing of SP1 precursor in a cell-free system from poly(A+) mRNA of human placenta. *Molecular Biology Reports* **13**, 45–51.

Boisson-Dernier, A., Roy, S., Kritsas, K., Grobei, M. A., Jaciubek, M., Schroeder, J. I. and Grossniklaus, U. (2009). Disruption of the pollen-expressed FERONIA homologs ANXUR1 and ANXUR2 triggers pollen tube discharge. *Development* **136**, 3279–3288.

Bondos, S. E. and Bicknell, A. (2003). Detection and prevention of protein aggregation before, during, and after purification. *Analytical Biochemistry* **316**, 223–231.

Booy, G., Krens, F. A. and Bino, R. J. (1992). Analysis of pollen-tube growth in cultured maize silks. *Sexual Plant Reproduction* **5**, 227–231.

Bou Daher, F. and Geitmann, A. (2011). Actin is involved in pollen tube tropism through redefining the spatial targeting of secretory vesicles. *Traffic* **12**, 1537–1551.

Braakman, I. and Hebert, D. N. (2013). Protein folding in the endoplasmic reticulum. *Cold Spring Harbor Perspectives in Biology* **5**, a013201.

Brennan, M. D., Warren, T. G. and Mahowald, A. P. (1980). Signal peptides and signal peptidase in Drosophila melanogaster. *The Journal of Cell Biology* **87**, 516–520.

Buckler, E. S. and Holtsford, T. P. (1996). Zea systematics: ribosomal ITS evidence. *Molecular Biology and Evolution* **13**, 612–622.

Bulaj, G. (2005). Formation of disulfide bonds in proteins and peptides. *Biotechnology Advances* **23**, 87–92.

Butenko, M. A., Patterson, S. E., Grini, P. E., Stenvik, G.-E., Amundsen, S. S., Mandal, A. and Aalen, R. B. (2003). Inflorescence deficient in abscission controls floral organ abscission in Arabidopsis and identifies a novel family of putative ligands in plants. *The Plant Cell* **15**, 2296–2307.

Canales, C., Bhatt, A. M., Scott, R. and Dickinson, H. (2002). EXS, a putative LRR receptor kinase, regulates male germline cell number and tapetal identity and promotes seed development in Arabidopsis. *Current Biology* **12**, 1718–1727.

Cannon, E. K., Birkett, S. M., Braun, B. L., Kodavali, S., Jennewein, D. M., Yilmaz, A., Antonescu, V., Antonescu, C., Harper, L. C., Gardiner, J. M., Schaeffer, M. L., Campbell, D. A., Andorf, C. M., Andorf, D., Lisch, D., Koch, K. E., McCarty, D. R., Quackenbush, J., Grotewold, E., Lushbough, C. M., Sen, T. Z. and Lawrence, C. J. (2011). POPcorn: An online resource providing access to distributed and diverse maize project data. *International Journal of Plant Genomics* **2011**, 923035.

Capron, A., Gourgues, M., Neiva, L. S., Faure, J.-E., Berger, F., Pagnussat, G., Krishnan, A., Alvarez-Mejia, C., Vielle-Calzada, J.-P., Lee, Y.-R., Liu, B. and Sundaresan, V. (2008). Maternal control of male-gamete delivery in Arabidopsis involves a putative GPI-anchored protein encoded by the LORELEI gene. *The Plant Cell* **20**, 3038–3049.

Carlson, E. D., Gan, R., Hodgman, C. E. and Jewett, M. C. (2012). Cell-free protein synthesis: applications come of age. *Biotechnology Advances* **30**, 1185–1194.

Chae, K. and Lord, E. M. (2011). Pollen tube growth and guidance: roles of small, secreted proteins. *Annals of Botany* **108**, 627–636.

Chang, S. Y., Tsai, P. C., Tseng, C. S. and Liang, P. H. (2001). Refolding and characterization of a yeast dehydrodolichyl diphosphate synthase overexpressed in Escherichia coli. *Protein Expression and Purification* **23**, 432–439.

Chen, H., Nelson, R. S. and Sherwood, J. L. (1994). Enhanced recovery of transformants of Agrobacterium tumefaciens after freeze-thaw transformation and drug selection. *BioTechniques* **16**, 664-668, 670.

Chen, J., Lausser, A. and Dresselhaus, T. (2014). Hormonal responses during early embryogenesis in maize. *Biochemical Society Transactions* **42**, 325–331.

Chen, Z. (2001). A superfamily of proteins with novel cysteine-rich repeats. *Plant Physiology* **126**, 473–476.

Chettoor, A. M., Givan, S. A., Cole, R. A., Coker, C. T., Unger-Wallace, E., Vejlupkova, Z., Vollbrecht, E., Fowler, J. E. and Evans, M. (2014). Discovery of novel transcripts and gametophytic functions via RNA-seq analysis of maize gametophytic transcriptomes. *Genome Biology* **15**, 414.

Cheung, A. Y., Wang, H. and Wu, H. M. (1995). A floral transmitting tissue-specific glycoprotein attracts pollen tubes and stimulates their growth. *Cell* **82**, 383–393.

Cheung, A. Y. and Wu, H.-M. (2008). Structural and signaling networks for the polar cell growth machinery in pollen tubes. *Annual Review of Plant Biology* **59**, 547–572.

Christensen, C. A., Subramanian, S. and Drews, G. N. (1998). Identification of gametophytic mutations affecting female gametophyte development in Arabidopsis. *Developmental Biology* **202**, 136–151.

Clark, S. E., Williams, R. W. and Meyerowitz, E. M. (1997). The CLAVATA1 gene encodes a putative receptor kinase that controls shoot and floral meristem size in Arabidopsis. *Cell* **89**, 575–585.

Clough, S. J. and Bent, A. F. (1998). Floral dip: a simplified method for Agrobacterium-mediated transformation of Arabidopsis thaliana. *The Plant Journal* **16**, 735–743.

Cock, J. M. and McCormick, S. (2001). A large family of genes that share homology with CLAVATA3. *Plant Physiology* **126**, 939–942.

Cong, L., Ran, F. A., Cox, D., Lin, S., Barretto, R., Habib, N., Hsu, P. D., Wu, X., Jiang, W., Marraffini, L. A. and Zhang, F. (2013). Multiplex genome engineering using CRISPR/Cas systems. *Science* **339**, 819–823.

Cordts, S., Bantin, J., Wittich, P. E., Kranz, E., Lörz, H. and Dresselhaus, T. (2001). ZmES genes encode peptides with structural homology to defensins and are specifically expressed in the female gametophyte of maize. *The Plant Journal* **25**, 103–114.

Cormack, B. P., Valdivia, R. H. and Falkow, S. (1996). FACS-optimized mutants of the green fluorescent protein (GFP). *Gene* **173**, 33–38.

Cornet, B., Bonmatin, J. M., Hetru, C., Hoffmann, J. A., Ptak, M. and Vovelle, F. (1995). Refined three-dimensional solution structure of insect defensin A. *Structure* **3**, 435–448.

Costa, L. M., Marshall, E., Tesfaye, M., Silverstein, K. A. T., Mori, M., Umetsu, Y., Otterbach, S. L., Papareddy, R., Dickinson, H. G., Boutiller, K., VandenBosch, K. A., Ohki, S. and Gutierrez-Marcos, J. F. (2014). Central cell-derived peptides regulate early embryo patterning in flowering plants. *Science* **344**, 168–172.

Costa, L. M., Yuan, J., Rouster, J., Paul, W., Dickinson, H. and Gutierrez-Marcos, J. F. (2012). Maternal control of nutrient allocation in plant seeds by genomic imprinting. *Current Biology* **22**, 160–165.

Crouch, E. and Longmore, W. (1987). Collagen-binding proteins secreted by type II pneumocytes in culture. *Biochimica et Biophysica Acta* **924**, 81–86.

Dang, X.-L., Tian, J.-H., Yang, W.-Y., Wang, W.-X., Ishibashi, J., Asaoka, A., Yi, H.-Y., Li, Y.-F., Cao, Y., Yamakawa, M. and Wen, S.-Y. (2009). Bactrocerin-1: a novel inducible antimicrobial peptide from pupae of oriental fruit fly Bactrocera dorsalis Hendel. *Archives of Insect Biochemistry and Physiology* **71**, 117–129.

Dash, S., van Hemert, J., Hong, L., Wise, R. P. and Dickerson, J. A. (2012). PLEXdb: gene expression resources for plants and plant pathogens. *Nucleic Acids Research* **40**, D1194-201.

de Conink, B., Cammue, B. P. and Thevissen, K. (2013). Modes of antifungal action and in planta functions of plant defensins and defensin-like peptides. *The British Mycological Society* **26**, 109–120.

de Marco, A. (2009). Strategies for successful recombinant expression of disulfide bond-dependent proteins in Escherichia coli. *Microbial Cell Factories* **8**, 26.

de Smet, I., Voss, U., Jürgens, G. and Beeckman, T. (2009). Receptor-like kinases shape the plant. *Nature Cell Biology* **11**, 1166–1173.

DeGrip, W. J. and Bovee-Geurts, P. H. (1979). Synthesis and properties of alkylglucosides with mild detergent action: improved synthesis and purification of β-1-octyl-, -nonyl-, and -decyl-glucose. Synthesis of β-1-undecylglucose and β-1-dodecylmaltose. *Chemistry and Physics of Lipids* **23**, 321–325.

Delay, C., Imin, N. and Djordjevic, M. A. (2013). CEP genes regulate root and shoot development in response to environmental cues and are specific to seed plants. *Journal of Experimental Botany* **64**, 5383–5394.

Demuth, D. R. and Irvine, D. C. (2002). Structural and functional variation within the alanine-rich repetitive domain of streptococcal antigen I/II. *Infection and Immunity* **70**, 6389–6398.

Derksen, E. J., Rutten, T. L., van Amstel, T., Win, A. de, Doris, F. and Steer, M. (1995). Regulation of pollen tube growth. *Acta Botanica Neerlandica* **44**, 93–119.

Diboll, A. G. and Larson, D. A. (1966). An electron microscopic study of the mature megagametophyte in Zea mays. *American Journal of Botany* **53**, 391–402.

Diego-García, E., Schwartz, E. F., D'Suze, G., González, S. A., Batista, C. V., García, B. I., de la Vega, R. C. and Possani, L. D. (2007). Wide phylogenetic distribution of Scorpine and long-chain beta-KTx-like peptides in scorpion venoms: identification of "orphan" components. *Peptides* **28**, 31–37.

Dong, J., Kim, S. T. and Lord, E. M. (2005). Plantacyanin plays a role in reproduction in Arabidopsis. *Plant Physiology* **138**, 778–789.

Dorokhov, Y. L., Skulachev, M. V., Ivanov, P. A., Zvereva, S. D., Tjulkina, L. G., Merits, A., Gleba, Y. Y., Hohn, T. and Atabekov, J. G. (2002). Polypurine (A)-rich sequences promote cross-kingdom conservation of internal ribosome entry. *Proceedings of the National Academy of Sciences of the United States of America* **99**, 5301–5306.

Doverskog, M., Tally, M. and Häggström, L. (1999). Constitutive secretion of an endogenous insulin-like peptide binding protein with high affinity for insulin in Spodoptera frugiperda (Sf9) cell cultures. *Biochemical and Biophysical Research Communications* **265**, 674–679.

Dresselhaus, T. and Franklin-Tong, N. (2013). Male-female crosstalk during pollen germination, tube growth and guidance, and double fertilization. *Molecular Plant* **6**, 1018–1036.

Dresselhaus, T., Lausser, A. and Márton, M. L. (2011). Using maize as a model to study pollen tube growth and guidance, cross-incompatibility and sperm delivery in grasses. *Annals of Botany* **108**, 727–737.

Dresselhaus, T., Lörz, H. and Kranz, E. (1994). Representative cDNA libraries from few plant cells. *The Plant Journal* **5**, 605–610.

Drews, G. and Koltunow, A. (2011). The female gametophyte. *The Arabidopsis Book* **9**, e0155.

Dube, D. H., Li, B., Greenblatt, E. J., Nimer, S., Raymond, A. K. and Kohler, J. J. (2010). A two-hybrid assay to study protein interactions within the secretory pathway. *PloS One* **5**, e15648.

Earley, K. W., Haag, J. R., Pontes, O., Opper, K., Juehne, T., Song, K. and Pikaard, C. S. (2006). Gateway-compatible vectors for plant functional genomics and proteomics. *The Plant Journal* **45**, 616–629.

Elayadi, A. N., Samli, K. N., Prudkin, L., Liu, Y.-H., Bian, A., Xie, X.-J., Wistuba, I. I., Roth, J. A., McGuire, M. J. and Brown, K. C. (2007). A peptide selected by biopanning identifies the integrin alphavbeta6 as a prognostic biomarker for nonsmall cell lung cancer. *Cancer Research* **67**, 5889–5895.

Ellis, R. J. and Van der Vies, S. M. (1991). Molecular chaperones. *Annual Review of Biochemistry* **60**, 321–347.

Elschenbroich, S., Kim, Y., Medin, J. A. and Kislinger, T. (2010). Isolation of cell surface proteins for mass spectrometry-based proteomics. *Expert Review of Proteomics* **7**, 141–154.

Escobar-Restrepo, J.-M., Huck, N., Kessler, S., Gagliardini, V., Gheyselinck, J., Yang, W.-C. and Grossniklaus, U. (2007). The FERONIA receptor-like kinase mediates male-female interactions during pollen tube reception. *Science* **317**, 656–660.

Esposito, D. and Chatterjee, D. K. (2006). Enhancement of soluble protein expression through the use of fusion tags. *Current Opinion in Biotechnology* **17**, 353–358.

Evans, M. and Grossniklaus, U. (2009). The maize megagametophyte. In: Bennetzen, J. L. and Hake, S.: *Handbook of maize - It's biology*, 79–104. Springer.

Farley, A. R. and Link, A. J. (2009). Identification and quantification of protein posttranslational modifications. *Methods in Enzymology* **463**, 725–763.

Fastner, A. (2010). Interspezifische Pollenschlauchanlockung durch EA1 Signale aus Zea mays (L.). *Cell Biology and Plant Biochemistry (University of Regensburg)*, Bachelor thesis.

Fitchette, A.-C., Dinh, O. T., Faye, L. and Bardor, M. (2007). Plant proteomics and glycosylation. *Methods in Molecular Biology* **355**, 317–342.

Fiume, E. and Fletcher, J. C. (2012). Regulation of Arabidopsis embryo and endosperm development by the polypeptide signaling molecule CLE8. *The Plant Cell* **24**, 1000–1012.

Fletcher, J. C., Brand, U., Running, M. P., Simon, R. and Meyerowitz, E. M. (1999). Signaling of cell fate decisions by CLAVATA3 in Arabidopsis shoot meristems. *Science* **283**, 1911–1914.

Folders, J., Tommassen, J., van Loon, L. C. and Bitter, W. (2000). Identification of a chitin-binding protein secreted by Pseudomonas aeruginosa. *Journal of Bacteriology* **182**, 1257–1263.

Frame, B., Main, M., Schick, R. and Wang, K. (2011). Genetic transformation using maize immature zygotic embryos. *Methods in Molecular Biology* **710**, 327–341.

Frame, B. R., Shou, H., Chikwamba, R. K., Zhang, Z., Xiang, C., Fonger, T. M., Pegg, S. E., Li, B., Nettleton, D. S., Pei, D. and Wang, K. (2002). Agrobacterium tumefaciens-mediated transformation of maize embryos using a standard binary vector system. *Plant Physiology* **129**, 13–22.

Franklin-Tong, V. E. (1999). Signaling and the modulation of pollen tube growth. *The Plant Cell* **11**, 727–738.

Frei, A. P., Jeon, O.-Y., Kilcher, S., Moest, H., Henning, L. M., Jost, C., Plückthun, A., Mercer, J., Aebersold, R., Carreira, E. M. and Wollscheid, B. (2012). Direct identification of ligand-receptor interactions on living cells and tissues. *Nature Biotechnology* **30**, 997–1001.

Frei, A. P., Moest, H., Novy, K. and Wollscheid, B. (2013). Ligand-based receptor identification on living cells and tissues using TRICEPS. *Nature Protocols* **8**, 1321–1336.

García-Mata, R., Bebök, Z., Sorscher, E. J. and Sztul, E. S. (1999). Characterization and dynamics of aggresome formation by a cytosolic GFP-chimera. *The Journal of Cell Biology* **146**, 1239–1254.

Gebert, M., Dresselhaus, T. and Sprunck, S. (2008). F-actin organization and pollen tube tip growth in Arabidopsis are dependent on the gametophyte-specific Armadillo repeat protein ARO1. *The Plant Cell* **20**, 2798–2814.

Gekko, K. and Timasheff, S. N. (1981). Mechanism of protein stabilization by glycerol: preferential hydration in glycerol-water mixtures. *Biochemistry* **20**, 4667–4676.

Geldner, N. and Robatzek, S. (2008). Plant receptors go endosomal: a moving view on signal transduction. *Plant Physiology* **147**, 1565–1574.

Giuliani, C., Consonni, G., Gavazzi, G., Colombo, M. and Dolfini, S. (2002). Programmed cell death during embryogenesis in maize. *Annals of Botany* **90**, 287–292.

Goldraij, A., Kondo, K., Lee, C. B., Hancock, C. N., Sivaguru, M., Vazquez-Santana, S., Kim, S., Phillips, T. E., Cruz-Garcia, F. and McClure, B. (2006). Compartmentalization of S-RNase and HT-B degradation in self-incompatible Nicotiana. *Nature* **439**, 805–810.

Gómez-Gómez, L. and Boller, T. (2000). FLS2: an LRR receptor-like kinase involved in the perception of the bacterial elicitor flagellin in Arabidopsis. *Molecular Cell* **5**, 1003–1011.

Gomord, V., Denmat, L. A., Fitchette-Lainé, A. C., Satiat-Jeunemaitre, B., Hawes, C. and Faye, L. (1997). The C-terminal HDEL sequence is sufficient for retention of secretory proteins in the endoplasmic reticulum (ER) but promotes vacuolar targeting of proteins that escape the ER. *The Plant Journal* **11**, 313–325.

Gray-Mitsumune, M. and Matton, D. P. (2006). The Egg apparatus 1 gene from maize is a member of a large gene family found in both monocots and dicots. *Planta* **223**, 618–625.

Guan, Y., Lu, J., Xu, J., McClure, B. and Zhang, S. (2014). Two mitogen-activated protein kinases, MPK3 and MPK6, are required for funicular guidance of pollen tubes in Arabidopsis. *Plant Physiology* **165**, 528–533.

Gui, J., Liu, B., Cao, G., Lipchik, A. M., Perez, M., Dekan, Z., Mobli, M., Daly, N. L., Alewood, P. F., Parker, L. L., King, G. F., Zhou, Y., Jordt, S.-E. and Nitabach, M. N. (2014). A tarantula-venom peptide antagonizes the TRPA1 nociceptor ion channel by binding to the S1-S4 gating domain. *Current Biology* **24**, 473–483.

Hafidh, S., Potěšil, D., Fíla, J., Feciková, J., Čapková, V., Zdráhal, Z. and Honys, D. (2014). In search of ligands and receptors of the pollen tube: the missing link in pollen tube perception. *Biochemical Society Transactions* **42**, 388–394.

Haji Abdolvahab, M., Fazeli, A., Fazeli, M. R., Brinks, V. and Schellekens, H. (2014). The effects of dodecyl maltoside and sodium dodecyl sulfate surfactants on the stability and aggregation of recombinant interferon Beta-1b. *Journal of Interferon & Cytokine Research* **34**, 894–901.

Hanks, J. N., Snyder, A. K., Graham, M. A., Shah, R. K., Blaylock, L. A., Harrison, M. J. and Shah, D. M. (2005). Defensin gene family in Medicago truncatula: structure, expression and induction by signal molecules. *Plant Molecular Biology* **58**, 385–399.

Hanson, S. R., Culyba, E. K., Hsu, T.-L., Wong, C.-H., Kelly, J. W. and Powers, E. T. (2009). The core trisaccharide of an N-linked glycoprotein intrinsically accelerates folding and enhances stability. *Proceedings of the National Academy of Sciences of the United States of America* **106**, 3131–3136.

Hara, K., Yokoo, T., Kajita, R., Onishi, T., Yahata, S., Peterson, K. M., Torii, K. U. and Kakimoto, T. (2009). Epidermal cell density is autoregulated via a secretory peptide, EPIDERMAL PATTERNING FACTOR 2 in Arabidopsis leaves. *Plant & Cell Physiology* **50**, 1019–1031.

He, Z. H., Cheeseman, I., He, D. and Kohorn, B. D. (1999). A cluster of five cell wall-associated receptor kinase genes, Wak1-5, are expressed in specific organs of Arabidopsis. *Plant Molecular Biology* **39**, 1189–1196.

Heese, A., Hann, D. R., Gimenez-Ibanez, S., Jones, A. M., He, K., Li, J., Schroeder, J. I., Peck, S. C. and Rathjen, J. P. (2007). The receptor-like kinase SERK3/BAK1 is a central regulator of innate immunity in plants. *Proceedings of the National Academy of Sciences of the United States of America* **104**, 12217–12222.

Helbig, A. O., Heck, A. J. and Slijper, M. (2010). Exploring the membrane proteome--challenges and analytical strategies. *Journal of Proteomics* **73**, 868–878.

Helenius, A., McCaslin, D. R., Fries, E. and Tanford, C. (1979). Properties of detergents. *Methods in Enzymology* **56**, 734–749.

Herbinière, J., Braquart-Varnier, C., Grève, P., Strub, J.-M., Frère, J., van Dorsselaer, A. and Martin, G. (2005). Armadillidin: a novel glycine-rich antibacterial peptide directed against gram-positive bacteria in the woodlouse Armadillidium vulgare (Terrestrial Isopod, Crustacean). *Developmental and Comparative Immunology* **29**, 489–499.

Heslop-Harrison, Y., Heslop-Harrison, J. and Reger, B. J. (1985). Pollen-tube guidance and the regulation of tube number in Zea mays L. *Acta Botanica Neerlandica* **34**, 193–211.

Hiei, Y. and Komari, T. (2008). Agrobacterium-mediated transformation of rice using immature embryos or calli induced from mature seed. *Nature Protocols* **3**, 824–834.

Higashiyama, T. and Hamamura, Y. (2008). Gametophytic pollen tube guidance. *Sexual Plant Reproduction* **21**, 17–26.

Higashiyama, T., Inatsugi, R., Sakamoto, S., Sasaki, N., Mori, T., Kuroiwa, H., Nakada, T., Nozaki, H., Kuroiwa, T. and Nakano, A. (2006). Species preferentiality of the pollen tube attractant derived from the synergid cell of Torenia fournieri. *Plant Physiology* **142**, 481–491.

Higashiyama, T., Kuroiwa, H., Kawano, S. and Kuroiwa, T. (1998). Guidance in vitro of the pollen tube to the naked embryo sac of Torenia fournieri. *The Plant Cell* **10**, 2019–2032.

Higashiyama, T. and Takeuchi, H. (2015). The mechanism and key molecules involved in pollen tube guidance. *Annual Review of Plant Biology* **66**, 393–413.

Higashiyama, T., Yabe, S., Sasaki, N., Nishimura, Y., Miyagishima, S., Kuroiwa, H. and Kuroiwa, T. (2001). Pollen tube attraction by the synergid cell. *Science* **293**, 1480–1483.

Hirakawa, Y., Shinohara, H., Kondo, Y., Inoue, A., Nakanomyo, I., Ogawa, M., Sawa, S., Ohashi-Ito, K., Matsubayashi, Y. and Fukuda, H. (2008). Non-cell-autonomous control of vascular stem cell fate by a CLE peptide/receptor system. *Proceedings of the National Academy of Sciences of the United States of America* **105**, 15208–15213.

Hoekema, A., Hirsch, P. R., Hooykaas, P. J. and Schilperoort, R. A. (1983). A binary plant vector strategy based on separation of vir- and T-region of the Agrobacterium tumefaciens Ti-plasmid. *Nature* **303**, 179–180.

Holloway, P. W. and Katz, J. T. (1972). A requirement for cytochrome b 5 in microsomal stearyl coenzyme A desaturation. *Biochemistry* **11**, 3689–3696.

Holsters, M., Silva, B., van Vliet, F., Genetello, C., Block, M. de, Dhaese, P., Depicker, A., Inzé, D., Engler, G. and Villarroel, R. (1980). The functional organization of the nopaline A. tumefaciens plasmid pTiC58. *Plasmid* **3**, 212–230.

Hruz, T., Laule, O., Szabo, G., Wessendorp, F., Bleuler, S., Oertle, L., Widmayer, P., Gruissem, W. and Zimmermann, P. (2008). Genevestigator v3: a reference expression database for the meta-analysis of transcriptomes. *Advances in Bioinformatics* **2008**, 420747.

Hsieh, J. C., Kodjabachian, L., Rebbert, M. L., Rattner, A., Smallwood, P. M., Samos, C. H., Nusse, R., Dawid, I. B. and Nathans, J. (1999). A new secreted protein that binds to Wnt proteins and inhibits their activities. *Nature* **398**, 431–436.

Huang, A. H. (1992). Oil Bodies and Oleosins in Seeds. *Annual Review of Plant Physiology and Plant Molecular Biology* **43**, 177–200.

Huang, Q., Dresselhaus, T., Gu, H. and Qu, L.-J. (2015). Active role of small peptides in Arabidopsis reproduction: Expression evidence. *Journal of Integrative Plant Biology* **57**, 518–521.

Hynes, R. O. (1992). Integrins: versatility, modulation, and signaling in cell adhesion. *Cell* **69**, 11–25.

Imredy, J. P., Chen, C. and MacKinnon, R. (1998). A snake toxin inhibitor of inward rectifier potassium channel ROMK1. *Biochemistry* **37**, 14867–14874.

Ingouff, M., Rademacher, S., Holec, S., Soljić, L., Xin, N., Readshaw, A., Foo, S. H., Lahouze, B., Sprunck, S. and Berger, F. (2010). Zygotic resetting of the HISTONE 3 variant repertoire participates in epigenetic reprogramming in Arabidopsis. *Current Biology* **20**, 2137–2143.

Ingram, G. and Gutierrez-Marcos, J. (2015). Peptide signalling during angiosperm seed development. *Journal of Experimental Botany* **66**, 5151–5159.

Inoue, H., Nojima, H. and Okayama, H. (1990). High efficiency transformation of Escherichia coli with plasmids. *Gene* **96**, 23–28.

Irani, N. G. and Russinova, E. (2009). Receptor endocytosis and signaling in plants. *Current Opinion in Plant Biology* **12**, 653–659.

Ito, Y., Nakanomyo, I., Motose, H., Iwamoto, K., Sawa, S., Dohmae, N. and Fukuda, H. (2006). Dodeca-CLE peptides as suppressors of plant stem cell differentiation. *Science* **313**, 842–845.

Iwano, M., Ngo, Q. A., Entani, T., Shiba, H., Nagai, T., Miyawaki, A., Isogai, A., Grossniklaus, U. and Takayama, S. (2012). Cytoplasmic Ca2+ changes dynamically during the interaction of the pollen tube with synergid cells. *Development* **139**, 4202–4209.

Iwano, M. and Takayama, S. (2012). Self/non-self discrimination in angiosperm self-incompatibility. *Current Opinion in Plant Biology* **15**, 78–83.

Jackson, R. C. and Blobel, G. (1977). Post-translational cleavage of presecretory proteins with an extract of rough microsomes from dog pancreas containing signal peptidase activity. *Proceedings of the National Academy of Sciences of the United States of America* **74**, 5598–5602.

Jackson, T., Blakemore, W., Newman, J. W., Knowles, N. J., Mould, A. P., Humphries, M. J. and King, A. M. (2000a). Foot-and-mouth disease virus is a ligand for the high-affinity binding conformation of integrin alpha5beta1: influence of the leucine residue within the RGDL motif on selectivity of integrin binding. *The Journal of General Virology* **81**, 1383–1391.

Jackson, T., Mould, A. P., Sheppard, D. and King, A. M. (2002). Integrin alphavbeta1 is a receptor for foot-and-mouth disease virus. *Journal of Virology* **76**, 935–941.

Jackson, T., Sharma, A., Ghazaleh, R. A., Blakemore, W. E., Ellard, F. M., Simmons, D. L., Newman, J. W., Stuart, D. I. and King, A. M. (1997). Arginine-glycine-aspartic acid-specific binding by foot-and-mouth disease viruses to the purified integrin alpha(v)beta3 in vitro. *Journal of Virology* **71**, 8357–8361.

Jackson, T., Sheppard, D., Denyer, M., Blakemore, W. and King, A. M. (2000b). The epithelial integrin alphavbeta6 is a receptor for foot-and-mouth disease virus. *Journal of Virology* **74**, 4949–4956.

Jauh, G. Y., Eckard, K. J., Nothnagel, E. A. and Lord, E. M. (1997). Adhesion of lily pollen tubes on an artificial matrix. *Sexual Plant Reproduction* **10**, 173–180.

Javelle, M., Marco, C. F. and Timmermans, M. (2011). In situ hybridization for the precise localization of transcripts in plants. *Journal of Visualized Experiments* **57**, e3328.

Johansson, T., Le Quéré, A., Ahren, D., Söderström, B., Erlandsson, R., Lundeberg, J., Uhlén, M. and Tunlid, A. (2004). Transcriptional responses of Paxillus involutus and Betula pendula during formation of ectomycorrhizal root tissue. *Molecular Plant-Microbe Interactions* **17**, 202–215.

Johnston, J. A., Ward, C. L. and Kopito, R. R. (1998). Aggresomes: a cellular response to misfolded proteins. *The Journal of Cell Biology* **143**, 1883–1898.

Jones, S. E. and Jomary, C. (2002). Secreted Frizzled-related proteins: searching for relationships and patterns. *BioEssays* **24**, 811–820.

Kaku, H., Nishizawa, Y., Ishii-Minami, N., Akimoto-Tomiyama, C., Dohmae, N., Takio, K., Minami, E. and Shibuya, N. (2006). Plant cells recognize chitin fragments for defense signaling through a plasma membrane receptor. *Proceedings of the National Academy of Sciences of the United States of America* **103**, 11086–11091.

Kakumanu, A., Ambavaram, M. M., Klumas, C., Krishnan, A., Batlang, U., Myers, E., Grene, R. and Pereira, A. (2012). Effects of drought on gene expression in maize reproductive and leaf meristem tissue revealed by RNA-Seq. *Plant Physiology* **160**, 846–867.

Kanaoka, M. M., Kawano, N., Matsubara, Y., Susaki, D., Okuda, S., Sasaki, N. and Higashiyama, T. (2011). Identification and characterization of TcCRP1, a pollen tube attractant from Torenia concolor. *Annals of Botany* **108**, 739–747.

Kapust, R. B. and Waugh, D. S. (1999). Escherichia coli maltose-binding protein is uncommonly effective at promoting the solubility of polypeptides to which it is fused. *Protein Science* **8**, 1668–1674.

Karimi, M., Inzé, D. and Depicker, A. (2002). GATEWAY vectors for Agrobacterium-mediated plant transformation. *Trends in Plant Science* **7**, 193–195.

Kasahara, R. D., Portereiko, M. F., Sandaklie-Nikolova, L., Rabiger, D. S. and Drews, G. N. (2005). MYB98 is required for pollen tube guidance and synergid cell differentiation in Arabidopsis. *The Plant Cell* **17**, 2981–2992.

Katoh, M. and Katoh, M. (2007). WNT signaling pathway and stem cell signaling network. *Clinical Cancer Research* **13**, 4042–4045.

Kehoe, J. W. and Bertozzi, C. R. (2000). Tyrosine sulfation: a modulator of extracellular protein-protein interactions. *Chemistry & Biology* **7**, R57-61.

Kerwin, B. A., Heller, M. C., Levin, S. H. and Randolph, T. W. (1998). Effects of Tween 80 and sucrose on acute short-term stability and long-term storage at -20 degrees C of a recombinant hemoglobin. *Journal of Pharmaceutical Sciences* **87**, 1062–1068.

Kessler, S. A., Shimosato-Asano, H., Keinath, N. F., Wuest, S. E., Ingram, G., Panstruga, R. and Grossniklaus, U. (2010). Conserved molecular components for pollen tube reception and fungal invasion. *Science* **330**, 968–971.

Kim, J. Y., Park, S. J., Jang, B., Jung, C.-H., Ahn, S. J., Goh, C.-H., Cho, K., Han, O. and Kang, H. (2007). Functional characterization of a glycine-rich RNA-binding protein 2 in Arabidopsis thaliana under abiotic stress conditions. *The Plant Journal* **50**, 439–451.

Kim, S., Mollet, J.-C., Dong, J., Zhang, K., Park, S.-Y. and Lord, E. M. (2003). Chemocyanin, a small basic protein from the lily stigma, induces pollen tube chemotropism. *Proceedings of the National Academy of Sciences of the United States of America* **100**, 16125–16130.

Kim, S. T., Zhang, K., Dong, J. and Lord, E. M. (2006). Exogenous free ubiquitin enhances lily pollen tube adhesion to an in vitro stylar matrix and may facilitate endocytosis of SCA. *Plant Physiology* **142**, 1397–1411.

Klein, R. M., Wolf, E. D., Wu, R. and Sanford, J. C. (1987). High-velocity microprojectiles for delivering nucleic acids into living cells. *Biotechnology* **327**, 70–73.

Klein, T. M., Gradziel, T., Fromm, M. E. and Sanford, J. E. (1988). Factors influencing gene deliver into Zea mays cells by high-velocity microprojectiles. *Nature Biotechnology* **6**, 559–563.

Kondo, T., Kajita, R., Miyazaki, A., Hokoyama, M., Nakamura-Miura, T., Mizuno, S., Masuda, Y., Irie, K., Tanaka, Y., Takada, S., Kakimoto, T. and Sakagami, Y. (2010). Stomatal density is controlled by a mesophyll-derived signaling molecule. *Plant & Cell Physiology* **51**, 1–8.

Kondo, T., Sawa, S., Kinoshita, A., Mizuno, S., Kakimoto, T., Fukuda, H. and Sakagami, Y. (2006). A plant peptide encoded by CLV3 identified by in situ MALDI-TOF MS analysis. *Science* **313**, 845–848.

Kopito, R. R. (2000). Aggresomes, inclusion bodies and protein aggregation. *Trends in Cell Biology* **10**, 524–530.

Kreilgaard, L., Jones, L. S., Randolph, T. W., Frokjaer, S., Flink, J. M., Manning, M. C. and Carpenter, J. F. (1998). Effect of Tween 20 on freeze-thawing- and agitation-induced aggregation of recombinant human factor XIII. *Journal of Pharmaceutical Sciences* **87**, 1597–1603.

Krohn, N. G., Lausser, A., Juranić, M. and Dresselhaus, T. (2012). Egg cell signaling by the secreted peptide ZmEAL1 controls antipodal cell fate. *Developmental Cell* **23**, 219–225.

Kubick, S., Gerrits, M., Merk, H., Stiege, W. and Erdmann, V. A. (2009). In vitro synthesis of posttranslationally modified membrane proteins. In: DeLucas, L. J.: *Membrane protein crystallization*, 25–51. Academic Press.

Kumpf, R. P., Shi, C.-L., Larrieu, A., Stø, I. M., Butenko, M. A., Péret, B., Riiser, E. S., Bennett, M. J. and Aalen, R. B. (2013). Floral organ abscission peptide IDA and its HAE/HSL2 receptors control cell separation during lateral root emergence. *Proceedings of the National Academy of Sciences of the United States of America* **110**, 5235–5240.

Kyte, J. and Doolittle, R. F. (1982). A simple method for displaying the hydropathic character of a protein. *Journal of Molecular Biology* **157**, 105–132.

Lacerda, A. F., Vasconcelos, E. A., Pelegrini, P. B. and Grossi de Sa, M. F. (2014). Antifungal defensins and their role in plant defense. *Frontiers in Microbiology* **5**, 116.

Laemmli, U. K. (1970). Cleavage of structural proteins during the assembly of the head of bacteriophage T4. *Nature* **227**, 680–685.

Larkin, M. A., Blackshields, G., Brown, N. P., Chenna, R., McGettigan, P. A., McWilliam, H., Valentin, F., Wallace, I. M., Wilm, A., Lopez, R., Thompson, J. D., Gibson, T. J. and Higgins, D. G. (2007). Clustal W and Clustal X version 2.0. *Bioinformatics* **23**, 2947–2948.

Lau, S., Slane, D., Herud, O., Kong, J. and Jürgens, G. (2012). Early embryogenesis in flowering plants: setting up the basic body pattern. *Annual Review of Plant Biology* **63**, 483–506.

Lausser, A. (2012). Studies on double fertilisation and early embryogenesis of Arabidopsis thaliana Heynh. and Zea mays L. *Cell Biology and Plant Biochemistry (University of Regensburg)*, PhD thesis.

Lausser, A., Kliwer, I., Srilunchang, K. and Dresselhaus, T. (2010). Sporophytic control of pollen tube growth and guidance in maize. *Journal of Experimental Botany* **61**, 673–682.

Lay, F. T. and Anderson, M. A. (2005). Defensins - components of the innate immune system in plants. *Current Protein & Peptide Science* **6**, 85–101.

Lay, F. T., Mills, G. D., Poon, I. K., Cowieson, N. P., Kirby, N., Baxter, A. A., van der Weerden, N. L., Dogovski, C., Perugini, M. A., Anderson, M. A., Kvansakul, M. and Hulett, M. D. (2012). Dimerization of plant defensin NaD1 enhances its antifungal activity. *The Journal of Biological Chemistry* **287**, 19961–19972.

Lease, K. A. and Walker, J. C. (2006). The Arabidopsis unannotated secreted peptide database, a resource for plant peptidomics. *Plant Physiology* **142**, 831–838.

Lease, K. A. and Walker, J. C. (2010). Bioinformatic identification of plant peptides. *Methods in Molecular Biology* **615**, 375–383.

Lee, A. G. (2004). How lipids affect the activities of integral membrane proteins. *Biochimica et Biophysica Acta* **1666**, 62–87.

Lee, J. S., Kuroha, T., Hnilova, M., Khatayevich, D., Kanaoka, M. M., McAbee, J. M., Sarikaya, M., Tamerler, C. and Torii, K. U. (2012). Direct interaction of ligand-receptor pairs specifying stomatal patterning. *Genes & Development* **26**, 126–136.

Leibly, D. J., Nguyen, T. N., Kao, L. T., Hewitt, S. N., Barrett, L. K. and Van Voorhis, W. C. (2012). Stabilizing additives added during cell lysis aid in the solubilization of recombinant proteins. *PloS One* **7**, e52482.

Li, H.-J., Xue, Y., Jia, D.-J., Wang, T., Hi, D.-Q., Liu, J., Cui, F., Xie, Q., Ye, D. and Yang, W.-C. (2011). POD1 regulates pollen tube guidance in response to micropylar female signaling and acts in early embryo patterning in Arabidopsis. *The Plant Cell* **23**, 3288–3302.

Li, S., Ge, F.-R., Xu, M., Zhao, X.-Y., Huang, G.-Q., Zhou, L.-Z., Wang, J.-G., Kombrink, A., McCormick, S., Zhang, X. S. and Zhang, Y. (2013). Arabidopsis COBRA-LIKE 10, a GPI-anchored protein, mediates directional growth of pollen tubes. *The Plant Journal* **74**, 486–497.

Lindner, H., Müller, L. M., Boisson-Dernier, A. and Grossniklaus, U. (2012). CrRLK1L receptor-like kinases: not just another brick in the wall. *Current Opinion in Plant Biology* **15**, 659–669.

Ling, Y., Chen, T., Jing, Y., Fan, L., Wan, Y. and Lin, J. (2013). γ-Aminobutyric acid (GABA) homeostasis regulates pollen germination and polarized growth in Picea wilsonii. *Planta* **238**, 831–843.

Liu, J., Zhong, S., Guo, X., Hao, L., Wei, X., Huang, Q., Hou, Y., Shi, J., Wang, C., Gu, H. and Qu, L.-J. (2013). Membrane-bound RLCKs LIP1 and LIP2 are essential male factors controlling male-female attraction in Arabidopsis. *Current Biology* **23**, 993–998.

Logemann, J., Schell, J. and Willmitzer, L. (1987). Improved method for the isolation of RNA from plant tissues. *Analytical Biochemistry* **163**, 16–20.

Lu, Y., Chanroj, S., Zulkifli, L., Johnson, M. A., Uozumi, N., Cheung, A. and Sze, H. (2011). Pollen tubes lacking a pair of K+ transporters fail to target ovules in Arabidopsis. *The Plant Cell* **23**, 81–93.

Luo, M., Dennis, E. S., Berger, F., Peacock, W. J. and Chaudhury, A. (2005). MINISEED3 (MINI3), a WRKY family gene, and HAIKU2 (IKU2), a leucine-rich repeat (LRR) KINASE gene, are regulators of seed size in Arabidopsis. *Proceedings of the National Academy of Sciences of the United States of America* **102**, 17531–17536.

MacDonald, M. R., McCourt, D. W. and Krause, J. E. (1988). Posttranslational processing of alpha-, beta-, and gamma-preprotachykinins. Cell-free translation and early posttranslational processing events. *The Journal of Biological Chemistry* **263**, 15176–15183.

Mädler, S., Bich, C., Touboul, D. and Zenobi, R. (2009). Chemical cross-linking with NHS esters: a systematic study on amino acid reactivities. *Journal of Mass Spectrometry* **44**, 694–706.

Mangelsdorf, P. C. and Reeves, R. G. (1931). Hybridization of maize, Tripsacum and Euchlaena. *Journal of Heredity* **22**, 343–344.

Mangeon, A., Junqueira, R. M. and Sachetto-Martins, G. (2010). Functional diversity of the plant glycine-rich proteins superfamily. *Plant Signaling & Behavior* **5**, 99–104.

Mangeon, A., Magioli, C., Menezes-Salgueiro, A. D., Cardeal, V., Oliveira, C. de, Galvão, V. C., Margis, R., Engler, G. and Sachetto-Martins, G. (2009). AtGRP5, a vacuole-located glycine-rich protein involved in cell elongation. *Planta* **230**, 253–265.

Manoli, A., Sturaro, A., Trevisan, S., Quaggiotti, S. and Nonis, A. (2012). Evaluation of candidate reference genes for qPCR in maize. *Journal of Plant Physiology* **169**, 807–815.

Marshall, E., Costa, L. M. and Gutierrez-Marcos, J. (2011). Cysteine-rich peptides (CRPs) mediate diverse aspects of cell-cell communication in plant reproduction and development. *Journal of Experimental Botany* **62**, 1677–1686.

Márton, M. L., Cordts, S., Broadhvest, J. and Dresselhaus, T. (2005). Micropylar pollen tube guidance by egg apparatus 1 of maize. *Science* **307**, 573–576.

Márton, M. L. and Dresselhaus, T. (2008). A comparison of early molecular fertilization mechanisms in animals and flowering plants. *Sexual Plant Reproduction* **21**, 37–52.

Márton, M. L. and Dresselhaus, T. (2010). Female gametophyte-controlled pollen tube guidance. *Biochemical Society Transactions* **38**, 627–630.

Márton, M. L., Fastner, A., Uebler, S. and Dresselhaus, T. (2012). Overcoming hybridization barriers by the secretion of the maize pollen tube attractant ZmEA1 from Arabidopsis ovules. *Current Biology* **22**, 1194–1198.

Matsubayashi, Y. (2014). Posttranslationally Modified Small-Peptide Signals in Plants. *Annual Review of Plant Biology* **65**, 385–413.

Matsubayashi, Y., Ogawa, M., Morita, A. and Sakagami, Y. (2002). An LRR receptor kinase involved in perception of a peptide plant hormone, phytosulfokine. *Science* **296**, 1470–1472.

Matsumoto-Nakano, M., Tsuji, M., Amano, A. and Ooshima, T. (2008). Molecular interactions of alanine-rich and proline-rich regions of cell surface protein antigen c in Streptococcus mutans. *Oral Microbiology and Immunology* **23**, 265–270.

Mayfield, J. A. and Preuss, D. (2000). Rapid initiation of Arabidopsis pollination requires the oleosin-domain protein GRP17. *Nature Cell Biology* **2**, 128–130.

McCormick, S. (2004). Control of male gametophyte development. *The Plant Cell* **16 Suppl**, S142-53.

McCormick, S. and Yang, H. (2005). Is there more than one way to attract a pollen tube? *Trends in Plant Science* **10**, 260–263.

McPherson, M., Yang, Y., Hammond, P. W. and Kreider, B. L. (2002). Drug receptor identification from multiple tissues using cellular-derived mRNA display libraries. *Chemistry & Biology* **9**, 691–698.

Medenbach, J., Seiler, M. and Hentze, M. W. (2011). Translational control via protein-regulated upstream open reading frames. *Cell* **145**, 902–913.

Meitzler, J. L., Hinde, S., Bánfi, B., Nauseef, W. M. and Ortiz de Montellano, P. R. (2013). Conserved cysteine residues provide a protein-protein interaction surface in dual oxidase (DUOX) proteins. *The Journal of Biological Chemistry* **288**, 7147–7157.

Meng, L., Ruth, K. C., Fletcher, J. C. and Feldman, L. (2010). The roles of different CLE domains in Arabidopsis CLE polypeptide activity and functional specificity. *Molecular Plant* **3**, 760–772.

Mergaert, P., Nikovics, K., Kelemen, Z., Maunoury, N., Vaubert, D., Kondorosi, A. and Kondorosi, E. (2003). A novel family in Medicago truncatula consisting of more than 300 nodule-specific genes coding for small, secreted polypeptides with conserved cysteine motifs. *Plant Physiology* **132**, 161–173.

Merk, H., Gless, C., Maertens, B., Gerrits, M. and Stiege, W. (2012). Cell-free synthesis of functional and endotoxin-free antibody Fab fragments by translocation into microsomes. *BioTechniques* **53**, 153–160.

Mirouze, M., Sels, J., Richard, O., Czernic, P., Loubet, S., Jacquier, A., François, I. E., Cammue, B. P., Lebrun, M., Berthomieu, P. and Marquès, L. (2006). A putative novel role for plant defensins: a defensin from the zinc hyper-accumulating plant, Arabidopsis halleri, confers zinc tolerance. *The Plant Journal* **47**, 329–342.

Miyakawa, T., Hatano, K.-i., Miyauchi, Y., Suwa, Y.-i., Sawano, Y. and Tanokura, M. (2014). A secreted protein with plant-specific cysteine-rich motif functions as a mannose-binding lectin that exhibits antifungal activity. *Plant Physiology* **166**, 766–778.

Miyawaki, K., Tabata, R. and Sawa, S. (2013). Evolutionarily conserved CLE peptide signaling in plant development, symbiosis, and parasitism. *Current Opinion in Plant Biology* **16**, 598–606.

Molina, A., Segura, A. and García-Olmedo, F. (1993). Lipid transfer proteins (nsLTPs) from barley and maize leaves are potent inhibitors of bacterial and fungal plant pathogens. *FEBS Letters* **316**, 119–122.

Mollet, J.-C., Park, S.-Y., Nothnagel, E. A. and Lord, E. M. (2000). A lily stylar pectin is necessary for pollen tube adhesion to an in vitro stylar matrix. *Plant Cell* **12**, 1737–1749.

Monaco, M. K., Stein, J., Naithani, S., Wei, S., Dharmawardhana, P., Kumari, S., Amarasinghe, V., Youens-Clark, K., Thomason, J., Preece, J., Pasternak, S., Olson, A., Jiao, Y., Lu, Z., Bolser, D., Kerhornou, A., Staines, D., Walts, B., Wu, G., D'Eustachio, P., Haw, R., Croft, D., Kersey, P. J., Stein, L., Jaiswal, P. and Ware, D. (2014). Gramene 2013: comparative plant genomics resources. *Nucleic Acids Research* **42**, D1193-9.

Mukhopadhyay, A. (1997). Inclusion bodies and purification of proteins in biologically active forms. *Advances in Biochemical Engineering/Biotechnology* **56**, 61–109.

Murashige, T. and Skoog, F. (1962). A revised medium for rapid growth and bio assays with tobacco tissue cultures. *Physiologia Plantarum* **15**, 473–497.

Murphy, E., Smith, S. and de Smet, I. (2012). Small signaling peptides in Arabidopsis development: how cells communicate over a short distance. *The Plant Cell* **24**, 3198–3217.

Muschietti, J., Dircks, L., Vancanneyt, G. and McCormick, S. (1994). LAT52 protein is essential for tomato pollen development: pollen expressing antisense LAT52 RNA hydrates and germinates abnormally and cannot achieve fertilization. *The Plant Journal* **6**, 321–338.

Nagahara, N. (2011). Intermolecular disulfide bond to modulate protein function as a redox-sensing switch. *Amino Acids* **41**, 59–72.

Nahirñak, V., Almasia, N. I., Hopp, H. E. and Vazquez-Rovere, C. (2012). Snakin/GASA proteins: involvement in hormone crosstalk and redox homeostasis. *Plant Signaling & Behavior* **7**, 1004–1008.

Nallamsetty, S., Austin, B. P., Penrose, K. J. and Waugh, D. S. (2005). Gateway vectors for the production of combinatorially-tagged His6-MBP fusion proteins in the cytoplasm and periplasm of Escherichia coli. *Protein Science* **14**, 2964–2971.

Nardmann, J. and Werr, W. (2009). Patterning of the maize embryo and the perspective of evolutionary developmental biology. In: Bennetzen, J. L. and Hake, S.: *Handbook of maize - It's biology*, 105–119. Springer.

Neagu, A., Neagu, M. and Dér, A. (2001). Fluctuations and the Hofmeister effect. *Biophysical Journal* **81**, 1285–1294.

Negbi, M. (1984). The structure and function of the scutellum of the Gramineae. *Botanical Journal of the Linnean Society* **88**, 205–222.

Nelson, B. K., Cai, X. and Nebenführ, A. (2007). A multicolored set of in vivo organelle markers for co-localization studies in Arabidopsis and other plants. *The Plant Journal* **51**, 1126–1136.

Ni, J. and Clark, S. E. (2006). Evidence for functional conservation, sufficiency, and proteolytic processing of the CLAVATA3 CLE domain. *Plant Physiology* **140**, 726–733.

Nicholas, K. B., Nicholas, H. B. and Deerfield, D. W. (1997). GeneDoc: analysis and visualization of genetic variation. *Embnet.news* **4**, 14.

Niwa, T., Kondo, T., Nishizawa, M., Kajita, R., Kakimoto, T. and Ishiguro, S. (2013). EPIDERMAL PATTERNING FACTOR LIKE5 peptide represses stomatal development by inhibiting meristemoid maintenance in Arabidopsis thaliana. *Bioscience, Biotechnology and Biochemistry* **77**, 1287–1295.

Nomura, T., Kono, Y. and Akazawa, T. (1969). Enzymic mechanism of starch breakdown in germinating rice seeds II. Scutellum as the site of sucrose synthesis. *Plant Physiology* **44**, 765–769.

Odell, J. T., Nagy, F. and Chua, N. H. (1985). Identification of DNA sequences required for activity of the cauliflower mosaic virus 35S promoter. *Nature* **313**, 810–812.

Oelkers, K., Goffard, N., Weiller, G. F., Gresshoff, P. M., Mathesius, U. and Frickey, T. (2008). Bioinformatic analysis of the CLE signaling peptide family. *BMC Plant Biology* **8**, 1.

Ogawa, M., Shinohara, H., Sakagami, Y. and Matsubayashi, Y. (2008). Arabidopsis CLV3 peptide directly binds CLV1 ectodomain. *Science* **319**, 294.

Ohyama, K., Ogawa, M. and Matsubayashi, Y. (2008). Identification of a biologically active, small, secreted peptide in Arabidopsis by in silico gene screening, followed by LC-MS-based structure analysis. *The Plant Journal* **55**, 152–160.

Ohyama, K., Shinohara, H., Ogawa-Ohnishi, M. and Matsubayashi, Y. (2009). A glycopeptide regulating stem cell fate in Arabidopsis thaliana. *Nature Chemical Biology* **5**, 578–580.

Okuda, S., Suzuki, T., Kanaoka, M. M., Mori, H., Sasaki, N. and Higashiyama, T. (2013). Acquisition of LURE-binding activity at the pollen tube tip of Torenia fournieri. *Molecular Plant* **6**, 1074–1090.

Okuda, S., Tsutsui, H., Shiina, K., Sprunck, S., Takeuchi, H., Yui, R., Kasahara, R. D., Hamamura, Y., Mizukami, A., Susaki, D., Kawano, N., Sakakibara, T., Namiki, S., Itoh, K., Otsuka, K., Matsuzaki, M., Nozaki, H., Kuroiwa, T., Nakano, A., Kanaoka, M. M., Dresselhaus, T., Sasaki, N. and Higashiyama, T. (2009). Defensin-like polypeptide LUREs are pollen tube attractants secreted from synergid cells. *Nature* **458**, 357–361.

Olsen, A. N., Mundy, J. and Skriver, K. (2002). Peptomics, identification of novel cationic Arabidopsis peptides with conserved sequence motifs. *In Silico Biology* **2**, 441–451.

Oltmanns, H., Frame, B., Lee, L.-Y., Johnson, S., Li, B., Wang, K. and Gelvin, S. B. (2010). Generation of backbone-free, low transgene copy plants by launching T-DNA from the Agrobacterium chromosome. *Plant Physiology* **152**, 1158–1166.

Onda, Y. (2013). Oxidative protein-folding systems in plant cells. *International Journal of Cell Biology* **2013**, 585431.

O'Reilly, David R.; Miller, Lois; Luckow, Verne A. (1992). Baculovirus expression vectors. A laboratory manual. W.H. Freeman.

Oyama, T., Sykes, K. F., Samli, K. N., Minna, J. D., Johnston, S. A. and Brown, K. C. (2003). Isolation of lung tumor specific peptides from a random peptide library: generation of diagnostic and cell-targeting reagents. *Cancer Letters* **202**, 219–230.

Palanivelu, R., Brass, L., Edlund, A. F. and Preuss, D. (2003). Pollen tube growth and guidance is regulated by POP2, an Arabidopsis gene that controls GABA levels. *Cell* **114**, 47–59.

Palanivelu, R. and Preuss, D. (2006). Distinct short-range ovule signals attract or repel Arabidopsis thaliana pollen tubes in vitro. *BMC Plant Biology* **6**, 7.

Palanivelu, R. and Tsukamoto, T. (2012). Pathfinding in angiosperm reproduction: pollen tube guidance by pistils ensures successful double fertilization. *Wiley Interdisciplinary Reviews Developmental biology* **1**, 96–113.

Pallotta, M. A., Graham, R. D., Langridge, P., Sparrow, D. H. and Barker, S. J. (2000). RFLP mapping of manganese efficiency in barley. *Theoretical and Applied Genetics* **101**, 1100–1108.

Pang, S. Z., DeBoer, D. L., Wan, Y., Ye, G., Layton, J. G., Neher, M. K., Armstrong, C. L., Fry, J. E., Hinchee, M. A. and Fromm, M. E. (1996). An improved green fluorescent protein gene as a vital marker in plants. *Plant Physiology* **112**, 893–900.

Park, A. R., Cho, S. K., Yun, U. J., Jin, M. Y., Lee, S. H., Sachetto-Martins, G. and Park, O. K. (2001). Interaction of the Arabidopsis receptor protein kinase Wak1 with a glycine-rich protein, AtGRP-3. *The Journal of Biological Chemistry* **276**, 26688–26693.

Park, C. J., Park, C. B., Hong, S. S., Lee, H. S., Lee, S. Y. and Kim, S. C. (2000). Characterization and cDNA cloning of two glycine- and histidine-rich antimicrobial peptides from the roots of shepherd's purse, Capsella bursa-pastoris. *Plant Molecular Biology* **44**, 187–197.

Parker, C. E., Mocanu, V., Mocanu, M., Dicheva, N. and Warren, M. R. (2010). Mass spectrometry for post-translational modifications. In: Alzate, O.: *Neuroproteomics*, Chapter 6. Taylor & Francis.

Parker, R. and Sheth, U. (2007). P bodies and the control of mRNA translation and degradation. *Molecular Cell* **25**, 635–646.

Pearce, G., Moura, D. S., Stratmann, J. and Ryan, C. A. (2001). RALF, a 5-kDa ubiquitous polypeptide in plants, arrests root growth and development. *Proceedings of the National Academy of Sciences of the United States of America* **98**, 12843–12847.

Pearson, W. R. (2013). An introduction to sequence similarity ("homology") searching. *Current Protocols in Bioinformatics* **Unit 3.1**.

Petersen, T. N., Brunak, S., Heijne, G. von and Nielsen, H. (2011). SignalP 4.0: discriminating signal peptides from transmembrane regions. *Nature Methods* **8**, 785–786.

Petrotchenko, E. V. and Borchers, C. H. (2010). Crosslinking combined with mass spectrometry for structural proteomics. *Mass Spectrometry Reviews* **29**, 862–876.

Philippar, K., Büchsenschutz, K., Abshagen, M., Fuchs, I., Geiger, D., Lacombe, B. and Hedrich, R. (2003). The K+ channel KZM1 mediates potassium uptake into the phloem and guard cells of the C4 grass Zea mays. *The Journal of Biological Chemistry* **278**, 16973–16981.

Piccolo, S., Agius, E., Leyns, L., Bhattacharyya, S., Grunz, H., Bouwmeester, T. and De Robertis, E. M. (1999). The head inducer Cerberus is a multifunctional antagonist of Nodal, BMP and Wnt signals. *Nature* **397**, 707–710.

Punwani, J. A. and Drews, G. N. (2008). Development and function of the synergid cell. *Sexual Plant Reproduction* **21**, 7–15.

Qin, Y., Leydon, A. R., Manziello, A., Pandey, R., Mount, D., Denic, S., Vasic, B., Johnson, M. A. and Palanivelu, R. (2009). Penetration of the stigma and style elicits a novel transcriptome in pollen tubes, pointing to genes critical for growth in a pistil. *PLoS Genetics* **5**, e1000621.

Qin, Y., Wysocki, R. J., Somogyi, A., Feinstein, Y., Franco, J. Y., Tsukamoto, T., Dunatunga, D., Levy, C., Smith, S., Simpson, R., Gang, D., Johnson, M. A. and Palanivelu, R. (2011). Sulfinylated azadecalins act as functional mimics of a pollen germination stimulant in Arabidopsis pistils. *The Plant Journal* **68**, 800–815.

Qin, Y. and Yang, Z. (2011). Rapid tip growth: insights from pollen tubes. *Seminars in Cell & Developmental Biology* **22**, 816–824.

Qu, L.-J., Li, L., Lan, Z. and Dresselhaus, T. (2015). Peptide signalling during the pollen tube journey and double fertilization. *Journal of Experimental Botany*, erv275.

Quilichini, T. D., Grienenberger, E. and Douglas, C. J. (2015). The biosynthesis, composition and assembly of the outer pollen wall: A tough case to crack. *Phytochemistry* **113**, 170–182.

Quintero-Hernández, V., Jiménez-Vargas, J. M., Gurrola, G. B., Valdivia, H. H. and Possani, L. D. (2013). Scorpion venom components that affect ion-channels function. *Toxicon* **76**, 328–342.

Rajesh, S., Knowles, T. and Overduin, M. (2011). Production of membrane proteins without cells or detergents. *New Biotechnology* **28**, 250–254.

Randolph, L. F. (1936). Developmental morphology of the caryopsis in maize. *Journal of Agricultural Research* **53**, 881–916.

Ray, S. M., Park, S. S. and Ray, A. (1997). Pollen tube guidance by the female gametophyte. *Development* **124**, 2489–2498.

Reiser, L. and Fischer, R. L. (1993). The ovule and the embryo sac. *The Plant Cell* **5**, 1291–1301.

Reyes, F. C., Buono, R. and Otegui, M. S. (2011). Plant endosomal trafficking pathways. *Current Opinion in Plant Biology* **14**, 666–673.

Roberts, I., Smith, S., de Rybel, B., Van Den Broeke, J., Smet, W., de Cokere, S., Mispelaere, M., de Smet, I. and Beeckman, T. (2013). The CEP family in land plants: evolutionary analyses, expression studies, and role in Arabidopsis shoot development. *Journal of Experimental Botany* **64**, 5371–5381.

Roberts, R. W. and Szostak, J. W. (1997). RNA-peptide fusions for the in vitro selection of peptides and proteins. *Proceedings of the National Academy of Sciences of the United States of America* **94**, 12297–12302.

Rogl, H., Kosemund, K., Kühlbrandt, W. and Collinson, I. (1998). Refolding of Escherichia coli produced membrane protein inclusion bodies immobilized by nickel chelating chromatography. *FEBS Letters* **432**, 21–26.

Rosano, G. L. and Ceccarelli, E. A. (2014). Recombinant protein expression in Escherichia coli: advances and challenges. *Frontiers in Microbiology* **5**, 172.

Rudd, P. M. and Dwek, R. A. (1997). Glycosylation: Heterogeneity and the 3D structure of proteins. *Critical Reviews in Biochemistry and Molecular Biology* **32**, 1–100.

Rymerson, R. T., Menassa, R. and Brandle J. E. (2002). Tobacco, a platform for the production of recombinant proteins. In: Erickson, L., Yu, W.-J., Brandle J. E. and Rymerson, R. T.: *Molecular farming of plants and animals for human and veterinary medicine*, 1–31. Springer Netherlands.

Ryser, U., Schorderet, M., Guyot, R. and Keller, B. (2004). A new structural element containing glycine-rich proteins and rhamnogalacturonan I in the protoxylem of seed plants. *Journal of Cell Science* **117**, 1179–1190.

Sachetto-Martins, G., Franco, L. O. and de Oliveira, D. E. (2000). Plant glycine-rich proteins: a family or just proteins with a common motif? *Biochimica et Biophysica Acta* **1492**, 1–14.

Sambrook, Joseph; Russell, David W. (2001). Molecular cloning. A laboratory manual 3rd edt. Cold Spring Harbor Laboratory Press.

Sargant, E. and Robertson, A. (1905). The anatomy of the scutellum in Zea mays. *Annals of Botany* **19**, 115–124.

Schägger, H. and Jagow, G. von (1987). Tricine-sodium dodecyl sulfate-polyacrylamide gel electrophoresis for the separation of proteins in the range from 1 to 100 kDa. *Analytical Biochemistry* **166**, 368–379.

Scheres, B., van Engelen, F., van der Knaap, E., van de Wiel, C., van Kammen, A. and Bisseling, T. (1990). Sequential induction of nodulin gene expression in the developing pea nodule. *The Plant Cell* **2**, 687–700.

Schnable, J. C., Freeling, M. and Lyons, E. (2012). Genome-wide analysis of syntenic gene deletion in the grasses. *Genome Biology and Evolution* **4**, 265–277.

Schreiber, D. N., Bantin, J. and Dresselhaus, T. (2004). The MADS box transcription factor ZmMADS2 is required for anther and pollen maturation in maize and accumulates in apoptotic bodies during anther dehiscence. *Plant Physiology* **134**, 1069–1079.

Schreiber, D. N. and Dresselhaus, T. (2003). Optimization of in vitro pollen germination and transient transformation of maize pollen and other species. *Plant Molecular Biology Reporter* **21**, 31–41.

Schwarz, F. and Aebi, M. (2011). Mechanisms and principles of N-linked protein glycosylation. *Current Opinion in Structural Biology* **21**, 576–582.

Seifert, T. B., Bleiweis, A. S. and Brady, J. L. (2004). Contribution of the alanine-rich region of Streptococcus mutans P1 to antigenicity, surface expression and interaction with the proline-rich repeat domain. *Infection and Immunity* **72**, 4699–4706.

Sekhon, R. S., Lin, H., Childs, K. L., Hansey, C. N., Buell, C. R., Leon, N. de and Kaeppler, S. M. (2011). Genome-wide atlas of transcription during maize development. *The Plant Journal* **66**, 553–563.

Sheridan, W. F. (1982). Black Mexican sweet corn: its uses for tissue cultures. In: Sheridan, W. F.: *Maize for biological research*, 385–388. Plant Molecular Biology Association.

Shimizu, K. K. and Okada, K. (2000). Attractive and repulsive interactions between female and male gametophytes in Arabidopsis pollen tube guidance. *Development* **127**, 4511–4518.

Shinoda, K., Yamaguchi, T. and Hori, R. (1961). The surface tension and the critical micelle concentration in aqueous solution of beta-D-alkyl glucosides and their mixtures. *Bulletin of the Chemical Society of Japan* **34**, 237–241.

Shinya, T., Osada, T., Desaki, Y., Hatamoto, M., Yamanaka, Y., Hirano, H., Takai, R., Che, F.-S., Kaku, H. and Shibuya, N. (2010). Characterization of receptor proteins using affinity cross-linking with biotinylated ligands. *Plant & Cell Physiology* **51**, 262–270.

Shiu, S. H. and Bleecker, A. B. (2001). Receptor-like kinases from Arabidopsis form a monophyletic gene family related to animal receptor kinases. *Proceedings of the National Academy of Sciences of the United States of America* **98**, 10763–10768.

Silverstein, K. A. T., Moskal, W. A., Wu, H. C., Underwood, B. A., Graham, M. A., Town, C. D. and VandenBosch, K. A. (2007). Small cysteine-rich peptides resembling antimicrobial peptides have been under-predicted in plants. *The Plant Journal* **51**, 262–280.

Simon, R. and Dresselhaus, T. (2015). Peptides take centre stage in plant signalling. *Journal of Experimental Botany* **66**, 5135–5138.

Sinz, A. (2006). Chemical cross-linking and mass spectrometry to map three-dimensional protein structures and protein-protein interactions. *Mass Spectrometry Reviews* **25**, 663–682.

Smith, D. B. and Johnson, K. S. (1988). Single-step purification of polypeptides expressed in Escherichia coli as fusions with glutathione S-transferase. *Gene* **67**, 31–40.

Solís, M.-T., Chakrabarti, N., Corredor, E., Cortés-Eslava, J., Rodríguez-Serrano, M., Biggiogera, M., Risueño, M. C. and Testillano, P. S. (2014). Epigenetic changes accompany developmental programmed cell death in tapetum cells. *Plant & Cell Physiology* **55**, 16–29.

Song, X., Zhang, M., Zhou, Z. and Gong, W. (2011). Ultra-high resolution crystal structure of a dimeric defensin SPE10. *FEBS Letters* **585**, 300–306.

Sparkes, I. A., Runions, J., Kearns, A. and Hawes, C. (2006). Rapid, transient expression of fluorescent fusion proteins in tobacco plants and generation of stably transformed plants. *Nature Protocols* **1**, 2019–2025.

Spelbrink, R. G., Dilmac, N., Allen, A., Smith, T. J., Shah, D. M. and Hockerman, G. H. (2004). Differential antifungal and calcium channel-blocking activity among structurally related plant defensins. *Plant Physiology* **135**, 2055–2067.

Springer, P. S., Zimmer, E. A. and Bennetzen, J. L. (1989). Genomic organization of the ribosomal DNA of sorghum and its close relatives. *Theoretical and Applied Genetics* **77**, 844–850.

Sprunck, S., Rademacher, S., Vogler, F., Gheyselinck, J., Grossniklaus, U. and Dresselhaus, T. (2012). Egg cell-secreted EC1 triggers sperm cell activation during double fertilization. *Science* **338**, 1093–1097.

Stadler, R. and Sauer, N. (1996). The Arabidopsis thaliana AtSUC2 gene is specifically expressed in companion cells. *Plant Biology* **109**, 299–306.

Stahl, Y., Wink, R. H., Ingram, G. C. and Simon, R. (2009). A signaling module controlling the stem cell niche in Arabidopsis root meristems. *Current Biology* **19**, 909–914.

Steffen, J. G., Kang, I.-H., Macfarlane, J. and Drews, G. N. (2007). Identification of genes expressed in the Arabidopsis female gametophyte. *The Plant Journal* **51**, 281–292.

Steu, S., Baucamp, M., Dach, G. von, Bawohl, M., Dettwiler, S., Storz, M., Moch, H. and Schraml, P. (2008). A procedure for tissue freezing and processing applicable to both intra-operative frozen section diagnosis and tissue banking in surgical pathology. *Virchows Archiv* **452**, 305–312.

Streitner, C., Danisman, S., Wehrle, F., Schöning, J. C., Alfano, J. R. and Staiger, D. (2008). The small glycine-rich RNA binding protein AtGRP7 promotes floral transition in Arabidopsis thaliana. *The Plant Journal* **56**, 239–250.

Stynen, B., Tournu, H., Tavernier, J. and van Dijck, P. (2012). Diversity in genetic in vivo methods for protein-protein interaction studies: from the yeast two-hybrid system to the mammalian split-luciferase system. *Microbiology and Molecular Biology Reviews* **76**, 331–382.

Suzuki, G., Kai, N., Hirose, T., Fukui, K., Nishio, T., Takayama, S., Isogai, A., Watanabe, M. and Hinata, K. (1999). Genomic organization of the S locus: Identification and characterization of genes in SLG/SRK region of S(9) haplotype of Brassica campestris (syn. rapa). *Genetics* **153**, 391–400.

Swartz, K. J. and MacKinnon, R. (1997). Hanatoxin modifies the gating of a voltage-dependent K+ channel through multiple binding sites. *Neuron* **18**, 665–673.

Takai, R., Isogai, A., Takayama, S. and Che, F.-S. (2008). Analysis of flagellin perception mediated by flg22 receptor OsFLS2 in rice. *Molecular Plant-Microbe Interactions* **21**, 1635–1642.

Takayama, S., Shiba, H., Iwano, M., Shimosato, H., Che, F. S., Kai, N., Watanabe, M., Suzuki, G., Hinata, K. and Isogai, A. (2000). The pollen determinant of self-incompatibility in Brassica campestris. *Proceedings of the National Academy of Sciences of the United States of America* **97**, 1920–1925.

Takayama, S., Shimosato, H., Shiba, H., Funato, M., Che, F. S., Watanabe, M., Iwano, M. and Isogai, A. (2001). Direct ligand-receptor complex interaction controls Brassica self-incompatibility. *Nature* **413**, 534–538.

Takeuchi, H. and Higashiyama, T. (2012). A species-specific cluster of defensin-like genes encodes diffusible pollen tube attractants in Arabidopsis. *PLoS Biology* **10**, e1001449.

Tang, W., Ezcurra, I., Muschietti, J. and McCormick, S. (2002). A cysteine-rich extracellular protein, LAT52, interacts with the extracellular domain of the pollen receptor kinase LePRK2. *The Plant Cell* **14**, 2277–2287.

Tang, W., Kelley, D., Ezcurra, I., Cotter, R. and McCormick, S. (2004). LeSTIG1, an extracellular binding partner for the pollen receptor kinases LePRK1 and LePRK2, promotes pollen tube growth in vitro. *The Plant Journal* **39**, 343–353.

Tao, H., Liu, W., Simmons, B. N., Harris, H. K., Cox, T. C. and Massiah, M. A. (2010). Purifying natively folded proteins from inclusion bodies using sarkosyl, Triton X-100, and CHAPS. *BioTechniques* **48**, 61–64.

Tessier, D. C., Thomas, D. Y., Khouri, H. E., Laliberté, F. and Vernet, T. (1991). Enhanced secretion from insect cells of a foreign protein fused to the honeybee melittin signal peptide. *Gene* **98**, 177–183.

The UniProt Consortium (2015). UniProt: a hub for protein information. *Nucleic Acids Research* **43**, D204-12.

Theillet, F.-X., Smet-Nocca, C., Liokatis, S., Thongwichian, R., Kosten, J., Yoon, M.-K., Kriwacki, R. W., Landrieu, I., Lippens, G. and Selenko, P. (2012). Cell signaling, post-translational protein modifications and NMR spectroscopy. *Journal of Biomolecular NMR* **54**, 217–236.

Timasheff, S. N. (1998). Control of protein stability and reactions by weakly interacting cosolvents: the simplicity of the complicated. *Advances in Protein Chemistry* **51**, 355–432.

Tomomura, M., Kadomatsu, K., Nakamoto, M., Muramatsu, H., Kondoh, H., Imagawa, K. and Muramatsu, T. (1990). A retinoic acid responsive gene, MK, produces a secreted protein with heparin binding activity. *Biochemical and Biophysical Research Communications* **171**, 603–609.

Truong, K. and Ikura, M. (2001). The use of FRET imaging microscopy to detect protein-protein interactions and protein conformational changes in vivo. *Current Opinion in Structural Biology* **11**, 573–578.

Tsuwamoto, R., Fukuoka, H. and Takahata, Y. (2008). GASSHO1 and GASSHO2 encoding a putative leucine-rich repeat transmembrane-type receptor kinase are essential for the normal development of the epidermal surface in Arabidopsis embryos. *The Plant Journal* **54**, 30–42.

Uebler, S. and Dresselhaus, T. (2014). Identifying plant cell-surface receptors: combining "classical" techniques with novel methods. *Biochemical Society Transactions* **42**, 395–400.

Uebler, S., Dresselhaus, T. and Márton, M.-L. (2013). Species-specific interaction of EA1 with the maize pollen tube apex. *Plant Signaling & Behavior* **8**, e25682.

Uebler, S., Márton, M. L. and Dresselhaus, T. (under review). Classification of EA1-box proteins and new insights into their role during reproduction in grasses.

Ueki, S. and Citovsky, V. (2005). Identification of an interactor of cadmium ion-induced glycine-rich protein involved in regulation of callose levels in plant vasculature. *Proceedings of the National Academy of Sciences of the United States of America* **102**, 12089–12094.

Unal, E. S., Zhao, R., Qiu, A. and Goldman, I. D. (2008). N-linked glycosylation and its impact on the electrophoretic mobility and function of the human proton-coupled folate transporter (HsPCFT). *Biochimica et Biophysica Acta* **1778**, 1407–1414.

Urech, D. M., Lichtlen, P. and Barberis, A. (2003). Cell growth selection system to detect extracellular and transmembrane protein interactions. *Biochimica et Biophysica Acta* **1622**, 117–127.

Urwin, P., Yi, L., Martin, H., Atkinson, H. and Gilmartin, P. M. (2000). Functional characterization of the EMCV IRES in plants. *The Plant Journal* **24**, 583–589.

Vabulas, R. M., Raychaudhuri, S., Hayer-Hartl, M. and Hartl, F. U. (2010). Protein folding in the cytoplasm and the heat shock response. *Cold Spring Harbor Perspectives in Biology* **2**, a004390.

van der Wijk, T., Overvoorde, J. and den Hertog, J. (2004). H2O2-induced intermolecular disulfide bond formation between receptor protein-tyrosine phosphatases. *The Journal of Biological Chemistry* **279**, 44355–44361.

Vanstraelen, M. and Benková, E. (2012). Hormonal interactions in the regulation of plant development. *Annual Review of Cell and Developmental Biology* **28**, 463–487.

Vernoud, V., Hajduch, M., Khaled, A. S., Depège, N. and Rogowsky, P. M. (2005). Maize embryogenesis. *Maydica* **50**, 469–483.

Vogler, F., Schmalzl, C., Englhart, M., Bircheneder, M. and Sprunck, S. (2014). Brassinosteroids promote Arabidopsis pollen germination and growth. *Plant Reproduction* **27**, 153–167.

Voinnet, O., Rivas, S., Mestre, P. and Baulcombe, D. (2003). An enhanced transient expression system in plants based on suppression of gene silencing by the p19 protein of tomato bushy stunt virus. *The Plant Journal* **33**, 949–956.

Vollbrecht, E. and Schmidt, R. J. (2009). Development of the inflorescences. In: Bennetzen, J. L. and Hake, S.: *Handbook of maize - It's biology*, 13–40. Springer.

Wagner, S., Klepsch, M. M., Schlegel, S., Appel, A., Draheim, R., Tarry, M., Högbom, M., van Wijk, K. J., Slotboom, D. J., Persson, J. O. and de Gier, J. W. (2008). Tuning Escherichia coli for membrane protein overexpression. *Proceedings of the National Academy of Sciences of the United States of America* **105**, 14371–14376.

Walter, M., Chaban, C., Schütze, K., Batistic, O., Weckermann, K., Näke, C., Blazevic, D., Grefen, C., Schumacher, K., Oecking, C., Harter, K. and Kudla, J. (2004). Visualization of protein interactions in living plant cells using bimolecular fluorescence complementation. *The Plant Journal* **40**, 428–438.

Wang, G. and Fiers, M. (2010). CLE peptide signaling during plant development. *Protoplasma* **240**, 33–43.

Webb, J. N., Webb, S. D., Cleland, J. L., Carpenter, J. F. and Randolph, T. W. (2001). Partial molar volume, surface area, and hydration changes for equilibrium unfolding and formation of aggregation transition state: high-pressure and cosolute studies on recombinant human IFN-gamma. *Proceedings of the National Academy of Sciences of the United States of America* **98**, 7259–7264.

Welinder, K. G. and Tams, J. W. (1995). Effects of glycosylation on protein folding, stability and solubility. Studies of chemically modified or engineered plant and fungal peroxidases. *Progress in Biotechnology* **10**, 205–210.

Wengier, D. L., Mazzella, M. A., Salem, T. M., McCormick, S. and Muschietti, J. P. (2010). STIL, a peculiar molecule from styles, specifically dephosphorylates the pollen receptor kinase LePRK2 and stimulates pollen tube growth in vitro. *BMC Plant Biology* **10**, 33.

Went, F. W.; Thimann, Kenneth Vivian (1937). Phytohormones. The Macmillan Company.

Wheeler, M. J., de Graaf, B. H., Hadjiosif, N., Perry, R. M., Poulter, N. S., Osman, K., Vatovec, S., Harper, A., Franklin, F. C. and Franklin-Tong, V. E. (2009). Identifi-

cation of the pollen self-incompatibility determinant in Papaver rhoeas. *Nature* **459**, 992–995.

Wollscheid, B., Bausch-Fluck, D., Henderson, C., O'Brien, R., Bibel, M., Schiess, R., Aebersold, R. and Watts, J. D. (2009). Mass-spectrometric identification and relative quantification of N-linked cell surface glycoproteins. *Nature Biotechnology* **27**, 378–386.

Woolaway, K. E., Lazaridis, K., Belsham, G. J., Carter, M. J. and Roberts, L. O. (2001). The 5' untranslated region of Rhopalosiphum padi virus contains an internal ribosome entry site which functions efficiently in mammalian, plant, and insect translation systems. *Journal of Virology* **75**, 10244–10249.

Wopereis, S., Lefeber, D. J., Morava, E. and Wevers, R. A. (2006). Mechanisms in protein O-glycan biosynthesis and clinical and molecular aspects of protein O-glycan biosynthesis defects: a review. *Clinical Chemistry* **52**, 574–600.

Woriedh, M., Merkl, R. and Dresselhaus, T. (2015). Maize EMBRYO SAC family peptides interact differentially with pollen tubes and fungal cells. *Journal of Experimental Botany*.

Wu, H.-M., Wong, E., Ogdahl, J. and Cheung, A. Y. (2000). A pollen tube growth-promoting arabinogalactan protein from Nicotiana alata is similar to the tobacco TTS protein. *The Plant Journal* **22**, 165–176.

Yalak, G. and Vogel, V. (2012). Extracellular phosphorylation and phosphorylated proteins: not just curiosities but physiologically important. *Science signaling* **5**, re7.

Yamaguchi, Y., Pearce, G. and Ryan, C. A. (2006). The cell surface leucine-rich repeat receptor for AtPep1, an endogenous peptide elicitor in Arabidopsis, is functional in transgenic tobacco cells. *Proceedings of the National Academy of Sciences of the United States of America* **103**, 10104–10109.

Yang, S.-L., Xie, L.-F., Mao, H.-Z., Puah, C. S., Yang, W.-C., Jiang, L., Sundaresan, V. and Ye, D. (2003). Tapetum determinant1 is required for cell specialization in the Arabidopsis anther. *The Plant Cell* **15**, 2792–2804.

Yang, Y.-S., Wang, C.-C., Chen, B.-H., Hou, Y.-H., Hung, K.-S. and Mao, Y.-C. (2015). Tyrosine sulfation as a protein post-translational modification. *Molecules* **20**, 2138–2164.

Yarden, Y. (2001). Biology of HER2 and its importance in breast cancer. *Oncology* **61 Suppl 2**, 1–13.

Yount, N. Y. and Yeaman, M. R. (2004). Multidimensional signatures in antimicrobial peptides. *Proceedings of the National Academy of Sciences of the United States of America* **101**, 7363–7368.

Yu, G.-H., Zou, J., Feng, J., Peng, X.-B., Wu, J.-Y., Wu, Y.-L., Palanivelu, R. and Sun, M.-X. (2014). Exogenous γ-aminobutyric acid (GABA) affects pollen tube growth via modulating putative Ca2+-permeable membrane channels and is coupled to negative regulation on glutamate decarboxylase. *Journal of Experimental Botany* **65**, 3235–3248.

Zardeneta, G. and Horowitz, P. M. (1992). Micelle-assisted protein folding. Denatured rhodanese binding to cardiolipin-containing lauryl maltoside micelles results in slower refolding kinetics but greater enzyme reactivation. *The Journal of Biological Chemistry* **267**, 5811–5816.

Zhao, D.-Z., Wang, G.-F., Speal, B. and Ma, H. (2002). The excess microsporocytes1 gene encodes a putative leucine-rich repeat receptor protein kinase that controls somatic and reproductive cell fates in the Arabidopsis anther. *Genes & Development* **16**, 2021–2031.

Zhou, L., Lan, W., Chen, B., Fang, W. and Luan, S. (2015). A calcium sensor-regulated protein kinase, CALCINEURIN B-LIKE PROTEIN-INTERACTING PROTEIN KINASE19, is required for pollen tube growth and polarity. *Plant Physiology* **167**, 1351–1360.

Zhou, X., Chang, Y.-C., Oyama, T., McGuire, M. J. and Brown, K. C. (2004). Cell-specific delivery of a chemotherapeutic to lung cancer cells. *Journal of the American Chemical Society* **126**, 15656–15657.

SUPPLEMENTARY MATERIAL

Genomic locations of EA1-box proteins

Supplement table 1 Genomic location of EA1-box proteins in different plant species.

Organism	Gene	Gene annotation	Chromosome location
Zea mays	*ZmEA1*	GRMZM2G456746	7: 164,503,140-164,503,655 reverse strand
	ZmEAL1		7: 164,505,108-164,505,816 forward strand
	ZmEAL1s		7: 164,507,585-164,507,837 forward strand
	ZmEAL2	GRMZM2G157505	7: 164,496,101-164,496,944 forward strand
	ZmEAG1a	GRMZM2G376674	8: 142,620,971-142,621,675 reverse strand
	ZmEAG1b	GRMZM2G075386	8: 142,651,683-142,652,309 reverse strand
	ZmEAG1c	GRMZM2G466856	8: 142,674,230-142,674,735 forward strand
	ZmEAG1d	GRMZM2G466848	8: 142,685,364-142,685,853 forward strand
	ZmEAG2	AC185611.3_FG001	1: 206,839,158-206,839,481 forward strand
	ZmEAC1	GRMZM5G849499	2: 211,059,193-211,060,310 reverse strand
	ZmEAC2	GRMZM2G435049	9: 123,261,233-123,262,209 forward strand
	ZmEAC3	GRMZM2G180950	2: 211,058,013-211,058,620 reverse strand
Sorghum bicolor	*SbEAL1*	Sb02g038810	2: 72,980,812-72,981,372 forward strand
	SbEAL2	Sb09g003110	9: 3,517,149-3,517,703 forward strand
	SbEAG1	Sb10g029350	10: 59,167,727-59,168,077 reverse strand
	SbEAC1	Sb02g038790	2: 72,970,764-72,972,049 forward strand
	SbEAC2	Sb01g032560	1: 55,447,215-55,447,868 forward strand
	SbEAC3	Sb02g038800	2: 72,973,061-72,973,534 forward strand
Oryza sativa Japonica	*OsEAL1*	OS07T0605900	7: 24,849,688-24,850,036 reverse strand
	OsEAL2	OS07T0605400	7: 24,809,650-24,810,354 forward strand
	OsEAL3	OS07T0605350	7: 24,805,571-24,805,912 forward strand
	OsEAG1	OS06T0706700	6: 29,871,368-29,871,718 reverse strand
	OsEAC1	Os03g0414100	3: 17,143,001-17,144,403 reverse strand
	OsEAC2	Os01g0340600	1: 13,396,264-13,397,109 reverse strand
	OsEAC3	Os01g0341200	1: 13,437,009-13,438,567 reverse strand
	OsEAC4	Os01g0341000	1: 13,422,910-13,424,625 reverse strand
	OsEAC5a	Os12g0575300	12: 23,739,977-23,740,564 reverse strand
	OsEAC5b	Os12g0575400	12: 23,750,068-23,750,655 reverse strand
	OsEAC5c	Os12g0576100	12: 23,782,933-23,783,505 reverse strand
Brachypodium distachyon	*BdEAL1*	BRADI1G21960	1: 17,624,930-17,625,160 reverse strand
	BdEAL2	BRADI1G21950	1: 17,619,462-17,620,094 reverse strand
	BdEAL3	BRADI1G21930	1: 17,612,750-17,612,980 reverse strand
	BdEAL4	LOC100823010	1: 17,674,234-17,674,809 forward strand
	BdEAL5	BRADI1G21970	1: 17,656,205-17,657,090 reverse strand
	BdEAG1	BRADI1G08960	1: 6,337,113-6,337,334 forward strand
	BdEAG2	BRADI1G34640	1: 30,233,938-30,234,459 reverse strand
	BdEAC1	BRADI1G60000	1: 59,144,023-59,144,701 forward strand
Arabidopsis thaliana	*AtEAG1*	AT5G61412	5: 24,686,755-24,687,042 reverse strand
	AtEAG2a	AT2G30560a	2: 13,017,347-13,017,569 forward strand
	AtEAG2b	AT2G30560b	2: 13,018,564-13,018,857 forward strand
	AtEAC1	AT4G33145	4: 15,984,643-15,985,064 reverse strand
	AtEAC2		2: 1,135,932-1,136,152 reverse strand
Arabidopsis lyrata	*AlEAG1*	ARALYDRAFT_685823	8: 20,001,998-20,002,234 reverse strand
	AlEAG2	ARALYDRAFT_668766	4: 14,250,745-14,251,014 forward strand
	AlEAC1	ARALYDRAFT_904655	5: 1,983,286-1,983,556 reverse strand
	AlEAC2	ARALYDRAFT_900363	3: 23,677,781-23,678,024 forward strand
	AlEAC3	ARALYDRAFT_913106	7: 3,385,899-3,386,139 forward strand
Glycine max	*GmEAG1*	GLYMA20G26010	20: 35,594,472-35,594,816 forward strand
	GmEAG2	GLYMA10G41250	10: 48,376,060-48,376,563 reverse strand
	GmEAC1a	GLYMA14G04196	14: 2,816,513-2,816,847 reverse strand
	GmEAC1b	GLYMA14G04235	14: 2,843,344-2,843,538 forward strand
Populus trichocarpa	*PtEAC1*	POPTR_0010s25020	10: 20,905,393-20,905,602 forward strand
	PtEAC2	POPTR_0626s00200	scaffold_626: 4,682-5,229 reverse strand
	PtEAC3	POPTR_0167s00240	scaffold_167: 46,849-47,744 forward strand
	PtEAC4	POPTR_0019s14980	19: 15,605,588-15,606,452 reverse strand
	PtEAC5	POPTR_0167s00200	scaffold_167: 3,293-4,238 forward strand
	PtEAC6	POPTR_0167s00230	scaffold_167: 42,797-43,414 forward strand
	PtEAC7	POPTR_0167s00210	scaffold_167: 8,605-9,226 forward strand
	PtEAC8	POPTR_0019s15010	19: 15,644,147-15,645,038 reverse strand
	PtEAC9	POPTR_0013s15230	13: 15,251,451-15,252,128 reverse strand
	PtEAC10	POPTR_0007s00260	7: 54,504-55,040 reverse strand

Primer sequences

Supplement table 2 Primers used in this study.

Primer name	Sequence
sEA1-fwd	CACCGGGATGATGATGAAGG
EA1-entr-rev	CGAGGATCCGCTAGCGATCGAAC
EAR-GFP	CGAGGATCCCGCTAGCGATCGAAC
1f	CCCCACTAGTATGGAGTACATACGTATCC
1r	CTCGGATCCACACGGCGAAG
2f	CCTCACTAGTCGAGAGCTAGCCATGGTGTC
2r	CTCAGGATCCACGCGGCGGCGG
3f	CCCTACTAGTCTCAAACCTCCAAAATTCT
3r	CTCAGGATCCACTTCTTGCTTTGTC
OsP0493C06-fwd	CGTGCGTACGTAATGTCGTC
OsP0493C06-rev	GTTGAGACCGCGATCGATCG
OsEAL2a-fwd	CTGTCGTTTTGGTTTGCTTAGC
OsEAL2b-rev	CGGATACCATTTCTTCCCTAC
OsEAL3-a(fwd-new)	GACGGAGGGATTATATATGGAG
OsEAL3-b(rev-new)	TCGTCGATTCGTCACGTCAC
GAPnew1	AGGGTCCACTCAAGGGTATCAT
GAPnew2	ACAAGCTTGACGAAGTGGTC
ER I	CCCCCGGGCTGCAGGAATTC
XI	GTACCGGGCCCCCCCTCGAG
MEPfwd	TGTACTCGGCAATGCTCTTG
MEPrev	TTTGATGCTCCAGGCTTACC
LUGfwd	TCCAGTGCTACAGGGAAGGT
LUGrev	GTTAGTTCTTGAGCCCACGC
CULfwd	GAAGAGCCGCAAAGTTATGG
CULrev	ATGGTAGAAGTGGACGCACC
FPGSfwd	ATCTCGTTGGGGATGTCTTG
FPGSrev	AGCACCGTTCAAATGTCTCC
spEAF	CGCGACTAGTATGGGAGCGGCGGTGGCGTT

ZE-GFP2-rev	CCAGGGTATCACCTTCGAAC
EA1-entr	CACCATGTCATCCTGCCC
spEA1-entr	CACCATGGGAGCGGCGGTGGCGTT
oSU17	CACCATGGCCACCGCCACCACTG
oSU19	CGCCAAAGCGGCGACCGC
oSU26	GGGCGGACTAGTATGGGGATGATGATGAAGG
oSU27	CGCGGATCCGCGATCGAACAGGCAGC
oSU38	CACCATGGCTATCACAGCACGG
oSU39	CCGCCGGACGCCAAAAAG
oSU40	CACCATGGCCACCCCCATTGC
oSU41	GTAGAGCATCTTTGCAGCCAAGTAGG
oSU44	TGTGTGACGCTCGTTGGGGA
oSU45	CGAGACTAGTCCTTTTGTTCTTGGG
oSU46	GCTCGTTGGGGAAGAGGGATGAC
oSU47	TAACCACTTGGTCAACATACAACCT
oSU48	CCGGGAATTCCAAGAACAAAAATGGC
oSU49	TACCTGCAGGCACCGCCGGAT
oSU50	CATGAATTCTGCTCGTCTCCCG
oSU51	TACCTGCAGGCTCAACACCAAC
oSU54	CAGTAAGCTTCAAGAACAAAAATGGCC
oSU55	ATTACGCGTCACCGCCGGATC
oSU56	CATAAGCTTTGCTCGTCTCCC
oSU57	TAACGCGTCTCAACACCAACG
oSU99	AGTCTCGACTCTCGAGTTTG
oSU100	GAAACCCACGTACTTTTACGGT
oSU104	CACCATGAAGAGCCGCAGC
oSU105	AGAAGGAGGAGGGGTGCAGG
oSU109	ATGAAGAAAGTGGCATCATCGTC
oSU110	GGAAGGAGGAGGGGTGCAG
oSU113	ATCAGCTCTAACTCTGTCGATAG
oSU117	CTATAGAATTCATGAAGAGCCGCAG

oSU118	ACTAGAGCTCAGAAGGAGGAGG
oSU119	CTATAGAATTCATGAAGAAAGTGGCATC
oSU120	ACTAGAGCTCGGAAGGAGGAGG
oSU121	CTATAGAATTCATGGCCCAAAACAAGC
oSU122	ACTAGAGCTCATCAGCTCTAACTC
oSU123	CTATAGAATTCATGTCATCCTGCCCG
oSU124	ACTAGAGCTCGCTAGCGATC
oSU125	CTATAGAATTCGGGATGATGATGAAGG
oSU126	ATAGAGCTCGCTAGCGATCG
oSU146	GGTTCATTCATTTCAAGGGGCTTCG
oSU147	GGGACGGACCTGGTCGTGTG
oSU148	GTTCTCGCTGAGCAGAGGCT
oSU149	CGCTAGTTTGTGCCCCGCTGA
oSU150	CCCAAGGACGGTTGACTAGGG
oSU151	GTGTGGGTTGCAGAAGGAGCCG
oSU154	CTGTACGGCAGGATCCAGTG
oSU155	AGATGGTTATCGGCTTATCGCA
oSU156	CGCTGATAGCAGAGGCAAAG
oSU157	AGTTCTCGCTGAGCAGAGGC
oSU158	AACGATGTGTGCCAACCCTA
oSU159	TGACTCCACATCACCTCTTCC
oSU175	CGCATGCGATAACCATCTGA
oSU176	GTTCCATCGACGGTATATTTGG

Vector maps

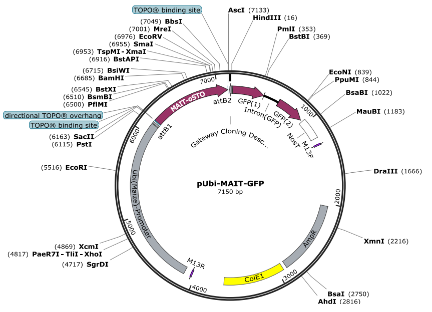
pUbi-MAIT-GFP
7150 bp

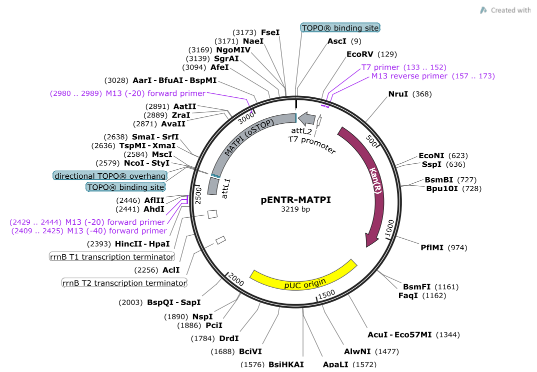
pENTR-MATPI
3219 bp

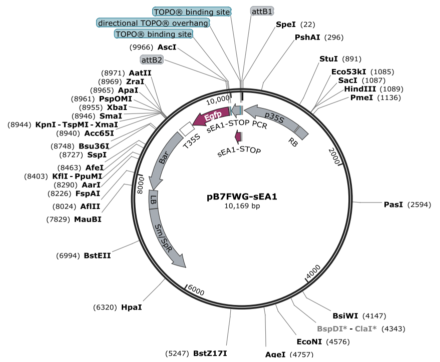
pB7FWG-sEA1
10,169 bp

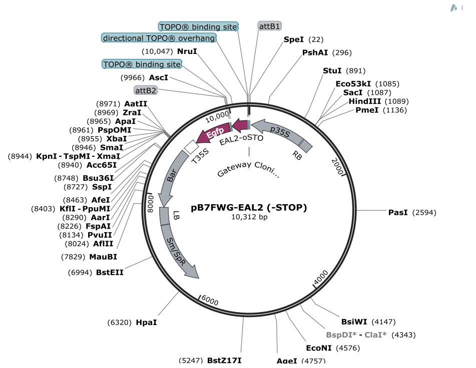
pB7FWG-EAL2 (-STOP)
10,312 bp

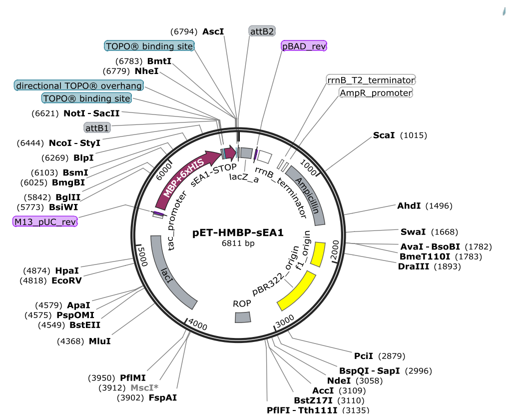
pET-HMBP-sEA1
6811 bp

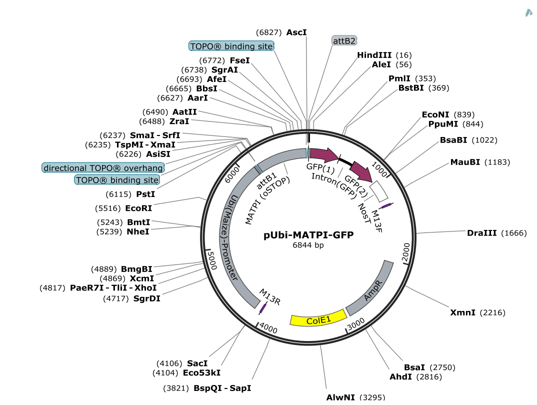
pUbi-MATPI-GFP
6844 bp

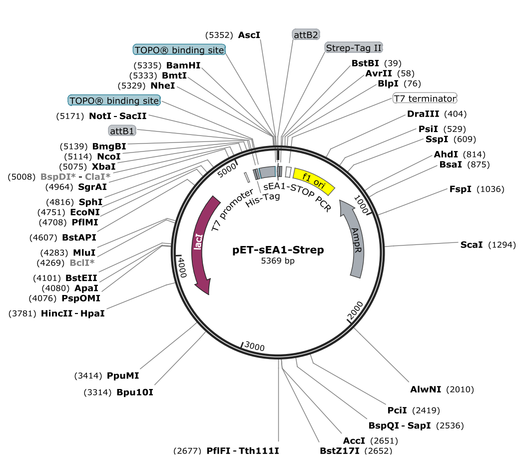
pET-sEA1-Strep
5369 bp

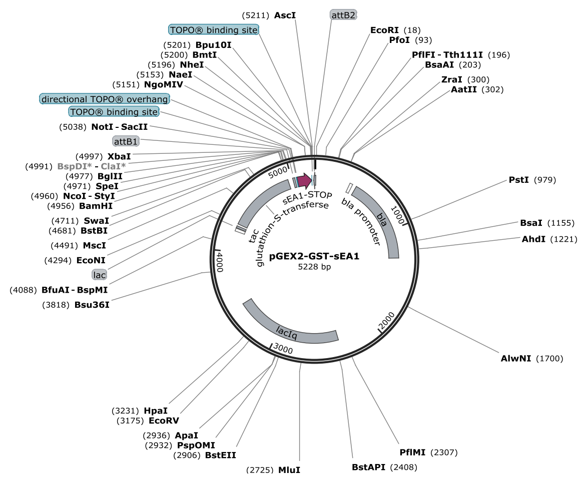
pGEX2-GST-sEA1
5228 bp

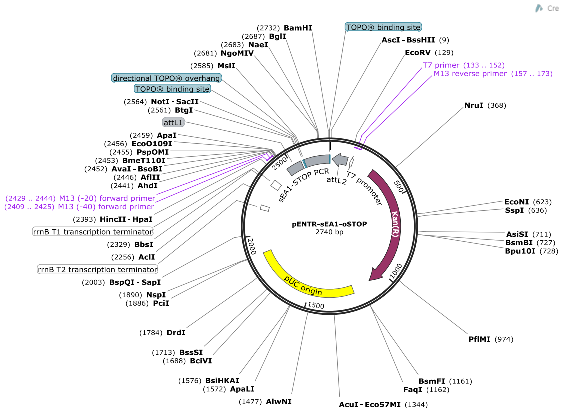
pENTR-sEA1-oSTOP
2740 bp
TOPO binding site
directional TOPO® overhang
TOPO® binding site
attL1
sEA1-STOP PCR
attL2
T7 promoter
Kan(R)
pUC origin
rrnB T1 transcription terminator
rrnB T2 transcription terminator
T7 primer (133 .. 152)
M13 reverse primer (157 .. 173)
(2429 .. 2444) M13 (-20) forward primer
(2409 .. 2425) M13 (-40) forward primer

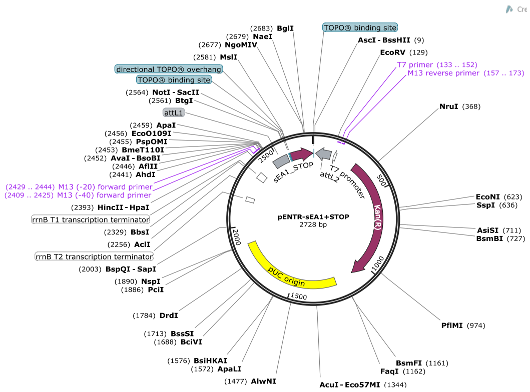
pENTR-sEA1+STOP
2728 bp
TOPO® binding site
directional TOPO® overhang
TOPO® binding site
attL1
sEA1_STOP
attL2
T7 promoter
Kan(R)
pUC origin
rrnB T1 transcription terminator
rrnB T2 transcription terminator
T7 primer (133 .. 152)
M13 reverse primer (157 .. 173)
(2429 .. 2444) M13 (-20) forward primer
(2409 .. 2425) M13 (-40) forward primer

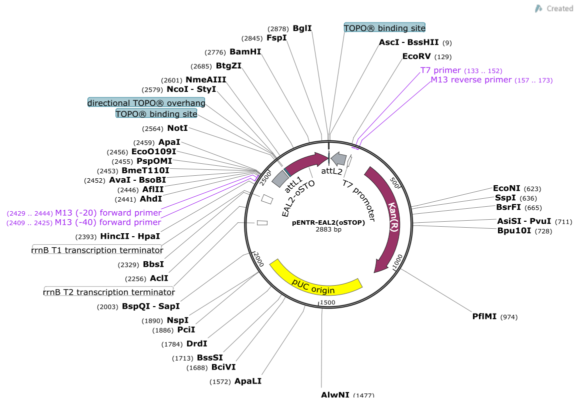
pENTR-EAL2(oSTOP)
2883 bp
TOPO® binding site
directional TOPO® overhang
TOPO® binding site
attL1
EAL2-oSTO
attL2
T7 promoter
Kan(R)
pUC origin
rrnB T1 transcription terminator
rrnB T2 transcription terminator
T7 primer (133 .. 152)
M13 reverse primer (157 .. 173)
(2429 .. 2444) M13 (-20) forward primer
(2409 .. 2425) M13 (-40) forward primer

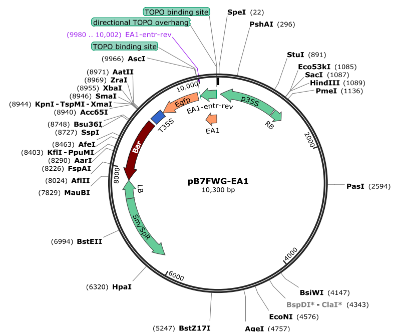
pB7FWG-EA1
10,300 bp
TOPO binding site
directional TOPO overhang
(9980 .. 10,002) EA1-entr-rev
TOPO binding site
Egfp
EA1-entr-rev
EA1
p35S
RB
T35S
Bar
LB
SmSpR

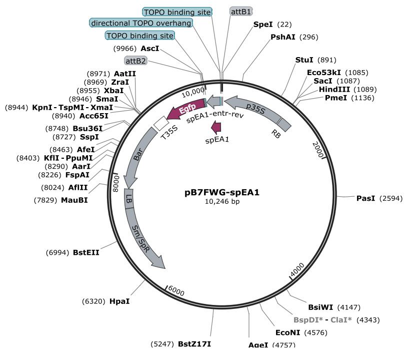
pB7FWG-spEA1
10,246 bp
TOPO binding site
attB1
directional TOPO overhang
TOPO binding site
attB2
Egfp
spEA1-entr-rev
spEA1
p35S
RB
T35S
Bar
LB
SmSpR

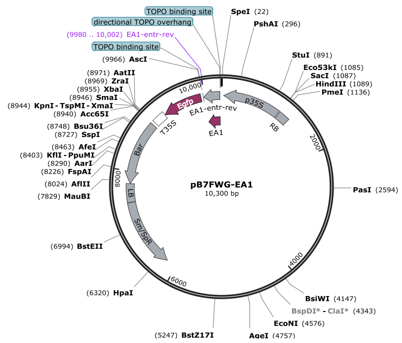
pB7FWG-EA1
10,300 bp
TOPO binding site
directional TOPO overhang
(9980 .. 10,002) EA1-entr-rev
TOPO binding site
Egfp
EA1-entr-rev
EA1
p35S
RB
T35S
Bar
LB
SmSpR

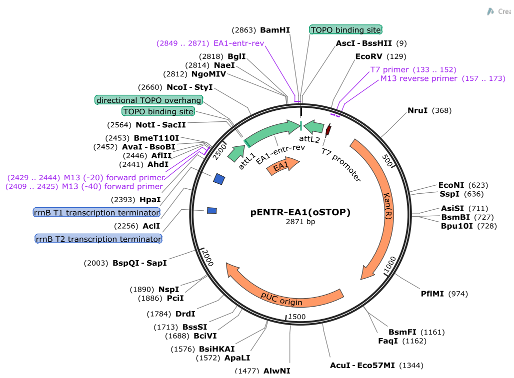
pENTR-EA1(oSTOP)
2871 bp
(2849 .. 2871) EA1-entr-rev
TOPO binding site
directional TOPO overhang
TOPO binding site
attL1
EA1-entr-rev
EA1
attL2
T7 promoter
Kan(R)
pUC origin
rrnB T1 transcription terminator
rrnB T2 transcription terminator
T7 primer (133 .. 152)
M13 reverse primer (157 .. 173)
(2429 .. 2444) M13 (-20) forward primer
(2409 .. 2425) M13 (-40) forward primer

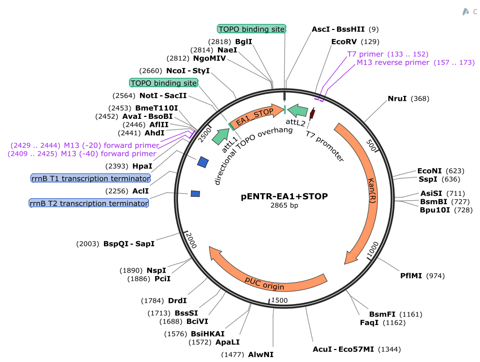
pENTR-EA1+STOP
2865 bp
TOPO binding site
TOPO binding site
attL1
EA1_STOP
directional TOPO overhang
attL2
T7 promoter
Kan(R)
pUC origin
rrnB T1 transcription terminator
rrnB T2 transcription terminator
T7 primer (133 .. 152)
M13 reverse primer (157 .. 173)
(2429 .. 2444) M13 (-20) forward primer
(2409 .. 2425) M13 (-40) forward primer

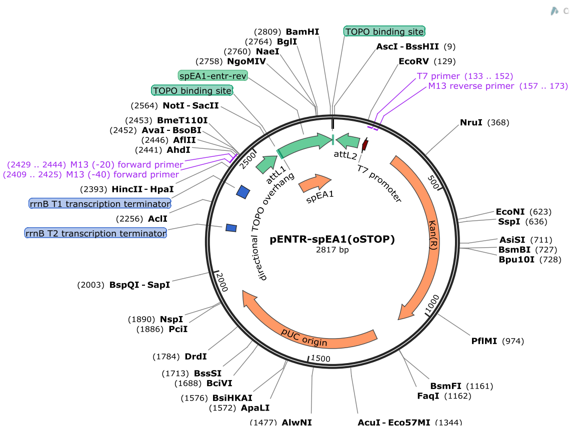
pENTR-spEA1(oSTOP)
2817 bp

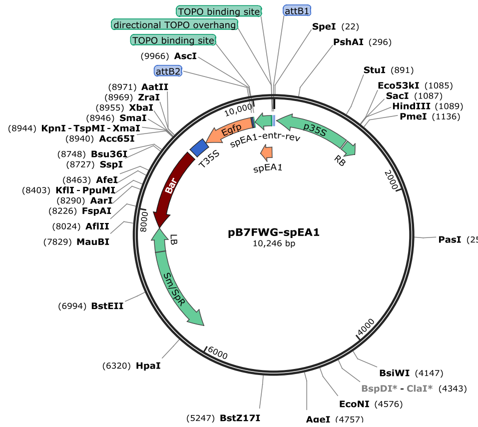
pB7FWG-spEA1
10,246 bp

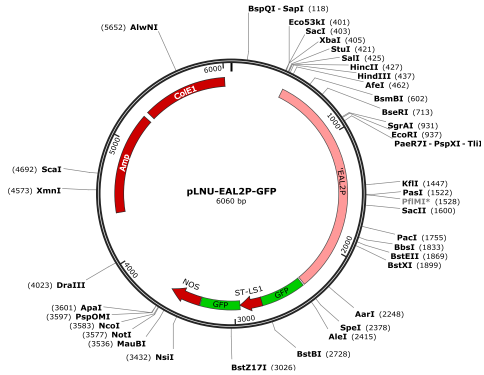
pLNU-EAL2P-GFP
6060 bp

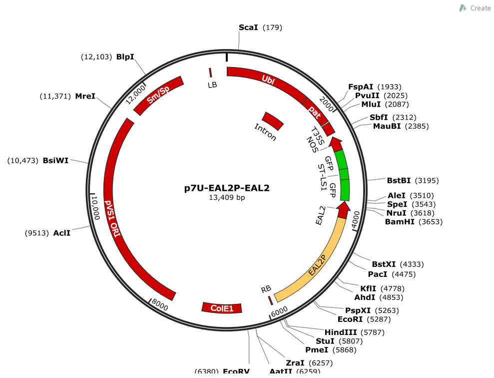
p7U-EAL2P-EAL2
13,409 bp

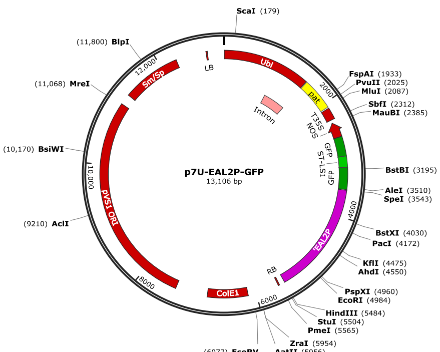
p7U-EAL2P-GFP
13,106 bp

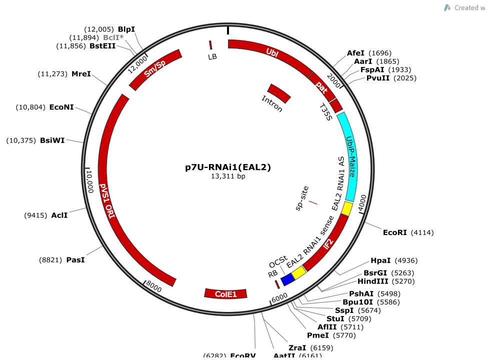
p7U-RNAi1(EAL2)
13,311 bp

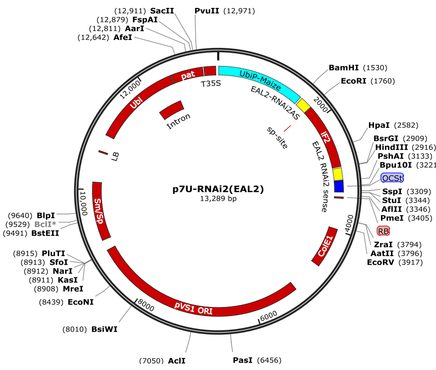
p7U-RNAi2(EAL2)
13,289 bp

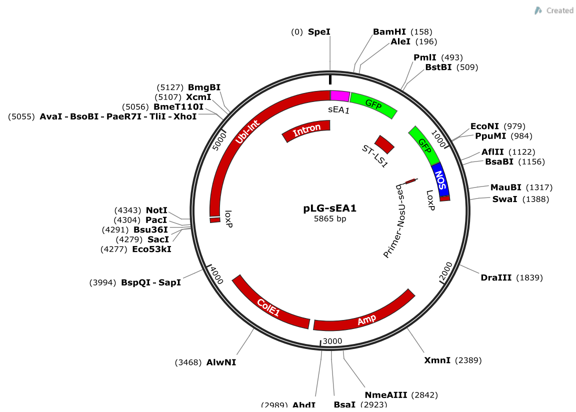
pLG-sEA1
5865 bp

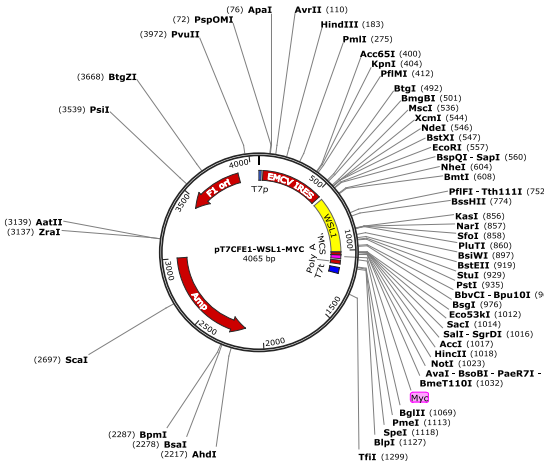
pT7CFE1-WSL1-MYC
4065 bp
T7p
EMCV IRES
WSL1
MCS
Poly A
T7t
Ori
Amp
Myc
(76) ApaI
AvrII (110)
(72) PspOMI
HindIII (183)
(3972) PvuII
PmlI (275)
Acc65I (400)
KpnI (404)
PflMI (412)
(3668) BtgZI
BtgI (492)
BmgBI (501)
(3539) PsiI
MscI (536)
XcmI (544)
NdeI (546)
BstXI (547)
EcoRI (557)
BspQI - SapI (560)
NheI (604)
BmtI (608)
PflFI - Tth111I (752
BssHII (774)
(3139) AatII
(3137) ZraI
KasI (856)
NarI (857)
SfoI (858)
PluTI (860)
BsiWI (897)
BstEII (919)
StuI (929)
PstI (935)
BbvCI - Bpu10I (9
BsgI (976)
Eco53kI (1012)
SacI (1014)
SalI - SgrDI (1016)
AccI (1017)
HincII (1018)
NotI (1023)
AvaI - BsoBI - PaeR7I -
BmeT110I (1032)
(2697) ScaI
BglII (1069)
PmeI (1113)
SpeI (1118)
(2287) BpmI
(2278) BsaI
(2217) AhdI
BlpI (1127)
TfiI (1299)

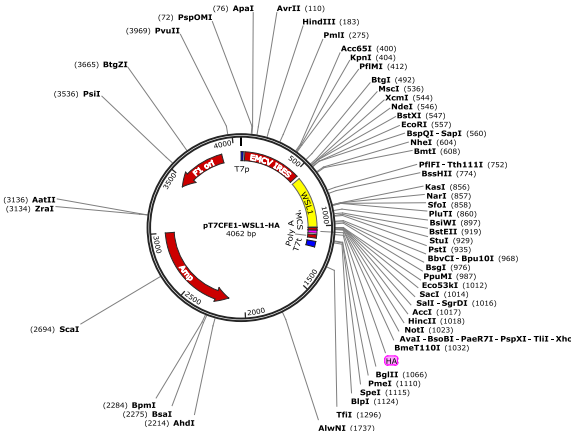
pT7CFE1-WSL1-HA
4062 bp
T7p
EMCV IRES
WSL1
MCS
Poly A
T7t
Ori
Amp
HA
(76) ApaI
AvrII (110)
(72) PspOMI
HindIII (183)
(3969) PvuII
PmlI (275)
Acc65I (400)
KpnI (404)
PflMI (412)
(3665) BtgZI
BtgI (492)
(3536) PsiI
MscI (536)
XcmI (544)
NdeI (546)
BstXI (547)
EcoRI (557)
BspQI - SapI (560)
NheI (604)
BmtI (608)
PflFI - Tth111I (752)
BssHII (774)
(3136) AatII
(3134) ZraI
KasI (856)
NarI (857)
SfoI (858)
PluTI (860)
BsiWI (897)
BstEII (919)
StuI (929)
PstI (935)
BbvCI - Bpu10I (968)
BsgI (976)
PpuMI (987)
Eco53kI (1012)
SacI (1014)
SalI - SgrDI (1016)
AccI (1017)
HincII (1018)
NotI (1023)
AvaI - BsoBI - PaeR7I - PspXI - TliI - Xho
BmeT110I (1032)
(2694) ScaI
BglII (1066)
PmeI (1110)
SpeI (1115)
BlpI (1124)
(2284) BpmI
(2275) BsaI
(2214) AhdI
TfiI (1296)
AlwNI (1737)

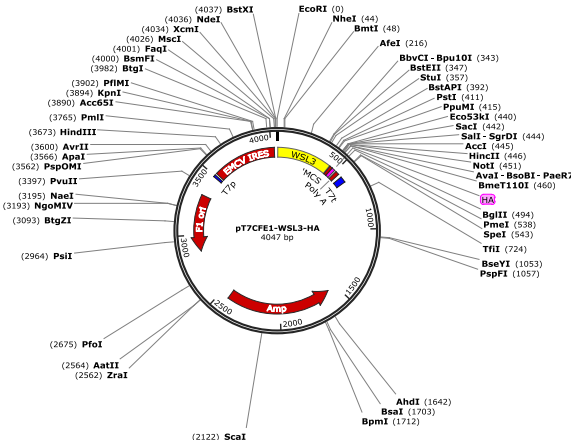
pT7CFE1-WSL3-HA
4047 bp
T7p
EMCV IRES
WSL3
MCS
Poly A
T7t
Ori
Amp
HA
(4037) BstXI
EcoRI (0)
(4036) NdeI
NheI (44)
(4034) XcmI
BmtI (48)
(4026) MscI
AfeI (216)
(4001) FaqI
(4000) BsmFI
BbvCI - Bpu10I (343)
(3982) BtgI
BstEII (347)
StuI (357)
(3902) PflMI
BstAPI (392)
(3894) KpnI
PstI (411)
(3890) Acc65I
PpuMI (415)
(3765) PmlI
Eco53kI (440)
(3673) HindIII
SacI (442)
SalI - SgrDI (444)
(3600) AvrII
AccI (445)
(3566) ApaI
HincII (446)
(3562) PspOMI
NotI (451)
(3397) PvuII
AvaI - BsoBI - PaeR7
BmeT110I (460)
(3195) NaeI
(3193) NgoMIV
BglII (494)
PmeI (538)
(3093) BtgZI
SpeI (543)
TfiI (724)
(2964) PsiI
BseYI (1053)
PspFI (1057)
(2675) PfoI
(2564) AatII
(2562) ZraI
AhdI (1642)
BsaI (1703)
BpmI (1712)
(2122) ScaI

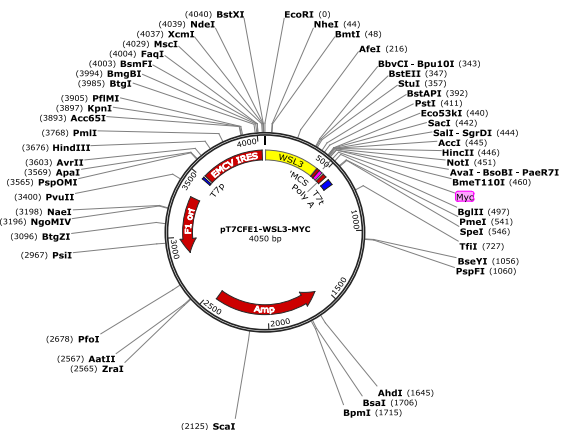
pT7CFE1-WSL3-MYC
4050 bp
T7p
EMCV IRES
WSL3
MCS
Poly A
T7t
Ori
Amp
Myc
(4040) BstXI
EcoRI (0)
(4039) NdeI
NheI (44)
(4037) XcmI
BmtI (48)
(4029) MscI
(4004) FaqI
AfeI (216)
(4003) BsmFI
BbvCI - Bpu10I (343)
(3994) BmgBI
BstEII (347)
(3985) BtgI
StuI (357)
BstAPI (392)
(3905) PflMI
PstI (411)
(3897) KpnI
Eco53kI (440)
(3893) Acc65I
SacI (442)
(3768) PmlI
SalI - SgrDI (444)
(3676) HindIII
AccI (445)
(3603) AvrII
HincII (446)
(3569) ApaI
NotI (451)
(3565) PspOMI
AvaI - BsoBI - PaeR7I
BmeT110I (460)
(3400) PvuII
BglII (497)
(3198) NaeI
PmeI (541)
(3196) NgoMIV
SpeI (546)
(3096) BtgZI
TfiI (727)
(2967) PsiI
BseYI (1056)
PspFI (1060)
(2678) PfoI
(2567) AatII
(2565) ZraI
AhdI (1645)
BsaI (1706)
BpmI (1715)
(2125) ScaI

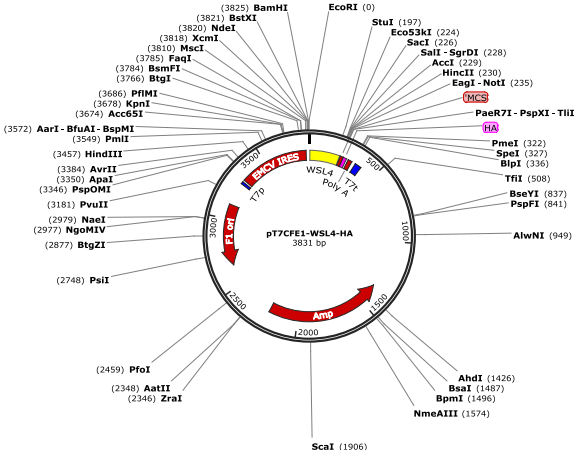
pT7CFE1-WSL4-HA
3831 bp
T7p
EMCV IRES
WSL4
Poly A
T7t
Ori
Amp
HA
(3825) BamHI
EcoRI (0)
(3821) BstXI
StuI (197)
(3820) NdeI
Eco53kI (224)
(3818) XcmI
SacI (226)
(3810) MscI
SalI - SgrDI (228)
(3785) FaqI
AccI (229)
(3784) BsmFI
HincII (230)
(3766) BtgI
EagI - NotI (235)
(3686) PflMI
MCS
(3678) KpnI
PaeR7I - PspXI - TliI
(3674) Acc65I
(3572) AarI - BfuAI - BspMI
(3549) PmlI
PmeI (322)
(3457) HindIII
SpeI (327)
(3384) AvrII
BlpI (336)
(3350) ApaI
TfiI (508)
(3346) PspOMI
BseYI (837)
(3181) PvuII
PspFI (841)
(2979) NaeI
(2977) NgoMIV
AlwNI (949)
(2877) BtgZI
(2748) PsiI
(2459) PfoI
(2348) AatII
(2346) ZraI
AhdI (1426)
BsaI (1487)
BpmI (1496)
NmeAIII (1574)
ScaI (1906)

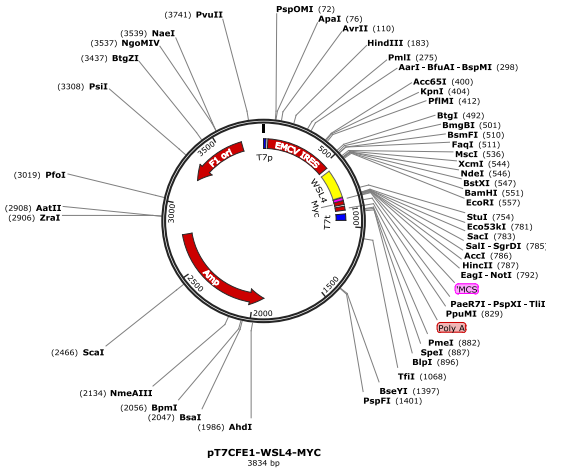
pT7CFE1-WSL4-MYC
3834 bp
T7p
EMCV IRES
WSL4
Myc
T7t
Ori
Amp
Poly A
(3741) PvuII
PspOMI (72)
ApaI (76)
(3539) NaeI
AvrII (110)
(3537) NgoMIV
HindIII (183)
(3437) BtgZI
PmlI (275)
AarI - BfuAI - BspMI (298)
(3308) PsiI
Acc65I (400)
KpnI (404)
PflMI (412)
BtgI (492)
BmgBI (501)
BsmFI (510)
FaqI (511)
MscI (536)
XcmI (544)
NdeI (546)
BstXI (547)
BamHI (551)
EcoRI (557)
(3019) PfoI
StuI (754)
Eco53kI (781)
(2908) AatII
(2906) ZraI
SacI (783)
SalI - SgrDI (785
AccI (786)
HincII (787)
EagI - NotI (792)
MCS
PaeR7I - PspXI - TliI
PpuMI (829)
Poly A
PmeI (882)
SpeI (887)
BlpI (896)
(2466) ScaI
TfiI (1068)
(2134) NmeAIII
BseYI (1397)
PspFI (1401)
(2056) BpmI
(2047) BsaI
(1986) AhdI

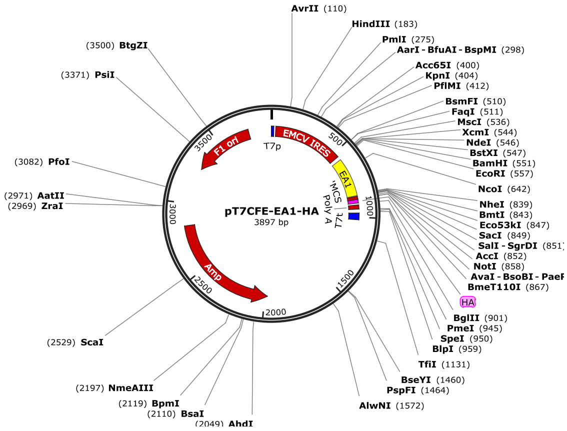
pT7CFE-EA1-HA
3897 bp
AvrII (110)
HindIII (183)
PmlI (275)
AarI - BfuAI - BspMI (298)
Acc65I (400)
KpnI (404)
PflMI (412)
BsmFI (510)
FaqI (511)
MscI (536)
XcmI (544)
NdeI (546)
BstXI (547)
BamHI (551)
EcoRI (557)
NcoI (642)
NheI (839)
BmtI (843)
Eco53kI (847)
SacI (849)
SalI - SgrDI (851)
AccI (852)
NotI (858)
AvaI - BsoBI - PaeR
BmeT110I (867)
HA
BglII (901)
PmeI (945)
SpeI (950)
BlpI (959)
TfiI (1131)
BseYI (1460)
PspFI (1464)
AlwNI (1572)
(2049) AhdI
(2110) BsaI
(2119) BpmI
(2197) NmeAIII
(2529) ScaI
(2969) ZraI
(2971) AatII
(3082) PfoI
(3371) PsiI
(3500) BtgZI
T7p
EMCV IRES
EA1
MCS
Poly A
T7t
F1 ori
Amp

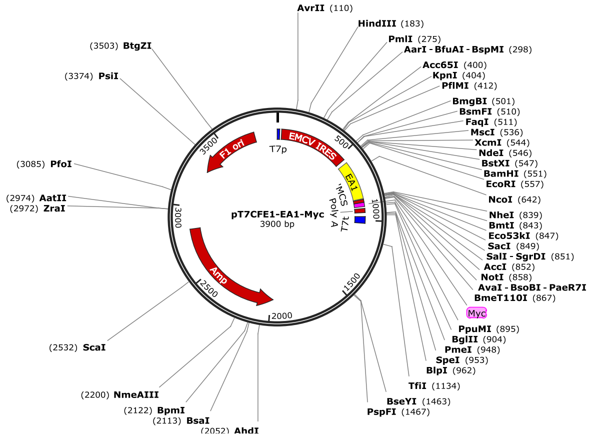
pT7CFE1-EA1-Myc
3900 bp
AvrII (110)
HindIII (183)
PmlI (275)
AarI - BfuAI - BspMI (298)
Acc65I (400)
KpnI (404)
PflMI (412)
BmgBI (501)
BsmFI (510)
FaqI (511)
MscI (536)
XcmI (544)
NdeI (546)
BstXI (547)
BamHI (551)
EcoRI (557)
NcoI (642)
NheI (839)
BmtI (843)
Eco53kI (847)
SacI (849)
SalI - SgrDI (851)
AccI (852)
NotI (858)
AvaI - BsoBI - PaeR7I
BmeT110I (867)
Myc
PpuMI (895)
BglII (904)
PmeI (948)
SpeI (953)
BlpI (962)
TfiI (1134)
BseYI (1463)
PspFI (1467)
(2052) AhdI
(2113) BsaI
(2122) BpmI
(2200) NmeAIII
(2532) ScaI
(2972) ZraI
(2974) AatII
(3085) PfoI
(3374) PsiI
(3503) BtgZI
T7p
EMCV IRES
EA1
MCS
Poly A
T7t
F1 ori
Amp

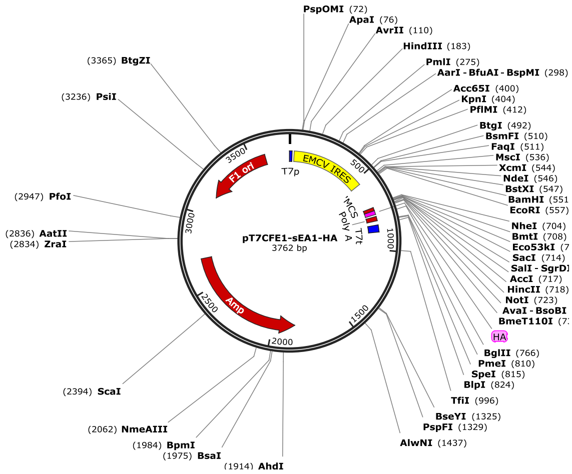
pT7CFE1-sEA1-HA
3762 bp
PspOMI (72)
ApaI (76)
AvrII (110)
HindIII (183)
PmlI (275)
AarI - BfuAI - BspMI (298)
Acc65I (400)
KpnI (404)
PflMI (412)
BtgI (492)
BsmFI (510)
FaqI (511)
MscI (536)
XcmI (544)
NdeI (546)
BstXI (547)
BamHI (551
EcoRI (557)
NheI (704)
BmtI (708)
Eco53kI (7
SacI (714)
SalI - SgrDI
AccI (717)
HincII (718)
NotI (723)
AvaI - BsoBI
BmeT110I (7
HA
BglII (766)
PmeI (810)
SpeI (815)
BlpI (824)
TfiI (996)
BseYI (1325)
PspFI (1329)
AlwNI (1437)
(1914) AhdI
(1975) BsaI
(1984) BpmI
(2062) NmeAIII
(2394) ScaI
(2834) ZraI
(2836) AatII
(2947) PfoI
(3236) PsiI
(3365) BtgZI
T7p
EMCV IRES
MCS
Poly A
T7t
F1 ori
Amp

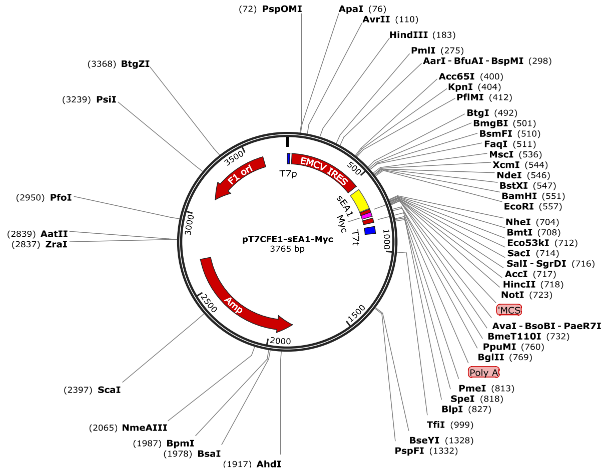
pT7CFE1-sEA1-Myc
3765 bp
(72) PspOMI
ApaI (76)
AvrII (110)
HindIII (183)
PmlI (275)
AarI - BfuAI - BspMI (298)
Acc65I (400)
KpnI (404)
PflMI (412)
BtgI (492)
BmgBI (501)
BsmFI (510)
FaqI (511)
MscI (536)
XcmI (544)
NdeI (546)
BstXI (547)
BamHI (551)
EcoRI (557)
NheI (704)
BmtI (708)
Eco53kI (712)
SacI (714)
SalI - SgrDI (716)
AccI (717)
HincII (718)
NotI (723)
MCS
AvaI - BsoBI - PaeR7I
BmeT110I (732)
PpuMI (760)
BglII (769)
Poly A
PmeI (813)
SpeI (818)
BlpI (827)
TfiI (999)
BseYI (1328)
PspFI (1332)
(1917) AhdI
(1978) BsaI
(1987) BpmI
(2065) NmeAIII
(2397) ScaI
(2837) ZraI
(2839) AatII
(2950) PfoI
(3239) PsiI
(3368) BtgZI
T7p
EMCV IRES
sEA1
Myc
T7t
F1 ori
Amp

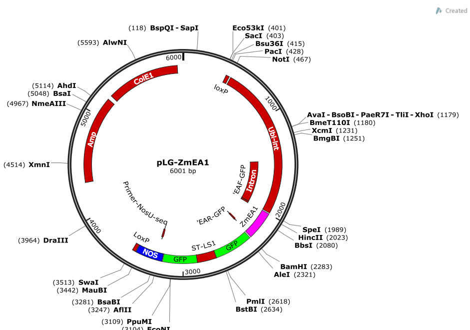
pLG-ZmEA1
6001 bp
(118) BspQI - SapI
(5593) AlwNI
Eco53kI (401)
SacI (403)
Bsu36I (415)
PacI (428)
NotI (467)
(5114) AhdI
(5048) BsaI
(4967) NmeAIII
AvaI - BsoBI - PaeR7I - TliI - XhoI (1179)
BmeT110I (1180)
XcmI (1231)
BmgBI (1251)
(4514) XmnI
(3964) DraIII
SpeI (1989)
HincII (2023)
BbsI (2080)
BamHI (2283)
AleI (2321)
PmlI (2618)
BstBI (2634)
(3513) SwaI
(3442) MauBI
(3281) BsaBI
(3247) AflII
(3109) PpuMI
(3104) EcoNI
ColE1
Amp
loxP
Ubi-int
Intron
ZmEA1
GFP
ST-LS1
NOS
LoxP
Primer-NosU-seq

ABBREVIATIONS

BiFC	bimolecular fluorescence complementation
BMS	Black Mexican Sweet
bp	base pairs
cDNA	complementary DNA
CMC	critical micelle concentration
CRP	cysteine-rich protein
DAG	days after germination
DAI	days after infiltration
DAP	days after pollination
DEFL	defensin-like
DNA	deoxyribonucleic acid
EMCV	encephalomyocarditis virus
ER	endoplasmic reticulum
FG	female gametophyte
FRET	Förster resonance energy transfer
GFP	GREEN FLUORESCENT PROTEIN
GRP	glycine-rich protein
IRES	internal ribosome entry site
IVT/T	*in vitro* transcription and translation
LRC	ligand-based receptor-capture technology
MS	mass spectrometry
MW	molecular weight
ORF	open reading frame
PCR	polymerase chain reaction
PGM	pollen germination medium
PT	pollen tube
PTCA	pollen tube competition assay
qRT-PCR	quantitative real-time PCR

RAM	root apical meristem
RLK	receptor-like kinase
RMA	robust multi-array average
RNA	ribonucleic acid
RNAi	RNA interference
RT	room temperature
RT-PCR	reverse transcriptase PCR
SAP	shoot apical meristem
SDS-PAGE	sodium dodecyl sulfate polyacrylamide gel electrophoresis
TI	trypsin inhibitor
UTR	untranslated region
WT	wild type

FIGURES AND TABLES

Figure 1.1 Megagametogenesis of *Zea mays* and *Arabidopsis*. 4
Figure 1.2 Development of the male gametophyte in maize. 5
Figure 1.3 Growth of pollen tube for fertilization of the female gametophyte in maize. 7
Figure 1.4 Morphological stages of embryogenesis of *Arabidopsis* and *Zea mays*. The different embryo stages are indicated. 10
Figure 2.1 Protein alignment of EA1-box proteins. 23
Figure 2.2 Partial protein sequence similarity between ZmEAL1 and ZmEAL1s. 25
Figure 2.3 Phylogenetic tree of proteins containing the EA1-box and genomic localization of EAL proteins. 28
Figure 2.4 Subcellular localization of EAL proteins in BMS suspension cells. 31
Figure 2.5 Subcellular localization of EAG and EAC proteins in BMS suspension cells. 32
Figure 2.6 *In silico* analysis of the expression profile of *ZmEAL2*. 33
Figure 2.7 ZmEAL2 protein level in maize endosperm was analyzed from 11 to 34 DAP using a ZmEAL2-specific antibody. 34
Figure 2.8 Expression analysis of *ZmEAL2*. 35
Figure 2.9 Immunolocalization of ZmEAL2 in the maize embryo. 36
Figure 2.10 Control experiments of immunohistochemically labeling of ZmEAL2 in the maize embryo. 37
Figure 2.11 Putative *ZmEAL2* promoter shows activity in BMS suspension cells. 39
Figure 3.1 Predicted mature ZmEA1 attracts and arrests maize pollen tubes *in vitro* and binds in a species-preferential manner to the subapical region of the PT tip. 48
Figure 3.2 Unspecific proteins are unable to attract and bind maize pollen tubes *in vitro* (related to Figure 3.1). 49
Figure 3.3 ZmEA1-GFP fusion protein is secreted to the filiform apparatus of *Arabidopsis* ovules. 51
Figure 3.4 ZmEA1 variants containing an internal or N-terminal signal recognition motif are secreted to the filiform apparatus of *Arabidopsis* ovules (related to Figure 3.3). 52

Figure 3.5 *In vitro* PT competition assay showing ZmEA1-mediated attraction of maize PTs by *Arabidopsis* ovules. 54
Figure 3.6 Secretion of ZmEA1-GFP fusion protein from *Arabidopsis* synergid cells enables *Arabidopsis* ovules to attract own competent pollen tubes and shows no significant influence on micropylar guidance and growth arrest of *Tripsacum dactyloides* pollen tubes (related to Figure 3.5). 56
Figure 4.1 EA1 peptide interacts with the maize pollen tube apex in a species-specific manner. 61
Figure 4.2 EA1-related EAL2 peptide does not interact with maize and *Tripsacum dactyloides* pollen tube tips. 62
Figure 4.3 DyLight-labeled synthetic EA1 peptide gets internalized in vesicles at the apical region of the maize pollen tube tip. 63
Figure 5.1 Pollen tube attractor EA1 binds to an unknown interaction partner at the apical maize pollen tube cell surface. 70
Figure 5.2 Ligand-based receptor-capture technology (LRC) after Frei *et al.*, 2013. 72
Figure 6.1 Male and female factors for ovular pollen tube guidance. 77
Figure 6.2 Production and purification of GST and GST-sEA1 in Rosetta™ (Coomassie stained gel). 91
Figure 6.3 Production of 6xHis-sEA1-StrepII in Lemo21(DE3) (Coomassie stained gel). 92
Figure 6.4 Production and purification of 6xHis-sEA1-StrepII in Rosetta™ (Coomassie stained gel). 93
Figure 6.5 Denaturing purification of 6xHis-sEA1-StrepII and refolding including agents for prevention of protein aggregation (Coomassie stained gel). 95
Figure 6.6 Purification of 6xHis-MBP-sEA1 in RosettaTM under native conditions. 97
Figure 6.7 Subcellular localization of ZmEA1, spEA1 and sEA1 fused to GFP in leave epidermis cells of tobacco. 99
Figure 6.8 Detection and purification of GFP-tagged ZmEA1, spEA1 and sEA1 produced in *Nicotiana benthamiana*. 100
Figure 6.9 Visualization of a putative interaction partner of sEA1. 101
Figure 6.10 Affinity purification of sEA1 binding partners. 104
Figure 6.11 Protein sequences and domain structure of WSL peptides, which were identified candidates for interaction with sEA1. 108
Figure 6.12 Analysis of 5'- and 3'-UTRs of WSL peptides. 109

Figure 6.13 Secondary structure prediction of WSL peptides. 111
Figure 6.14 *In vitro* transcription and translation (IVT/T) of ZmEA1/sEA1 and WSL peptides fused to affinity tags. 113
Figure 6.15 Heterologous production of Myc-WSL in tobacco and test for interaction with sEA1. 114
Figure 6.16 Heterologous production of WSL peptides fused to GFP in tobacco leaves and test for interaction with sEA1. 115
Figure 6.17 *In silico* analysis of the expression profile of *WSL* genes. 117
Figure 6.18 Quantitative expression profile of *WSL* genes in *in vitro* germinated maize pollen tubes. 118
Figure 6.19 Detection of tobacco-produced WSL peptides fused to GFP with anti-WSL1 antibody. 119
Figure 6.20 WSL1 peptide in germinated maize pollen. 120
Figure 6.21 Subcellular localization of WSL1 in *Nicotiana benthamiana* leaf cells. 122
Figure 6.22 Subcellular localization of WSL3 in *Nicotiana benthamiana* leaf cells. 123
Figure 6.23 Subcellular localization of WSL4 in *Nicotiana benthamiana* leaf cells. 124
Figure 6.24 Model for involvement of WSL peptides in micropylar pollen tube attraction of maize. 130

Table 4.1 Summary of *in vitro* pollen tube binding assays of three maize inbred lines, *Tripsacum dactyloides*, *Lilium* "Stargazer" and *Nicotiana benthamiana*, respectively. 60
Table 6.1 Bacterial strains used in this study. 79
Table 6.2 Additives used to stabilize recombinant protein and to prevent aggregation. .. 94
Table 6.3 Critical micellar concentrations (CMCs) of detergents utilized for refolding of denatured purified 6xHis-sEA1-StrepII. 96
Table 6.4 Protein groups identified in biotin-directed pull-down of pollen tubes after incubation with sEA1. 106

Supplement table 1 Genomic location of EA1-box proteins in different plant species. 165
Supplement table 2 Primers used in this study. 166

ACKNOWLEDGEMENTS

First of all, I want to thank Prof. Dr. Thomas Dresselhaus for giving me the great opportunity to work in his lab. I'm grateful for all his support during these years and his critical remarks on this manuscript and want to appreciate that he gave me the chance to visit numerous international conferences and to meet the scientific world.

Great thanks to Dr. Mihaela-Luiza Márton for supervising my work in the lab, sharing her knowledge with me, for scientific discussions and always having amusing chats and a cup of coffee. Furthermore, I would like to thank Prof. Dr. Reinhard Sterner and PD Dr. Joachim Griesenbeck for being part of the examination committee and my external mentor Prof. Dr. Ueli Grossniklaus (University of Zurich) for advice and support during my PhD student time.

I gratefully acknowledge Prof. Dr. Klaus Grasser and Dr. Marion Grasser for providing their equipment and Dr. Liang-Zi Zhou, Dr. Junyi Chen, PD Dr. Stefanie Sprunck, Dr. Mariana Mondragon-Palomino, Dr. Andrea Bleckmann and PD Dr. Ulrich Hammes for scientific advices and help on experimental questions. I also want to appreciate the kind support of Veronika Mrosek in all administrative questions, which can be as challenging as lab work.

I also would like to thank our collaborators Dr. Igor Paron (MPI of Biochemistry, Martinsried) for Orbitrap MS analysis, Dr. Jan Medenbach (University of Regensburg) for providing support for *in vitro* translation experiments and Dr. Urte Schlüter (formerly University of Erlangen) for microarray hybridization and statistical analysis.

My warm thanks go to Annemarie Taffner for her great technical support in the lab and for being a wonderful colleague and friend. I also want to thank all current and former members of the maize lab: our technicians Angelika Rechenmacher and Ingrid Fuchs for always having an open ear and my PhD colleagues Sandra Bertrand, Ajay John Arputharaj, Philipp Alter, Andreas Lausser and Martina Juranić for helping in word and deed and always having a fun time. Special thanks go to Ursula Wittmann, Günther Peissig and Armin Hildebrand for taking care of all my plants.

Furthermore, I want to thank all other members of the department, as there is never enough space for acknowledgements to mention everybody that I would like to. But if you read this and were somebody who accompanied me during my years as PhD student, be it for months or just weeks, then you can feel certain that I also thank you for this time. And if you don't know me, well, then I'm also grateful that you spent your time reading this.

Finally, I want to thank the people I love the most, especially my parents Edeltraud and Lothar, who gave me the opportunity to focus on my studies and supported me through all these years. Thank you for always welcoming me and providing me all the basic equipment a student needs, be it technical stuff, technical support for the technical stuff, family support or the knowledge about it. I'm also grateful for my sisters, Monika and Claudia, and my brother Christian, for being the best friends somebody can have. Knowing that Monika will always take her time to call and talk with me, and looking forward to meeting Claudia in the University made me feel like always being so close to both of you. And a special thank goes to our new family member, my nephew Lukas, for being a little sunshine.

Last but not least, I want to honor my fiancé Martin. Love of my life, you were always my bastion of calm and made me happy for all these years. Thank you for making me laugh, building me up, needing me, accompanying me, protecting me and reading these mawkish little words I wrote for you.